REFERENCE ONLY

UNIVERSITY OF LONDON THESIS

Degree PhD Year 2005 Name of Author GEE V-J

Molecular and functional characterization of neuronal nicotinic and 5-HT_3 receptors

Veronica Josephine Gee

August 2005

A thesis presented for the degree of Doctor of Philosophy to the University of London

Department of Pharmacology
University College London
London, WC1E 6BT

ProQuest LLC
789 East Eisenhower Parkway
P.O. Box 1346
Ann Arbor, MI 48106-1346

ABSTRACT

Unlike many nicotinic subunits, the α7 nicotinic subunit and the 5-HT_{3A} subunit are able to form functional homomeric receptors. Despite sharing this ability, they have differences in cell-surface expression in human embryonic kidney (HEK) cells, with $5HT_{3A}$ subunits forming a large number of functional receptors, whereas the α7 subunit forms few or no correctly folded receptors as assayed by radioligand binding with [^{125}I]α-BTX. A series of chimeras between α7 and $5HT_{3A}$ were constructed to investigate which domains of the subunits were important for folding and cell surface expression. Only chimeras that contained the region from the beginning of M1 to the end of M3, and M4 domain of the $5HT_{3A}$ subunit were able to form correctly folded receptors.

The chimeras that gave high levels of radioligand binding were also found to be functional using whole-cell patch-clamp recording. Functional characteristics were examined, and differences were found in single channel conductance and desensitization. Chimeras with the large cytoplasmic loop and the extracellular N-terminal region of α7 had larger single channel conductances than the $5HT_{3A}$ receptor, with the inclusion of the α7 large cytoplasmic loop and the N-terminal domain increasing the conductance by approximately 10 and 2 fold respectively

Co-expression of α7 with RIC3 (a protein originally identified in *C. elegans*) in HEK cells, results in high levels of cell surface expression. These receptors were shown to be functional, with whole cell responses from 20-300 pA. showing fast desensitization (time constant of 66±13 ms) and strong inward rectification. RIC3 was also shown to increase the functional expression of the α8 and the rat α3β2 nAChRs, which rarely formed detectable functional receptors when expressed alone. On co-expression with RIC3 almost all cells expressing α8 responded giving an average response of 240 pA, and all cells expressing α3β2 responded giving an average response of 99 pA. *C. elegans* RIC3 has been shown to increase the functional expression of the human $5HT_{3A}$ receptor by 168 %. Human RIC3 had no effect on human $5HT_{3A}$ and in fact decreased the functional expression of the murine $5HT_{3A}$ by 59 %.

AKNOWLEDGEMENTS

My thanks to Dr Neil Millar, for the opportunity to work in his laboratory, and for all his support during the last year. Also, huge thanks to Dr Alasdair Gibb for collaborating with me and being a very present second supervisor. I would also like to thank the rest of the Millar group for being so supportive and understanding, especially Patricia Harkness and Dr Stuart Lansdell.

Many thanks to all the people who contributed subunit cDNAs and antibodies that make my work possible.

Thanks to my Dad and Francine for supporting me in every way and most importantly letting me live with them for the last year. Thanks also to my brothers and all my friends who have given me moral support all the way along.

And finally, thank you Paul, I never would have finished the PhD with out you.

This work was funded by grants from the Wellcome Trust.

TABLE OF CONTENTS

LIST OF FIGURES AND TABLES

CHAPTER 1

Introduction

CHAPTER 2

Materials and Methods

CHAPTER 3

α7/5-HT_3 Chimeras

CHAPTER 4

RIC3 affects functional expression of multiple nicotinic ACh receptor subtypes and the 5-HT_{3A} receptor.

ABBREVIATIONS

2-Me-5-HT	2-methyl-5-hydroxytryptamine
5-HT	5-hydroxytryptamine
$5\text{-HT}_{1\text{-}7}\text{R}$	5-hydroxytryptamine receptors types 1 to 7
$5\text{-HT}_3\text{R}$	5-hydroxytryptamine type 3 receptor
5-HT_{3A}	'A' subunit of the 5-hydroxytryptamine type 3 receptor
$5\text{-HT}_{3B,C...}$	'B', 'C'... subunit of the 5-hydroxytryptamine type 3 receptor
A_1	area of 1st lorentzian component
A_2	area of 2nd lorentzian component
α-BTX	alpha bungarotoxin
AC	alternating current
ACh	acetylcholine
AChBP	acetylcholine binding protein
ADNFLE	autosomal dominant nocturnal frontal lobe epilepsy
Amp	ampicillin
Arg	arginine
Asn	asparagine
Asp	aspartate
Bgh	bovine growth hormone
BiP	immunoglobulin binding protein
BSA	bovine serum albumin
cDNA	clonal deoxyribonucleic acid
CIP	calf intestinal alkaline phosphatase
CMV	cytomegalovirus
C-terminal	carboxy (COOH) terminal
Cys	cysteine
DC	direct current
DMEM	Dulbecco's modified Eagles's medium
DMPP	1,1-dimethyl-4-phenylpiperazinium
dNTPs	deoxynucleotide triphosphate
E8	embryonic day 8

EC_{50}	median effective concentration
EDTA	ethylenediaminetetraacetic acid
E_{rev}	reversal potential
FCS	foetal calf serum
FLIPR	fluorescence imaging plate reader
GABA	gamma-aminobutyric acid
$GABA_AR$	gamma-aminobutyric acid type A receptor
$GABA_BR$	gamma-aminobutyric acid type B receptor
GFP	green fluorescent protein
Glu	glutamate
HBSS	Hank's buffered saline solution
$HBSS^{++}$	Hank's buffered saline solution with 25 μM $MgCl_2$ and 25μM $CaCl_2$
HCA	high calcium buffer
HEK	human embryonic kidney
HEK tsA201	a subclone of the HEK 293 cell line
HRP	horse radish peroxidase
GH_4C_1	rat pituitary cell line
i	single-channel current
I	mean current
I_{40}	mean current at 40 mV
I_{-60}	mean current at -60 mV
Ile	isoleucine
LB	Luria-Bertani
Leu	leucine
M1/M2/M3/M4	transmembrane domains 1/2/3/4
mCPBG	meta-chlorophenylbiguanide
MLA	methyllycaconitine
MOPS	3-N-morpholinopropanesulphonic acid
mRNA	messenger ribonucleic acid
N	number of channels
NAc	nucleus accumbens
nAChR	nicotinic acetylcholine receptor
NB41A3	murine C-1300 Neuroblastoma cell line

NCB-20	murine neuroblastoma/Chinese hamster embryonic brain cell hybrid
NG108-15	murine/rat, neuroblastoma x glioma hybrid cell line
NMDA	N-methyl-D-aspartate
N-terminal	amino (NH_2) terminal
p	open channel probability
P14	postnatal day 14
PBG	phenylbiguanide
PCR	polymerase chain reaction
P_f	percentage of current carried by calcium ions
Phe	phenylalanine
Poly-A	poly-adenylation
Pro	proline
RIC3	resistant to inhibitors of cholinesterase protein 3
rpm	revolutions per minute
σ^2_I	current variance (or standard deviation squared)
SDM	site-directed mutagenesis
Ser	serine
SV40	simian virus
τ_1	time constant 1
τ_2	time constant 2
τ_w	weighted mean time constant
TAE	tris-acetate with EDTA
Tet	tetracyline
Trp	tryptophan
Tyr	tyrosine
Val	valine
VILIP-1	visinin-like protein-1
VTA	ventral tegmental area

CHAPTER 1
INTRODUCTION

1.1 Neurotransmitter receptors

The nicotinic ACh receptors and the 5-hydroxytryptamine type 3 receptors are the focus of this thesis. These two neurotransmitter receptor classes are both ligand-gated ion channels. When ligand-gated ion channels are activated by an agonist or drug, an ion-permeable transmembrane channel opens, thus transferring a signal from outside the cell to within the cell. Nicotinic acetylcholine receptors (nAChRs) and 5-hydroxytryptamine type 3 receptors (5-HT_3Rs) are oligomeric proteins with five membrane-spanning subunits and a conserved cysteine loop in the N-terminal extracellular region formed from a disulphide bond between two cysteine residues, at positions 126 and 142 for the α7 nAChR subunit and at 138 and 153 in the 5-HT3A subunit. Analysis of the gene sequences of these receptors and others sharing these characteristics has shown that they have a common evolutionary ancestor, and thus are all part of a large gene super-family (Ortells and Lunt, 1995). The first ligand-gated ion channel from this family to be biochemically isolated and studied extensively was the *Torpedo* nAChR (Changeaux *et al.*, 1970). Subsequently, many more members of this family have been identified, for example the gamma-aminobutyric acid receptors $GABA_AR$ and $GABA_CR$, and glycine receptors in vertebrates, and 10 nAChRs in *Drosophila* over 40 nAChRs in *C. elegans*.

1.1.1 The nicotinic acetylcholine receptors (nAChRs):

There are two types of AChRs, named nicotinic and muscarinic. Nicotinic AChRs are ligand-gated ion channels, whereas muscarinic AChRs are G-protein coupled receptors. These two types of AChRs were originally distinguished pharmacologically by their sensitivity to nicotine (isolated from the tobacco plant) and muscarine (isolated from the poisonous mushroom *Amanita muscaria*) (Dale, 1914).

1.1.1.1 A short history of *Torpedo* nAChR

As mentioned above, the first well-characterised ligand-gated ion channel was the acetylcholine- (ACh) activated cationic channel protein from the electric organ of the ray. (La Torre *et al.*, 1970, Changeux *et al*, 1970). The electric organs of two species of ray, *Torpedo* (*californica* and *marmorata*) and the electric eel *Electrophorus electricus*, contain a very high density of nAChRs that have been

shown to resemble the nAChR at the neuromuscular junction (Sealock *et al.*, 1982). A snake toxin α-bungarotoxin (α-BTX), that was shown to bind and inactivate the *Torpedo* nAChR almost irreversibly (Lee and Chang, 1966), has been used to purify large quantities of the *Torpedo* nAChR protein (Changeux *et al.*, 1970; Miledi *et al.*, 1971).

The purified *Torpedo* electric organ receptor has been shown to be made up of four different proteins, of molecular weights 40, 48, 62 and 60 kDa (Hucho *et al.*, 1976) named α, β, γ and δ respectively. The total molecular weight of the assembled nAChR is approximately 250 kDa (Reynolds and Karlin, 1978). The receptor was proposed to be pentameric, containing two α, and then one of each of the β, γ and δ subunits as there appeared to be more α subunit protein compared to the other subunits when separated by electrophoresis (Hucho *et al.*, 1976). Functional characterisation of the *Torpedo* electric organ nAChR was achieved by reconstitution of the four subunit proteins in planar lipid bilayers (Labarca *et al.*, 1984) and also by injection of the four subunit mRNAs into *Xenopus* oocytes (Sumikawa *et al.*, 1981, Barnard *et al.*, 1982). It was shown properties of this receptor were different to the native ACh-activated receptors in oocytes (Kusano *et al.*, 1977), which are muscarinic AChRs.

Torpedo nAChR α, β, γ and δ subunits were the first ligand-gated ion channel subunits to be cloned (Noda *et al.*, 1982, Claudio *et al*, 1983, Noda *et al.*, 1983a). The nAChR subunits expressed at the neuromuscular junction and in the central nervous system of vertebrates and invertebrates have now also been identified and cloned. The *Torpedo* nAChR is still used as a model nAChR, for example ultrastructural studies have given us insight into the three-dimensional structure of the nAChR at very high resolution (4 Å; Unwin *et al.*, 2003). This has not been possible for other nAChRs, due to the absence of suitably pure source of receptors.

1.1.1.2 Vertebrate neuromuscular nAChRs

It was known from the 1940s that there were receptors at the skeletal neuromuscular junction that responded to ACh (Fatt, 1949). The cDNA sequences of *Torpedo* nAChR subunits were used to isolate homologous proteins in muscle. Mammalian

α, β, γ and δ were identified (Noda *et al.*, 1983a; Lapolla *et al.*, 1984, Nef *et al.*, 1984, Tanabe *et al.*, 1984) and a novel subunit was cloned (ε) that exhibited close sequence similarity to the γ subunit (Takai *et al.*, 1985). The ε subunit and was shown to be expressed predominately in the adult form of the vertebrate neuromuscular nAChR, whilst the γ subunit is only expressed in the foetal form (Mishina *et al.*, 1986). These two forms of the muscle nAChR have different functional characteristics including greater single channel conductance, greater calcium permeability and faster desensitization in receptors containing the ε subunit (Mishina *et al.*, 1986; Villarroel and Sakmann, 1996) thus there is a developmental switch that changes the functional characteristics of the muscle nAChR. The muscle nAChR was thought to resemble the *Torpedo* receptor, also having a pentameric subunit structure (Sealock *et al.*, 1982).

1.1.1.3 Vertebrate neuronal nAChRs

Nicotinic AChRs are present throughout the central and peripheral nervous systems, as demonstrated by nicotine and α-BTX binding (Clarke, 1985; McGehee and Role, 1995). However, these nAChR are not a homogeneous group of receptors as at the neuromuscular junction. It has been shown that the nAChRs activated in sympathetic neurones do not bind to α-BTX (Patrick and Stallcup, 1977), and are not blocked by α-BTX (Carbonetto *et al.*, 1978). Thus, it was demonstrated that there was more than one subtype of nAChR in the nervous system, with some nicotinic receptors that, unlike the muscle nAChR, do not bind α-BTX. In fact it has since been demonstrated that there is much greater diversity of nAChR subtypes (Sargent, 1993).

Molecular cloning has identified 12 vertebrate neuronal nicotinic subunits (Boulter *et al.*, 1985; Boulter *et al.*, 1987; Deneris *et al.*, 1988; Deneris *et al.*, 1989; Wada *et al.*, 1988; Boulter *et al.*, 1990; Couturier *et al.* 1990a; Elgoyhen *et al.*, 1994; Elgoyhen *et al.*, 2001), and these have been divided into two categories, α and "non-α" (Boulter *et al.*, 1987). The α8 subunit has been identified in chick (Schoepfer *et al.*, 1990), but not in any other vertebrates. Subunits are classified as α subunits by the presence of an adjacent pair of cysteine residues in the extracellular amino- (N-) terminus, equivalent to Cys^{192} and Cys^{193} of the *Torpedo* nAChR α subunit. These

cysteine residues form a disulphide bond and are thought to contribute to the ligand-binding domain of the *Torpedo* nAChR, shown by labelling with a tritiated nicotinic ligand (Kao *et al.*, 1984; Kao and Karlin, 1986). The neuronal β subunits do not show particular sequence similarity with muscle β subunit compared to the γ or δ, and have been referred to as "structural" subunits (Schoepfer *et al.*, 1988), although the neuronal β2 and β4 subunits contribute some residues to the ligand binding site (Parker *et al.*, 1998, Wang *et al.*, 1998).

1.1.2 5-hydroxytryptamine type 3 receptors (5-HT_3Rs)

There are a number of different subtypes of the 5-hydroxytryptamine receptors (5-HT_{1-7}R), however, most of the 5-HT receptor subtypes are G-protein coupled receptors and are not discussed in this thesis.

The 5-HT type 3 receptors (5-HT_3Rs), like the nAChRs, are excitatory cation-selective ligand-gated ion channels (Derkach *et al.*, 1989). The 5-HT_{3A} subunit was cloned from NCB-20 cells (a murine/hamster hybrid brain cell line; Maricq *et al.*, 1991). This subunit is able to generate functional homomeric receptors when expressed in *Xenopus* oocytes. A homologous subunit has been cloned in a number of other species including rat (Johnson and Heinemann, 1992), human (Belelli *et al.*, 1995) and guinea pig (Lankiewicz *et al.*, 1998). There is some diversity in 5-HT_3R subunits generated through alternative splicing. The first cloned murine variant is now referred to as the long form, whereas an alternative splice variant (which lacks 6 amino acids in the intracellular loop) is termed the "short" form (Hope *et al.*, 1993). There is no significant difference in function of the short and long forms of the murine 5-HT_{3A} receptor (Glitsch *et al.*, 1996) and the only pharmacological differences are in the efficacy of 2-methyl-5-hydroxytryptamine (2-Me5-HT) and meta-chlorophenylbiguanide (mCPBG) (Niemeyer and Lummis, 1998) and the potency of ondansetron (Hope *et al.*, 1993).

5-HT_{3A} subunits, equivalent to the short splice variant identified in mouse, have been cloned in rat (Miquel *et al.*, 1995; Isenberg *et al.*, 1993), human (Belelli *et al.*, 1995; Miyake *et al.*, 1995) and guinea pig (Lankiewicz *et al.*, 1998). Two additional splice variants of the human 5-HT_{3A} subunit have also been identified, but are unable to

form functional homomeric receptors (Brüss *et al.*, 2000). However, both the truncated splice variant and the long splice variant modify the function of the receptor when co-expressed with the short form (Brüss *et al*, 2000).

Although the 5-HT_{3A} subunit is able to form recombinant homomeric receptors, this is not sufficient to explain the properties of some native 5-HT_3Rs, even with incorporating the splice variants into the receptor (Hussy *et al.*, 1994). More recently, additional 5-HT_3R subunits have been cloned. The 5-HT_{3B} subunit is unable to form functional homomeric receptors, however it can form heteromeric receptors with the 5-HT_{3A} subunit (Davies *et al.*, 1999b). This heteromeric receptor has different properties to the homomeric receptor (Dubin *et al.*, 1999). The 5-HT_{3C} subunit alters the functional response to 5-hydroxytrptamine (5-HT) when co-expressed with the 5-HT_{3A} subunit (Dubin *et al.*, 2002). Other putative subunits have also been cloned (5-HT_{3D} and 5-HT_{3E}, Niesler *et al.*, 2003), but have not been well characterized.

1.2 The Structure of nAChRs and 5-HT_3Rs

The nAChR and 5-HT_3R subunits share structural characteristics that are common to the members of the super-family of ligand-gated ion channels to which they belong. Both contain an N-terminal signal peptide, which is cleaved to form the mature protein. The subunits have a similar overall topology, with a large extracellular N-terminal domain, four putative transmembrane domains (M1-M4) and a short extracellular carboxy- (C-) terminal domain (Noda, 1983; Maricq *et al.*, 1991), see Figure 1.1.

1.2.1 Primary amino-acid sequences and homology

Comparison of the nucleotide sequence of genes within this ligand-gated ion channel super-family suggests that all the members originated from a common ancestral gene (Ortells and Lunt, 1995), see Figure 1.2. All members of the super-family of ligand-gated ion channels, including the nAChR, 5-HT_3R and $GABA_A$R subunits, have two conserved cysteine residues in the N-terminal region, which forms an important disulphide bond. The protein sequence in the N-terminal forms the ligand-binding

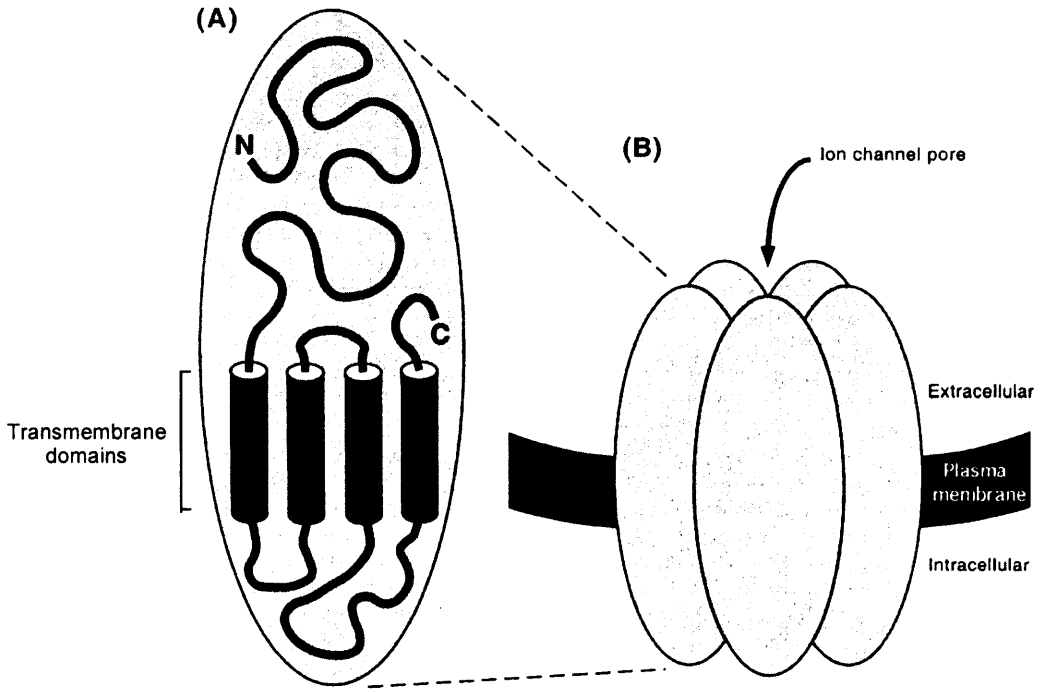

Figure 1.1 *The predicted topology of the nAChR and 5-HT_3R subunits, and pentameric structure of the assembled receptor*

(A), The subunits have a large extracellular N-termial domain which contains the ligand binding site, the main immunogenic region and sites for N-glycosylation. Following the N-terminal domain are four transmembrane (M1-M4) domains and then a short extracellular C-terminal domain. There is a large hydrophilic cytoplamsic loop in between M3 and M4, and this contains a number of putitive sites for phosphorylation. (B), The receptors are formed of five subunits arranged around a central ion channel pore. Adapted from Millar, 2003.

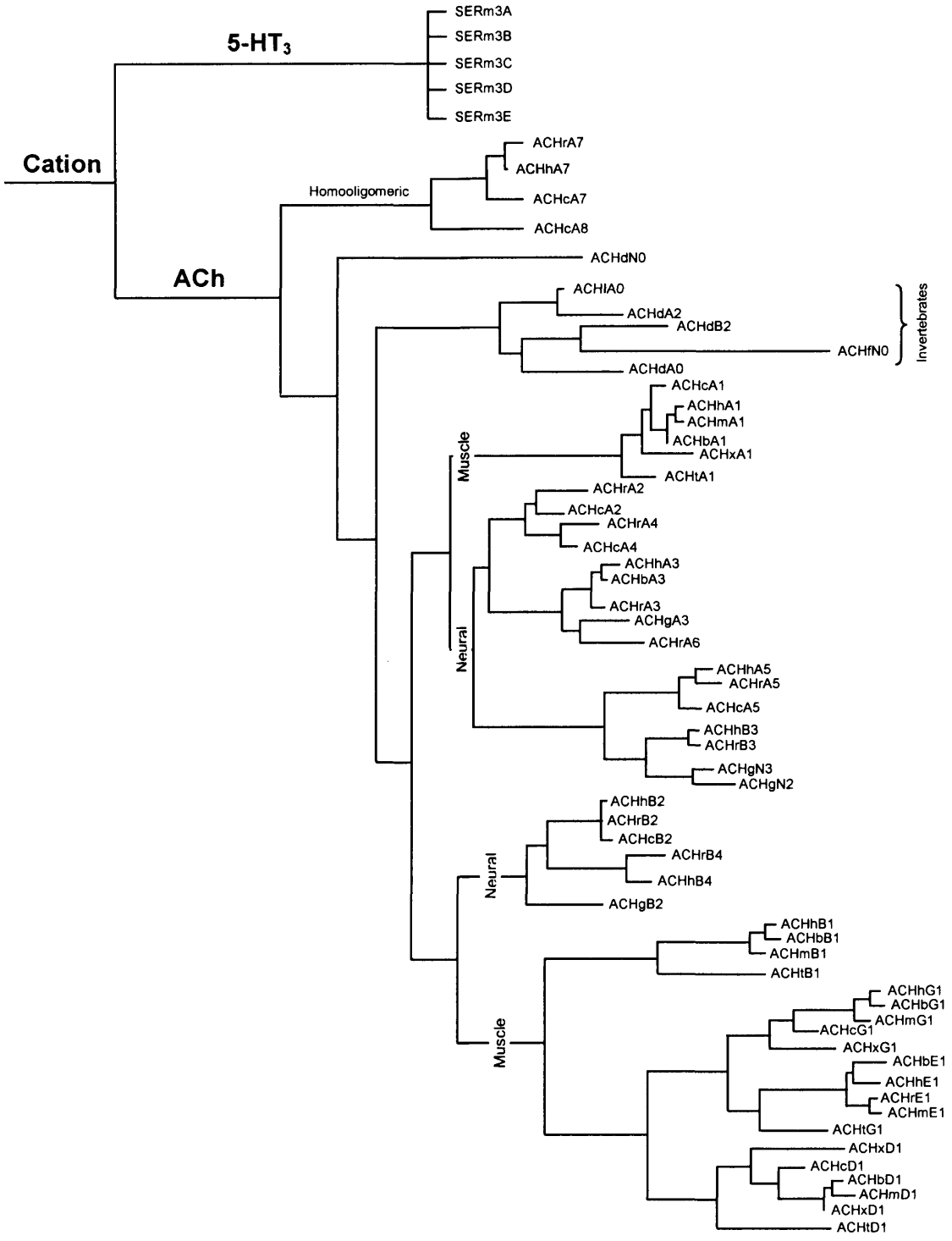

Figure 1.2 *Evolutionary tree of the ligand-gated ion channel superfamily.* Adapted from Ortells and Lunt, 1995. This evolutionary tree was constructed from the alignment of the amino acids of ligand-gated ion channels.

domain and determines the agonist specificity (Eiselé *et al.*, 1993) and contains sites for asparagine-linked glycosylation (Nomoto *et al.*, 1986; Quirk *et al.*, 2004). The large M3-M4 cytoplasmic loop shows the least sequence similarity between subunits, and contains several potential sites of phosphorylation (Huganir and Greengard, 1990; Lankiewicz *et al.*, 2000). A possible consequence of the variability of the large M3-M4 cytoplasmic loop is that intracellular interactions can be specific to certain subunits and receptors. This would allow receptors to be functionally modulated, trafficked and targeted selectively.

1.2.2 Arrangement and subunit stoichiometry: Pentameric receptors

The *Torpedo* nAChR contains four subunit proteins, α, β, γ and δ (Hucho *et al.*, 1976). These subunits form a pentameric receptor with the subunit stoichiometry of αγαδβ (Karlin *et al.*, 1983, Pedersen and Cohen, 1990). This native receptor forms dimers in the *Torpedo* membranes that are cross-linked at the δ subunits (Hamilton *et al.*, 1979; DiPaola *et al.*, 1989). The pentameric structure has been confirmed by high resolution electron microscopy (Brisson and Unwin, 1985), which showed five rod shaped subunits at 25 Å resolution, and a pentameric transmembrane region at 4Å resolution (Miyazawa *et al.*, 2003).

A soluble ACh binding protein (AChBP) has been isolated from snail glia and has 24% sequence similarity with the α7 subunit, and 20-24% sequence similarity with the other nicotinic subunits (Smit *et al.*, 2001). The AChBP forms a soluble pentameric transmitter receptor that can suppress cholinergic transmission by binding to ACh. The AChBP has been demonstrated to also bind nicotine, d-tubocurarine and α-BTX (Brejc *et al.*, 2001). The crystal structure of the AChBP has been determined at 2.7 Å and shows structural similarity to the extracellular region of the *Torpedo* nAChRs (Brejc *et al.*, 2001). This is a useful tool to predict more precisely the position of individual amino acids in the nAChRs and 5-HT_3Rs. Recently the structure of the *Torpedo* nAChR resolved at 4 Å has been refined and the structure of the AChBP was compared to that of the α subunit (Unwin, 2005).

The nAChR in murine skeletal muscle has a similar predicted topology to the *Torpedo* receptor (Sealock, 1982). Once homologous subunits (muscle α,β,γ and δ)

were cloned, sucrose gradient sedimentation showed muscle nAChR had a similar apparent molecular weight to the *Torpedo* receptor, implying that it assembled into a oligomer with five subunits. The γ subunit is only expressed at high levels in embryonic muscle or following denervation. After birth the levels of γ decrease and instead the homologous ε is expressed a high levels selectively by the muscle cell nuclei located under the neuromuscular junction. The ε subunit replaces the γ subunit within the pentamer (Mishina *et al.*, 1986).

There is evidence that neuronal nAChRs are also pentameric complexes. Expression of α4β2 receptors containing reporter mutations has been used to estimate the number of subunits in each receptor (Cooper *et al.*, 1991). This suggested that there were five subunits, and has been confirmed by metabolic labelling of methionine residues (Anand *et al.*, 1991). Elucidating which subunits make up neuronal AChRs is complex, as most cells express more that two subunits and evidence suggests that more that two subunits may co-assemble (see section 1.4). Two well studied heteromeric receptors contain α4 and β2 subunits (Boulter *et al.*, 1987, Schoepfer *et al.*, 1988) and α3 and β4 subunits (Duvoisin *et al.*, 1989; Parker *et al.*, 1998). These combinations are thought to have two α subunits and three β subunits (Cooper *et al.*, 1991; Anand *et al.*, 1991; Boorman *et al.*, 2000), although other ratios have been proposed depending on the expression ratio of the two subunits (Zwart and Vijverberg, 1998, Nelson *et al.*, 2003). Some nAChR subunits are capable of forming homomeric receptors (e.g. α7, α9; Couturier *et al.*, 1990a, Elgoyhen *et al.*, 1994) and it has been reported that homomeric α7 receptors have five binding sites for the ligand methylycaconitine (MLA) (Palma *et al.*, 1996a) implying a pentameric structure.

The 5-HT_{3A} subunit can also form homomeric receptors (Maricq *et al.*, 1991). The molecular weight of the 5-HT_3R is consistent with the receptor being made of up five of the 5-HT_{3A} subunits. This receptor has more directly been shown have a pentameric structure using electron microscopy with receptors purified from NG108-15 cells (Boess *et al.*, 1995). Although the resolution was much lower than studies on the *Torpedo* nAChR, five densities of protein can be seen around a hollow pore. The stoichiometry of the heteromeric 5-HT_3R is as yet unknown.

1.2.3 The ligand-binding domain

1.2.3.1 The nAChRs ligand-binding domain

The ligand-binding domain in *Torpedo* and muscle nAChR has been shown to be at two non-equivalent sites (Neubig *et al*, 1979, Prince and Sine, 1996), and is located between the α and non-α subunits (Pederson and Cohen, 1990, Galzi *et al.*, 1991, Taylor *et al.*,2000). The subunit pairs, αγ and αδ, form an α-BTX binding site (Kurosaki *et al.*, 1987). Residues from both the α (Kao *et al.*, 1984, Kao and Karlin, 1986, Galzi *et al.*, 1990) and the δ/γ subunits (Czajkowski *et al.*, 1993, Sine, 1993, Martin *et al.*, 1996) contribute to the binding site. Electron microscopy of the *Torpedo* nAChRs at 4 Å has demonstrated the presence of two cavities in the extracellular region that are proposed to form the ligand binding sites (Unwin, 2005).

It has been suggested that heteromeric neuronal receptors contain two α subunits and three β subunits ($\alpha_2\beta_3$) (Cooper *et al.*, 1991; Anand *et al.*, 1991; Boorman *et al.*, 2000), and would therefore be expected to contain two binding sites, similar to the muscle and *Torpedo* nAChRs. The different affinities of nicotinic ligands observed with the αδ verses αγ ligand binding sites is similar to that seen with α4β2 versus α4β4 binding sites (Parker *et al.*, 1998). Thus the diversity of neuronal nAChR subunits means that heterogeneous populations of receptors with varying affinities for agonist and antagonists, and varying functional properties, can occur within the nervous system. Homomeric nAChRs would be expected to have five ligand binding sites, with the same subunit contributing the principal and complimentary components (Corringer *et al.*, 2000). It has been reported that recovery of the homomeric α7 nAChR from MLA inhibition is best fitted with a five binding site model (Palma *et al.*, 1996). In functional experiments, the Hill coefficient in obtained for homomeric receptors (α7 or a chimeric receptor) from concentration-response curves is usually approximately 2 (Corringer *et al.*, 1995; Servent *et al.*, 1997), which implies that activation of the receptor may only require agonist binding to two sites within the receptor.

Important amino acids on the principal and complimentary components that are involved in binding nicotinic ligands have been identified on the *Torpedo* nAChR by affinity labelling and site directed mutagenesis. These have then been modelled into

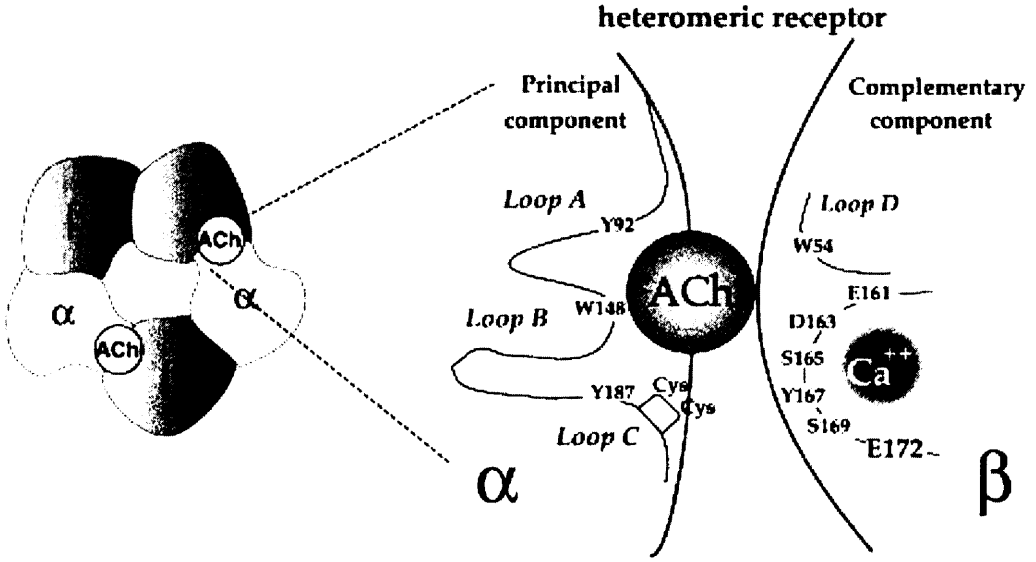

Figure 1.3 *Model of the nAChR ligand binding domain.*

The pentameric complex of subunits is shown, with two α and three β subunits around the central pore. The two binding sites are shown at two α/β interfaces. The schematic of this interface is enlarged and shows the six loops of amino acids that form the ligand binding site. The priciple component of the binding site comes from the α subunit (loops A-C) and the complimentary component from the β subunit (loops E and F). Adapted from Iter and Bertrand, 2001

six loops of amino acids (Corringer *et al.*, 2000), with loops A-C from the α subunit and loops D-F from the δ, or γ subunit (Figure 1.3). The residues on the α subunit include Trp^{86} and Tyr^{93} in loop A, Trp^{149} in loop B and Cys^{192}, Cys^{193} Tyr^{190} and Tyr^{198} in loop C (Galzi and Changeux, 1995). The residues identified in the α subunit are present in the α2, α3, α4, α6, α7 and α8 subunits. The α5 subunit lacks conserved tyrosine residues, from loops A and C (Boulter *et al.*, 1990, Couturier *et al.*, 1990b), and may actually be a structural non-α subunit (Ramirez-Latorre *et al.*, 1996, Wang *et al.*, 1996, Kuryatov *et al.*, 2000). The residues on the γ or δ subunits include Trp^{55} ad Trp^{57} in loop D, Tyr^{111} and Arg^{113} in loop E and Asp^{180} in loop F (Chiara *et al.*, 1998; Chiara *et al.*, 1999; Martin *et al.*, 1996). The residues in the D loop are conserved in β2, β4, α7 and α8 subunits (Corringer *et al.*, 2000). Mutations of residues homologous to those in the six loops show significant changes in the apparent affinity of nicotinic agonists and competitive antagonists (Corringer *et al.*, 2000).

1.2.3.2 The 5-HT_3R ligand-binding domain

The extracellular N-terminal region of the 5-HT_{3A} subunit has been demonstrated to contain the ligand-binding domain (Eiselé *et al.*, 1993). The ligand-binding domain has been proposed to be similar to that of the nAChRs, and residues important for serotonergic agonist binding have been predicted on the basis of the known structure of the AChBP (described in Section 1.2.2) (Reeves *et al.*, 2003). The residues are proposed to be organised in domains equivalent to the loops A-F of the nAChRs (Reeves and Lummis, 2002).

Site-directed mutagenesis has been performed on residues in the 5-HT_{3A} subunit predicted to be important for ligand binding (Reeves and Lummis, 2002). In loop A, mutation of Glu^{129} and Phe^{130} altered the binding characteristics of the receptor (Boess *et al.*, 1997; Steward *et al.*, 2000). Additionally mutation of Trp^{121} and Pro^{123} resulted in receptors that showed no ligand binding (Spier and Lummis, 2000; Deane and Lummis, 2001). In loop B, mutation of Trp^{183} altered the potency of agonists (Spier and Lummis, 2000). The region in 5-HT_{3A} subunit equivalent to the C loop is involved in the binding of the serotonergic agonist m-chlorophenylbiguanide (mCPBG) (Mochizuki *et al.*, 1999). In loop D, mutation of Trp^{90}, Arg^{92} and Tyr^{94}

affect ligand binding (Yan *et al.*, 1999). Finally, in loop E, Tyr^{141}, Tyr^{143} and Tyr^{153} are also involved in ligand binding. The similarity of the $5\text{-}HT_{3A}$ ligand-binding domain is illustrated by the mutation of Phe^{130} to Asn (the equivalent residue in *Torpedo* α nAChR subunit), which results in a receptor that is activated by ACh (Steward *et al.*, 2000).

1.2.4 The channel domain

1.2.4.1 The nAChR ion channel

The nAChRs are permeable to both monovalent and divalent cations (Fucile, 2004). The ion channel of the *Torpedo* nAChR is formed by amino acid residues contributed by the transmembrane domains of the α, β, γ, δ subunits (Hucho *et al.*, 1986). The importance of the M2 sequence for channel properties has been demonstrated with chimeras of bovine and *Torpedo* γ subunits, and point mutations of the residues within M2 and at each end of the channel (Imoto *et al.*, 1986, Imoto *et al.*, 1988; Leonard *et al.*, 1988). This has been confirmed by labelling with non competitive blockers such as [^{3}H]chlorpromazine, that bind inside the channel once it is opened by agonist. Labelling was detected in δ-Ser^{262} in M2 (Giraudat *et al.*, 1986), the homologous residues α-Ser^{248} and β-Ser^{254} (Hucho *et al.*, 1986), γ-Ser^{257} (Revah *et al.*, 1990), γ-Leu^{260}, β-Leu^{257}, and γ-Thr^{253} (Revah *et al.*, 1990). This contribution from each subunit forms rings of residues within the channel (Figure 1.4). The residues which are accessible to labelling by [^{3}H chlorpromazine from inside the channel provide evidence for an α-helical structure for M2 (Revah *et al.*, 1990).

In addition to these polar and non-polar rings of residues there are also three rings of negatively charged residues within M2. The *Torpedo* nAChR residues α-Asp^{238}, α-Glu^{241} and α-Glu^{262} and the equivalent residues in β,γ and δ form negatively charged rings around the lumen of the channel (Figure 1.4; Imoto *et al.*, 1988; Stroud *et al.*, 1990). These negatively charged rings are thought to attract cations and repel anions both from inside and outside the cell. These rings are know as the outer (extracellular), intermediate and inner (cytoplasmic) rings (Imoto *et al.*, 1988). Equivalent residues have been mutated in the α7 receptor and have been shown to be involved in ion channel properties. The α7 subunit can be converted into an anion

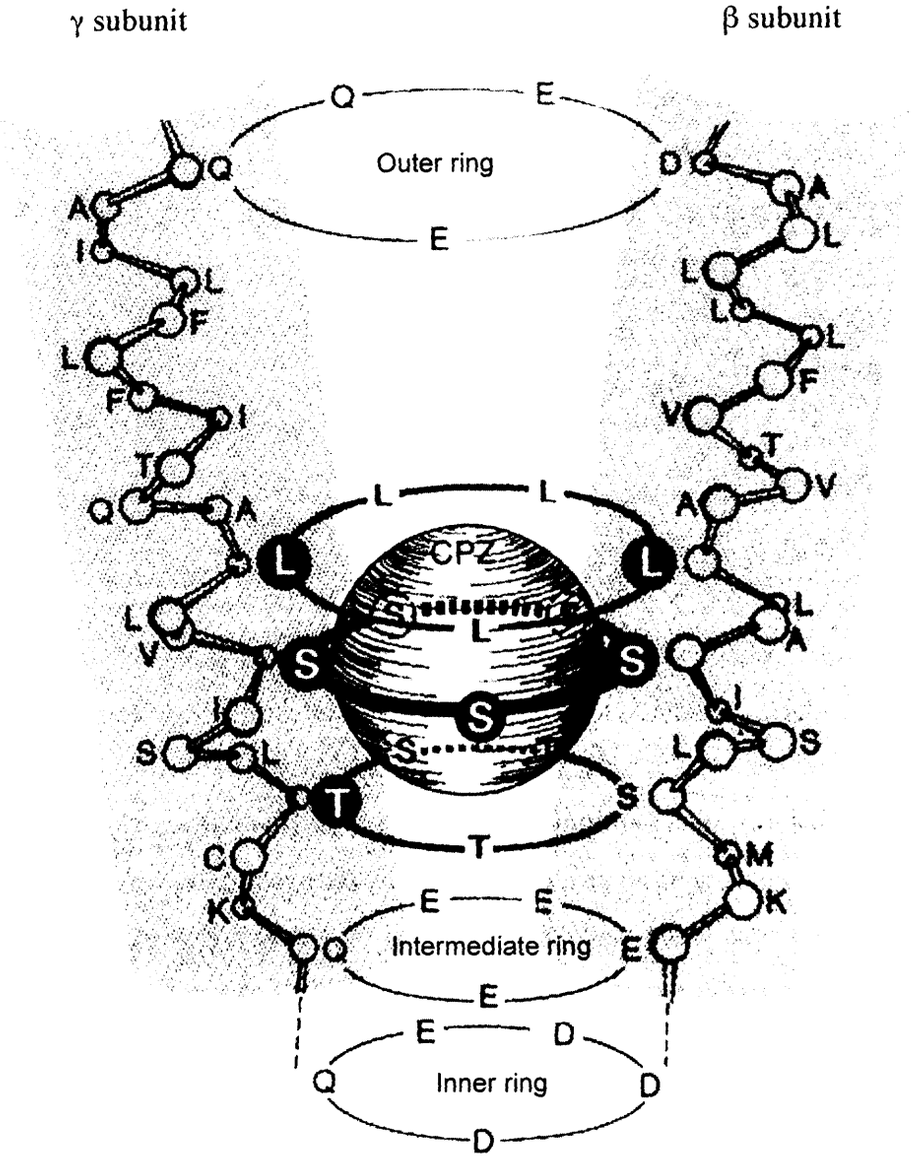

Figure 1.4 *A model of the high affinity binding site for the open channel blocker, chlorpromazine.*

The M2 amino acids of the β and γ subunits are shown in a helical conformation. The sphere labelled CPZ represents the space filled by chlorpromazine. The filled circles are amino acids labelled by [^{3}H]-CPZ, showing the rings of polar and non-polar residues in the channel. The rings of charged resides at either end of M2 (labelled inner, intermediate and outer) are also shown. Adapted from Revah *et al,* 1990.

channel with the appropriate mutations (Galzi *et al.*, 1992). The removal of a negative charge at the Glu^{237} residue abolishes the normally very high calcium permeability of α7 but does not alter the flow of monovalent cations (Bertrand *et al.*, 1993). For complete conversion to an anionic channel this negative charge must be removed and additional proline residue needs to be added between residues 234-237 (Galzi *et al.*, 1992, Corringer *et al.*, 1999). This small loop of residues has been hypothesized to be a gating region in this receptor (Corringer *et al.*, 1999).

The α7 subunit has been used extensively as a model receptor in a number of mutagenesis studies. Because the α7 subunit is able to form homomeric channels, mutagenesis of only one cDNA will alter that residue in all five subunits of the receptor. The homomeric α7 nAChR is more permeable to calcium than the muscle and *Torpedo* and most other neuronal nAChRs (review Fucile, 2004). The α7 nAChR has a calcium permeability (fractional current carried by calcium in%, P_f) of approximately 10-20 % (Fucile, 2004), which is higher than the calcium permeable NMDA receptors. Mutation of α7-Leu^{247} (homologous to *Torpedo* γ-Leu^{260}) to serine or threonine altered ion channel properties, including loss of desensitization and rectification, and the proposed addition of another conductance state (Revah *et al.*, 1991, Bertrand *et al.*, 1992). It has been suggested that the leucine ring is involved in preventing ion permeation in a desensitized state, and mutation to non-hydrophobic residues results in this state becoming conducting.

The structure of the *Torpedo* nAChR channel has been visualized with electron microscopy (Figure 1.5; Miyazawa *et al.*, 1999, Miyazawa *et al.*, 2003, Unwin, 2005). High resolution (4 Å) images indicate that M2 is α-helical, as are the other transmembrane domains. This method also revealed more about the topology of the M2 helix and how the protein forms a gate or barrier against ions when shut. The M2 helix is about 40 Å long and tilts radially inwards from the extracellular region until the middle of the membrane where it kinks at α-Leu^{251}. This is the narrowest point is at α-Leu^{251} and α-Ser^{252}, α-Val^{255} and α-Phe^{256}, which form a hydrophobic girdle around the pore that is less than 3.5 Å in diameter for about 8Å until α-Val259. This is too small for the monovalent and divalent cations to pass though and thus creates a closed gate. When the receptor is activated the proposed

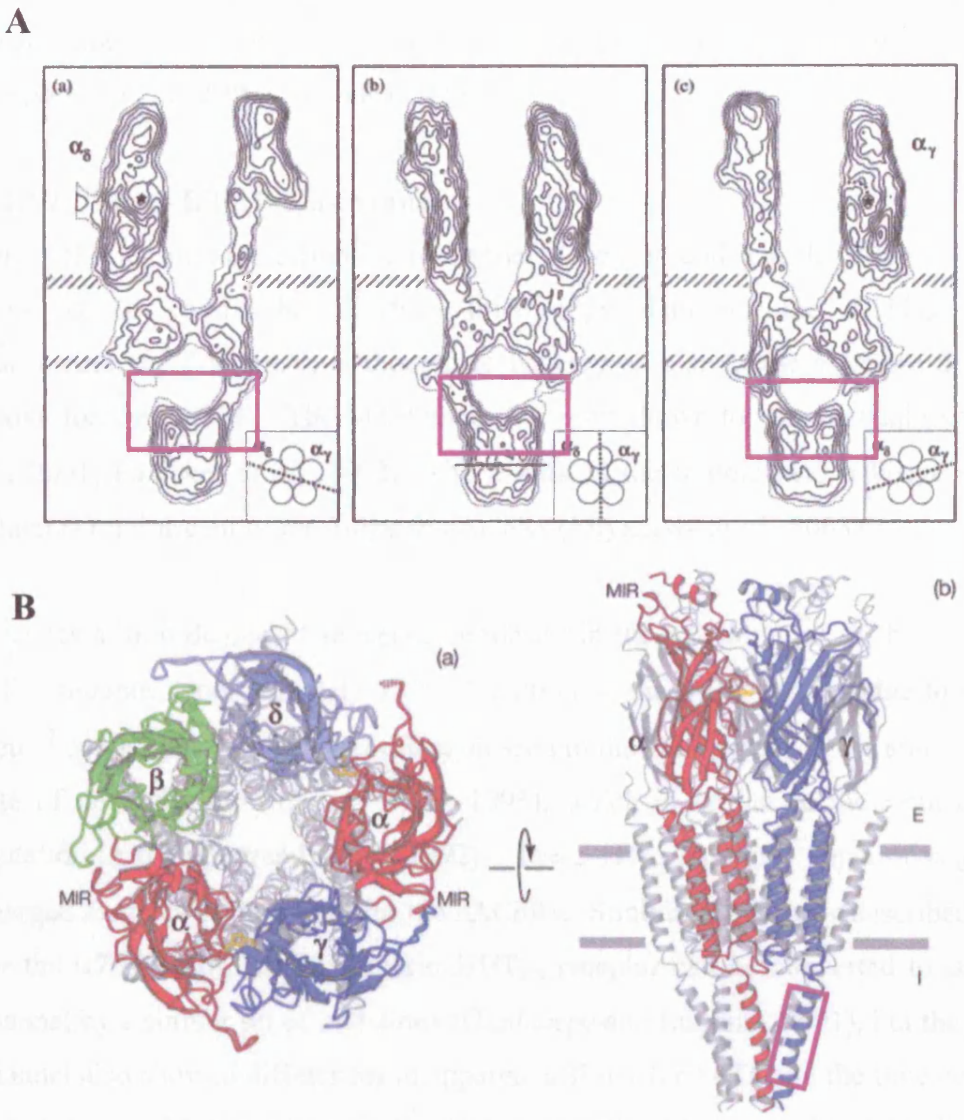

Figure 1.5 *The 3-dimensional structure of the nAChR, visualized by electron microscopy.*

(A), Three cross sections views through the *Torpedo* nAChR at 4.6 Å resolution, from Miyazawa *et al.*, 1999. (B), Ribbon diagrams of the receptor (from the amino-acid sequence fitted to the density map obtained by electron microscopy) viewed from the (a) synaptic cleft (b) the plane of the membrane. The α-Trp[149] is highlighted in yellow, and the subunits in red (α), green (β), blue (γ) and light blue (δ). The purple boxes in (A) and (B) indicate the equivalent positioning within the *Torpedo* subunits of the three arginine residues within the $5HT_{3A}$ subunit which are thought to determine the single channel conductance. E, extracellular; I, intracellular. Adapted from Unwin, 2005.

mechanism for opening the channel is a rotation of the M2 helix which causes a weakening of the hydrophobic forces in the girdle so that it comes apart, widening the pore (Unwin, 1993; Auerbach, 2003).

1.2.4.2 The 5-HT_{3A}R ion channel

The 5-HT_3Rs are also cationic ion channels (Jackson and Yakel, 1995). Although there is no comparable electron microscopy data for the 5-HT_{3A} subunit transmembrane domain, it is thought to be very similar to the structure described above for the nAChR. The M2 domain has been shown to be α-helical (Reeves *et al.*, 2001, Panicker *et al.*, 2002), with a kink in the middle near a lysine residue, which is reminiscent of the *Torpedo* nAChRs (Miyazawa *et al.*, 2003).

There is a high degree of sequence similarity in the M2 domains of the α7 and 5-HT_{3A} subunits (approximately 75%). Mutation of the equivalent residue to the α7-Leu^{247} nearly eliminated the rectification seen in the wild type receptor and slows the rate of desensitization (Yakel *et al.*, 1993), which is similar to the results of the mutation in α7 (Bertrand *et al.*, 1992). The 5-HT_{3A} has three rings of negatively charged residues as described for the nAChRs. Similar to the study described above for the α7 receptor, the homomeric 5-HT_{3A} receptor can be converted to an anion channel by a similar set of mutations (Gunthorpe and Lummis, 2001), but the mutant channel also showed differences in apparent affinity for 5-HT and the time course of the response. Mutation of only the glutamate residue to an alanine neutralized one ring of negative charge at the intracellular region of M2, and made the ion channel non-selective (Thompson and Lummis, 2003). Introduction a ring of positive charge at the extracellular end of M2 made the ion channel anion selective without largely changing other properties of the receptor (Thompson and Lummis, 2003). A mutation of an Ile^{294} in M2 decreases the calcium permeability of the 5-HT_{3A} receptor (Reeves and Lummis, 2000), which is similar to the results of a mutation in a homologous position of the α7 subunit (Bertrand *et al.*, 1993).

The heteromeric 5-HT_3R, with 5-HT_{3A} and 5-HT_{3B} subunits, has a lower calcium permeability compared to the homomeric 5-HT_{3A} receptor (Davies *et al.*, 1999b). This may be due to the lack of the rings of negatively charged residues in the M2

domain of the 5-HT_{3B} subunit (Dubin *et al.*, 1999). The heteromeric channel also has a larger single-channel conductance, however this has been attributed to residues the large cytoplasmic loop of the 5-HT_{3B} subunit rather than the ion channel (Kelley *et al.*, 2003). Three arginine residues in the intracellular loop within the amphipathic helix (Position shown in Figure 1.5), when mutated to the equivalent residues in the 5-HT_{3B} subunit, cause the homomeric receptor to have a conductance comparable to the heteromeric receptor. These arginine residues are positively charged and may act as an electrostatic barrier to positively charged ions trying to flow through the receptor on channel opening.

1.3 Folding and assembly, trafficking and targeting of nAChRs and 5-HT_3R

The ligand-gated ion channels described in the previous sections have a complex 3-dimensional structure. To produce the final receptor from a number of linear protein sequences, the subunits must fold into the correct membrane spanning topology and assemble with other subunits in the correct stoichimetry and arrangement (Green and Millar, 1995). This occurs in the endoplasmic reticulum, where the receptor also undergoes post-translational modifications before being exported to the plasma membrane.

1.3.1 Folding and assembly

Nicotinic receptors assemble slowly and inefficiently (Merlie and Lindstrom, 1983) in comparison to other transmembrane proteins. This is thought to be due to inaccurate folding of the subunit proteins, which has been monitored by the formation of ligand binding sites and conformational epitopes for monoclonal antibodies (Merlie and Lindstrom, 1983). It has been shown for the *Torpedo* subunits that correct folding requires interactions with other subunits (Paulson *et al.*, 1991). It is thought that much of the secondary structures form during synthesis of the protein, the formation of the tertiary structure occurs after subunit oligomerization (Gething and Sambrook, 1992).

1.3.1.1 Chaperone proteins and other receptor-associated proteins

Chaperone proteins are thought to be involved in the folding of nAChR subunits, and may retain misfolded subunits within the endoplasmic reticulum. The chaperones BiP (immunoglobulin binding protein) and calnexin associate with the α, β and δ subunits of muscle nAChRs and the 5-HT_3 receptor subunits (Blount and Merlie, 1991; Forsayeth *et al.*, 1992; Gelman *et al.*, 1995; Keller *et al.*, 1996; Boyd *et al.*, 2002). Co-expression of calnexin with the muscle nAChR subunits enhances assembly and surface expression of the receptor (Chang *et al.*, 1997). The chaperone protein 14-3-3η associates with the α4β2 nAChRs, and co-expression with α4β2 increases steady-state levels of the α4 subunit (Jeanclos *et al.*, 2001).

In additional to chaperones, other proteins have been demonstrated to affect surface expression of nAChR and 5-HT_3Rs. Rapsyn (43K) is involved in the clustering of muscle nAChRs (Froehner *et al.*, 1991), but not for neuronal nAChRs. Co-expression of the visinin-like protein-1 (VILIP-1) with α4β2 AChRs caused an up-regulation of the surface expression of receptors (Lin *et al.* 2002). The RIC3 (resistant to inhibitors of cholinesterase) protein interacts with both nAChR subunits and the 5-HT_{3A} subunit (Williams *et al.*, 2005; Lansdell *et al.*, 2005; Cheng *et al.*, 2005). Human RIC3 has been shown to enhance the correct folding of the α7 subunit (Williams *et al.*, 2005; Lansdell *et al.*, 2005) and also enhance the functional expression of heteromeric nAChRs (Lansdell *et al.*, 2005) and human 5-HT_{3A} receptors (Cheng *et al.*, 2005).

1.3.1.2 Post-translational modifications in folding and assembly

Both the nAChRs and the 5-HT_3R subunits have putative sites of phosphorylation and N-glycosylation, and it has been demonstrated that post-translational modifications can effect receptor expression. Examples with the nAChRs include phosphorylation of α4β2 receptors which may be involved in the up-regulation of this receptor in HEK cells by nicotine (Gopalakrishnan *et al.*, 1997), and N-glycosylation at specific sites is required to form correctly folded $\alpha_2\beta\gamma\delta$ receptors in *Xenopus* oocytes (Gehle *et al.*, 1997). Post-translational modifications also affect 5-HT_3Rs. Receptor stability is affected by the N-glycosylation sites on the 5-HT_3R subunits (Boyd *et al.*, 2002), and glycosylation at N^{109} on the 5-HT_{3A} subunit has

been demonstrated to be important for receptor assembly (Quirk *et al.*, 2004). In addition to phosphorylation and glycosylation, palmitoylation of assembling α7 receptors has a role in forming receptors able to bind α-BTX (Drisdel *et al.*, 2004).

1.3.1.3 Models of nAChR assembly

There are at present two models that describe the assembly of α, β, γ and δ subunits into the nAChR in the endoplasmic reticulum (Wanamaker *et al.*, 2003). The first model involves the association mature subunits to form the heterodimers αδ and αγ, and then the pentameric receptor including the β subunit (Blount *et al.*, 1990). This model is not consistent with results obtained with pulse-labelled subunits, and the method of solubilisation performed in experiments that support the first model may have dissociated subunit complexes (Wanamaker *et al.*, 2003).

In second model the subunits associated in the order: αβγ →αβγδ→α_2βγδ (Green and Claudio, 1993). The subunits are not folded into their mature form before association with each other. Folding events that bury a disulfide bond loop in the α subunit N-terminus occur after its association with β and γ, and once this loop is buried the trimer αβγ can bind α-BTX and also form the tetramer αβγδ (Green and Wanamaker, 1997). The same event then occurs on the β subunit, which allows the formation of the pentamer α_2βγδ. However this model is probably too simple, as it does not take into account the results that show that αβδ and αγδ are able to form α-BTX binding sites (Gu *et al.*, 1991) and that αβδ form functional channels (Kurosaki *et al.*, 1987). Thus *in vivo* is it likely to be more complex, with other subunit combinations and assembly pathways present to a greater or lesser extent. The assembly of neuronal nicotinic and 5-HT_{3A} subunits has not been well characterized. It has been shown that α7 only binds α-BTX after forming pentamers (Anand *et al.*, 1993).

1.3.1.4 Subunit combinations

It has been possible to express functional recombinant receptors with the *Torpedo*, muscle and most neuronal nAChR subunits, with the right combination of subunits. The minimum requirment for heteromeric receptors is the subunits needed to make the binding site; at least one α subunit containing the Cys^{192} and Cys^{193} residues, and

another subunit to form the complimetary component of the binding site. Despite containing the two adjacent Cys residues α5 cannot form homomeric, or heteromeric receptors with only β subunits (Boulter *et al.*, 1990; Couturier *et al.*, 1990b). The α5 subunit only forms functional receptors with other α subunit and β subunit heteromeric combination, such as α3β4 (Wang *et al.*, 1996; Gerzanich *et al.*, 1998).

In contrast to these heteromeric receptor formations, the α7 and α8 subunits form functional homomeric receptors in *Xenopus* oocytes (Couturier *et al.*, 1990a, Gerzanich *et al.*, 1994). However, they generally do not form functional receptors in a number of cell lines examined (e.g. HEK cells), despite having sufficient protein expressed (Cooper and Millar, 1997; Cooper and Millar, 1998; Sweileh *et al.*, 2000). In one case a stable HEK cell line expressing functional α7 receptors was established (Gopalakrishnan, 1995), however this is likely to be due to this isolate expressing factors that other HEK cells lack that enable the α7 subunit to form functional receptors (see Chapter 4 Section 4.1). The expression of other nicotinic subunits with α7 or α8 in HEK cells made no difference (Cooper and Millar, 1997; Cooper and Millar, 1998). The 5-HT_{3A} folds more efficiently that nAChR subunits and forms homomeric functional receptors in all the cell lines tested (Hargreaves *et al.*, 1994; Cooper and Millar, 1997; Gunthorpe *et al.*, 2000). A chimera constructed from the NH_2-terminal domain of the α7 subunit and the transmembrane and COOH-terminal of 5-HT_{3A} subunit forms functional channels when expressed in oocytes (Eiselé *et al.*, 1993). When a similar chimera was tested in the cell lines that did not express functional α7 receptors (e.g. HEK cells) they did form functional channels with the ligand binding properties of the α7 subunit (Cooper and Millar, 1997; Corringer *et al.*, 1998). It has been suggested that the α7 subunit cannot form the correct conformation in these cell lines for ligand binding (Rakhilin *et al.*, 1999). Thus it seems that there are important interactions between parts of the subunit protein beyond the extracellular N-terminus that allow the correct folding of the α7 protein.

1.3.2 Trafficking and targeting

Assembled proteins are transported from the endoplasmic reticulum to the plasma membrane. To prevent unassembled or incorrectly folded protein leaving the endoplasmic reticulum, many receptors have endoplasmic reticulum retention signals

in their amino acid sequence that are only masked when the subunit is assembled into oligomeric complexes (Ma and Jan, 2003). Endoplasmic reticulum retention signals have been identified in some nAChR subunits, for example the muscle α subunit has a PLYFXXN sequence in M1 that is involved in the retention of the subunit in the endoplasmic reticulum (Wang *et al.*, 2002). This motif is conserved in all muscle-type nAChR subunits and most neuronal subunits (α2-α6 and β2-β4). A retention motif has also been found in the 5-HT_{3B} subunit, in the first cytoplasmic loop between M1 and M2, which is sufficient to cause the retention of the 5-HT_{3A} subunit when it is transplanted into the homologous region (Boyd *et al.*, 2003). The correct folding of the α7 protein may hide a retention motif, and when it misfolds and is exposed this may cause less receptor to be transported to the cell surface (Rakhilin *et al.*, 1999).

The fact that certain ligand-gated ion channels do not reach the cell surface of a specific type of cell could be an important way of regulating the pharmacological profile of that cell. For example, as well as the α7 receptor, there have been few reports of the heteromeric α9α10 nAChR forming ligand binding sites in cells other than oocytes. The α9 subunit forms functional homomeric receptors in a murine cochlear cell line (Jaggar *et al.*, 2000). This is not surprising since these α9 and α10 are not generally found in the CNS or PNS, and one of the few sites of high levels of expression are the cochlear hair cells (Elgoyhen *et al.*, 1994; Elgoyhen *et al.*, 2001). Thus, cochlear hair cells must presumably express something that permits expression of this nAChR.

There have also been studies of subcellular targeting of nAChRs. For example, muscle nAChRs are denser at the thickened postjunctional folds of the endplate as compared to the non-thickened bottom folds, which are equivalent to the extrajunctional regions (Salpeter and Harris, 1983). There is evidence from an *in vivo* study that the long internal loop of the α3 subunit targets the receptors to specialized postsynaptic membranes (Williams *et al.*, 1998). The α7 subunit has been shown to be targeted to distal locations of the chick sciatic nerve (Roth *et al.*, 2000), and to the somato-dendritic portion of neurones in the chick nucleus semilunaris (Sorenson *et al.*, 2001). The distribution of the splice variant of the α7

nAChR subunit overlaps with that of the α7 subunit when expressed in cultured rat cortical neurones, but is also targeted to distinct areas (Severance and Cuevas, 2004). This implies that the differences in sequence allow the subunits be targeted to different regions.

1.4 Native neuronal nAChRs and 5-HT_3Rs

The distribution of nAChR and 5-HT_3R subunit mRNA and protein has been thoroughly investigated, however the subunit composition of all native receptors is as yet unknown. Some work has been done to elucidate the subunit combinations that form receptors in native cells, for example, chick ganglion neurons there are thought to be only 3 populations of receptors (Conroy and Berg, 1995).

1.4.1 Native nAChR distribution and subtypes

Ligand binding with [^{3}H]ACh and [^{125}I]α-BTX has been investigated in the brain to examine the distribution of potential neuronal nAChRs. Both these ligands bound to muscle nAChRs but showed a differential pattern of binding in the brain (Clarke *et al.*, 1985). This has been shown to be more complex than just two types of neuronal nAChRs. This is due to the number of different possible receptors that could contain five subunits from α2-α7, α9,α10 and β2-β4 (also α8 in chick).

In situ hybridisation and immunohistochemistry experiments investigated the distribution of specific subunit mRNA and protein and demonstrated the differing expression patterns of the nAChR subunits. For example the β2 subunit mRNA is widely distributed throughout the brain (Swanson *et al.*, 1987; Paterson and Nordberg 2000). In contrast the α2 subunit mRNA is only seen in the interpeduncular nucleus (Wada *et al.*, 1988). As there is considerable overlap in the expression of many of the subunit mRNA, suggesting that the proteins they encode may have the opportunity to come together to form receptors.

1.4.1.1 Subtypes of nAChRs in the Central Nervous System

The α4 and β2 subunit mRNAs and proteins are widely expressed in the central nervous system (Goldman *et al.*, 1987; Deneris *et al.*, 1988; Swanson *et al.*, 1987).

They form functional heteromeric receptors when expressed recombinantly (Boulter *et al.*, 1987; Buisson *et al.*, 1996) with high affinity to nicotine (Connolly *et al.*, 1992). Immunodepletion experiments in chick brain have shown that a large proportion of the epibatidine binding receptors contain α4 and β2 (Conroy and Berg, 1998). These two subunits probably form the primary site for high affinity nicotine binding in the central nervous system (Zoli *et al.*, 1998). Both α4 and β2 knockout mice lack high affinity [^{3}H]-nicotine binding sites (Marubio *et al.*, 1999, Picciotto *et al.*, 1995).

Additional subunits combine with the α4β2 receptor to form diverse receptors in the central nervous system. The α5 subunit has been shown to assemble with α4 subunits in the brain (Conroy *et al.*, 1992). The β3 and β4 subunits have been shown to co-assemble with α4β2 in rat cerebellum (Forsayeth and Kobrin, 1997). However, there are also nAChRs that contain no β2 subunit. When the β2 subunit is knocked out there are still high affinity [^{3}H]-epibatidine sites in the dorsocaudal medulla oblongata, pineal gland and habenula-ventral interpeduncular system, which are consistent with the pharmacology of α3β4 (Zoli *et al.*, 1998).

Radioligand binding of [^{125}I]α-BTX in the brain is thought to be due to α7 nAChRs. The localization of α7 mRNA has been shown to overlap with [^{125}I]α-BTX binding sites (Séguéla *et al.*, 1993) and α7 knockout mice lack α-BTX binding. Nicotine induced currents in rat hippocampal slices that are blocked by α-BTX and MLA are not present in the knockout mice (Orr-Urtreger *et al.*, 1997).

The radioligand [^{125}I]α-BTX also binds to the α8 subunit, however, this subunit has only been identified in chick (Schoepfer *et al.*, 1990). The α7 homomeric receptors are thought to account for 74% of α-BTX binding sites in chick brain (Keyser *et al.*, 1993) and 65-70% of α-BTX receptors in the chick optic lobe (Gotti *et al.*, 1994). The α8 homomeric nAChRs are thought to account for 9% of α-BTX binding sites in chick brain (Keyser *et al.*, 1993) and heteromeric α7α8 nAChRs account for 20-25% of the α-BTX binding sites in the chick optic lobe (Gotti *et al.*, 1994).

1.4.1.2 Subtypes of nAChRs in the Peripheral Nervous System

Little or no α4 subunit is expressed in the periphery (Rust *et al.*, 1994). In contrast, the α3 and β4 transcripts are highly expressed and thought to be the primary high affinity nicotinic receptors in the periphery (Corriveau and Berg, 1993; Mandelzys *et al.*, 1994). The α3 subunit has been shown to co-immunoprecipitate with the β4 subunit in the rat trigeminal ganglion (Flores *et al.*, 1996). Other subunits are thought to co-assemble with some α3β4, including α5 and β2 in the chick ciliary ganglion (Vernallis *et al.*, 1993; Conroy and Berg, 1995) and the rat trigeminal ganglion (Flores *et al.*, 1996). The α6 and β3 subunits were shown to assemble with α3β4 in the chick retina (Vailati *et al.*, 2000).

[^{125}I]α-BTX binding sites are seen in cultured sympathetic neurones (Patrick and Stallcup, 1977; Carbonetto *et al.*, 1978). The α7 mRNA is highly expressed in the rat superior cervical ganglion and adrenal medulla (Rust *et al.*, 1994) and chick ciliary ganglion (Corriveau and Berg, 1993). In the chick peripheral nervous system, the α7 homomeric receptors are thought to account for only 14% of α-BTX receptors in the chick retina whereas the α8 homomeric receptors account for 69% (Keyser *et al.*, 1993). The chick retina also has heteromeric α7α8 nAChRs which account for 17% of α-BTX receptors (Keyser *et al.*, 1993). Some evidence suggests that α7 may assemble with subunits other than α8. In both rat and chick there are thought to be at least three subtypes of receptor that may contain the α7 subunit, because there are distinct pharmacological subtypes that are sensitive to α-BTX and MLA (Yu and Role, 1998b, Cuevas *et al.*, 2000). Possible subunits that could assemble with α7 are β2 (Britto *et al.*, 1992) or β3 (Palma *et al.*, 1999). There is also a splice variant of the α7 subunit, that forms receptors that have different functional and pharmacological properties to the original homomeric α7 receptor (Severance *et al.*, 2004). This splice variant has been detected in the peripheral nervous system and could account for α-BTX sensitive receptors that have distinct properties to the original α7 subunit.

There is the possibility that there are more nAChR subunits to be found and cloned in some species, although this is unlikely in humans since the whole genome has been sequenced and searched for homologous sequences. In chick ciliary ganglion

there is a population of nAChRs that are sensitive to α-BTX but have not yet been shown to immunoprecipitate any known subunit (Pugh *et al.*, 1995).

1.4.1.3 The α9 and α9α10 nAChRs

Responses to ACh have been detected in cochlear hair cells (Art *et al.*, 1984), but most AChR subtypes are not expressed there (Hiel *et al.*, 1996). Only the α9 and α10 nAChR subunits are expressed in cochlear hair cells, with their expression generally restricted to the peripheral vestibular system (Elgoyhen *et al.*, 1994; Elgoyhen *et al.*, 2001), although α9 is found in the rat dorsal root ganglion neurones (Lips *et al.*, 2002). The expression pattern of α9 and α10 is not exactly the same and α9 is expressed alone in areas such as nasal epithelium (Elgoyhen *et al.*, 2001).

1.4.2 Native 5-HT_3R subtypes and distribution

The 5-HT_3R is present in the nervous system in a number of areas including cortical areas, olfactory regions, the hippocampus and the amygdala (Kilpatrick *et al.*, 1988; Marazziti *et al.*, 2001). There are two subtypes of 5-HT_3Rs in the nervous system; the homomeric 5-HT_{3A}R and the heteromeric 5-HT_3R. The 5-HT_{3A} subunit mRNA is expressed in both central and peripheral rat neurones whereas the 5-HT_{3B} subunit mRNA is mostly restricted to the peripheral nervous system (Morales and Wang, 2002). There have been reports of 5-HT_{3B} subunit protein in the hippocampus (Monk *et al.*, 2001), and also in cell lines of neuronal origin (Hanna *et al.*, 2000). Thus, there may be a mixture of homomeric and heteromeric receptors in the brain, with a larger proportion of homomeric receptors in the CNS. The mRNA of the 5-HT_{3C} is found in the adult human brain, however no 5-HT_{3D} and 5-HT_{3E} subunit mRNA has been detected in the brain (Niesler *et al.*, 2003).

1.4.3 Developmental changes in neuronal subunit expression

There are developmental changes in the expression of some of the nAChR subunits. For example, in chick ciliary ganglion there is a significant increase in the expression of the α5 subunit from embryonic day 8 (E8) to E18 (Corriveau and Berg, 1993). There also is a significant increase in the expression of α3 and α7 subunits from postnatal day 1(P1) to P14 in rat superior cervical gangion neurones (Mandelzys *et al.*, 1994).

1.5 Functional expression of recombinant nAChRs and 5-HT_3Rs

The *Torpedo* nAChR was the first ion channel to be expressed in a heterologous system (Barnard *et al.*, 1982). Since then, functional expression has been used to examine the pharmacological and functional properties of all the ligand-gated ion channels in a variety of expression systems. *Xenopus* oocytes have been used extensively as a model system to express recombinant DNA, and receptor properties have been studied using two electrode voltage clamp and patch-clamp recording. Many mammalian cell lines have also been used to express receptor subunits, as they are more representative of the conditions the native protein encounters. Both patch-clamp recording and calcium-influx assays have been used to examine functional characteristics. It is important to note that there is variability in functional characteristics of the same receptor depending on the cell type it is expressed in, the experimental conditions used and the system used to examine function. For example, there have been differences noted in functional characteristics of receptors expressed in *Xenopus* oocytes compared to mammalian cells, such as the single-channel conductance of α7 and α3β4 nAChRs (Lewis *et al.*, 1997; Section 1.5.3). Differences are also observed between patch-clamping and calcium-influx assays. When the human 5-HT_{3B} subunit is co-expressed with the human 5-HT_{3A} subunit in HEK cells, the EC_{50} for 5-HT is ten fold greater when 5-HT responses were recorded using patch-clamp experiments compared with a calcium-influx assay (see Section 1.5.1). This could be due to calcium influx assays being more sensitive, or that the response to calcium has a different EC_{50} to the whole cell responses observed.

1.5.1 Agonist potency and efficacy

Agonists to the nAChRs include ACh, nicotine, 1,1-dimethyl-4-phenylpiperazinium (DMPP), cytosine, epibatidine, and choline. These have varying binding affinites, potencies and efficacies on different nAChR subtypes such as those listed in Section 1.4. There are also differences between the same receptor subtype in different species, for example DMPP has a much lower efficacy of 3% on chick α7 compared to 78% on rat α7 (Vazquez and Oswald, 1999).

Choline is a product of the break down of ACh, and is known to have low potency at heteromeric receptors such that the physiological concentrations would be

ineffective. However, it has been shown that choline has a much higher potency at the α7 receptor (Alkondon *et al.*, 1997) which allows α7 nAChRs to be activated at physiological concentrations. This could allow a paracrine method of nAChRs activation, and suggests a physiological role for α7 nAChRs in places where there are no cholinergic inputs. Nicotine is more potent at α4β2 receptors than other subtypes. The EC_{50} values range from 0.8 μM (chick, Ramirez-Latorre *et al.*, 1996) to 15 μM (rat, Fenster 1997) compared to 106 μM for human α3β4 (Gerzanich *et al.*, 1998).

The agonists of 5-HT_3Rs include (in rank order of potency for murine 5-HT_{3A}) mCPBG > 5-HT > 2-Me-5-HT > PBG (Hope *et al.*, 1993; Mair *et al.*, 1998). As with nAChRs there are some species differences, for example 2-Me5-HT only has a efficacy of 9.1% in murine 5-HT_{3A} as compared to 87% in human 5-HT_{3A} (Hope *et al.*, 1993; Belelli *et al.*, 1995). The new diversity of the 5-HT_3R subunits introduces potential control over the function of the 5-HT_3R. With the addition of the 5-HT_{3B} subunit the heteromeric receptor has different apparent affinities for agonists. For example, both 5-HT and 2-Me-5-HT become less potent agonists, but mCPBG and 1-PBG become more potent agonists with heteromeric receptors expressed in *Xenopus* oocytes (Davies *et al.*, 1999b; Dubin *et al.*, 1999), and a mammalian cell line (Stewart *et al.*, 2003). There was no difference seen in efficacies at the homomeric and heteromeric receptors (Dubin *et al.*, 1999). There are also small differences between splice variants of the 5-HT_{3A} subunit. For example, the potency and efficacy of mCPBG is greater at the short compared to the long splice variant of the murine 5-HT_{3A} subunit (Niemeyer and Lummis, 1998).

1.5.2 Antagonist potency

There are antagonists that show a much higher potency for certain receptor subtypes, thus allowing selective antagonism. The α7 and α8 nAChRs are antagonised by low concentrations of α-BTX and MLA (Couturier *et al.*, 1990a; Palma *et al.*, 1996a; Gerzanich *et al.*, 1994; Gotti *et al.*, 1994). The toxin α-conotoxin MII is a selective antagonist for α3β2 nAChRs (Cartier *et al.*, 1996). In comparison d-tubocurarine is regarded as a typical competitive antagonist at all the nicotinic receptors. Although d-tubocurarine acts as an competitive antagonist at the muscle nAChR, it has been

demonstrated to open nACh channels in rat myotubes (Trautmann, 1982), thus it may be viewed as a very bad agonist, which can occlude the binding site for more efficient agonists.

It has been reported that long-term exposure to nicotine can causes persistent inactivation of α4β2 and α7 nAChRs when expressed in oocytes (Hsu *et al.*, 1996; Olale *et al.*, 1997). This has been demonstrated for the α4β2 in a mammalian cell line (Gentry *et al.*, 2003) however other reports show no long-lasting inactivation when α4β2 or α7 were expressed in a mammalian cell line or in native cells (Kawai and Berg, 2001; Buisson and Bertrand, 2001). The α3 nAChRs are only desensitized by much higher concentrations of nicotine compared to the α4β2 receptors, and this inactivation is rapidly reversible (Olale *et al.*, 1997).

1.5.3 Rectification

Nicotinic AChRs have been observed to have strong voltage dependency or inward rectification (Forster and Bertrand, 1995). In comparison, the homomeric 5-HT_{3A} receptor does not display as great a rectification, and the heteromeric 5-$HT_{3A/3B}$ receptor shows no rectification at all (Davies *et al.*, 1999b). Mutations in the M2 region of the α7 subunit have been reported to abolish rectification (Leu ^{247}, Revah *et al.*, 1991; Glu^{237}, Forster and Bertrand, 1995).

1.5.4 Desensitization

The characteristics of desensitization vary between the nAChRs (Quick and Lester, 2002). Different subunits alter the desensitization distinctly when they are included into the nAChR. This allows a mechanism to vary the length of time the current, including calcium ions, is allowed into the cell during exposure to agonist. The amount of calcium entering the cell is very important as calcium levels control many aspects of cell function such as neurotransmitter release. The α7 and α8 receptors desensitize very quickly with time constants of a few 10s of ms, whereas the α4β2 desensitizes more slowly, with a time constant of about 1 second (Ragozzino *et al.*, 1997). In contrast to the homomeric α7 and α8 receptors, the homomeric α9 receptor desensitization is very slow and is incomplete even after long agonist applications (Elgoyhen *et al.*, 2001). When α10 forms a heteromeric receptors with

α9 the desensitization is much faster. The α7 subunit has been reported to associate with the β2 subunit and the resulting receptor has a slower rate of desensitization (Khiroug *et al.*, 2002). The splice variant of the α7 subunit recently reported forms homomeric receptors that also desensitize more slowly (Severance *et al.*, 2004).

The β4 containing nAChRs have even slower kinetics of desensitization than β2 receptors, which has been attributed to the N-terminal domain of these subunits (Bohler *et al.*, 2001). Residues in the loop B and C region of the ligand-binding domain affect the potency of ligands to desensitize the receptor (Corringer *et al.*, 1998).

The 5-HT_{3A} homomeric receptor desensitizes more slowly than most nAChRs (Ragozzino *et al.*, 1997; Gunthorpe *et al.*, 2000), but the heteromeric 5-$HT_{3A/3B}$ has a faster rate of desensitization compared to the homomeric receptor (Dubin *et al.*, 1999). Single residues have been demonstrated to be important for the characteristics of desensitization of the 5-HT_{3A} receptor including Leu^{286} in the M2 domain (Yakel *et al.*, 1993) and Ser^{248} in the M1 domain (Lobitz *et al.*, 2001).

1.5.5 Conductance

All the nAChRs have relatively large single-channel currents that can be resolved with outside-out patch-clamp recording. The conductances range from 5 to 55 pS (Papke *et al.*, 1989; Role, 1992). Some of the receptors have more than one conductance state which can be clearly seen in single-channel recordings, for example chick α4β2 (22.3±1.0 and 41.8±1.5 pS; Ragozzino *et al.*, 1997). Although the single-channel conductance should be an intrinsic characteristic of the protein there are some differences seen when comparing receptors expressed in *Xenopus* oocytes as compared to mammalian cell lines. For example chick α7 has a single-channel conductance of 45 pS in *Xenopus* oocytes, but two conductance levels are observed in mammalian cell lines and the largest measured conductance was only 32 pS (Ragozzino *et al.*, 1997).

The homomeric 5-HT_{3A} receptor has a low sub-pS single-channel conductance (Brown *et al.*, 1998) that cannot be resolved with single-channel recordings. The

single-channel conductance can be estimated by noise analysis of the current during agonist application (Traynelis and Jaramillo, 1998). In contrast to the homomeric 5-HT_{3A} receptor, the heteromeric 5-$HT_{3A/3B}$ receptor has a conductance of 16 pS (Davies *et al.*,1999b) which is comparable to the nAChRs. Adding to previous studies which attributed the characteristics of the single-channel current to the ion channel (Imoto *et al.*, 1988), it has been demonstrated that residues in the large cytoplasmic loop determine the size of the single-channel conductance of both the α7 (Chapter 3, Section 3.6.3) and the 5-HT_3R subunits (Kelley *et al.*, 2003).

1.5.6 Calcium permeability

The calcium permeability of a receptor can have important effects on the host cell. Many cellular processes are dependent on the specific levels of calcium in a closely localized area, for example modulation of neurotransmitter release at synapses, regulation of calcium sensitive ion channels or control of calcium sensitive second messenger systems. The nAChRs are permeable to both monovalent and divalent cations. Different subtypes of the nAChRs have different calcium permeabilities, with P_f values ranging from 1.5% for the α4β4 nAChR (Lax *et al.*, 2002) to 70% calculated in a murine cochlear cell line where AChRs are thought to contain the α9 subunit (Jagger *et al.*, 2000). Considering that the α9 homomeric receptor does not desensitize very rapidly (Section 1.5.7.1), depending on the receptor density, a large amount of calcium could enter the cell on ACh release. Muscle nAChR subtypes have a significant calcium permeability although generally less than most neuronal nAChRs (Fucile *et al.*, 2004). They have P_f values comparable to some neuronal subtypes, and in fact murine α1β1εδ has a greater P_f than the human α4β4 subtype mentioned above (P_f = 4.1%, Ragozzino *et al.*, 1998).

The range of calcium permeabilities of nAChRs allows them to have varied roles within the cell. Many subunit combinations have not been measured yet, but so far it seems that the heteromeric combinations α4β2, α4β4 and α3β4 have lower calcium permeability than the homomeric α7 and α9 or the α9α10 receptors (review, Fucile *et al.*, 2004). There are much more complex subunit combinations, and it has been shown that when α5 is incorporated into a number of heteromeric receptors, one of the consequences is an increase in calcium permeability (Gerzanich *et al.*, 1998). A

mutation found in some patients suffering from a rare form of epilepsy replaces a serine residue in the M2 region of the α4 subunit with phenylalanine and results in a receptor with virtually no calcium permeability (Kuryatov *et al.*, 1997). Thus calcium influx through at least the α4 containing receptors seems to be important for normal brain function.

The homomeric 5-HT_{3A} receptor was thought to be impermeable to calcium (Eiselé *et al.*, 1993) however direct visualisation of calcium influx upon agonist application indicated that there was some permeability to divalent cations (Hargreaves *et al.*, 1994; Reeves and Lummis, 2000). As discussed above, co-expression of 5-HT_{3A} and 5-HT_{3B} subunits result in a receptor with a much greater single-channel conductance. However there is evidence that the calcium permeability is drastically reduced (Stewart *et al,.* 2003), although another publication showed significant calcium influx comparable to that of the homomeric receptor (Dubin *et al.*, 1999). At present the calcium permeability of the heteromeric 5-HT_3 receptors remains uncertain.

1.5.7 Comparison of native to recombinant receptors

In many cases the characteristics of recombinant receptors are very similar to native nAChRs, but there are important differences. This implies that either the subunit combination of the recombinant receptor, or the environment of the host cell do not match that of native receptors. For example, the native *Torpedo* nAChR is in dimeric form with two receptor cross-linked at the δ subunit, but when the *Torpedo* nAChR subunits are expressed in *Xenopus* oocytes only single pentameric receptors are formed (Sumikawa *et al.*, 1981; DiPaola *et al.*, 1989). This demonstrates the differences in host cell environment can affect the biochemical properties of the receptor.

1.5.7.1 Homomeric nAChRs

The α7, α8 and α9 subunits are able to form homomeric receptors when expressed in *Xenopus* oocytes and some mammalian cell lines. However, there have been some questions as to whether these subunits form homomeric or heteromeric receptors in the brain. Neuronal α-BTX binding receptors have been proposed to be homomeric α7 receptors (Chen and Patrick, 1997; Drisdel and Green, 2000).

However, homomeric recombinant and native α7 nAChRs have been demonstrated to have similar but non-identical pharmacological properties in the chick brain. For example, native α7 receptors have a 50 fold lower affinity for cytisine compared to recombinant homomeric receptors expressed in *Xenopus* oocytes (Anand *et al.*, 1993). Also, the EC_{50} for ACh and nicotine differs between native and recombinant α7 and α8 nAChRs (Gotti *et al.*, 1994).

The different properties of native α7 nAChRs when compared to recombinant homomeric receptors may be due to the assembly of α7 with other nicotinic subunits (Virginio *et al.*, 2002). The α7 subunit has been proposed to form heteromeric receptors with the α5 subunit (Yu and Role, 1998a; Cuevas *et al.*, 2000), the β3 subunit (Palma *et al.*, 1999), the β2 subunit (Khiroug *et al.*, 2002) and the α8 subunit (Keyser *et al.*, 1993). The α5 subunit may affect the single-channel conductance of α7 nAChRs (Yu and Role, 1998a). The β2 subunit has been demonstrated to co-assemble with α7 and cause the resultant receptor to have a slower rate of desensitization (Khiroug *et al.*, 2002). Alternatively the α7 nAChRs may indeed be homomeric, but may undergo post-translational modification only in native cell lines, providing them with specific pharmacological and functional characteristics (Blumenthal *et al.*, 1997).

It has been shown that the biophysical characteristics of the α9α10 heteromeric receptor, compared to the α9 homomeric receptor, are more similar to those of some of the nAChRs found in the cochlea (Elgoyhen *et al.*, 2001). For example the rate of desensitization is much faster for some native and α9α10 receptors, compared to the homomeric α9 receptor.

1.5.7.2 Heteromeric nAChRs

A number of paired combinations of nAChR subunits have been tested in recombinant systems, but the characteristics do not account for all native nAChRs. Subsequently, three, four and even five subunit combinations have been tested (Vernallis *et al.*, 1993; Kuryatov *et al.*, 2000). The inclusion of α5 into α3β2 and α3β4 receptors has produced characteristics that are more similar to the receptors in some areas of the brain (Wang *et al.*, 1996; Gerzanich *et al.*, 1998).

1.5.7.3 Homomeric verses heteromeric 5-HT_3 receptors

The 5-HT_{3A} subunit is able to form homomeric receptors in *Xenopus* oocytes (Maricq *et al.*, 1991) and in mammalian cells lines (Hope *et al.*, 1996). However, the functional and pharmacological properties of the homomeric receptor do not match those of the native channels (Brüss *et al.*, 1999). Splice variants of the 5-HT_{3A} receptor have some functional diversity, but is not sufficient to account for the differences observed between recombinant and native receptors (Hubbard *et al.*, 2000). For example, estimates of the single-channel conductance of some of the native receptors are much larger than that of the homomeric 5-HT_{3A} (Hussy *et al.*, 1994; Gunthorpe *et al.*, 2000) and the efficacies of 2-Me5-HT and mCPBG are greater at native 5-HT_3 receptors (van Hooft *et al.*, 1997a).

Recently the 5-HT_{3B} subunit was cloned, and can form a heteromeric receptor with the 5-HT_{3A} subunit (Davies *et al.*, 1999b). The recombinant heteromeric receptor has characteristics that are more similar to native 5-HT_3 receptor, including a larger single-channel conductance (Davies *et al.*, 1999b; Dubin *et al.*, 1999; Hanna *et al.*, 2000). The 5-HT_{3B} mRNA has been shown to be present in many cell lines that express endogenous 5-HT_3 receptors (Hanna *et al.*, 2000) but it should be noted that the neuroblastoma cell line, NB41A3, contains the 5-HT_{3B} transcript but has 5-HT_3Rs with the characteristics of the homomeric receptor (Stewart *et al.*, 2003). When the 5-HT_{3B} subunit is introduced by transient transfection, the 5-HT_3 receptors expressed have the characteristics of the heteromeric receptor. Thus, it seems the NB41A3 cells may not have sufficient 5-HT_{3B} transcripts to produce the heteromeric 5-HT_3 receptor.

Three additional 5-HT_3 subunits have been cloned (Dubin *et al.*, 2002; Niesler *et al.*, 2003). The 5-HT_{3C} has also been reported to associate with the 5-HT_{3A} subunit and affect its function (Dubin *et al.*, 2002). The transcripts for the 5-HT_{3D} and 5-HT_{3E} subunits have not been shown to be present in the nervous system (Niesler *et al.*, 2003).

1.6 Function of nAChRs and 5-HT_3Rs in the central nervous system

The nAChRs have been shown to have important roles outside the central nervous system. The muscle nAChR is essential for transmission from the nerve to the muscle. The α3 subunit has been demonstrated to be essential for survival in mice, as α3 knockout mice die during the first post-natal week. This is presumably because α3 nAChRs mediate fast transmission in the autonomic nervous system (Cordero-Erausquin *et al.*, 2000). Nicotinic AChRs in the central nervous system are thought to be involved in cognitive functions such as learning and memory. Nicotine can improve memory in rats (Levin and Simon, 1998) however mice that lack the β2 subunit also have improved memory, but there is no improvement with nicotine (Jones *et al.*, 1999; Cordero-Erausquin *et al.*, 2000). This may implicate the β2-containing receptors in a dual role of inhibition memory formation, but mediating the positive effects of nicotine. The β2 and β4 subunits are also important for survival as knockout mice lacking both have retarded development and die young, (Cordero-Erausquin *et al.*, 2000). This suggests that β4 probably can substitute for β2 in places necessary for development as these problems are not seen in the β2 only knock out mice (Picciotto *et al.*, 1995).

5-HT_3 receptors have been shown to be involved in cardiac, intestinal and lung function in the body. The role of the 5-HT_3 receptors in the central nervous system is not fully understood, but they may be involved in anxiety and cognition (Barnes and Sharp, 1999). In experiments with a 5-HT_{3A} knockout mice, the lack of this subunit has an ambiguous effect upon anxiety, with differing results depending on which behavioural tests are used (Bhatnagar *et al.*, 2004a). However, mice that lack the 5-HT_{3A} subunit show less of the sex differences that are seen in tests for anxiety (Bhatnagar *et al.*, 2004b).

1.6.1 Pre and post-synaptic nAChRs

The primary role for nAChRs in the central nervous system is thought to be presynaptic modulation of neurotransmitter release resulting in regulation of synaptic transmission (Role and Berg, 1996; Wonnacott, 1997; Levin and Simon, 1998). The

modulation of release can also occur through receptors that are not in the terminal region (preterminal) and this distinction can be shown by the blockage of modulation by tetrodotoxin (Wonnacott, 1997). The modulation of release of a number of neurotransmitters have been demonstrated, including dopamine, GABA, noradrenaline and glutamate (Role and Berg, 1996; Wonnacott, 1997). For example, $\alpha4\beta2$ containing nAChRs are found on the terminals of dopamine neurones in the striatum, and modulation of dopamine release by $\beta2$ containing nAChRs has been demonstrated (Wonnacott, 1997; Wonnacott *et al.*, 2000). The population of these receptors may be heterogeneous as some may also contain either or both of $\alpha5$ and $\beta3$.

GABA synaptic transmission in the hippocampus is also modulated by nAChRs. This has been demonstrated to be due to $\alpha7$-containing nAChRs located on the hippocampal interneurones (Alkondon *et al.*, 2000). The $\alpha7$ agonist choline triggers action potentials in hippocampal interneurones, which are blocked by the $\alpha7$ selective antagonist MLA. Presynaptic nAChRs may also act as autoreceptors to modulate ACh release via a feedback mechanism. Release of ACh from the nerve terminal would activate the presynaptic nAChRs enhancing mobilisation of more ACh and thus aiding continual ACh release in situations of sustained nerve stimulation (Wonnacott, 1997).

Presynaptic nAChRs may have functions other than modulation of neurotransmitter release. The receptors could act to modulate other aspects of nerve terminal function, for example via calcium signalling. Nicotinic AChRs participate in regulating neurite outgrowth and pathfinding of growth cones (Role and Berg, 1996).

Postsynaptic nAChRs have been demonstrated to mediate fast transmission outside the central nervous system. The signal from the motor neurone to the muscle is transmitted by a homogenous population of nicotinic receptors on muscle cells. Nicotinic AChRs also mediate fast transmission at the Renshaw cell-motorneurone synapse (Dourado and Sargent, 2002), and the efferent synapses of the cochlea hair cells and within the autonomic ganglia (Role and Berg, 1996). Within the central nervous system few cases of fast nicotinic transmission have been documented,

indicating that the primary role of nAChRs in the brain may be other than fast transmission. Fast transmission has been shown in the hippocampus and visual cortex (Jones *et al.*, 1999), and possibly a few other areas (Role and Berg, 1996). Nicotinic AChRs occur in areas where there are no cholinergic projections to mediate fast transmission, and their role may instead be paracrine. This would be feasible for α7 containing receptors which are activated by physiological concentrations of choline, which is a metabolite of ACh (Alkondon *et al.*, 1997). ACh is broken down by cholinesterase too quickly to mediate paracrine transmission, but choline is removed much more slowly.

1.6.2 Pre- and post-synaptic 5-HT_3Rs

There is evidence for fast transmission which is mediated by cholinergic neurones in the amygdala (Sugita *et al.*, 1992), in hippocampal interneurones (McMahon *et al.*, 1997) and the developing visual cortex (Roerig *et al.*, 1997).). Also, postsynaptic 5-HT_3 receptors are found on GABAergic interneurones in the central nervous system (van Hooft and Vijverberg, 2000).

There is also evidence of the presence of presynaptic 5-HT_3 receptors in the CNS and they are thought to have a role in the modulation of neurotransmitter release. However, presynaptic 5-HT_3 receptor modulation of neurotransmitter release has not been decisively proved (Lambert *et al.*, 1995; van Hooft and Vijverberg, 2000). Presynaptic 5-HT_3Rs have been implicated in the modulation of release of a number of neurotransmitters including dopamine, 5-HT, GABA and cholecystokinin. 5-HT_3R mediated 5-HT release has been investigated in the amygdala: the presence of presynaptic 5-HT_3 receptors has been shown in synaptosomes from the amygdala by immunocytochemistry, and when the serotonerigic system is chemically lesioned the number of 5-HT_3R is significantly reduced. However, there has been no demonstration of 5-HT_3 receptor mediated 5-HT release in this system (van Hooft and Vijverberg, 2000). 5-HT_3R mediated 5-HT release has been shown in other brain regions but the presence of presynaptic 5-HT_3 receptor on these nerve terminals has not been confirmed.

5-HT_3 mediated dopamine release has been investigated in the nucleus acumbens. There is some evidence it occurs from *in vivo* studies but it has not been corroborated by *in vitro* experiments, and the exact location of the receptors is inconclusive (van Hooft and Vijverberg, 2000). There is conflicting evidence for 5-HT_3 mediated dompaine release in the striatum (van Hooft and Vijverberg, 2000).

Thus, the 5-HT_3 receptor has been implicated in mediating the release of a number of neurotransmitters, however the results remain ambiguous. There is little direct evidence for presynaptic 5-HT_3 receptor influence on GABA release and the results on the influence on ACh and noradrenaline release vary from inhibition, to no effect, to enhancement (van Hooft and Vijverberg, 2000).

1.6.3 Tobacco dependence

Tobacco smoking has been demonstrated to be highly addictive, and the principal addictive component is nicotine (Jones *et al.*, 1999). Both tobacco smoking and nicotine self administration in animals are associated with an increase in dopamine release in the nucleus accumbens (NAc) upon nicotine intake (Mansvelder and McGehee, 2002). These dopamine neurones are part of the mesolimbic dopaminergic pathway which is thought to be the primary area that reinforces the effects of natural rewards such as food. Drugs such as nicotine and cocaine are thought to exploit this pathway to result in an unnatural addiction (Jones *et al.*, 1999).

The principal dopaminergic projections to the nucleus accumbens come from the ventral tegmental area (VTA). The release of dopamine onto the NAc neurones is modulated by the nAChRs in the VTA rather than in the NAc (Nisell *et al.*, 1994). In the VTA there are dopamine neurones, GABAergic neurones and glutamatergic presynaptic terminals that synapse onto the dopamine neurones (Mansvelder and McGehee, 2002). The glutamatergic excitatory inputs to the dopamine neurones may originate from the prefrontal cortex, and contain α7 nAChRs (Mansvelder and McGehee, 2000). The GABAergic inhibitory inputs to the dopamine neurones originate from local interneurones, the NAcc and ventral pallidum, and these are likely to contain $\alpha4\beta2$ receptors (Mansvelder *et al.*, 2002). The excitatory and

inhibitory inputs contain different nAChRs and they respond differently to the low dose of nicotine that occurs upon smoking. This dose of nicotine has been shown to cause long term enhancement of glutamatergic transmission, due to long term potentiation and a lack of desensitization of the α7 nAChRs at this nicotine concentration (Mansvelder and McGehee, 2000). This long term potentiation of the glutamatergic synapse is aided by the activation of nAChRs (probably α4β2) on the dopamine neurone. This provides additional post synaptic activation to remove the magnesium block of the NMDA receptor and hence facilitate potentiation of excitatory transmission at these synapses. In β2 knockout mice there is no nicotine self-administration, and there is no long term activation as a result of nicotine application. This supports the idea that β2 containing nAChR activation in the postsynaptic dopamine neurone may be necessary for the induction of long term potentiation (Picciotto *et al.*, 1998).

Long term depression of GABAergic transmission occurs as the α4β2 receptors desensitize rapidly at this concentration of nicotine (Mansvelder *et al.*, 2002). As a result the dopamine neurones receive a net increase in excitatory input, which could explain the prolonged excitation of the mesolimbic dopamine system that is the result of a single application of nicotine (Mansvelder and McGehee, 2002).

The mechanism described above involves a single dose to a naïve system that has had no previous exposure to nicotine. Most smokers maintain chronic levels of nicotine. Chronic exposure to nicotine has been shown to upregulate a number of nAChRs. There is increased [^{3}H]-nicotine binding in postmortem brain tissue of smokers (Benwell *et al.*, 1988) and in mice with continuous nicotine administration (Marks *et al.*, 1992). The concentration of nicotine required to upregulate different subtypes of nAChRs differs, with only α4β2 upregulated at nicotine concentrations equivalent to the plasma concentration in smokers (Peng *et al.*, 1997; Molinari *et al.*, 1998). The number of surface α4β2 receptors are also upregulated to a greater extent than α3 or α7 containing receptors (Peng *et al.*, 1997). The concentrations of nicotine required to desensitize nAChRs also differ, as does the extent of the desensitization. The α3β2 containing receptors are much less sensitive to desensitization by nicotine than α4β2. The α3β2 receptors also are not fully

desensitized even at high nicotine concentrations, compared to the full ablation of the α4β2 responses at nM concentrations (Hsu *et al.*, 1996; Olale *et al.*, 1997). These results suggest that only α3β2 receptors would not be affected by the nicotine concentrations present in smokers.

1.6.4 Pathology

Nicotinic receptors have been implicated in a number of neurological disorders including epilepsy, Alzheimer's disease, Parkinson's disease, schizophrenia, anxiety and depression, Tourette's syndrome and Lewy-body disease (Paterson and Nordberg, 2000; Picciotto and Zoli, 2002). Some of these are discussed in more detail below.

The hypersensitivity of the gastro-intestinal tract that is thought to cause the symptoms in irritable bowel syndrome may be mediated partially through 5-HT_3 receptors (Jones and Blackburn, 2002). The 5-HT_3 receptor has not been specifically linked to neurological disorders, but antagonists to this receptor may prove useful for treatment for psychoses and anxiety (Jones and Blackburn, 2002).

1.6.4.1 Epilepsy

A number of specific mutations of nicotinic subunits have been identified in patients suffering from a rare form of epilepsy, autosomal dominant nocturnal frontal lobe epilepsy (ADNFLE) (Corcia *et al*, 2005). These mutations involve the α4 and β2 subunits. A misssense mutation in the M2 domain of the α4 subunit, at Ser^{247} that causes it to be replaced by a phenylalanine, is associated with ADNFLE (Steinlein *et al.*, 1995). When the mutant α4 subunit is expressed with β2 in *Xenopus* oocytes, the resultant α4β2 receptors desensitizes faster and recover from desensitization more slowly than with the wild type receptors (Weiland *et al.*, 1996). The mutant receptor also has a higher EC_{50}, less inward rectification, virtually no calcium permeability and loses the larger of two single-channel conductance states (Kuryatov *et al.*, 1997). The overall result is a decrease in function for this receptor. This could result in epilepsy if the receptor is part of an inhibitory circuit, for example modulating a GABA synapse. Other mutations that have been identified in α4 also cause a loss in function, whereas two mutations in the β2 subunit cause a gain of

function (Corcia *et al.*, 2005). Other loci containing other nicotinic subunits have also been linked to ADNFLE but no specific mutations have been identified (Corcia *et al.*, 2005)

1.6.4.2 Alzheimer's disease

The loss of nicotinic binding sites has been seen in a number of neurodegenerative diseases including Alzheimer's disease (Picciotto and Zoli, 2002) and anticholinesterases have been used with some success to treat this disease (Racchi *et al.*, 2004). The α4β2 nAChR has been implicated, as it is the major subtype lost in Alzheimer's disease (Paterson and Nordberg, 2000). Radioligand binding and immunoblotting in the temporal cortex show a decrease in [^{3}H]-epibatidine binding and α4 protein levels, but no difference in α3 or α7 protein levels (Martin-Ruiz *et al.*, 1999). β-Amyloid has been shown to modulate α7 activity (Pym *et al.*, 2005) and it has been reported that activation of α7 nAChRs may mediate the protective effect of nicotine against β-Amyloid induced neurotoxicity that occurs in Alzheimer's disease (Kihara *et al.*, 2001).

1.6.4.3 Parkinson's disease

Parkinson's disease is linked to the decrease in dopamine neurones in the substantial nigra, but there is also a decrease in the number of cholinergic neurones (Whitehouse *et al.*, 1983) and a loss of nAChR binding sites in the cortex (Whitehouse *et al.*, 1988). There is evidence that nicotine may have a protective effect against Parkinson's disease (Morens *et al.*, 1995; Quik and Kulak, 2002), and that the α6 subunit may be an important new drug target (Quik and Kulak, 2002).

1.6.4.4 Schizophrenia

This is a complex condition that is still not well understood. It is reported that the percentage of smokers in the schizophrenic population is much higher than normal (Paterson and Nordberg, 2000), however this may be due to patients compensating for the deficits induced by the antipsychotic drugs used for treatment (Lena and Changeux, 1998). Schizophrenia has been linked to a polymorphism at chromosome 15q14 which is the locus of the α7 gene (Paterson and Nordberg, 2000). A decrease in the expression of α7 nAChRs in the hippocampus has been reported for

schizophrenic patients (Freedman *et al.*, 2000). It has been reported that the α7 receptor mediates inhibition of the response to repeated auditory stimuli, and loss of this inhibition, through loss of the α7 receptor, may cause the sensory gating disturbances seen in schizophrenic patients (Freedman *et al.*, 2000).

1.6.4.5 Anxiety and depression

Nicotine has been reported to have an effect on both anxiety and depression, however the effects are complex as they can be anxiolytic or anxiogenic (Picciotto *et al.*, 2002). The α4β2 receptor and the α7 subunit have been implicated in anxiety through mutant mice studies and the action of specific agonists (Picciotto *et al.*, 2002). These two nAChRs have also been linked to depression through increased levels of cytosine binding in animal models and linkage studies to the α7 subunit gene (Picciotto *et al.*, 2002).

1.6.5 Therapeutic potential

The involvement of nicotinic receptors in a number of disorders (described above) place them in an important position as a potential target for drug treatments. The protective nature of smoking against disorders such as Parkinson's disease points to therapeutic potential of nicotinic agonists. Nicotine has been reported to have beneficial effects upon memory and thus could aid patients with cognitive dysfunction (Levin and Simon, 1998). Agonists to the α7 receptor could increase neuroprotection against β-Amyloid induced neurotoxicity (Geerts, 2005). Alternative nicotinic agonists could play an important role in helping patients with smoking cessation.

5-HT_3 antagonists, for example ondansetron, have revolutionised the treatment of cancer by inhibiting the emesis caused by chemotherapy and radiotherapy (Jones and Blackburn, 2002). The 5-HT_3 receptor has not been directly linked to many disorders or diseases. However 5-HT_3 antagonists have been reported to have beneficial effects in preclinical trials for psychoses, cognitive dysfunction and anxiety disorders (Barnes and Sharp, 1999; Jones and Blackburn, 2002). No benefit has been shown in clinical trials as yet.

1.7 Co-assembly and cross-pharmacology of the nAChRs and the 5-HT_3R

The co-assembly of recombinant 5-HT_{3A} and nicotinic subunits has been reported. The 5-HT_{3A} subunit has been shown to co-assemble with the α4 nicotinic subunit and form a heteromeric receptor that has increased calcium permeability in HEK cells, and a distinct sensitivity to block by the nicotinic antagonist d-tubocurarine in *Xenopus* oocytes (van Hooft *et al.*, 1998). The α4 subunit forms part of the lining of the ion channel pore in these heteromeric receptors when expressed in *Xenopus* oocytes (Kriegler *et al.*, 1999). The β2 subunit has also been reported to associate with the 5-HT_{3A} subunit, but the association with the 5-HT_{3A} subunit does not enable the α4 or β2 subunit to be detected on the surface of HEK cells (Harkness and Millar, 2001). These results are ambiguous and functional significance of the co-assembly remains unclear. A study of the porcine brain indicated that nicotinic subunits are not part of native 5-HT_3 receptors (Fletcher *et al.*, 1998), so it remains uncertain whether native α4 and 5-HT_{3A} do co-assemble and form heteromeric receptors (Nayak *et al.*, 2000). There has been no indication that the 5-HT_{3A} subunit co-assembles with other nicotinic subunits.

There is some pharmacological cross-reactivity between the nAChRs and the 5-HT_3 receptors, with opposing effect of ligands. Nicotinic agonists including ACh and nicotine act as competitive antagonists at the 5-HT_3 receptor (Gurley and Lanthorn, 1998). 5-HT has been demonstrated to antagonise α7 receptors (Palma *et al.*, 1996b) and the 5-HT_3 antagonist tropisetron is a potent and selective α7 nAChR partial agonist (Macor *et al.*, 2001). However, some ligands have been identified that act in the same way upon the α7 and 5-HT_3 receptors. PSAB-OFP is an agonist (Broad *et al.*, 2002) and 5-hydroxyindole potentiates the currents produced by agonists (van Hooft *et al.*, 1997b; Zwart *et al.*, 2002) at both these receptors.

1.8 Aim of this study

The nAChRs and the 5-HT_3Rs are widely expressed in the nervous system, and the importance of these receptors in brain function has been highlighted by the number of neurological disorders in which they are implicated. One aim of this study was to

gain a better understanding of the structural and functional properties of the α7 nAChR and the 5-HT_{3A} receptor, which show a number of similarities. Recombinant subunits were expressed in HEK cells to compare differences between the α7 and 5-HT_{3A} receptors. The 5-HT_{3A} subunit efficiently forms functional receptors, however the α7 subunit does not, so chimeras of these two subunits were constructed to investigate which domains caused this difference. The functional differences between the 5-HT_{3A} and α7 subunits were examined using the chimeras, again to identify which regions of the subunit determine these differences.

The α7 subunit is able to form functional receptors in some expression systems and recently the RIC3 protein has been shown to enable the α7 subunit to form α-BTX binding sites. Another aim of this study was to examine whether these binding sites represented functional receptors, and how RIC3 affected other receptors including the 5-HT_{3A} receptor and the α8 and α3β2 receptors. Part of the work on RIC3 in Chapter 4 has been published (Lansdell *et al.*, 2005).

CHAPTER 2
MATERIALS AND METHODS

2.1 Materials

All chemicals were obtained from BDH unless otherwise specified. All restriction enzymes with buffers were obtained from Promega unless otherwise stated. A Biofuge 13 (Heraeus Instruments) was used to centrifuge samples unless otherwise specified.

2.1.1 Original plasmid constructs

Rat α7 nAChR subunit cDNA in pcDNA1neo (Invitrogen) was obtained from Dr. Jim Patrick (Baylor College of Medicine, Houston) and excised and subcloned into the *Hind*III/*Xho*I sites of pZeoSV2(+) (Invitrogen). Human α7 and chick α8 nAChR subunit cDNAs (Peng *et al.*, 1994; Schoepfer *et al.*, 1990) were obtained from Dr Jon Lindstrom (University of Pennsylvania, PA., USA). Human α7 subunit cDNA was subcloned into pcDNA3neo (Invitrogen) in this laboratory by Dr Sandra Cooper (Cooper, 1998). Chick α8 subunit cDNA was subcloned from pBluescript SK(-) (Stratagene) and subcloned into pcDNA3neo in this laboratory by Dr Sandra Cooper (Cooper, 1998).

Murine 5-$HT_{3A(L)}$ subunit cDNA in pCDM6x1 (Maricq *et al.*, 1991) was obtained from Dr David Julius, (University of California) and subcloned into both pZeoSV2(+) and pRK5 in this laboratory by Dr Sandra Cooper (Cooper, 1998) and Dr Elizabeth Baker (Baker, 2003) respectively. Human 5-HT_{3A} in pcDM8 was obtained from Ewen Kirkness (Institute for Genomic Research, Rockville, Maryland).

The *C. elegans* RIC3 cDNA was obtained from Millet Treinin (Hebrew University, Israel) and was subcloned into pcDNA3 in this laboratory by Dr Stuart Lansdell. Human and *Drosophila* RIC3 cDNA were cloned into pcDNA3neo in this laboratory by Dr Stuart Lansdell and Dr Anne Doward (Doward, 2005).

The properties of the plasmid expression vectors used in this project are summarised in Table 2.1. All subunit cDNAs or chimeric constructs were in the expression vector pZeoSV2(+) for experiments in Chapter 3. For experiments in Chapter 4, chick α8, human α7 and all RIC3 constructs were in pcDNA3neo. Rat α3 and β2

were in pRK5. Rat α7 was in pcDNA1neo. Murine 5-HT_{3A} was in pRK5. Human 5-HT_{3A} was in pcDM8.

Table 2.1 *Summary of the plasmid expression vectors used in this study*

Expression Vector	Promotor	Inducible/ Constitutive	Poly-A Signal	Selection
pcDNA1neo	CMV	Constitutive	SV40	Kanamycin SupF* (amp/tet)
pcDNA3neo	CMV	Constitutive	Bgh	Kanamycin Ampicillin
pRK5	CMV/SP6	Constitutive	SV40	Ampicillin
pcDM8	CMV/SP6	Constitutive	SV40	SupF* (amp/tet)
pZeoSV2(+)	SV40	Constitutive	SV40	Zeocin

Abbreviations: amp – ampicillin, Bgh – bovine growth hormone, CMV – cytomegalovirus, tet – tetracycline, poly-A – polyadenylation, SV40 – Simian virus

* SupF: Plasmids with the SupF gene require growth in a bacterial strain that contains the P3 episome (MC1061; Invitrogen). The P3 episome contains ampicillin and tetracyclin selectable markers which contain amber mutations that are complemented by the SupF transfer RNA.

2.2 Subcloning techniques

2.2.1 Polymerase chain reaction (PCR)

Polymerase chain reaction amplification was performed in a peltier thermal cycler, PTC-225 (MJ Research) (PCR). Typical reactions were carried out in 30-50 µl and contained 10-200 ng of plasmid DNA, 0.05-0.5 µM forward and reverse primers (synthetic oligonucleotide primers were obtained from Genosys), 250 µM dNTPs, 1x polymerase buffer plus $MgCl_2$ (for *Taq* only) or $MgSO_4$ (for KOD only), and 2.5 U of a DNA polymerase enzyme. One of three enzymes were used, *Taq* (Promega), *Pfu* (Stratagene) or KOD (Novogen). *Taq* only has 5'to 3' exonuclease activity whereas the other two enzymes also have 3' to 5' exonuclease activity. As a consequence, *Taq* has a lower DNA synthesis fidelity and was only used for standard diagnostic PCR reactions, or to add TA overhangs onto *Pfu* or KOD PCR products.

2.2.2 Agarose gel electrophoresis

PCR products, digested plasmid DNA fragments and excised DNA inserts were separated by molecular weight by electrophoresis through a 1% agarose gel. Electrophoresis-grade agarose (Invitrogen) was dissolved in TAE buffer (Tris-acetate: 0.04 M Tris-acetate, 0.0001 M EDTA) and 0.3 μg/ml of ethidium bromide was added. DNA samples were run along-side DNA size markers either, 1 μg of *Hind*III digested Lamda (λ) DNA (Invitrogen) or PCR markers (Promega). This enabled estimation of the size of the sample DNA. Samples and markers were loaded in 1X blue/orange loading dye (Promega). DNA was visualized by means of a UV transilluminator (UVP).

When DNA was required for subsequent purification, low melting point agarose was used (Invitrogen) and DNA fragments were excised after electrophoresis using a sterile scalpel. DNA was extracted from the agarose gel using the Wizard™ DNA clean up system (Promega). The agarose gel was melted in a hot block and mixed with 1ml of Wizard™ DNA-binding resin. DNA was isolated from the resin using a Wizard™ clean up column and washed with 2 ml of 80% isopropanol. The isopropanol was removed from the column by centrifugation and evaporation. The DNA was then eluted with 50 μl of sterile pre-warmed milli-Q water and centrifuged for 1 minute at 13,000 rpm. 5 μl of this DNA was run on a diagnostic agarose gel to estimate the yield.

2.2.3 Restriction digestion of DNA

All restriction enzymes and reaction buffers were obtained from Promega unless specified otherwise. Reactions were carried out in 30 μl, containing 1-2 μg of DNA, 5-10 U of restriction enzyme in the appropriated buffer. The reaction was incubated at an appropriate temperature (typically 37°C) for 1-2 hours. For "double digests" in which the DNA was digested with two restriction enzymes requiring incompatible buffers, the first reaction was performed as above. The reaction was then made up to 100 μl in the preferred digestion buffer and incubated with the second enzyme for 1-2 hours. After plasmid DNA was digested it was run on an agarose gel along side uncut DNA to ensure that the restriction enzyme had cut the DNA as expected. For double digests of plasmid vectors, plasmid DNA was digested by each enzyme

singly with the same protocol and run along side on an agarose gel to ensure that both enzymes had cut the DNA as expected.

2.2.4 Dephosphorylation of DNA

When subcloning involving digestion with a single restriction enzyme or two enzymes that had compatible overhangs, 5' phosphate groups were removed using calf intestinal alkaline phosphatase (CIP) (Promega). This was done to prevent re-ligation of the plasmid DNA. CIP (2-3 U) was added to the restriction digest reaction. This was incubated at 37°C for 30 minutes and then another 2-3 U of CIP was added to the mixture and incubated at 37°C for a further 30 minutes.

2.2.5 DNA ligation

Ligation was carried out in a volume of 10 µl, and contained a molar ratio of vector: insert of 1:3, 0.5 U of the T4 DNA ligase (Roche) and 1x T4 DNA ligase buffer. Background re-ligated vector was determined by performing a 'control' ligation which contained no insert. Ligation reactions were incubated overnight at 14°C.

2.2.6 Competent cells for transformation

The XL1-blue strain of *Escherichia coli* (*E. coli*) bacteria (Stratagene) were prepared as follows: from a frozen glycerol stock, cells were streaked onto a Luria-Bertani (LB) agar plate and grown overnight at 37°C. A single colony was picked and used to inoculate 20ml of LB medium (10 g/l bacto-tryptone, 5 g/l Bacto-yeast extract, 10 g/l NaCl, adjusted to pH 7.0 with NaOH) and grown overnight at 37°C with shaking at 225 rpm. The culture was transferred to 500ml of SOB (20 g/l bacto^{TM}-peptone (DIFCO, Becton Dickinson), 5 g/l bacto-yeast extract, 0.5 g/l NaCl, 2.5 mM KCl, 10 mM $MgCl_2$). The culture was then incubated at 37°C with shaking at 225 rpm until the optical density measured at 550 nm was 0.5-0.55. The culture was then centrifuged at 2500 rpm (using a Beckman J2-M1 centrifuge, JA-14 rotor), for 15 minutes at 4°C. The supernatant was poured off and the cells resuspended in 20 ml of ice-cold RF1 (100 mM RbCl (Sigma), 50 mM $MnCl_2.4H_2O$ (Sigma), 30 mM potassium acetate, 10 mM $CaCl_2.2H_2O$, 15% w/v glycerol (Sigma), pH adjusted to 5.8 with 0.2 M acetic acid, filter sterilized (0.22 µM)) and incubated on ice for 15 minutes. This was then centrifuged at 2500 rpm for 9 minutes at 4°C, the

supernatant poured off and the pellet resuspended in 3.5 ml of ice-cold RF2 (10 mM RbCl, 10 mM MOPS (3-N-morpholinopropanesulphonic acid) (Sigma), 75 mM $CaCl_2.2H_2O$, 15% w/v glycerol, pH adjusted to 6.8 with 0.2 M acetic acid, filter sterilised (0.22 μM)). The cells were incubated on ice for 15 minutes. Aliquots were fast frozen in a dry ice/ethanol bath and stored at -80°C.

2.2.7 Bacterial transformation

Bacterial transformations were performed using 50 μl frozen stocks of competent *E.coli* cells prepared as described in Section 2.1.6. 1-20 ng of plasmid DNA, or 2-4 μl of ligation mixture was gently mixed with the cells in a Falcon 352005 polypropylene tube (Becton Dickinson) and incubated on ice for 30 minutes. The cells were then subjected to a heat shock at 42°C for 90 seconds and then placed on ice for 2 minutes. 500 μl of SOC (SOB with 20 mM glucose from Sigma) was added and this was incubated at 37°C with shaking at 225 rpm for 1 hour to allow expression of the antibiotic resistance gene. Aliquots of this were plated on to LB-agar plates containing inhibitory concentrations of the appropriate antibiotic (50 μg/ml ampicillin (Sigma) or 25 μg/ml Zeocin from Invitrogen).

2.2.8 Preparation of plasmid DNA

2.2.8.1 Small scale preparation of plasmid DNA by alkaline lysis extraction

LB medium (2 ml) containing the appropriate antibiotic was inoculated with a single bacterial colony. This was grown at 37°C overnight with shaking at 225 rpm. The bacterial culture was then centrifuged at 13,000 rpm for 30 seconds and the supernatant aspirated off. The cells were resuspended in 100 μl of ice-cold solution I (50 mM glucose, 25mM Tris.HCl – pH 8, 10 mM EDTA (Sigma) – pH 8) with vortexing. 200 μl of Solution II (0.2 NaOH, 1% SDS) was added and carefully mixed by inversion. 150 μl of ice cold solution III (3 M potassium acetate, glacial acetic acid) was added and mixed carefully by inversion and stored on ice for 5 minutes. This mixture was then centrifuged at 13,000 rpm for 5 minutes and the supernatant transferred to a new eppendorf. 400 μl of Phenol/chlorophorm (Amresco) (1:1) was added and mixed with vortexing to extract the protein from the sample. This was then centrifuged at 10,000 rpm for 2 minutes. The top layer of

liquid was transferred into a tube containing 800 µl of 100% ethanol, vortexed and centrifuged at 13,000 rpm for 5 minutes. The supernatant was aspirated off and the pellet washed with 70% ethanol. The remaining ethanol was evaporated off by placing the tube into a hot block for a few minutes. The DNA was then resuspended in 20 µl of MQ water containing 50 µg/ml RNAse A (Roche).

2.2.8.2 Large scale preparation of plasmid DNA

Plasmid purification kits from Qiagen (Qiagen Plasmid Maxi Kit and Qiagen HiSpeed™ plasmid Midi Kit) were used according to the manufacturers instructions. LB medium (250 ml – maxi, or 50 ml - midi) of was inoculated with a single colony or a stab from a glycerol stock and grown overnight at 37°C with shaking at 225 rpm. Cells were harvested by centrifugation at 6,000 rpm (using a Beckman J2-M1 centrifuge, JA-14 rotor) for 15 minutes at 4°C. The pellet was resuspended in ice cold buffer P1 (50mM Tris.Cl (pH 8.0), 10 mM EDTA, 100µg/ml RNAse A) by vortexing. Buffer P2 (200mM NaOH, 1% SDS) was added and mixed gently by inverting, and incubated on ice for 5 minutes. Buffer P3 (3 M potassium acetate, pH 5.5) was added and mixed gently by inverting, and incubated on ice for 10-15 minutes (room temperature for the midi kit). Different volumes of buffers were used for the two kits, 10 ml of buffers P1-3 were used for the maxi kit, and 6 ml for the midi kit.

Centrifugation was used to isolate the DNA in the maxi kit protocol. The mixture was centrifuged at 13,000 rpm (using a Beckman J2-M1 centrifuge, JA-14 rotor) for 30 minutes at 4°C. The supernatant was added to a Qiagen tip, previously equilibrated with 10 ml QBT (750mM NaCl, 50mM MOPS, 15% isopropanol, 0.15% Triton X-100). The supernatant moved through the tip by gravity flow, then the tip was washed twice with 30 ml of QC (1 M NaCl, mM MOPS, 15% isopropanol), and the DNA eluted with 15 ml of QF (1.25 M NaCl, 50 mM Tris.HCl (pH 8.5), 15% isopropanol) into a glass tube. The DNA was precipitated with 0.7 volumes of room temperature isopropanol and this was centrifuged at 10,500 rpm (using a Beckman J2-M1 centrifuge, JA-17 rotor) for 30 minutes at 4°C. The supernatant was then poured off and the pellet washed with 5 ml of room

temperature 70% ethanol, and then air-dried for 10-15 minutes. The pellet was then resuspended in 1 ml of TE buffer (10 mM Tris.Cl, 1mM EDTA, pH 8.0).

The HiSpeed midi kit (Qiagen) used filtration to isolate the DNA. The cell lysate was forced gently through a QIAfilter cartridge and into a Qiagen tip that was previously equilibrated with 4 ml QBT. When this had passed through by gravity flow the tip was washed with 20 ml of QC, and the DNA eluted with 5 ml of QF. The DNA was precipitated with 0.7 volumes of room temperature isopropanol and incubated at room temperature for 5 minutes. The precipitated DNA was then forced through a QIA precipitator with a syringe, and the QIA precipitator was washed with 2 ml of 70% ethanol. Air was then forced through repeatedly to dry the membrane of the QIA precipitator. The DNA was then eluted with 600 µl of TE buffer.

The yield of the DNA preparation was determined using ether a BIORAD SmartSpec™ 3000 spectrophotometer or a Beckman Coulter DU 800 spectrophotometer. The absorbance at 260 nm (A_{260}) and 280nm (A_{280}) was measured. The DNA concentration was determined from the absorbance measured at 260 nm. A solution containing 50 µg/ml of double-stranded DNA has an absorbance of 1 at 260 nm, calculated assuming that the mass of a nucleotide pair in DNA is 660 daltons. The purity of the DNA was determined from the value of A_{260}/A_{280}, with approximately 1.8 indicating pure DNA. The DNA preparation was also run on an agarose gel to visualize the DNA.

2.2.9 Site-directed Mutagenesis used to construct $\alpha 7^{1TM\text{-}5\text{-}HT3A}$

Site-directed mutagenesis (SDM) was performed using the QuikChange™ site-directed mutagenesis kit (Stratagene) to the manufacturers instructions. Two complimentary oligonucleotide primers (typically of length 25-45 bp) were designed, containing the desired. Oligonucleotide primers were designed so that the GC base content (%GC) was a minimum of 40%, the melting temperature (T_m) was greater than or equal to 78°C using the equation:

T_m=81.5+0.41(%GC) - 657/N -% mismatch

Where N is the primer length in bases. Primers were designed to end in G or C to ensure then ends of the primer hybridise to the template DNA. Primers were purified by polyacrylamide gel electrophoresis by the supplier (Genosys).

Site-directed mutagenesis reactions were performed in a volume of 50 µl containing 50 ng of template, 125 ng of each of the two oligonucleotides, 1 µl of dNTP mix from kit, 1x reaction buffer and 1 µl of *Pfu*Turbo DNA polymerase (2.5 U/µl). The reaction was heated to 95°C for 30 seconds and then the thermocycling reaction was performed for 12-18 cycles as follows:
95°C for 30 seconds (denaturation)
55°C for 1 minute (annealing)
68°C for 1/ minute per kilobase of plasmid length (extension).

The reaction mixture was then cooled on ice for 2 minutes and then 1 µl of the restriction enzyme *Dpn*I (10 U/µl) was added to digest the methylated, non-mutated parental template DNA. DNA was incubated with *Dpn*I at 37°C for 1 hour. Bacterial cells were then transformed with the DNA product. 1 µl of digested DNA was mixed with 50 µl of XL1-blue supercompetant *E. coli* cells in a chilled Falcon 2059 polypropylene tube (Becton Dickinson) and incubated on ice for 30 minutes. The cells were then heat shocked at 42°C for 45 seconds, put on ice for 2 minutes and then incubated in 500 µl of NZY^+ broth (10 g/l of NZ amine (casein hydrosylate enzymatic, Invitrogen), 5 g/l yeast extract, 5 g/l NaCl – pH 7.5, 12.5 ml/l of 1 M $MgCl_2$, 12.5 ml/l of $MgSO_4$ and 10 ml/l of 2 M glucose) for 1 hour with shaking at 225 rpm. 250 µl of this transformation mix was plated onto LB agar plates containing the appropriate antibiotic and incubated at 37°C overnight.

The mutation was verified by nucleotide sequencing, and in cases where mutagenesis created a novel restriction enzyme site, by restriction enzyme digestion.

2.2.10 Nucleotide sequencing

Fluorescent-based cycle sequencing was carried out using the ABI Prism® BigDye™ Terminator Cycle Sequencing Ready Reaction Kit 1.0 and 1.1 (ABI Applied Biosystems, Applera UK) according to the manufacturer's instructions. The reaction

was carried out in a volume of 20 µl and contained 200-500 ng of template DNA, 3.2 pmol of primer and 8 µl of Terminator Ready Reaction Mix (dye-labelled ddNTP terminators, unlabelled dNTPs, AmpliTaq DNA polymerase, $MgCl_2$ and buffer). The thermocycling reaction was performed for 25 cycles as follows:

96°C for 30 seconds (denaturation)

50°C for 15 seconds (annealing)

60°C for 4 minutes (extension)

DNA was precipitated by the addition of sodium acetate (2 µl, pH 5.2) and 99% ethanol (50µl) per 20µl of reaction. This was incubated on ice for 15 minutes and then centrifuged at 13,000 rpm for 15 minutes. The supernatant was aspirated off and the pellet washed in 500µl of 70% ethanol. The remaining ethanol was evaporated off by placing the tube in a hot block for a few minutes, and then resuspended in 10 µl of formamide. Samples were sequenced using an ABI Prism® 3100-*Avant* Genetic Analyzer (ABI Applied Biosystems). Fluorescent DNA fragments were run on a 50 cm capillary array using POP 6 polymer (ABI Applied Biosystems) and the data was extracted using 3100-*Avant* Data Collection Software Version 1.0 (ABI Applied Biosystems). Sequences were analysed using either SeqEd™ (ABI Applied Biosystems) or MacVector™ 7.2.2 (Accelrys).

2.3 Mammalian cell line and transfection

A subclone of the human embryonic kidney (HEK) 293 cell line, tsA201cells, were obtained from Dr William Green (University of Chicago, IL, USA). This HEK cell line stably expresses an SV40 temperature sensitive T antigen.

2.3.1 Cell culture

Human embryonic kidney tsA201 cells were cultured in Dulbecco's modified Eagle's medium (DMEM) (Gibco-Invitrogen) in a humidified incubator containing 5% CO_2 at 37°C. DMEM contains 2 mM L-GlutamaxTM (Gibco-Invitrogen), 10% heat inactivated foetal calf serum (FCS) (Sigma), 100 units/ml penicillin and 100 µg/ml streptomycin (Gibco-Invitrogen).

2.3.2 Transient transfection

Cells were transfected using the Effectene™ Transfection Kit (Qiagen) according to the manufacturer's instructions. Cells were trypsinised and re-plated the day before transfection, and then again 4-6 hours before transfection to 25-30% confluency. The cells were left for 4-6 hours to allow them to adhere to the bottom of the plate, and then media was removed to make the appropriate volume. For radioligand binding, western blotting and calcium-influx assays, 10 cm plates (Corning) were used containing 3 ml of medium. To transfect a 10 cm dish, 0.6 μg of plasmid DNA was added to 120 μl of Buffer EC in a sterile microfuge tube. 4.8 μl of Enhancer (DNA condensing enhancer solution) was added and incubated for 5 minutes. 13 μl of Effectene (non liposomal lipid formulation which coats condensed DNA with cationic lipids) was added and incubated for 10 minutes. 600 μl of growth medium was added and this mixture was dropped onto the cells making a final volume of approximately 3.7 ml. After 16 hours, 7 ml of growth medium was added.

For electrophysiological studies and enzyme-linked assays, cells were plated onto 13 mm glass cover slips (VWR international) coated with collagen (10 μg/ml) and polylysine (Sigma) (10 μg/ml) in a 3.5 cm dish (Falcon, Becton Dickinson) containing 1 ml of medium. The same procedure was used as above with 0.2 μg DNA, 1.6 μl of Enhancer, 4.3 μl of Effectene and 200μl of growth medium. Cells were used 38-48 hours after transfection.

2.4 Radioligand binding

Radioligand binding was were used to estimate the amount of expressed receptor. Binding was performed on either intact cells (to determine levels of receptor expressed on the cells surface) or permeabilised cells (to determine the level of total cellular receptor). All calculations were performed using Microsoft Excel.

2.4.1 Iodinated α-bungarotoxin ([^{125}I]α-BTX) binding

The radioligand [^{125}I]α–bungarotoxin ([^{125}I]α–BTX; specific activity 200 Ci/mmol) was purchased from Amersham. Cells were rinsed and harvested with Hanks' buffered saline solution (HBSS; 1.26 mM $CaCl_2$, 0.49 mM $MgCl_2.6H_2O$, 0.41 mM

$MgSO_4.7H_2O$, 5.33 mM KCl, 0.44 mM KH_2PO_4, 137.9 mM NaCl, 0.34 mM $Na_2HPO_4.7H_2O$, 5.56 mM D-Glucose) and split into two samples for total and whole-cell binding. For total binding, cell membranes were prepared by freeze/thawing and were resuspended in phosphate buffer containing protease inhibitors (4 μg/ml pepstatin, 8 μg/ml leupeptin, 8 μg/ml apoprotinin) and 2.5% bovine serum albumin (BSA) (Sigma). Membranes were incubated with 15 nM α–BTX radioligand (5 nM [^{125}I]α–BTX and 10 nM unlabelled α–BTX, Calbiochem) for 2 hours on ice. Non-specific [^{125}I]α–BTX binding was determined by adding 1.25 mM nicotine (Sigma) and 1.25 mM carbamylcholine-chloride (Sigma). Samples were harvested onto Whatman GF/A filters pre-soaked in 0.5% w/v polyethylene-imine (Sigma) with a Brandel cell harvester (Model M36, Semaat, UK) and assayed in a gamma counter. To assay cell-surface [^{125}I]α–BTX binding, cells were incubated and harvested at room temperature as described above for cell membranes using HBSS instead of phosphate buffer.

The values obtained using the gamma counter (counts per minute, cpm) were converted into fmol of ligand bound using the following equation:

Specific counts per minute/(E x S x 2.2 x 10^{-12})

Where the specific counts per minute is equal to the total counts minus the non-specific counts, E is the efficiency of the counter and S is the specific activity of the radioligand in Ci/mmol. This value was then converted into fmol per mg of protein or fmol per 10^6 according to the amount of protein or number of cells per assay tube (see section 2.4.3). Cells were counted using a haemocytometer.

2.4.2 Tritiated radioligand binding

The radioligand [^{3}H]GR65630 (specific activity 75 Ci/mmol) was purchased from Perkin Elmer. This radioligand is membrane permeable and was therefore used for binding to permeabilised cells. Cell membranes were prepared by freeze/thawing and were resuspended in phosphate buffer containing protease inhibitors (4 μg/ml pepstatin, 8 μg/ml leupeptin, 8 μg/ml apoprotinin). Membranes were incubated with radioligand (10 nM [^{3}H]GR65630) for 2 hours on ice. Non-specific binding of

[^{3}H]GR65630 was determined by adding 12.5 mM 5-hydroxytryptamine (5-HT) (Sigma). Samples were harvested onto Whatman GF/B filters pre-soaked in 0.5% w/v polyethylene-imine with a Brandel cell harvester, and assayed by scintillation counting. The values obtained using the scintillation counter (disintegrations per minute, dpm) were converted into fmol of ligand bound using the equation:

Specific disintegrations per minute/(S x 2.2 x 10^{-12})

Where specific disintegrations per minute is equal to the total disintegrations minus the non-specific disintegrations, and S is the specific activity of the radioligand in Ci/mmol. There is no need to include the efficiency of the counter as the scintillation counter was set to give the disintegrations per minute, which is equal to the counts per minute divided by the efficiency of the counter.

2.4.3 Protein assay and cell counting

The protein concentration of cell membrane preparations was determined using a BioRad *DC* protein assay according to the manufacturer's instructions. Typically, 20 µl of diluted sample (1/10) or bovine serum albumin (BSA) standard was added to a semi-microcuvette (Starstedt) and mixed with 100 µl of Reagent A (alkaline copper tartrate solution). 800 µl of Reagent B (a dilute Folin Reagent) was added and mixed with vortexing. This was incubated at room temperature for 15-30 minutes. Protein concentration was determined by measurement of the absorbance at 750 nm with a spectrophotometer. Samples were compared to BSA standards at concentrations of 0.1, 0.2, 0.4, 0.8, 1.0, 1.2 mg/ml.

2.5 Cell surface enzyme-linked antibody assay

The antibody pAb120 (Spier *et al.*, 1999) was used to label the extracellular N-terminal domain of the 5-HT_{3A} subunit and the 5-$HT_{3A}^{3\text{-}4Loop\text{-}\alpha7}$ chimera. The primary antibody pAb120 was used at 1/750 and the secondary antibody goat-anti-rabbit was used at 1/2000. Cells transiently transfected onto 13 mm glass cover slips, were washed with HBSS supplemented with 25 µM $MgCl_2$ and 25 µM $CaCl_2$ ($HBSS^{++}$).

Non-specific binding was blocked by incubation in $HBSS^{++}$ with 2% BSA (BLOCK). Cells were incubated with the primary antibody in BLOCK and 10% FCS for 1 hour in a humidified chamber. Cells were then washed five times in HBSS and fixed using 3% paraformaldehyde (Sigma) for 15 minutes. Cells were incubated in the secondary antibody conjugated to horseradish peroxidase (HRP) in BLOCK and 5% FCS for 1 hour in a humidified chamber. Cells were washed five times and then incubated in 750 µl of a liquid HRP substrate (3,3',5,5'-tetramethylbenzidine, Amersham) to quantify antibody binding. The density of the colour change was measured with a spectrophotometer at 655 nm

2.5.1 Total cell receptor enzyme-linked antibody assay

The assay was performed essentially as described above but with the following changes: Cells were first fixed using 3% paraformaldehyde and permeabilised with 0.1% Triton-X100, and then non-specific binding was blocked. The BLOCK solution contained 2% BSA, 10% FCS, 5% milk and 0.1% Triton-X100. 0.1% Triton-X100 was also included in the wash solution.

2.5.2 Immunofluorescent microscopy

The protocol used for immunofluorescent labelling was very similar to that described for the enzyme-linked assay (Section 2.4). Cells were transfected as described in Section 2.2.2. Rhodamine α–BTX (Molecular Probes) was used to visualize receptor localization in the cell. Cells were first fixed using 3% paraformaldehyde and permeabilised with 0.1% Triton-X100, and then non-specific binding was blocked. The BLOCK solution contained 2% BSA. The cells were incubated with 250 nM rhodamine α-BTX in BLOCK for 1-2 hours in a dark humidified chamber then washed five times with $HBSS^{++}$ and then once in water. The glass cover slips were mounted onto glass slides (BDH) in FluorSave (Calbiochem), and examined with a Zeiss Axiophot microscope using a Plan-Apochromat 100X 1.4 oil-immersion objective.

2.6 Intracellular calcium assay

Cells were re-plated into dark-walled 96-well tissue culture plates (Falcon, Becton Dickinson) 12-16 hours after transfection. The assay was performed 40-48 hours after transfection. The medium was removed from the cells which were then incubated in the membrane-permeable ratiometric calcium-sensitive dye Fluo 4 acetoxymethyl ester (1 μM) plus 0.02% Pluronic® F-127 (Sigma) in HBSS at room temperature for 1 hour. The cells were then washed 2-3 times in HBSS and then incubated in an appropriate buffer, either HBSS or high calcium (HCA). The composition of the HCA buffer is as follows: 35 mM sucrose, 75 mM $CaCl_2$, 25 mM Hepes pH 7.4). The response of the cells to agonist was then assayed using a fluorometric imaging plate reader (FLIPR) (Molecular Devices, Winnersh) (Schroeder and Heagle, 1996). Cells were excited by light of 488 nm from a 4 W argon-ion laser and the emitted fluorescence passed through a 510 to 570 nm bandpass interference filter before detection with a cooled 'charge coupled device' camera (Princeton Instruments). A range of concentrations of agonist were prepared in a separate 96-well plate (Nunclon) for each assay, such that each column had a different concentration. The agonist was added to the cells and, after the continued presence of the agonist for 2 minutes, 2 μM ionomycin (Sigma) was applied to the cells. Ionomycin permeablilsed the cell membranes and allows calcium to enter.

The data was exported and analysed using Microsoft Excel. The background level of fluorescence was calculated for each well using the average of the values and time points before agonist application. The fluorescence value at each time point was divided by the backgound level to normalise the data. Each 96-well plate had at least two rows of mock transfected cells. Data averaged from these cells were used as a negative control. To calculate the actual response of each well of transfected cells, the values at each time point of the mock transfected cells were subtracted from the values of the transfected cells at equivalent agonist concentration applications within the same 96-well plate. There were two to four rows of cells transfected with the same DNA, and the results of these were averaged.

The size of the peak of the response was plotted against the concentration of agonist used to produce concentration-response curves. The data was imported into SigmaPlot, which was then used to fit the data with the Hill equation:

$$R=R_{max} \times (A^{nH}/(A^{nH} + EC_{50}{}^{nH}))$$

Where R is the response to agonist, R max is the maximum response to agonist, A is the concentration of agonist, nH is the Hill coefficient and EC_{50} is the concentration that evokes the half maximal response.

2.7 Electrophysiological recording

HEK tsA201 cells, grown on glass cover slips coated in collagen and polylysine, were co-transfected with pEGFP-C2 (Clontech), encoding green fluorescent protein, and plasmids containing either wild type or chimeric subunit cDNA in the ratio of 1:20.

2.7.1 Whole-cell patch-clamp recording

Whole-cell recordings were performed at room temperature, 38-48 hours after transfection. All chemicals listed in this section were obtained from Sigma. Recording solution contained (in mM): 110 NaCl, 5.4 KCl, 0.8 $MgCl_2$, 1.8 $CaCl_2$, 25 glucose, 0.9 NaH_2PO_4, 44 $NaHCO_3$ equilibrated with 95% O_2 and 5% CO_2. Borosilicate glass pipettes (Harvard GC150F-7.5) of resistance 2-8 MΩ contained (in mM) 140 CsCl, 10 Hepes, 10 EGTA, 0.5 $CaCl_2$, 29.53 CsOH, pH adjusted to 7.26, osmolarity 283 mOsm/Kg H_2O. The series resistance and the whole cell capacitance were measured, and for all cells patched they were 28±0.4 MΩ and 33±3 pF respectively (n=388). For cells transfected with 5-HT_{3A} the series resistance was compensated by at least 80 %. Unless otherwise specified, the holding potential was –60 mV. Fast cell superfusion was achieved with a theta-barrelled application pipette made from 1.5 mm diameter borosilicate glass theta tubing (Harvard AH-30-0114), which was moved laterally using a stepper motor.

Agonist evoked currents were recorded using an Axopatch 200B amplifier. These were stored on magnetic or digital audio tape for subsequent analysis or digitised online at 10 kHz using WinEDR (Strathclyde Electrophysiology Software; www.strath.ac.uk/Departments/PhysPharm) after filtering and further amplification to provide a low-gain DC, 2 kHz record that was used to measure the agonist-induced mean current.

2.7.2 Antagonist block and time course of recovery

Whole-cell responses were blocked by the appropriate antagonist (Chapter 4). Antagonist was applied by exchanging the recording solution flowing through the bath for recording solution plus antagonist. The theta-barrelled application pipette was moved away from the cell to allow antagonist to wash on between agonist applications. Once a block of the responses was achieved the bath flow was changed back to recording solution alone to wash off the antagonist. The time course of recovery from block was examined for receptors that gave repeatable whole-cell responses every 10 seconds. The percentage of block of the response (as compared to the size of the response before the block) was plotted against time and the data fitted with an exponential equation:

$$C=C_{max} \times e^{-(t/\tau)}$$

Where C is the percentage block, C_{max} is the maximum block, t is the time after the antagonist was removed and τ the decay time constant for recovery from block. This allowed the estimation of the time constant, τ, of recovery.

2.7.3 Reversal potential and rectification analysis

Rectification was investigated over the voltage range from –60 to +40 mV in 10 mV steps using three 500 ms agonist applications at 10 second intervals every minute. The size of agonist responses were verified at –40 and –60 mV after the final response at +40 mV. The data points were then fitted with a polynomial equation and the reversal potential (E_{rev}) was calculated from the solved equation. The rectification was then quantified as follows:

Rectification Index=$[I_{40}/(40-E_{rev})]/[I_{-60}/(-60-E_{rev})]$

Where I_{40} is the current at +40mV, I_{-60} is the current at -60 mV.

2.7.4 Desensitization analysis

The kinetics of desensitization were analysed on 20 second agonist applications for most constructs. For rat α7 subunit, shorter (500 ms) agonist applications were used because of the rapid and complete desensitization of this receptor. Responses were inverted and fitted with single or double exponential functions:

$I=SS+I_{max} \times e^{-(t/\tau)}$ (single) or $I=SS+I_{max1} \times e^{-(t/\tau 1)} + I_{max2} \times e^{-(t/\tau 2)}$ (double)

Where I is the whole cell current, I_{max} is the peak of the whole cell current, SS is the steady state current, t is the time after the peak of the whole cell current and τ is the time constant of desensitization. The fit of a single or double exponential was fitted by eye. Thus the time constants (τ) and relative amplitude for double exponential function and the steady state desensitization were obtained. Where a double exponential fit was used, a weighted time constant was calculated by multiplying each time constant by the proportion of its' starting amplitude.

2.7.5 Conductance estimation from noise analysis

A high-gain band pass (2 Hz –2 kHz) record was recorded for variance and spectral density analysis. Both this high gain AC recording and the low gain DC recording were divided into segments of 0.82 seconds duration and edited to remove any segments with obvious artefacts.

2.7.5.1 Noise variance analysis

The relationship between the variance and the single-channel current can be derived from the binomial theorem, assuming that channels open independently from one another (Traynelis and Jaramillo, 1998). For a cell with N channels that have a single-channel current of i, the mean current (I) is equal to:

$I=iNp$

where p is the probability that the channel is open. The current variance (σ^2_I) is equal to:

$$\sigma^2_I=i^2Np(1-p)$$

When this is rearranged and N is substituted for:

$$\sigma^2_I=iI(1-p)$$

This means that when p is small (<0.1) then the variance is directly proportional to the mean current, with the single-channel current as the constant of proportion. The variance of each high gain AC segment was determined and plotted against the mean current of the equivalent low gain DC segment. This was then fitted with a straight line by linear regression and the single-channel conductance derived from the slope of the line (i), divided by the holding potential of the recording (-60mV in this case).

2.7.5.2 Noise power spectral density analysis

The relationship between the variance of the current fluctuations and the kinetics of receptor activation was examined by generating a power spectrum. The objective was to show how energy (amplitude squared per frequency) is distributed across the frequencies of the variance. A 10% cosine taper window was applied to each segment and the single-sided spectral density computed by fast Fourier transform and averaged over 16–32 logarithmically spread frequency ranges. The mean background spectrum was subtracted from the mean spectrum in the presence of the agonist to give the net agonist-induced noise spectrum. The single-channel conductance was calculated from the integration of the net power spectrum fitted with a single or the sum of two lorentzian components as judged by eye (Dempster 2001);

$$S=S_{(0)}/(1+(f/f_c)^2 \text{ (single) or } S= S_{(0)1}/(1+(f/f_{c1})^2+ S_{(0)2}/(1+(f/f_{c2})^2$$

Where S is the spectral density, $S_{(0)}$ is the asymptotic spectral density at zero frequency, f is the frequency of the variation and f_c is half power frequency. The

time constant $\tau=1/(2\pi f_c)$ is an estimate of the mean single channel open time (reviewed Traynelis and Jaramillo, 1998). For two-component spectra a weighted noise time constant was calculated from $\tau_w = \tau_1 A_1 + \tau_2 A_2$ where A_1 and A_2 are the relative areas of each Lorentzian component. The number of lorenztian equations used to fit the data does not reflect the number of conductance states. The single channel conductance, γ, was calculated from;

$$\gamma = S_{(0)} / 4I_m(V-V_{rev})$$

Where I_m is the mean current, V is the holding potential and V_{rev} is the reversal potential of the receptor.

2.8 Statistical analysis

All statistical analysis was performed on Microsoft Excel, with a minimum significance level of $p<0.05$. For most comparisons in Chapter 3 and all in Chapter 4, an F test was performed to examine whether data had the similar variances. If the variances were not significantly different a student's t-test was performed. In cases where the variances were significantly different a modified Z test was performed. For the binding data in Chapter 3 Section 3.3.2 a 1-way analysis of variance and subsequent Tukey's test was performed to determine whether any sample were significantly different.

CHAPTER 3

α7/5-HT_{3A} Subunit Chimeras

3.1 Introduction

The nAChR α7 subunit was first cloned in 1990 and, although it has been shown to generate functional homomeric receptors when expressed in *Xenopus* oocytes (Couturier *et al.*, 1990a; Campos-Caro *et al.*, 1997), considerable difficulties have been encountered in attempts to generate functional nAChRs by heterologous expression of α7 in a range of mammalian cell types (Cooper and Millar, 1997; Kassner and Berg, 1997; Rangwala *et al.*, 1997; Zhao *et al.*, 2003). In contrast, such difficulties have not been encountered in heterologous expression of homomeric 5-hydroxytryptamine (5-HT; serotonin) type 3 receptors (5-HT_3Rs). Heterologous expression of the 5-HT_{3A} subunit results in efficient formation of functional 5-HT_3Rs in all cell types which have been examined (Maricq *et al.*, 1991; Hargreaves *et al.*, 1994; Cooper and Millar, 1997; Gunthorpe *et al.*, 2000).

A subunit chimera containing the extracellular domain of the α7 subunit and the transmembrane and intracellular domains of the murine 5-HT_{3A} subunit generates high levels of functional cell-surface receptors in all cell lines tested, including cells in which α7 fails to do so, for example human embryonic kidney (HEK) cells (Eiselé *et al.*, 1993; Blumenthal *et al.*, 1997; Rangwala *et al.*, 1997; Cooper and Millar, 1998). These findings have suggested that inefficient folding, assembly or trafficking of the α7 subunit can be attributed to regions other than the N-terminal domain (transmembrane and intracellular regions). This conclusion is supported by studies conducted with chimeras of α7 and 5-HT_{3A} (Campos-Caro *et al.*, 1996; Dineley and Patrick, 2000; Valor *et al.*, 2002) and chimeras containing other nAChR subunits fused with α7 (Campos-Caro *et al.*, 1997) or with parts of the 5-HT_{3A} subunit (Cooper and Millar, 1998; Cooper *et al.*, 1999; Harkness and Millar, 2001).

In the present study a series of subunit chimeras were constructed. The aim of this project was to identify which domains of the nAChR α7 subunit and the 5-HT_{3A} subunit are important for folding, assembly or trafficking of these receptors. By heterologous expression of these chimeras in HEK tsA201 cells, domains have been identified which markedly influence folding, assembly, cell-surface expression and ion-channel conductance.

3.2 Construction of chimeras

A number of chimeric subunits (Figure 3.1) were constructed containing regions of the rat nAChR α7 subunit (Séguéla *et al.*, 1993) and the murine 5-HT_{3A} subunit (Maricq *et al.*, 1991). All constructs were verified by nucleotide sequencing.

The $\alpha7^{(V201)}$/5-HT_{3A} chimera (here referred to as $\alpha7^{V201\text{-}5\text{-}HT3A}$) has been described previously (Eiselé *et al.*, 1993; Cooper and Millar, 1998). Three further α7/5-HT_{3A} subunit chimeras ($\alpha7^{S235\text{-}5\text{-}HT3A}$, $\alpha7^{D265\text{-}5\text{-}HT3A}$ and $\alpha7^{G301\text{-}5\text{-}HT3A}$) each of which contained an N-terminal α7 domain and a C-terminal 5-HT_{3A} domain have also been described previously (Cooper, 1998).

Chimeras in which the M1 and M2 domains of α7 were replaced by the corresponding regions of the 5-HT_{3A} subunit ($\alpha7^{2TM\text{-}5\text{-}HT3A}$), and M1-M3 domains of α7 were replaced by the corresponding regions of the 5-HT_{3A} subunit ($\alpha7^{3TM\text{-}5\text{-}HT3A}$), have been described previously (Cooper, 1998). Additional subunit chimeras were constructed, details of which are in the subsequent Sections (Section 3.2.1-3.2.7).

3.2.1 $\alpha7^{1TM\text{-}5\text{-}HT3A}$

A chimera was constructed, in which the M1 domain of α7 was replaced by the corresponding region of the 5-HT_{3A} subunit ($\alpha7^{1TM\text{-}5\text{-}HT3A}$). A *Bsp*EI site was introduced into the $\alpha7^{V201\text{-}5\text{-}HT3A}$ chimeric DNA after M1 (at Ser^{235}) by amplification using PCR with olignucleotides $OL_{694(+)}$ and $OL_{695(-)}$. The resulting fragment was subcloned into a *Hind*III site (in the 5' end of the multiple cloning site) and a *Bsp*EI site (introduced by site directed mutagenesis at Ser^{235}) in α7.

Oligonucleotides used to amplify $\alpha7^{V201\text{-}5\text{-}HT3A}$ fragment:

$OL_{694(+)}$ $^{5'}$ CGA CTC ACT ATA GCG AGA CCC **AAG CTT** GCT AG $^{3'}$

*Hind*III

$OL_{695(-)}$ $^{5'}$ CTT GAA AGA GAC TCT CTC **TCC GGA** GTC CG $^{3'}$

*Bsp*EI

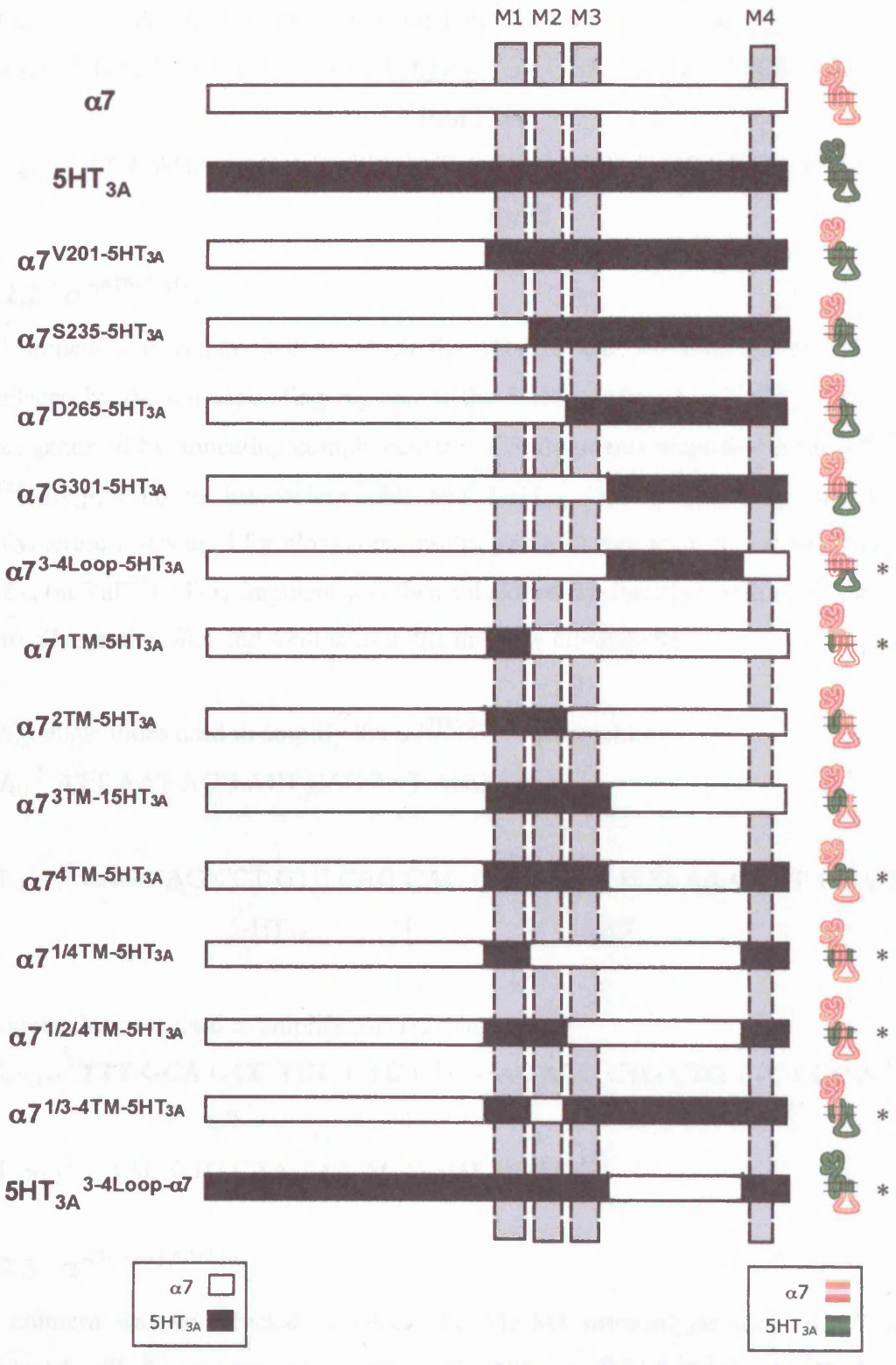

Figure 3.1 *Diagram of α7/5-HT$_{3A}$ chimeras.*

The α7 and 5-HT$_{3A}$ domains are shown are shown, see keys. The four transmembrane (M1-M4) domains are indicated by the dashed boxes. TM-transmembrane domain. Loop – M3 to M4 cytoplasmic loop. * indicates constructs prepared by the author.

Oligonucleotides used for the site directed mutagenesis of α7:

$OL_{692(+)}$ $^{5'}$ GCT GCC TGC AGA C**TC CGG A**GA GAA AAT CTC TCT TGG $^{3'}$

*Bsp*EI

$OL_{693(-)}$ $^{5'}$ CCA AGA GAG ATT TTC TC**T CCG GA**G TCT GCA GGC AGC $^{3'}$

*Bsp*EI

3.2.2 $\alpha7^{4TM\text{-}5\text{-}HT_{3A}}$

A chimera was constructed in which the M1-M3 and M4 domains of α7 were replaced by the corresponding regions of the 5-HT_{3A} subunit ($\alpha7^{4TM\text{-}5\text{-}HT3A}$). This was achieved by annealing complementary PCR fragments amplified from $\alpha7^{3TM\text{-}5\text{-}HT3A}$ (region up to just before M4) and 5-HT_{3A} (M4 to the end), and DNA polymerase I was used for elongation resulting in a change from α7 (at Val^{443}) to 5-HT_{3A} (at Val^{433}). This fragment was then subcloned by digestion with *Nhe*I and *Sal*I into pZeo at the *Nhe*I and *Xho*I sites in the multiple cloning site.

Oligonucleotides used to amplify the $\alpha7^{3TM\text{-}5\text{-}HT3A}$ fragment:

$T7_{(+)}$ $^{5'}$ ATT AAT ACG ACT CAC TAT AGG G $^{3'}$

$OL_{292(-)}$ $^{5'}$CAG CAG CCT GTC CAG **CAC GCA GGC TCG AAA CTT CCA T** $^{3'}$

5-HT_{3A} | **α7**

Oligonucleotides used to amplify 5-HT_{3A} fragment:

$OL_{291(+)}$ $^{5'}$**TTT GCA GCC TGC GTG** CTG GAC AGG CTG CTG TTC CGC A $^{3'}$

α7 | 5-HT_{3A}

$OL_{276(-)}$ $^{5'}$ - AAG CTG CAA TAA ACA AGT TGG GC $^{3'}$

3.2.3 $\alpha7^{3\text{-}4Loop\text{-}5\text{-}HT3A}$

A chimera was constructed in which the M3-M4 intracellular loop of α7 was replaced with the corresponding region of 5-HT_{3A} ($\alpha7^{3\text{-}4Loop\text{-}5\text{-}HT3A}$). An *Xba*I site was introduced into the $\alpha7^{G301\text{-}5\text{-}HT3A}$ chimeric DNA (at Leu^{419}) by amplification using PCR with oligonucleotides T7 and $OL_{509(-)}$. The resulting fragment was subcloned into a *Bam*HI site and an *Xba*I site in the multiple cloning site of pRK5 (pRK5G301*).

Oligonucleotides used to amplify $\alpha7^{G301\text{-}5\text{-}HT3A}$ fragment:

T7 - as shown above in Section 3.2.2

$OL_{509(-)}$ 5' GCA GCC TG**T CTA GA**A CGT ATC CCA C 3'

*Xba*I

An *Xba*I site was introduced into the α7 cDNA (at Val^{444}) by amplification using PCR with olignucleotides $OL_{508(+)}$ and $SP6_{(-)}$. The resulting fragment was subcloned into an *Xba*I site in pRK5G301*. As pRK5G301* was cut with a single restriction enzyme, to prevent religation the linearized plasmid was dephosphorylated by treatment with calf intestinal phosphatase (Chapter 2 Section 2.1.4).

Oligonucleotides used to amplify the α7(M4) fragment:

$OL_{508(+)}$ 5' CTG CTG **TCT AGA** CCG CTT GTG CCT 3'

*Xba*I

$SP6_{(-)}$ 5' TCT AGC ATT TAG GTG ACA CTA TAG 3'

3.2.4 $5\text{-}HT_{3A}^{3\text{-}4Loop\text{-}\alpha7}$

A chimera was constructed in which the M3-M4 loop of $5\text{-}HT_{3A}$ was replaced with the corresponding region of α7 ($5\text{-}HT_{3A}^{3\text{-}4Loop\text{-}\alpha7}$). A section of the $\alpha7^{4TM\text{-}5\text{-}HT3A}$ chimera was subcloned from an *Acc*I site at the position Val^{271} to an *Apa*I site in the 3' end of the multiple cloning site, into an *Acc*I site at Val^{286} to a *Apa*I site after the 3' end of the cDNA in $5\text{-}HT_{3A}$ subunit.

3.2.5 $\alpha7^{1/4TM\text{-}5\text{-}HT3A}$

A chimera was constructed in which the M1 and M4 domains of α7 were replaced with the corresponding regions of the $5\text{-}HT_{3A}$ subunit ($\alpha7^{1/4TM\text{-}5\text{-}HT3A}$). A *Bst*Z17I site was introduced into the $\alpha7^{1TM\text{-}5\text{-}HT3A}$ chimeric DNA (at Val^{443}) by amplification using PCR with oligonucleotides $T7_{long}$ and $OL_{745(-)}$. The resulting fragment was subcloned into an *Eco*RI site (at the 5' end of the multiple cloning site) and a

*Bst*Z17I site in the $\alpha7^{4TM\text{-}5\text{-}HT3A}$ (introduced by site directed mutagenesis at α7 Val^{443} making V443I, by Sebastian Kracun, this laboratory).

Oligonucleotides used to amplify the $\alpha7^{1TM\text{-}5\text{-}HT3A}$ fragment:

$T7_{long(+)}$ $^{5'}$ GAA ATT AAT ACG ACT CAC TAT AGG GAG $^{3'}$

$OL_{745(-)}$ $^{5'}$ CGG TCC A**GT ATA C**AG GCT GC $^{3'}$

*Bst*Z17I

Oligonucleotides used for site directed mutagenesis of $\alpha7^{4TM\text{-}5\text{-}HT3A}$

$OL_{591(+)}$ $^{5'}$GGA AGT TTG CAG CCT **GTA TAC** TGG ACA GGC TGC TGT TCC GC$^{3'}$

*Bst*Z17I

$OL_{592(-)}$ $^{5'}$GCG GAA CAG CAG CCT GTC CA**G TAT AC**A GGC TGC AAA CTT CC$^{3'}$

*Bst*Z17I

3.2.6 $\alpha7^{1/2/4TM\text{-}5\text{-}HT3A}$

A chimera was constructed in which the M1-M2 and M4 domains of α7 were replaced with the corresponding regions of the $5\text{-}HT_{3A}$ subunit ($\alpha7^{1/2/4TM\text{-}5\text{-}HT3A}$). Exactly the same method was used as described for the $\alpha7^{1/4TM\text{-}5\text{-}HT3A}$ chimera in section 3.2.5, but using a fragment of the $\alpha7^{2TM\text{-}5\text{-}HT3A}$ chimera instead of the $\alpha7^{1TM\text{-}5\text{-}HT3A}$ chimera.

3.2.7 $\alpha7^{1/3\text{-}4TM\text{-}5\text{-}HT3A}$

A chimera was constructed in which the M1 and M3-M4 domains of α7 were replaced with the corresponding regions of the $5\text{-}HT_{3A}$ subunit ($\alpha7^{1/3\text{-}4TM\text{-}5\text{-}HT3A}$). A *Kpn*I site was introduced into the $\alpha7^{1TM\text{-}5\text{-}HT3A}$ chimeric DNA between M2 and M3 (at a position equivalent to Ser^{266} in α7) by amplification using PCR with oligonucleotides $T7_{long}$ and $OL_{169(-)}$. The resulting fragment was subcloned into an *Eco*RI site (in the 5' end of the multiple cloning site) and a *Kpn*I site in the $\alpha7^{D265\text{-}5\text{-}HT3A}$ chimera (at α7 Ser^{266}).

Oligonucleotides used to amplify $\alpha7^{1TM\text{-}5\text{-}HT3A}$ fragment:

$T7_{long}$ - as shown above in section 3.2.5

$OL_{169(-)}$ $^{5'}$ GGG **GGT ACC** ATC AGA TGT TGC TGG CAT GAT CTC $^{3'}$

*Kpn*I

RESULTS

3.3 Radioligand binding to assay correctly folded receptor protein

3.3.1 The $\alpha7^{V201\text{-}5\text{-}HT3A}$ chimera

Human embryonic kidney tsA201 cells were transiently transfected with plasmid expression vectors encoding either the nAChR α7 subunit or a previously described subunit chimera, $\alpha7^{V201\text{-}5\text{-}HT3A}$ (Cooper and Millar, 1998). The subunit chimera $\alpha7^{V201\text{-}5\text{-}HT3A}$ contains the N-terminal extracellular domain of the nAChR α7 subunit together with the C-terminal (intracellular and transmembrane) domain of $5\text{-}HT_{3A}$. Radioligand binding was performed with [^{125}I]α–BTX on transfected cells (as described in Chapter 2, Section 2.4). A Student's t-test was used to test for significant differences. As has been reported previously (Eiselé *et al.*, 1993; Blumenthal *et al.*, 1997; Rangwala *et al.*, 1997; Cooper and Millar, 1998), high levels of [^{125}I]α–BTX binding were detected on the surface of cells transfected with $\alpha7^{V201\text{-}5\text{-}HT3A}$ subunit chimera (3.0±0.4 pmol/mg protein, n=12; Figure 3.2), which were significantly different from background (p<0.001) and from the levels of binding seen with cells transfected with α7 (p<0.005). High levels of [^{125}I]α–BTX binding were also detected in permeabilised cells (3.4±0.7 pmol/mg protein, n=11, significantly above background p<0.001). In contrast, no significant specific binding of [^{125}I]α–BTX was detected on the surface of cells (0.01±0.01 pmol/mg protein) or in permeabilised cells (0.01±0.01 pmol/mg protein) transfected with the α7 subunit. These findings are in agreement with previous studies (Cooper and Millar, 1997) which have demonstrated that the lack of specific [^{125}I]α–BTX binding is a consequence of an inability of the α7 subunit to assemble efficiently into an appropriately folded nAChR in this host cell environment.

These and previous findings have clearly implicated regions within the C-terminal region of the α7 subunit in inefficient assembly of functional nAChRs (Eiselé *et al.*,

1993; Blumenthal *et al.*, 1997; Rangwala *et al.*, 1997; Cooper and Millar, 1998). Similar conclusions have been made from studies conducted with similar subunit chimeras which contain the N-terminal region of other nAChR subunits (e.g. α4 and β2 subunits) fused to the C-terminal region of 5-HT_{3A} (Cooper *et al.*, 1999; Harkness & Millar, 2001).

3.3.2 Additional α7/5-HT_{3A} chimeras

With the aim of identifying more precisely subunit domains influencing nAChR folding and assembly, several further α7/5-HT_{3A} subunit chimeras were constructed as described in Section 3.1 (Figure 3.1) and the statistical significance was tested using an analysis of variance and a subsequent Tukey's test. Chimeric subunits were expressed in tsA201 cells and examined for their ability to form a high-affinity binding site for [^{125}I]α–BTX. As illustrated in Figure 3.2 and 3.3, no specific binding of [^{125}I]α–BTX was detected in cells transfected with α7/5-HT_{3A} chimeras containing an N-terminal α7 subunit domain which terminated after transmembrane region M1 ($\alpha7^{S235\text{-}5\text{-}HT3A}$), M2 ($\alpha7^{D265\text{-}5\text{-}HT3A}$), or M3 ($\alpha7^{G301\text{-}5\text{-}HT3A}$). It would appear, therefore, that α7 sequences within the region of M1 (i.e. contained in $\alpha7^{S235\text{-}5\text{-}HT3A}$ but absent in $\alpha7^{V201\text{-}5\text{-}HT3A}$) are important in regulating efficient subunit folding and assembly. A similar conclusion was made by a previous study of α7/5-HT_{3A} chimeras (Dineley and Patrick, 2000).

Additional α7/5-HT_{3A} subunit chimeras were constructed which contained the entire α7 sequence, except for selected transmembrane domains and in between transmembrane domains derived from the analogous regions of 5-HT_{3A} ($\alpha7^{1TM\text{-}5\text{-}HT3A}$, $\alpha7^{2TM\text{-}5\text{-}HT3A}$, $\alpha7^{3TM\text{-}5\text{-}HT3A}$, $\alpha7^{4TM\text{-}5\text{-}HT3A}$, Figure 3.1). Chimeras containing the M1 region of 5-HT_{3A} ($\alpha7^{1TM\text{-}5\text{-}HT3A}$), M1 and M2 plus M1-M2 intracellular loop of 5-HT_{3A} ($\alpha7^{2TM\text{-}5\text{-}HT3A}$) or the M1, M2 and M3 plus the M1-M2 intracellular and M2-M3 extracellular regions ($\alpha7^{3TM\text{-}5\text{-}HT3A}$) showed little or no specific [^{125}I]α–BTX binding on the cell surface or within the cell (Figure 3.2). Replacement of the M1 domain of α7 alone with the analogous region of 5-HT_{3A} is, therefore, not sufficient to permit efficient folding of α7. Expression of a chimera ($\alpha7^{4TM\text{-}5\text{-}HT3A}$), which contained all four of the predicted transmembrane domains and the M1-M2 and M2-M3 regions from 5-HT_{3A}, but containing the N-terminal and the large M3-M4

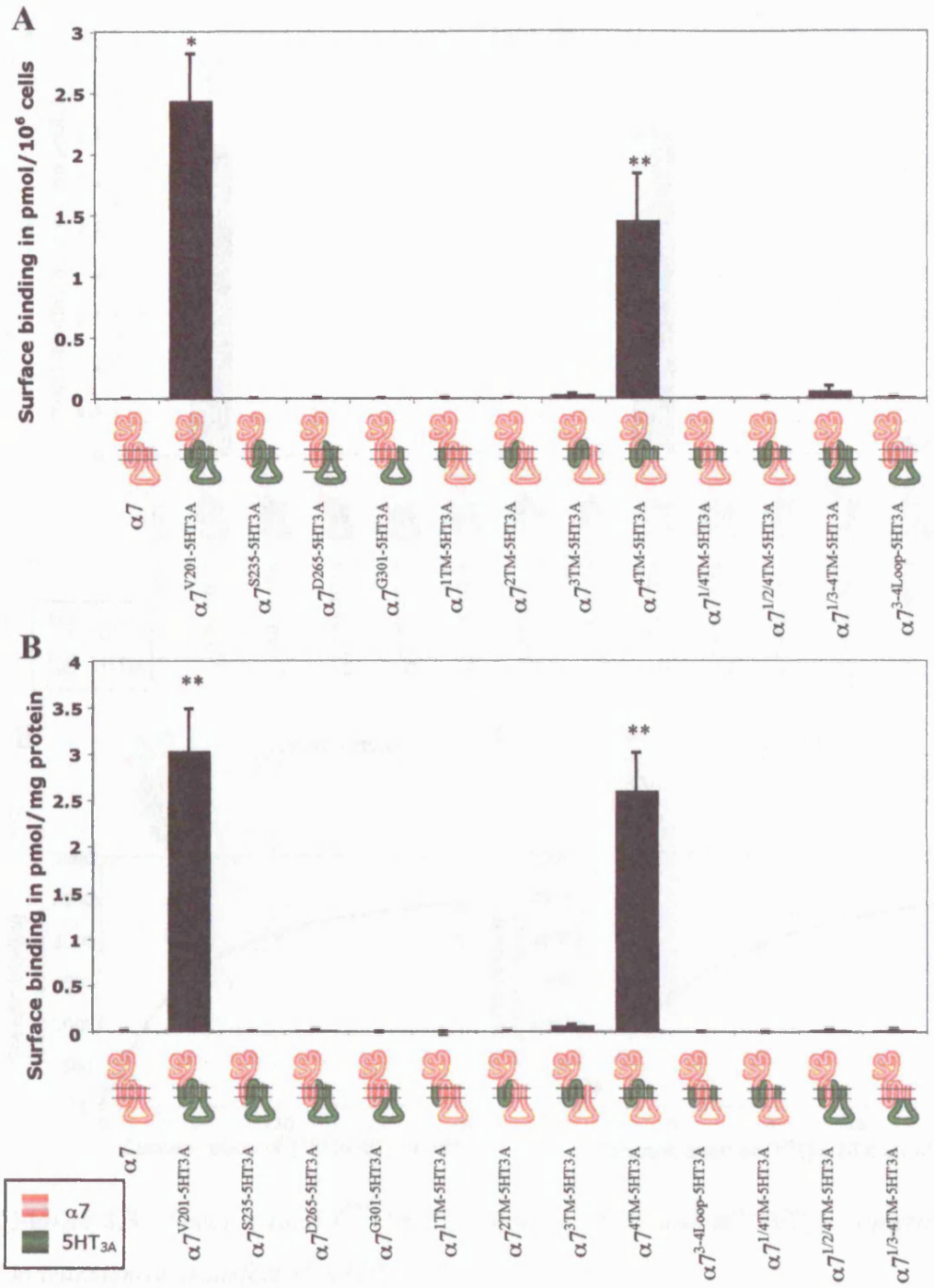

Figure 3.2 *Specific surface [^{125}I]α-BTX binding of α7 and α7/5-HT$_{3A}$ chimeras in transiently transfected tsA201 cells.*

Cells were counted and protein was assayed for each experiment to give (A), specific binding in pmol per 10^6 cells and (B), specific binding in pmol per mg of protein. n=6-12. The results were tested for significant differences using an analysis of variance and a subsequent Tukey's test. * $p<0.05$ and ** $p<0.01$ when compared to all other samples except $\alpha7^{V201\text{-}5HT3A}$ and $\alpha7^{4TM\text{-}5HT3A}$

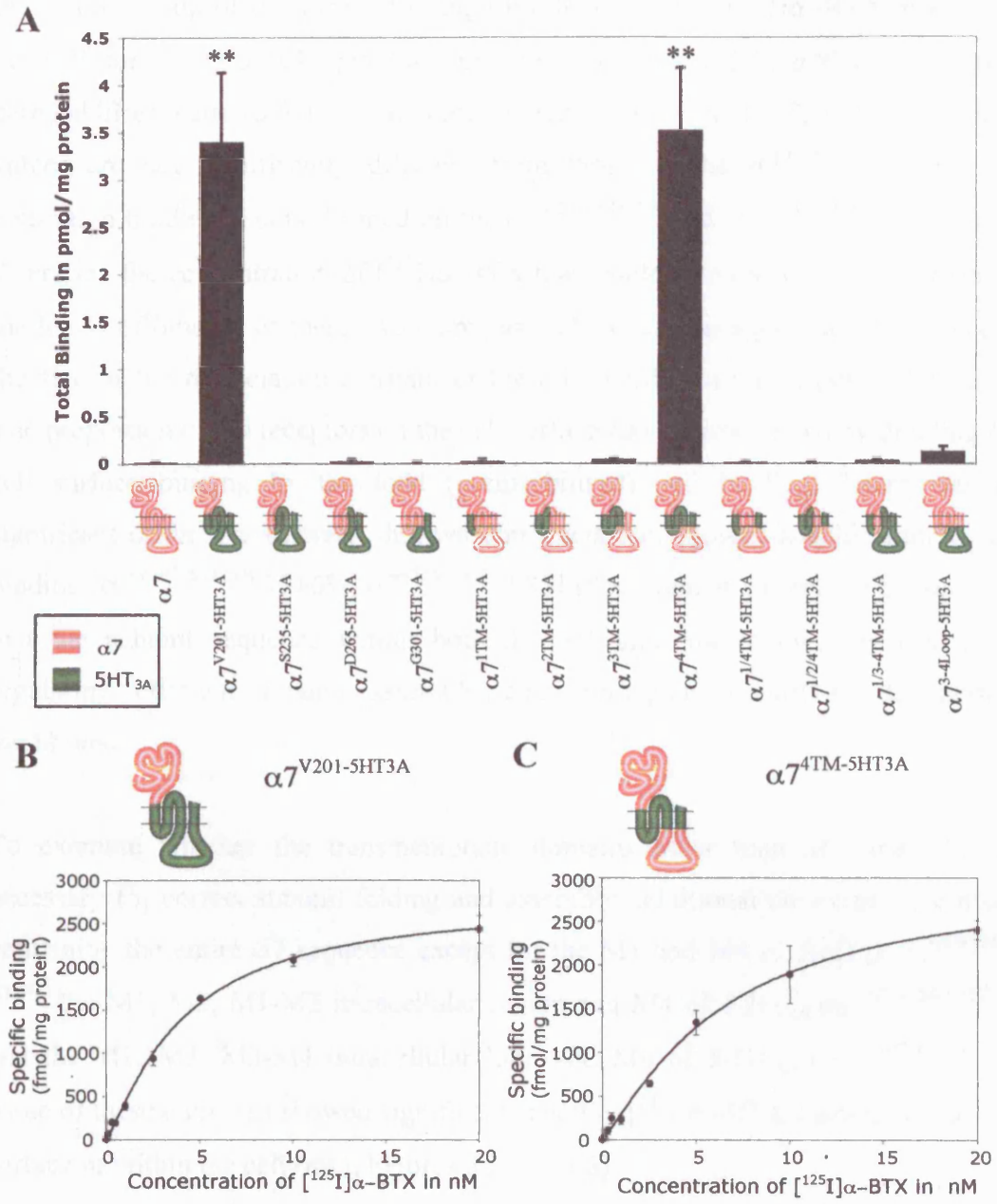

Figure 3.3 *Specific total [^{125}I]α-BTX binding of α7 and α7/5HT$_{3A}$ chimeras in transiently transfected tsA201 cells.*

(A) Binding was done on the same cells as for whole cell binding, but cells were permeabilized, see methods section 2.3.1. n=6-12. The results were tested for significant differences using an analysis of variance and a subsequent Tukey's test. ** p<0.01 when compared to all other samples except $\alpha7^{V201\text{-}5HT3A}$ and $\alpha7^{4TM\text{-}5HT3A}$ Saturation binding in cells transfected with (B) the $\alpha7^{V201\text{-}5HT_{3A}}$ and (C) the $\alpha7^{4TM\text{-}5HT_{3A}}$, n=2. Data was fitted with the Hill equation in SigmaPlot. K_d values of 4.1±0.5 nM, 6.1±0.6 nM, and n_H values of 1.3±0.1, 1.3±0.3 respectively.

intracellular loop of α7, resulted in high levels of specific [^{125}I]α–BTX binding on the cell surface (2.6±0.4 pmol/mg protein, n=6; Figure 3.2, p<0.001) and with permeablilsed cells (3.5±0.7 pmol/mg protein, n=6; Figure 3.3, p<0.001). These values are not significantly different from those of the $\alpha7^{V201\text{-}5\text{-}HT3A}$ chimera. Saturation binding was performed on the $\alpha7^{V201\text{-}5\text{-}HT3A}$ and $\alpha7^{4TM\text{-}5\text{-}HT3A}$ chimeras to determine the concentration of [^{125}I]α-BTX that would provide a fair comparison of the levels of binding of these two chimeras. There was no significant difference in the size of the dissociation constant or the hill coefficient tested (student's t-test). The proportion of the receptors on the cell surface can be determined by dividing the cell surface binding by the total (permeabilised) cell binding. There was no significant difference between the two constructs that showed specific radioligand binding ($\alpha7^{V201\text{-}5\text{-}HT3A}$ 73±6%, $\alpha7^{4TM\text{-}5\text{-}HT3A}$ 85±19%, student's t-test). This suggests that the subunit sequence within both the M1 and M4 regions are critical in regulating efficient subunit assembly and subsequent export to the plasma membrane.

To examine whether the transmembrane domains other than M1 and M4 are necessary for correct subunit folding and assembly, additional chimeras were made containing the entire α7 sequence except for the M1 and M4 of 5-HT_{3A} ($\alpha7^{1/4TM\text{-}5\text{-}HT3A}$) the M1, M2, M1-M2 intracellular region and M4 of 5-HT_{3A} ($\alpha7^{1/2/4TM\text{-}5\text{-}HT3A}$) and the M1, M3, M3-M4 intracellular loop and M4 of 5-HT_{3A} ($\alpha7^{1/3\text{-}4TM\text{-}5\text{-}HT3A}$). None of these chimeras showed significant specific [^{125}I]α–BTX binding on the cell surface or within the cell (n=4, Figures 3.2 and 3.3).

These findings demonstrate that efficient subunit folding and assembly (as assayed by [^{125}I]α–BTX binding) is possible in tsA201 cells only for those subunits examined which contain the region from the beginning of M1 to the end of M3, and including M4 from 5-HT_{3A} ($\alpha7^{V201\text{-}5\text{-}HT3A}$ and $\alpha7^{4TM\text{-}5\text{-}HT3A}$). Replacement of the large intracellular loop of $\alpha7^{V201\text{-}5\text{-}HT3A}$ with that of the α7 subunit ($\alpha7^{4TM\text{-}5\text{-}HT3A}$) did not have a significant effect on levels of [^{125}I]α–BTX binding (Figures 3.2 and 3.3). To examine further the influence of the large intracellular loop, two additional chimeras ($\alpha7^{3\text{-}4Loop\text{-}5\text{-}HT3A}$ and 5-$HT_{3A}^{3\text{-}4Loop\text{-}\alpha7}$) were constructed (Figures 3.1). No [^{125}I]α–BTX binding was detected in cells transfected with $\alpha7^{3\text{-}4Loop\text{-}5\text{-}HT3A}$ (Figures

3.2 and 3.3). High levels of specific binding of the 5-HT_{3A} receptor ligand [^{3}H]GR65630 (a membrane-permeable ligand) were detected in permeabilised cells transfected with 5-$HT_{3A}^{3\text{-}4Loop\text{-}\alpha7}$ (0.47±0.14 pmol/mg protein, n=4; Figure 3.4A). When this construct was compared with the 5-HT_{3A} subunit (0.30±0.09 pmol/mg protein, n=4; Figure 3.4A) there appeared to slightly greater specific binding with the 5-$HT_{3A}^{3\text{-}4Loop\text{-}\alpha7}$ chimera, however this was not a statistically significant difference (student's t-test). These findings are consistent with the conclusion that only those subunit chimeras containing regions from the beginning of M1 to the end of M3, and including M4 of 5-HT_{3A} fold and assemble efficiently in tsA201 cells. These findings also provide further evidence that efficient or inefficient subunit folding is not determined by sequences present within the large intracellular loop region.

3.3.3 Enzyme-linked assay to determine cell surface receptors

As the serotonergic radioligand [^{3}H]GR65630 is membrane permeable, it was not possible for it to be used selectively to detect cell surface receptors. For this reason an enzyme-linked assay was used with tsA201 cells transfected with the 5-HT_{3A} subunit and the 5-$HT_{3A}^{3\text{-}4Loop\text{-}\alpha7}$ chimera to examine levels of cell surface receptor. The antibody pAb120, which is immuno-reactive to the extracellular N-terminal domain of the 5-HT_{3A} subunit (Spier *et al.*, 1999), was used with the protocol described in Chapter 2, Section 2.5, for both intact cells (n=7) and permeabilised cells (n=5) and either a student's t-test or modified z-test has been used to test significance. As expected, the 5-HT_{3A} subunit showed a significant signal above background for cell surface receptors (p<0.005) and total cell protein (p<0.005) (Figure 3.4). The 5-$HT_{3A}^{3\text{-}4Loop\text{-}\alpha7}$ chimera showed significant total cell protein (p<0.01), in agreement with data from radioligand binding. Again, this appeared to be greater than with the 5-HT_{3A} subunit, but was not a statistically significant difference. With intact cells there was also a significant signal (p<0.005), however this was consistently higher in cells transfected with the 5-$HT_{3A}^{3\text{-}4Loop\text{-}\alpha7}$ chimera compared to the 5-HT_{3A} subunit (p<0.01). Thus it seems that the 5-$HT_{3A}^{3\text{-}4Loop\text{-}\alpha7}$ chimera is more efficiently expressed at the cell surface than the 5-HT_{3A} subunit. It was not possible to compare the cell surface to total cell signals, because the background levels of antibody binding in permeablilsed cells was much greater than

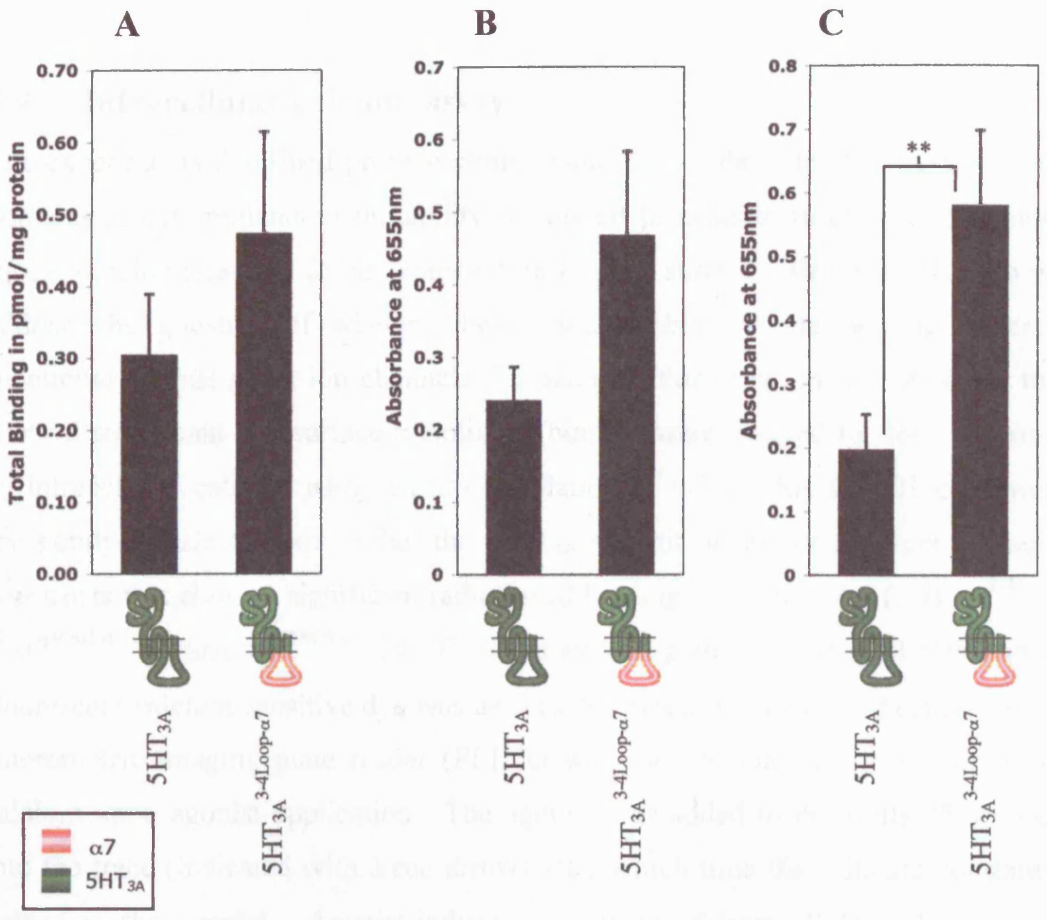

Figure 3.4 *Surface and total expression of 5-HT_{3A} and the 5-$HT_{3A}^{3\text{-}4Loop\text{-}\alpha7}$ chimera transiently transfected in tsA201 cells.*

(A), specific total [^{3}H]GR65630 binding in permeabilised cells n=4. Enzyme-linked assay on (B) permeablilsed, n=4 and (C) whole cells, n=7. The results were tested for significant differences using a student's t-test or a modified Z test, ** $p<0.01$.

with intact cells, thus probably masking some of the 5-HT_{3A} N-terminal protein levels.

3.4 Intracellular calcium assay

The experiments described provide strong evidence for the role of discrete subunit domains as determinants of the ability of subunit proteins to form correctly folded ligand-binding sites and to be expressed on the cell surface. However, they do not address the question of whether these subunit chimeras are able to generate functional agonist-gated ion channels. To examine this question, the chimeras that showed significant cell surface radioligand binding were assayed for function using an intracellular calcium assay with a population of cells. HEK tsA201 cells were transiently transfected with either the 5-HT_{3A} subunit or one of the three chimeric constructs that showed significant radioligand binding in Section 3.4 (5-$HT_{3A}^{3\text{-}4Loop\text{-}\alpha7}$,$\alpha7^{V201\text{-}5\text{-}HT3A}$ and $\alpha7^{4TM\text{-}5\text{-}HT3A}$). The cells were re-plated into 96-well plates and a fluorescent calcium-sensitive dye was used as described in Chapter 2, Section 2.6. A fluorometric imaging plate reader (FLIPR) was used to measure in the influx of calcium upon agonist application. The agonist was added to the wells 35 seconds into the trace (indicated with a red arrow) after which time the cells are constantly bathed in the agonist. Agonist-induced elevations of intracellular calcium were detected in cells transfected with the 5-HT_{3A} subunit, as would be expected (Figure 3.5A), and also the three chimeric subunits. As would be expected from the presence of the N-terminal region of 5-HT_{3A}, the 5-$HT_{3A}^{3\text{-}4Loop\text{-}\alpha7}$ chimera responded to 5-HT_3 receptor agonist (mCPBG), Figure 3.5B. The agonist mCPBG was chosen, as it is a more potent ligand at the homomeric 5-HT_{3A} receptor than 5-HT (EC_{50} 0.8 μM, Mair *et al.*, 1998). Similarly, nicotinic agonists (DMPP and nicotine) induced elevations of intracellular calcium were detected in cell transfected with the $\alpha7^{V201\text{-}5\text{-}HT3A}$ and $\alpha7^{4TM\text{-}5\text{-}HT3A}$ chimeras, which have the α7 N-terminal regions (see Figure 3.5 C and D). More consistent increases in intracellular calcium were detected with DMPP compared to nicotine, where the increase in calcium did not always relate to the concentration of nicotine used. Thus, the chimeras that showed binding also showed significant calcium influx upon application of agonist. This was interpreted as showing function of these constructs.

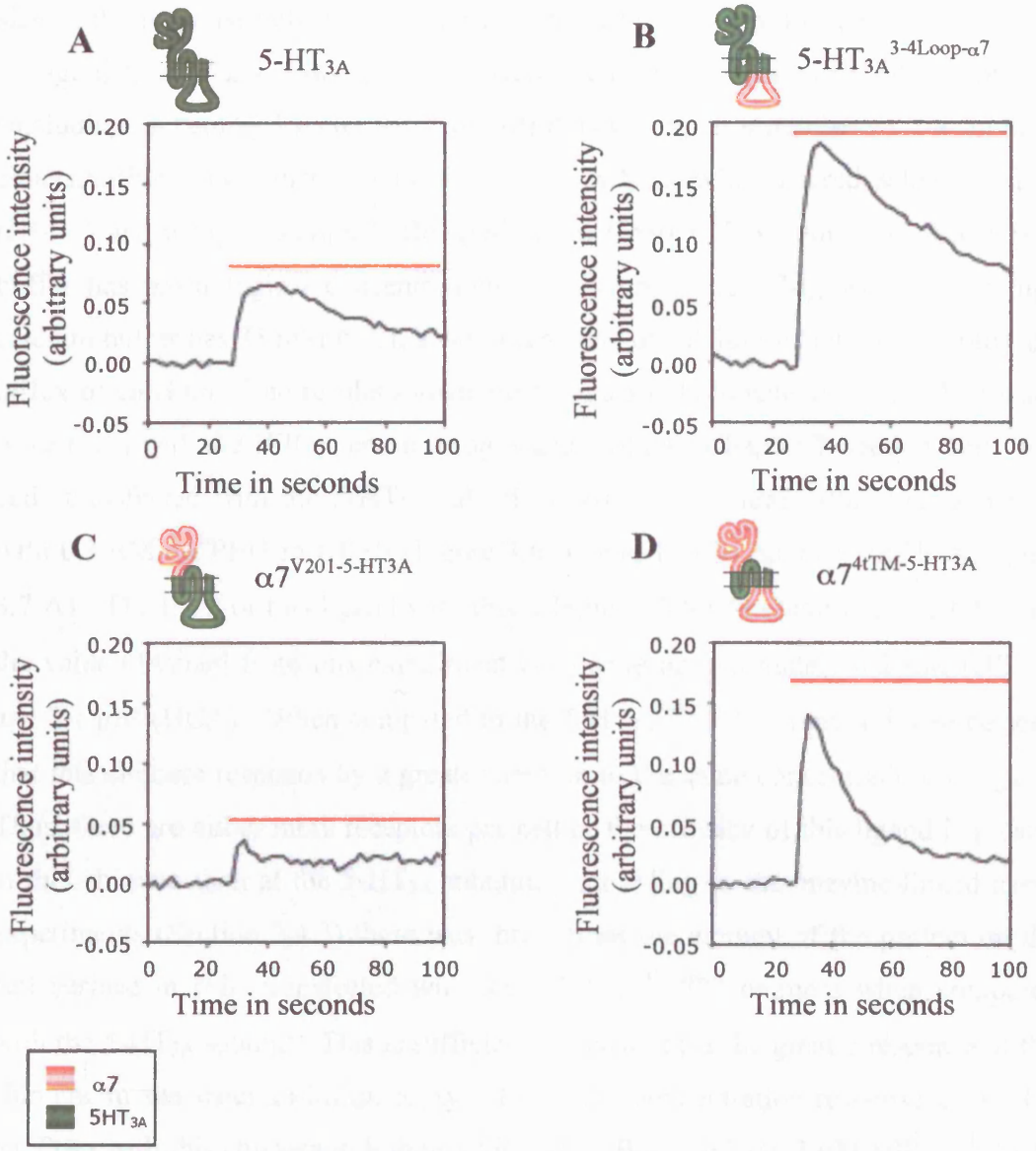

Figure 3.5 *Agonist-induced calcium responses in tsA201 cells transiently transfected with 5-HT$_{3A}$ and α7/5-HT$_{3A}$ chimeras.*

(A), 10 μM CPBG applied to cell transfected with 5HT$_{3A}$ subunit. (B), 10 μM CPBG applied to cells transfected with 5HT$_{3A}^{3\text{-}4Loop\text{-}\alpha7}$ chimera. (C), 17 μM DMPP applied to cells transfected with the $\alpha7^{V201\text{-}5HT_{3A}}$ chimera. (D), 1.8 μM DMPP applied to cells transfected with the $\alpha7^{4TM\text{-}5HT_{3A}}$ chimera. The red line indicates when the agonist was applied.

Agonist concentration-response curves were determined using a 96-well FLIPR assay, to give a rough estimate of the potency of the agonists and the comparative size of the responses obtained. Each column of wells had a different concentration of agonist, and 2-4 rows of wells were transfected with each DNA contruct (including an "empty" vector as a control) thus giving an *n* number of 2-4 for each concentration. Two different buffers were used, Hank's buffered saline solution (HBSS) and a high calcium buffer (HCA, see Chapter 2 Section 2.6). The HBSS buffer has physiological concentrations of calcium (1.26 mM), whereas the high calcium buffer has 75 mM CaCl, a very high level of calcium which may amplify the influx of calcium. The results shown are from a single transfection, and the results were fitted with the Hill equation using SigmaPlot (see Chapter 2 Section 2.6). For cells transfected with the 5-HT_{3A} subunit, maximum calcium influx was achieved with 0.3 μM mCPBG in HBSS (Figure 3.6 A) and 10 μM mCPBG in HCA(Figure 3.7 A). The EC_{50} of this ligand with this subunit is 0.8 μM (Mair *et al.*, 1998), and the value obtained from this experiment is close at approximately 0.2 μM (HBSS) and 2.1 μM (HCA). When compared to the 5-$HT_{3A}^{3\text{-}4Loop\text{-}\alpha7}$ chimera, it can be seen that this chimera responds by a greater amount to the same concentration of ligand. Thus, there are either more receptors per cell or the efficacy of this ligand is greater at this chimera than at the 5-HT_{3A} subunit. According to the enzyme-linked assay experiments (Section 3.4.3) there was three times the amount of the protein on the cell surface in cells transfected with the 5-$HT_{3A}^{3\text{-}4Loop\text{-}\alpha7}$ chimera when compared with the 5-HT_{3A} subunit. This is sufficient to account for the greater response of the chimera in the calcium-influx assay. From the concentration-response curve for mCPBG with this chimera in Figure 3.6B and 3.7B the EC_{50} (0.3 μM HBSS, 1.3 μM HCA) is similar to that of the 5-HT_{3A} subunit.

The concentration-response curves for the nicotinic ligand DMPP were obtained with the $\alpha7^{V201\text{-}5\text{-}HT3A}$ and $\alpha7^{4TM\text{-}5\text{-}HT3A}$ chimeras (Figures 3.6 C and D, 3.7 C and D). It can be seen that the $\alpha7^{4TM\text{-}5\text{-}HT3A}$ chimeras respond to a greater extent to the same concentration of ligand when compared to the $\alpha7^{V201\text{-}5\text{-}HT3A}$ chimera by approximately four times (at 50 μM DMPP). The level of surface radioligand binding was not significantly different between these two chimeras, thus the difference in the calcium influx may be due to differences in efficacy of this ligand

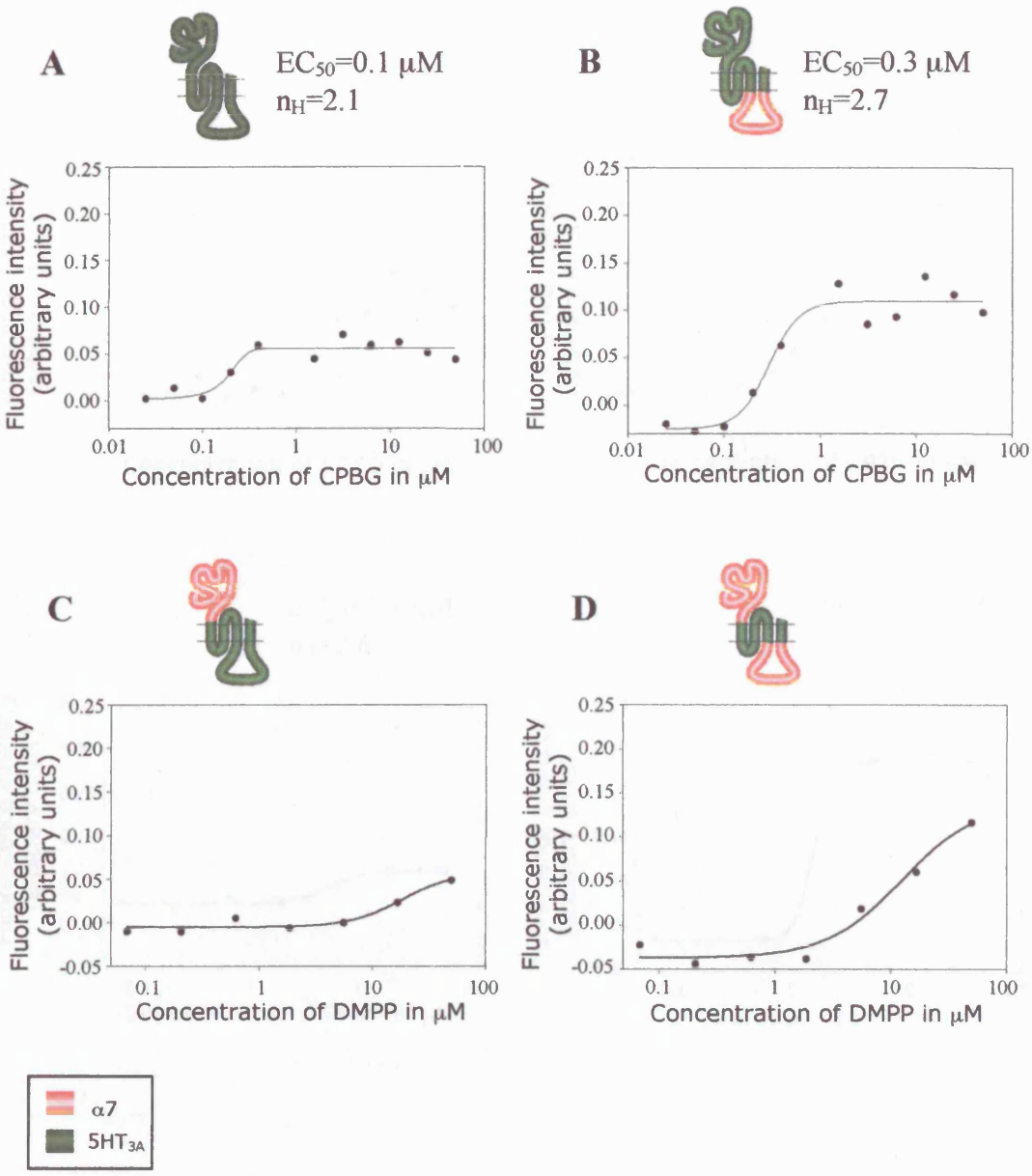

Figure 3.6 *Concentration-response relationship for agonist induced calcium responses from tsA201 cells in HBSS, transiently transfected with 5-HT$_{3A}$ and α7/5-HT$_{3A}$ chimeras.*

From one experiment with (A), CPBG applied to cells transfected with 5-HT$_{3A}$ subunit. (B), CPBG applied to cells transfected with 5-HT$_{3A}^{3\text{-}4Loop\text{-}\alpha7}$ chimera. (C) DMPP applied to cells transfected with the $\alpha7^{V201\text{-}5HT_{3A}}$ chimera. (D), DMPP applied to cells transfected with the $\alpha7^{4TM\text{-}5HT_{3A}}$ chimera.

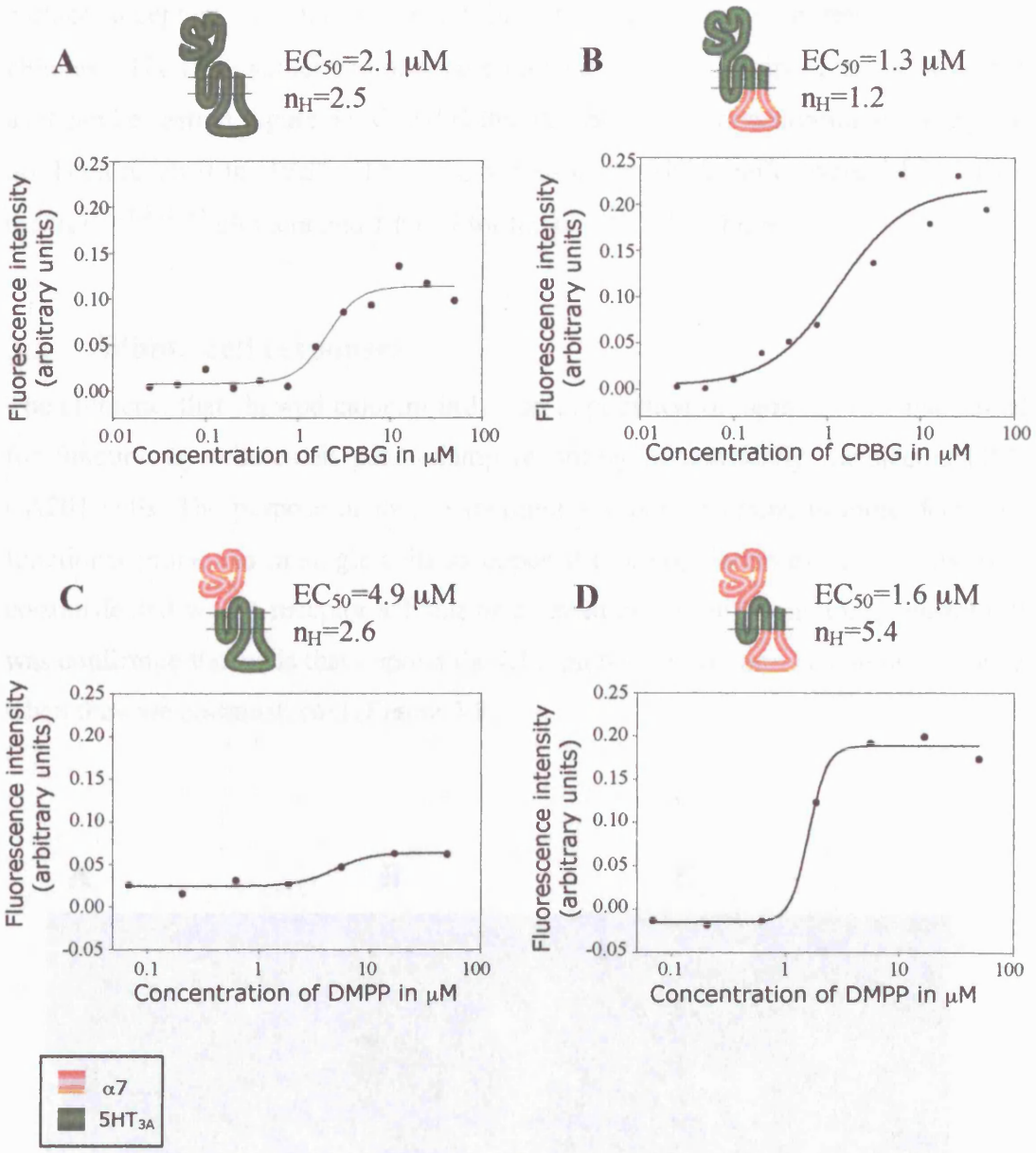

Figure 3.7 *Concentration-response relationship for agonist induced calcium responses in tsA201 cells in high (75mM) calcium buffer transiently transfected with 5-HT$_{3A}$ and α7/5-HT$_{3A}$ chimeras.*

From one experiment with (A), CPBG applied to cells transfected with 5HT$_{3A}$ subunit. (B), CPBG applied to cells transfected with 5-HT$_{3A}^{3\text{-}4Loop\text{-}\alpha7}$ chimera. (C) DMPP applied to cells transfected with the $\alpha7^{V201\text{-}5HT_{3A}}$ chimera. (D), DMPP applied to cells transfected with the $\alpha7^{4TM\text{-}5HT_{3A}}$ chimera.

between the two receptors. Alternatively, it is possible that a proportion of the surface receptors are non-functional in cells transfected with the $\alpha7^{V201\text{-}5\text{-}HT3A}$ chimera. The EC_{50} values can only be estimated from the results in the HCA buffer, as it can be seen in Figure 3.6 C and D that the saturating concentration of ligand has not been reached in HBSS. The EC_{50} values in the HCA buffer were 4.87 μM for the $\alpha7^{V201\text{-}5\text{-}HT3A}$ chimera and 1.6 μM for the $\alpha7^{4TM\text{-}5\text{-}HT3A}$ chimera.

3.5 Whole-cell responses

The chimeras that showed calcium influx on application of agonist were also tested for function by whole-cell patch-clamp recording in transiently transfected HEK tsA201 cells. The purpose of these experiments was to examine in more detail the functional properties in single cells as opposed to a population of cells. Cells were co-transfected with a receptor subunit or chimera and a GFP containing plasmid. It was confirmed that cells that express the GFP protein also express a chimeric protein when they are co-transfected (Figure 3.8).

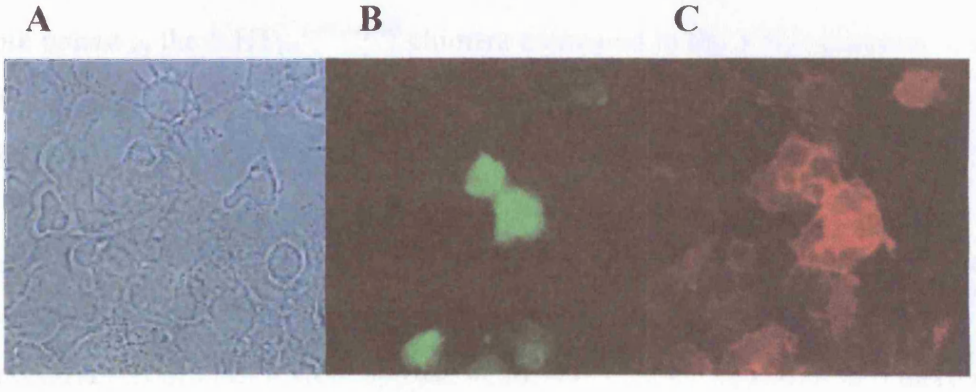

Figure 3.8 *HEK tsA201 cells co-transfected with $\alpha7^{4TM\text{-}5\text{-}HT3A}$ and pEGFP-C2, stained with rhodomine αBTX.*

(A) light micrograph and the same cells (B) showing GFP fluorescence and (C) rhodomine fluorescence. There is a good correlation between cells that show fluorescence in (B) and (C).

In each case, functional responses to rapid agonist application were obtained at -60 mV holding potential (unless stated otherwise), as illustrated in Figure 3.9. Either a student's t-test or modified z-test was used to test for significance when comparing either the size or the functional characteristics of the responses. The 5-HT_{3A} and 5-$HT_{3A}^{3\text{-}4Loop\text{-}\alpha7}$ receptors responded to 5-HT_3 receptor agonists (mCPBG and 5-HT) with inward currents. 5-HT was chosen to be used for the subsequent experiments as it is less potent than mCPBG, and it was desirable to have responses less than 2 nA. The average response of the 5-HT_{3A} receptor to different concentrations of 5-HT were as follows: 0.139±0.039 nA to 1μM 5-HT (n=6) and 1.28±0.439 nA to 4 μM 5-HT (n=4). The 5-$HT_{3A}^{3\text{-}4Loop\text{-}\alpha7}$ chimera had significantly larger responses at 1 μM 5-HT (1.3±0.5 nA n=10, p<0.05). This is an order of magnitude greater than the 5-HT_{3A} responses to this concentration. This cannot be solely accounted for by the approximately three fold greater amount of protein on the cell surface (Figure 3.4). A number of responses were obtained from this chimera at a higher concentration (2 μM 5-HT), with an average response of 0.8±0.2 nA (n=6). This is not significantly different from the responses at 1 μM 5-HT, suggesting that 1 μM is equal to or greater than the maximally effective concentration. The EC_{50} of 5-HT on the homomeric 5-HT_{3A} receptor is 2.6 μM (Hubbard *et al.*, 2000), thus 5-HT seems to be more potent at the 5-$HT_{3A}^{3\text{-}4Loop\text{-}\alpha7}$ chimera compared to the 5-HT_{3A} subunit assuming that this EC_{50} is equal to that of the homomeric 5-HT_{3A} receptor in these experiments.

The $\alpha7^{V201\text{-}5\text{-}HT3A}$ and $\alpha7^{4TM\text{-}5\text{-}HT3A}$ chimeras responded to the nicotinic agonist DMPP (Figure 3.9 C and D, 400 μM and 100 μM respectively). Three concentrations of DMPP were applied to the $\alpha7^{V201\text{-}5\text{-}HT3A}$ chimera, and there was no significant difference in the size of the response, (100 μM, 287±117 pA, n=6; 200 μM, 245±54 pA, n=5; 400 μM, 295±121 pA, n=5) it was therefore concluded that 100 μM is equal to or greater than the maximally effective concentration. Concentrations below 100 μM were tried but the responses were not reliable. In contrast to the $\alpha7^{V201\text{-}5\text{-}HT3A}$ chimera, the $\alpha7^{4TM\text{-}5\text{-}HT3A}$ chimera showed responses at concentrations as low as 20μM DMPP. The average response at 20 μM DMPP (372±94 pA, n=7) was not significantly different from the responses of the $\alpha7^{V201\text{-}5\text{-}HT3A}$ chimera at 100 μM DMPP. A higher concentration of DMPP was applied to

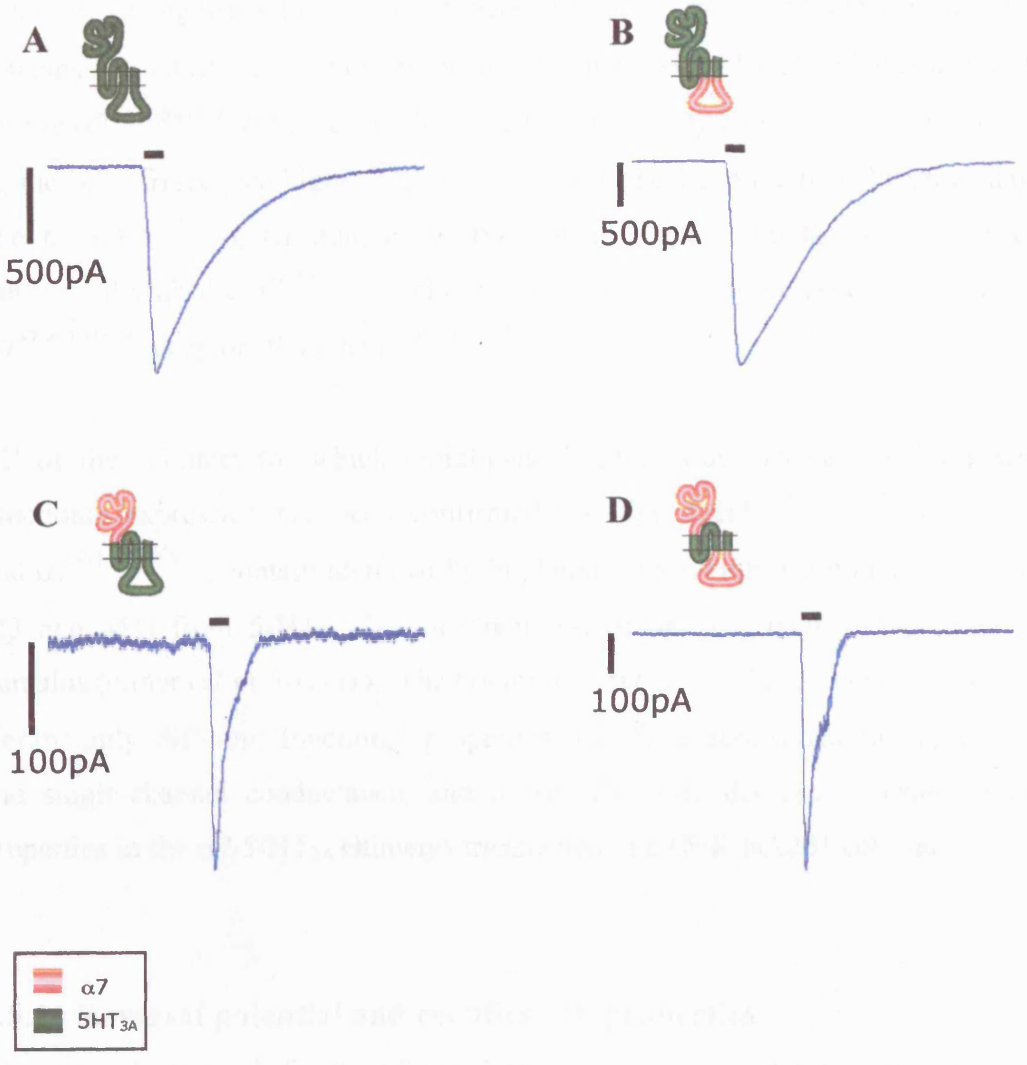

Figure 3.9 *Whole-cell responses in tsA201 cells transiently transfected with 5-HT_{3A} and α7/5-HT_{3A} chimeras.*

The bar above the responses indicates a 500 ms application of agonist with (A), 4 μM CPBG applied to a cell transfected with the 5-HT_{3A} subunit. (B), 4 μM CPBG applied to a cell transfected with $5HT_{3A}^{3\text{-}4Loop\text{-}\alpha7}$ chimera. (C), 400 μM DMPP applied to a cell transfected with the $\alpha7^{V201\text{-}5HT_{3A}}$ chimera. (D), 100 μM DMPP applied to a cell transfected with the $\alpha7^{4TM\text{-}5HT_{3A}}$ chimera. Holding potential was -60 mV.

cells expressing the $\alpha7^{4TM\text{-}5\text{-}HT3A}$ chimera (100μM DMPP, 439±64 pA, n=4), but there was no significant difference between responses to 20 μM and 100μM. Thus, it seems that 20 μM may be greater or equal to the maximally effective concentration for the $\alpha7^{4TM\text{-}5\text{-}HT3A}$ chimera. As there are approximately equal numbers of receptors on the cell surface (see Figure 3.2), the differences between the two chimeras may be due to either a greater number of functional receptors on the surface of cells transfected with the $\alpha7^{4TM\text{-}5\text{-}HT3A}$ chimera, or DMPP is a more potent agonist at the $\alpha7^{4TM\text{-}5\text{-}HT3A}$ receptors than the $\alpha7^{V201\text{-}5\text{-}HT3A}$.

All of the subunits for which radioligand binding was detected, and for which functional expression has been confirmed (5-HT_{3A}, 5-$HT_{3A}^{3\text{-}4Loop\text{-}\alpha7}$, $\alpha7^{V201\text{-}5\text{-}HT3A}$ and $\alpha7^{4TM\text{-}5\text{-}HT3A}$), contain identical hydrophobic transmembrane domains (M1, M2, M3 and M4) from 5-HT_{3A}, but different N-terminal and large cytoplasmic loop domains (either α7 or 5-HT_{3A}). The homomeric α7 and 5-HT_{3A} receptors have some significantly different functional properties including desensitization, rectification and single-channel conductance, and it was therefore decided to examine these properties in the α7/5-HT_{3A} chimeras transfected in a HEK tsA201 cell line.

3.5.1 Reversal potential and rectification properties

The reversal potentials for the α7 and 5-HT_{3A} subunit receptors are not significantly different from each other (Puchacz *et al.*, 1994; Hubbard *et al.*, 2000), however there is a large difference in the rectification properties. The reversal potential and rectification of the subunits were investigated by obtaining triplicate responses at holding potentials from -60 to +40 mV (an example of a cell transfected with the 5-$HT_{3A}^{3\text{-}4Loop\text{-}\alpha7}$ chimera, with brief (500 ms) agonist applications shown in Figure 3.10). There were no significant differences in these two functional characteristics between the four subunits. The reversal potentials for the 5-HT_{3A} subunit and the 5-$HT_{3A}^{3\text{-}4Loop\text{-}\alpha7}$, $\alpha7^{V201\text{-}5\text{-}HT3A}$ and $\alpha7^{4TM\text{-}5\text{-}HT3A}$ chimeras were 1.15±1.25, 5.83±2.62, 4.78±2.55 and 3.64±2.40, mV respectively, similar to that previously described for the wild-type 5-HT_{3A} subunit (-2.7mV; Hubbard *et al.*, 2000) and the rat α7 subunit (0mV; Puchacz *et al.*, 1994). The rectification profile for the four subunits showed little inward rectification, the rectification indices (see Chapter 2, Section 2.7.3) were

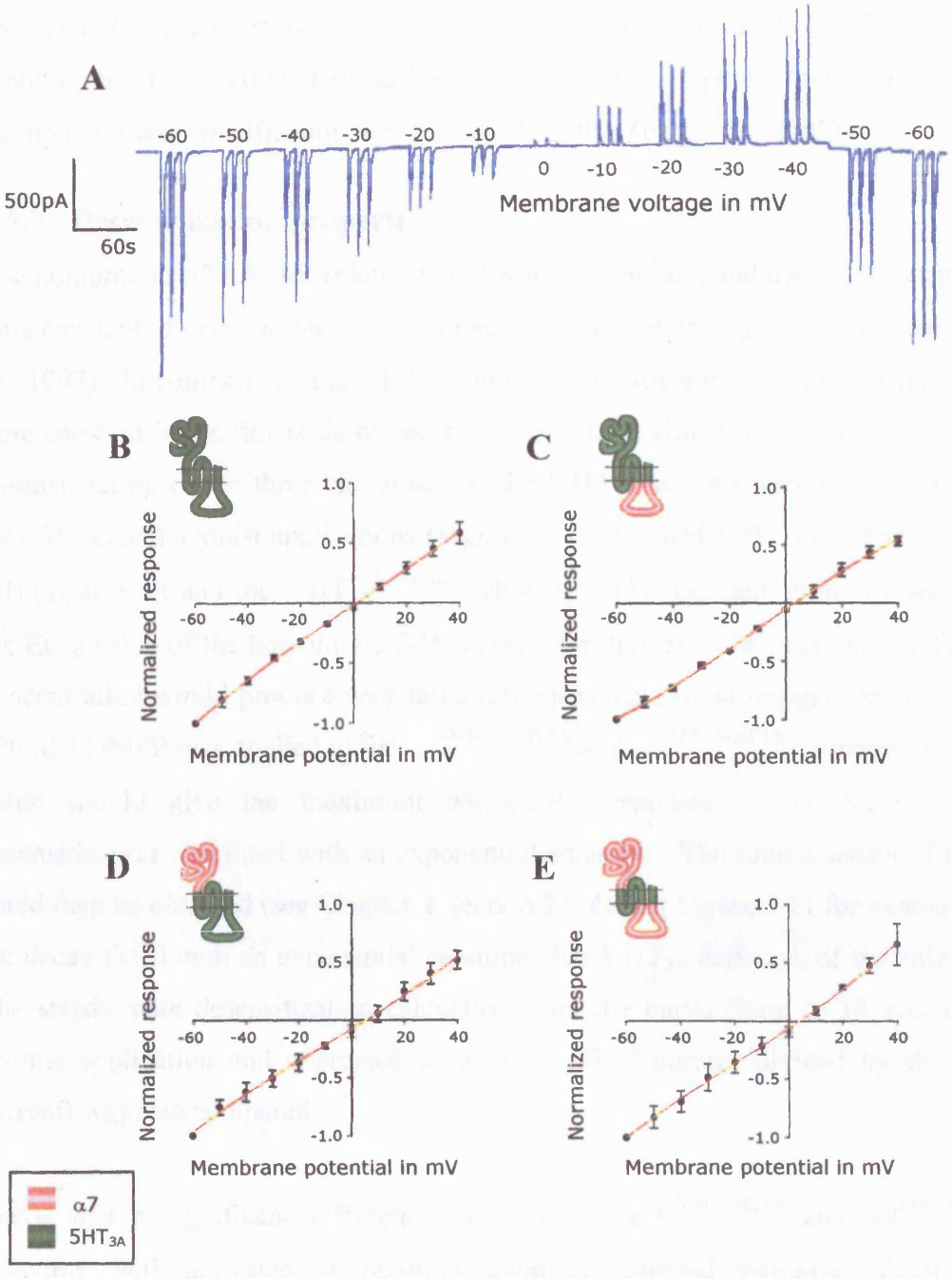

Figure 3.10 *Reversal potential and rectification of whole-cell responses from tsA201 cells transiently transfected with 5-HT$_{3A}$ and α7/5-HT$_{3A}$ chimeras.*
(A), an example of brief agonist applications done in triplicate to obtain current-voltage relation, with a cell transfected with the 5-HT$_{3A}^{3\text{-}4Loop\text{-}\alpha7}$ chimera. (B)-(E), mean current voltage relations for the 5-HT$_{3A}$ subunit (B), the 5-HT$_{3A}^{3\text{-}4Loop\text{-}\alpha7}$ chimera (C), the $\alpha7^{V201\text{-}5HT_{3A}}$ chimera (D) and the $\alpha7^{4TM\text{-}5HT_{3A}}$ chimera (E). The responses were normalised to the response obtained at -60 mV. *n*=5.

0.93±0.09, 1.08±0.04, 0.94±0.08 and 1.01±0.15 respectively. These functional characteristics are more similar to those shown previously for the 5-HT_{3A} receptor (Gunthorpe *et al.*, 2000, Hubbard *et al.*, 2000) as compared to the α7 subunit (complete inward rectification; Puchacz *et al.*, 1994, Zhao *et al.*, 2003).

3.5.2 Desensitization properties

The homomeric α7 nAChR is known to desensitise rapidly, and the responses have a time constant of decay in the region of tens of milliseconds (e.g. 75 ms, Ragozzino *et al.*, 1997). In comparison, the 5-HT_{3A} subunit desensitises much more slowly with a time constant in the timescale of seconds (e.g. 2.13 s, Gunthorpe *et al.*, 2000). The desensitization of the three chimeras and the 5-HT_{3A} subunit were compared using long 20 second agonist applications (Figure 3.11 A). 1 μM 5-HT was applied to the 5-HT_{3A} subunit and the 5-$HT_{3A}^{3\text{-}4Loop\text{-}\alpha7}$ chimera. This concentration is lower than the EC_{50} value of the homomeric 5-HT_{3A} receptor, however the maximally effective concentration would produce very large responses that would not give reliable data. 200 μM DMPP was applied to the $\alpha7^{V201\text{-}5\text{-}HT3A}$ and $\alpha7^{4TM\text{-}5\text{-}HT3A}$ chimeras, and this value should give the maximum whole-cell responses. The decay of the desensitization was fitted with an exponential equation. The time constant of decay could then be obtained (see Chapter 2 Section 2.7.4), see Figure 3.11 for examples of the decay fitted with an exponential equations for 5-HT_{3A} and each of the chimeras. The steady state desensitization calculated from the curve fitted to 18 seconds of agonist application and expressed as a % (he final current divided by the peak current) was also compared.

There was a significant difference between the $\alpha7^{V201\text{-}5\text{-}HT3A}$ and $\alpha7^{4TM\text{-}5\text{-}HT3A}$ chimeras, both activated by nicotinic agonists (denoted nicotinic subunits) as compared to the 5-$HT_{3A}^{3\text{-}4Loop\text{-}\alpha7}$ chimeras and 5-HT_{3A} subunit, activated by serotonergic agonists (denoted serotonergic subunits). However, the rate of decay was not determined from the maximally effective concentration of 5-HT, thus the nicotinic and serotonergic subunits cannot be directly compared. The time constant for decay for the two nicotinic subunits were 223±32 ms for $\alpha7^{V201\text{-}5\text{-}HT3A}$ and 925±220 ms for $\alpha7^{4TM\text{-}5\text{-}HT3A}$ (Figure 3.13A). These values are smaller than previously published values obtained for the homomeric 5-HT_{3A} receptor (2.13 s,

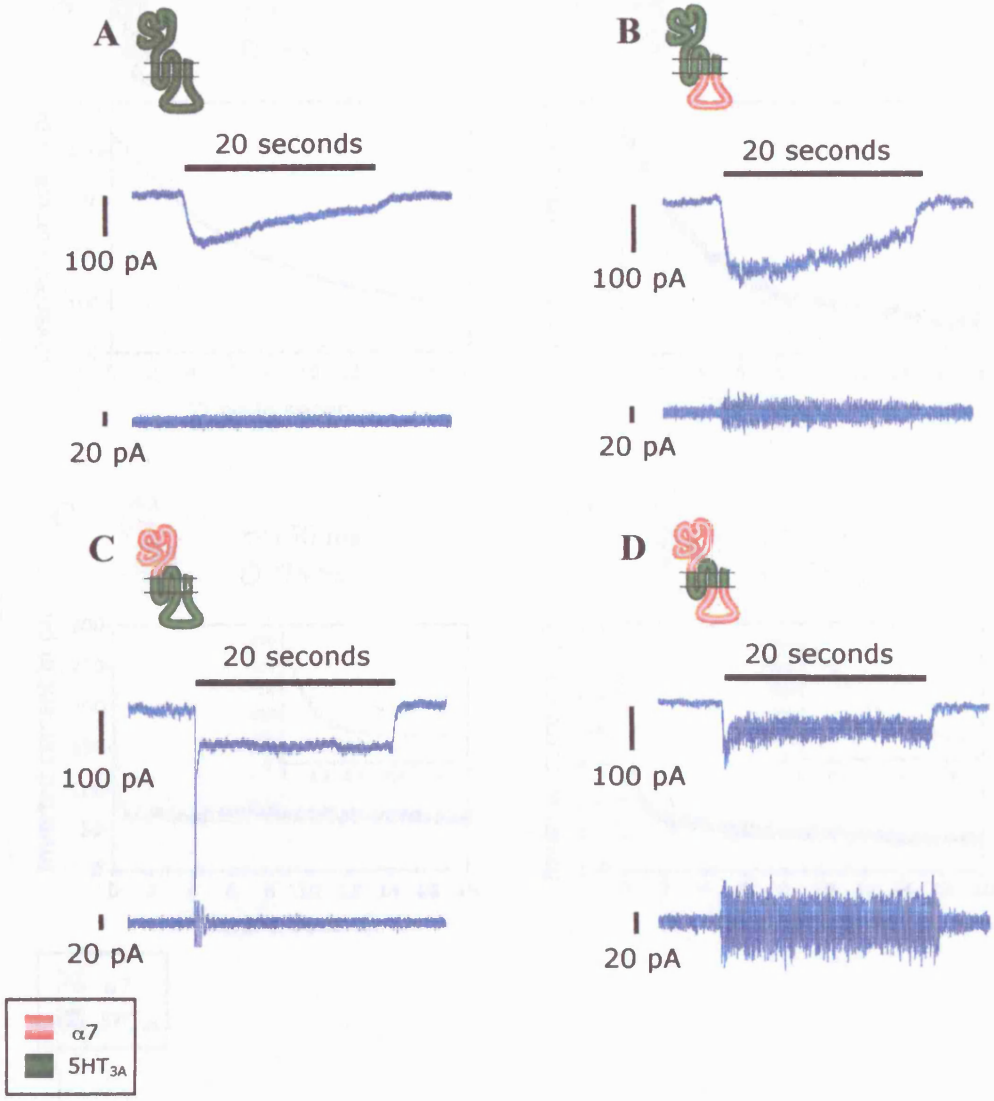

Figure 3.11 *Long agonist applications: whole cell responses from tsA201 cells transiently transfected with 5-HT$_{3A}$ and α7/5-HT$_{3A}$ chimeras.*

(A), 1 μM CPBG applied to a cell transfected with 5-HT$_{3A}$ subunit. (B), 1 μM CPBG applied to a cell transfected with the 5-HT$_{3A}^{3\text{-}4\text{Loop-}\alpha7}$ chimera. (C), 200 μM DMPP applied to a cell transfected with the $\alpha7^{V201\text{-}5HT_{3A}}$ chimera. (D), 20 μM DMPP applied to a cell transfected with the $\alpha7^{4TM\text{-}5HT_{3A}}$ chimera. The black bar above the trace indicates the agonist application.

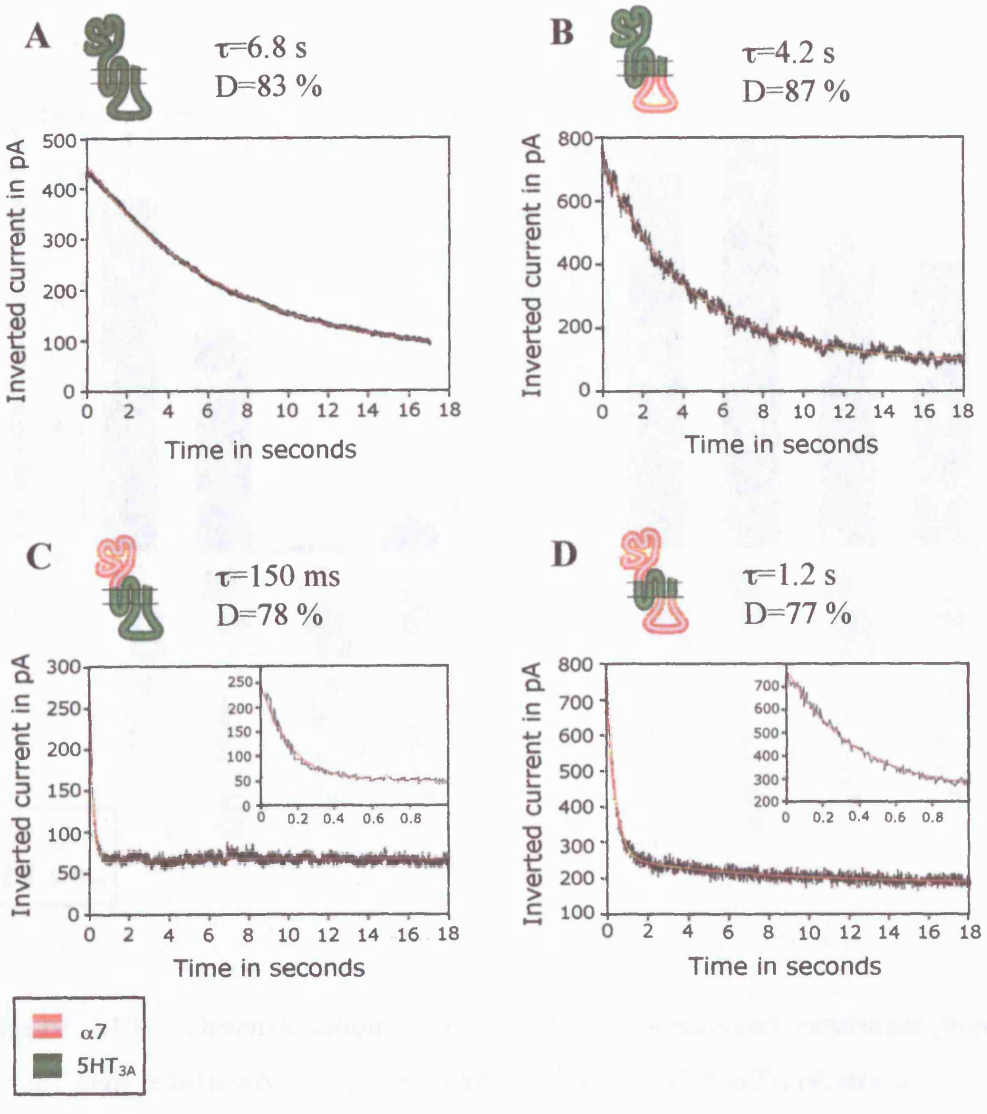

Figure 3.12 *Inverted whole-cell responses from tsA201 cells transiently transfected with 5-HT$_{3A}$ and α7/5-HT$_{3A}$ chimeras, fitted with an exponential equation to detemine desensitization characteristics*

20 second agonist applications were analysed to obtain the time constant of decay and the percentage of desensitization of the 5-HT$_{3A}$ subunit (A) the 5-HT$_{3A}^{3\text{-}4Loop\text{-}\alpha7}$ chimera (B) the $\alpha7^{V201\text{-}5HT_{3A}}$ chimera (C) and the $\alpha7^{4TM\text{-}5HT_{3A}}$ chimera (D) see methods section 2.6.4. D, percentage desensitization; τ, time constant of decay, n=5. A single exponential was used to fit to the data in (A), (B) and (C) and a double exponential was used to fit the data in (D).

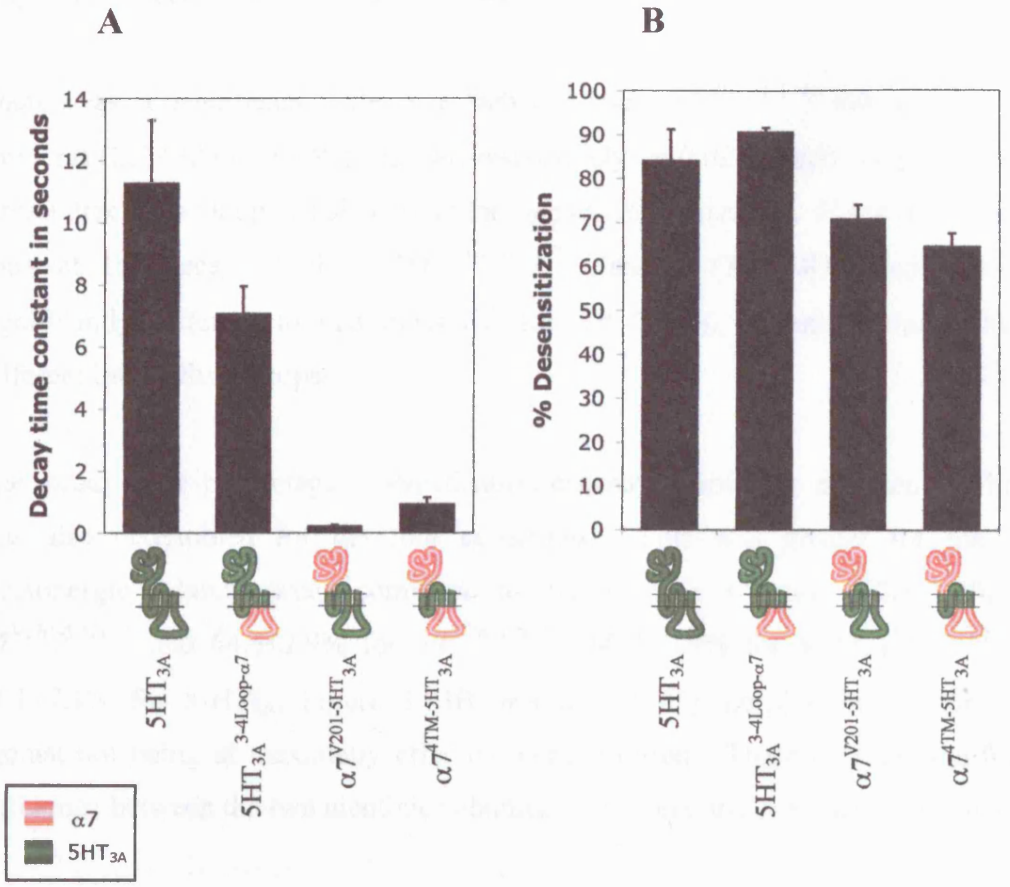

Figure 3.13 *Desensitisation characteristics of whole-cell responses from tsA201 cells transiently transfected with 5-HT$_{3A}$ and α7/5-HT$_{3A}$ chimeras.*

20 second agonist applications were analysed, to obtain the mean time constant of the decay of desensitization (A) and the mean percentage of desensitization (B) in cells transfected with the 5-HT$_{3A}$ subunit and the 5-HT$_{3A}^{3\text{-}4Loop\text{-}\alpha7}$, α7-$^{V201\text{-}5HT}_{3A}$ and α7$^{4TM\text{-}5HT}_{3A}$ chimeras. n=6-8.

Gunthorpe *et al.*, 2000). This indicates that the N-terminal extracellular domain may play a role in determining the rate of desensitization.

There was a significant difference between the $\alpha7^{V201\text{-}5\text{-}HT3A}$ and $\alpha7^{4TM\text{-}5\text{-}HT3A}$ chimeras (223±32 ms and 925±220 ms respectively, $p<0.02$), which suggests that the large intracellular loop can also affect the rate of desensitization. However, the time constant for decay of the $5\text{-}HT_{3A}^{3\text{-}4Loop\text{-}\alpha7}$ chimera (7067±878 ms) was not significantly different to that measured for the $5\text{-}HT_{3A}$ subunit, despite having different intracellular loops.

The steady state percentage desensitization estimated from the exponential fitting was also determined for the four constructs. This was greater for the two serotonergic subunits when compared to the nicotinic subunits (70.8±3.2% for $\alpha7^{V201\text{-}5\text{-}HT3A}$ and 64.6±2.9% for $\alpha7^{4TM\text{-}5\text{-}HT3A}$, 90.7±0.9% for $5\text{-}HT_{3A}^{3\text{-}4Loop\text{-}\alpha7}$ and 84.1±7.1% for $5\text{-}HT_{3A}$, Figure 3.13B, n=6-8, $p<0.05$), despite the serotonerigic agonist not being at maximally effective concentration. There was no significant difference between the two nicotinic subunits, or between the serotonergic subunits.

3.5.3 Estimate of the single-channel conductance from noise analysis

Previous studies have reported that homomeric $5\text{-}HT_{3A}$ receptors, produced by the heterologous expression of $5\text{-}HT_{3A}$, exhibit very small (sub-pS) single-channel openings (Hussy *et al.*, 1994; Kelley *et al.*, 2003) in contrast to the homomeric rat α7 subunit that have been shown to have a significantly larger single-channels of 72 and 87 pS when expressed in *Xenopus* oocytes (Fucile *et al.*, 2002), although it should be noted that the conductance for chick α7 is lower in mammalian cell lines (18.5 and 31.5 pS; Ragozzino *et al.*, 1997) when compared to *Xenopus* oocytes (45 pS; Revah *et al.*, 1991). Historically the single-channel properties of nAChRs have been attributed to the M2 transmembrane domain (Imoto *et al.*, 1986; Leonard *et al.*, 1988).

Surprisingly, considerable differences were apparent in the noise variance of functional responses obtained with these chimeras with long agonist applications

(Figure 3.10), suggesting that regions outside of the four proposed transmembrane domains exert an influence upon ion channel properties.

Consistent with previous studies (Hussy *et al.*, 1994; Kelley *et al.*, 2003) tsA201 cells expressing 5-HT_{3A} generated whole-cell responses with little detectable noise during agonist application (Figure 3.10A). Noise analysis of responses obtained with 5-HT_{3A} was used to estimate a single-channel conductance of 0.7±0.1 pS, (n=8; Figures 3.14 and 3.15). There was no significant difference in the values obtained by the noise analysis variance method compared to the noise power spectral density estimate (student's t-test). Surprisingly, the 5-$HT_{3A}^{3\text{-}4Loop\text{-}\alpha7}$ chimera, in which the M3-M4 cytoplasmic loop of 5-HT_{3A} was replaced with that of the α7 subunit, generated receptors with a single-channel conductance of 9.6±1.9 pS (n=11), which was significantly higher than that of 5-HT_{3A} (p<0.05). Analysis of whole-cell responses recorded from cells transfected with the $\alpha7^{V201\text{-}5\text{-}HT3A}$ chimera revealed an average single-channel conductance of 2.2±1 pS (n=9), but this was not significantly different from the sub-pS conductance observed with 5-HT_{3A}. (0.7±0.1 pS). This was because 4/9 of the cells had low single-channel conductances. Their average of 0.8±0.1 pS was the same as the 5-HT_{3A} receptors. The average of the other 5 cells was 2.4±0.9 pS and was significantly different from 5-HT_{3A} subunit (p<0.05). Cells transfected with the $\alpha7^{4TM\text{-}5\text{-}HT3A}$ chimera expressed receptors with a single-channel conductance of 21.5±2.4 pS (n=8). This was significantly larger (p<0.05) than the conductance of receptors generated by the 5-$HT_{3A}^{3\text{-}4Loop\text{-}\alpha7}$ chimera. These results indicate that replacement of the two domains, the extracellular N-terminal domain and the M3-M4 cytoplasmic loop of 5-HT_{3A} with that of α7 lead to a significant increase in channel conductance.

The noise power spectrum can also be used to estimate the of the mean single-channel open time from the τ value obtained from the lorentzian fit. There was no significant difference in the τ values estimated for the 5-HT_{3A} subunit (24.2±4.3 ms, n=8), the $\alpha7^{V201\text{-}5\text{-}HT3A}$ chimera (18.0±5.3 ms, n=9) and the $\alpha7^{4TM\text{-}5\text{-}HT3A}$ chimera (18.6±6.8 ms, n=8). The τ value for the 5-$HT_{3A}^{3\text{-}4Loop\text{-}\alpha7}$ chimera was significantly greater than the other constructs (38.0±3.3 ms, n=11, p<0.05).

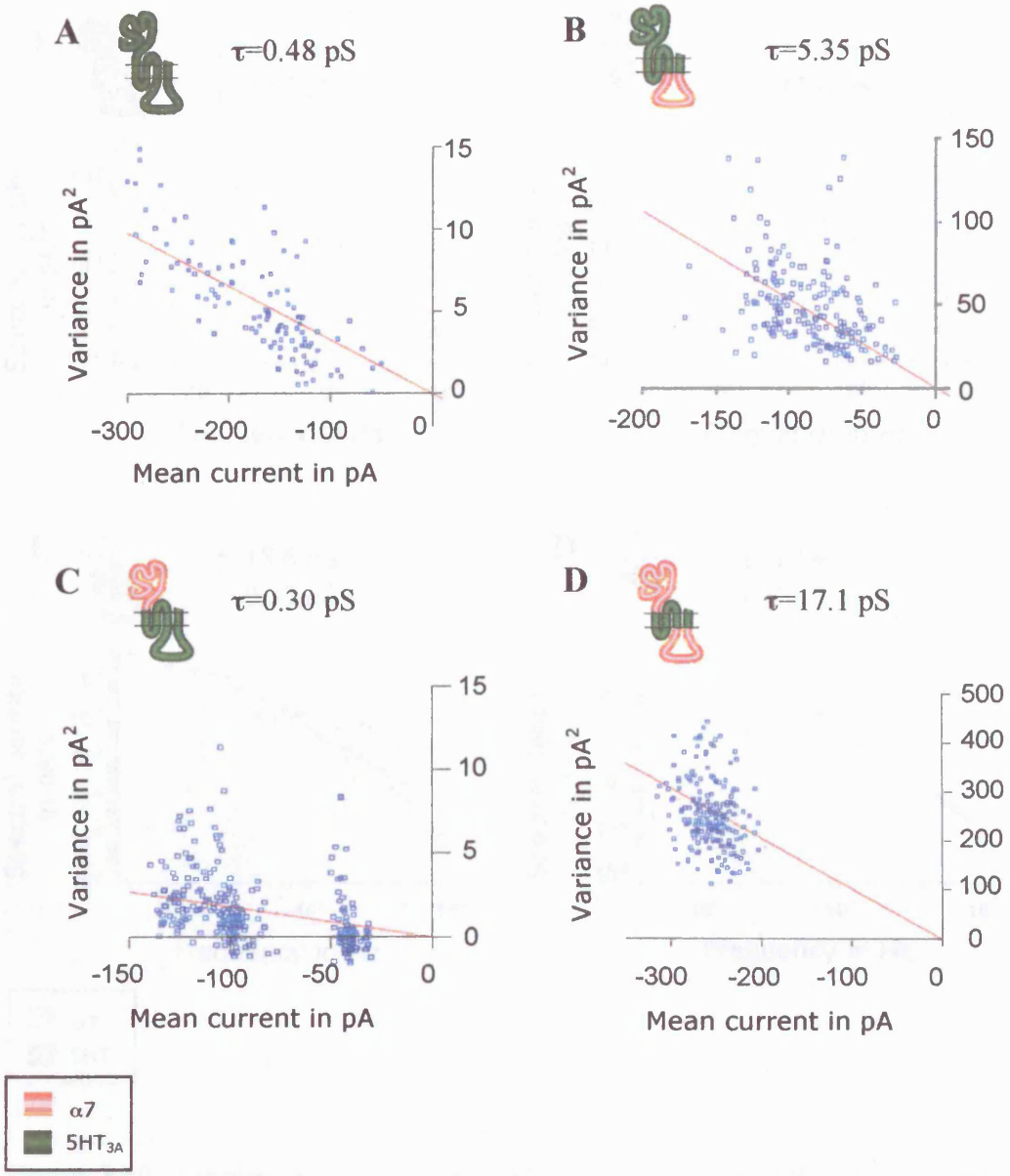

Figure 3.14 *Estimation of single-channel conductance using the noise analysis variance method to analyse whole-cell responses from tsA201 cells transiently transfected with 5-HT$_{3A}$ and α7/5-HT$_{3A}$ chimeras.*

20 second agonist applications were analysed to obtain the single channel conductance of the 5-HT$_{3A}$ subunit (A) the 5-HT$_{3A}^{3\text{-}4Loop\text{-}\alpha7}$ chimera (B) the α7-$^{V201\text{-}5HT_{3A}}$ chimera (C) and the $\alpha7^{4TM\text{-}5HT_{3A}}$ chimera (D) see methods section 2.6.5.1. *n*=8-11.

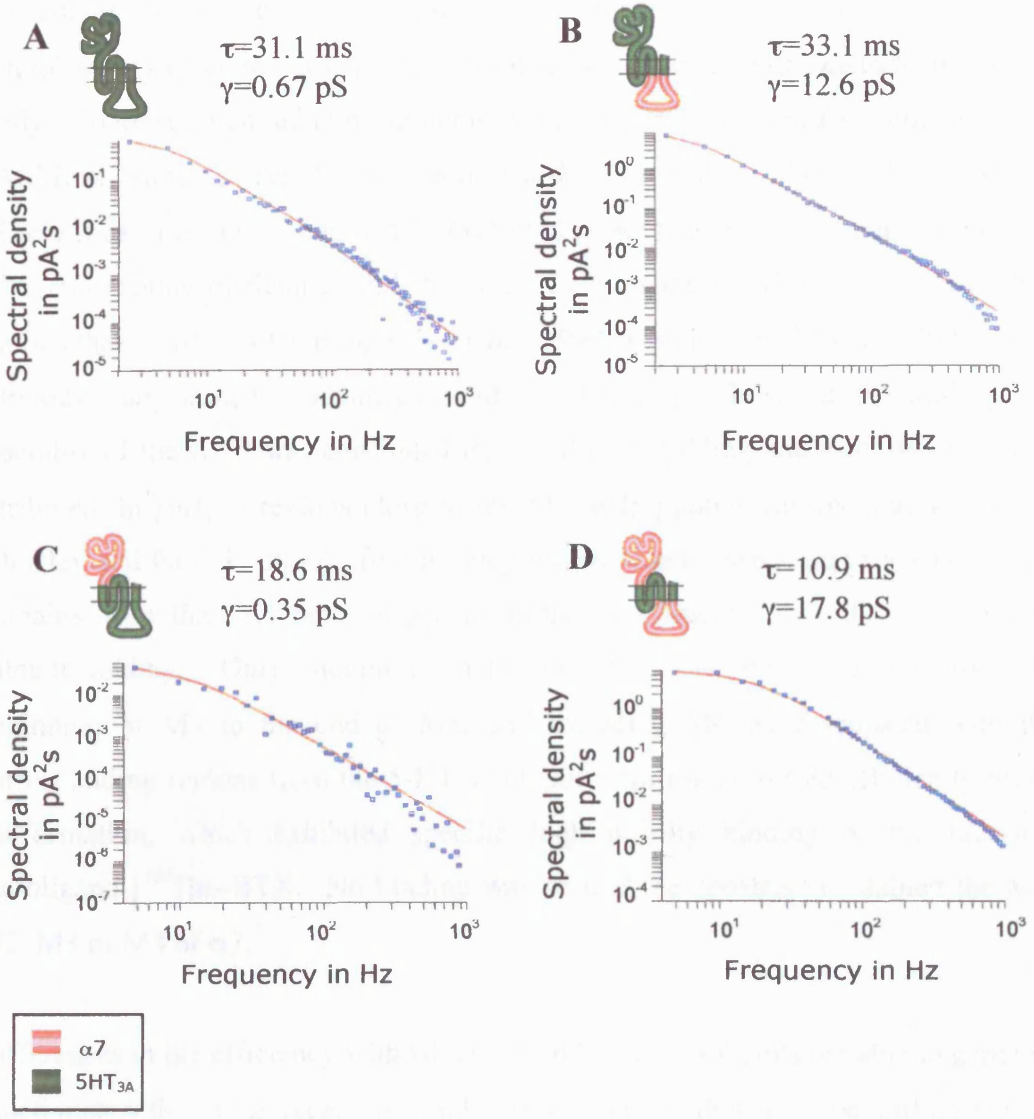

Figure 3.15 *Estimation of single-channel conductance using the noise power spectral density method to analyse whole-cell responses from tsA201 cells transiently transfected with 5-HT$_{3A}$ and α7/5-HT$_{3A}$ chimeras.*

20 second agonist applications were analysed to obtain the single channel conductance of the 5-HT$_{3A}$ subunit (A) the 5-HT$_{3A}^{3\text{-}4Loop\text{-}\alpha7}$ chimera (B) the α7-$^{V201\text{-}5HT}_{3A}$ chimera (C) and the α7$^{4TM\text{-}5HT}_{3A}$ chimera (D) see methods section 2.6.5.2. τ, estimate of mean single-channel open time, γ, estimate of single-channel conductance . *n*=8-11. A double lorenztian was used to fit the data in (A) and (B) and a single lorentzian was used to fit the data in (C) and (D).

3.6 Discussion

Difficulties in the efficient expression of functional α7 nAChRs in many heterologous expression systems have been a considerable hindrance to their detailed study. Evidence that subunit chimeras containing the extracellular domain of the nAChR α7 subunit fused to the C-terminal domain of the 5-HT_3R subunit 5-HT_{3A} (Eiselé *et al.*, 1993) has been widely exploited by several research groups as a means of circumventing difficulties in heterologous expression of α7 (Eiselé *et al.*, 1993; Blumenthal *et al.*, 1997; Rangwala *et al.*, 1997; Cooper and Millar, 1998). In a previous study aimed at identifying subunit domains influencing the folding and assembly of the α7 it was concluded that inefficient folding and assembly could be attributed, in part, to regions close to the M1 hydrophobic transmembrane domain (Dineley and Patrick, 2000). In this study we provide evidence that transmembrane domains other than M1 have an equally profound influence upon the efficiency of subunit folding. Only subunit chimeras in which the regions of α7 from the beginning of M1 to the end of M3, and including M4 were replaced with the corresponding regions from the 5-HT_{3A} subunit were found to fold efficiently into a conformation, which exhibited specific high affinity binding of the nicotinic radioligand [^{125}I]α–BTX. No binding was seen if the construct contained the M1, M2, M3 or M4 of α7.

Differences in the efficiency with which α7 and 5-HT_{3A} subunits are able to generate functional cell-surface receptors might have been predicted to be influenced by regions such as their large cytoplasmic M3-M4 domain. This region of nAChR subunits has been shown to interact with a range of intracellular proteins (Maimone and Enigk, 1999; Jeanclos *et al.*, 2001; Lin *et al.*, 2002) and to influence receptor targeting (Williams *et al.*, 1998). Our findings suggest that it is not this region of α7 that is responsible for inefficient folding, assembly and cell-surface expression. In fact when the intracellular loop of 5-HT_{3A} was replaced with that of α7 there was a statistically significant increase in the amount of receptor protein on the cell surface (Figure 3.5C).

The chimeras that showed significant binding have also been shown to be functional with two different methods. Using a calcium-influx assay, consistent responses were

obtained that were dependent on agonist concentration. This method can be used in the future to examine in more detail the concentration-response relationship, however there are some reports of variability in values such as the EC_{50} when comparing calcium-influx assays to whole-cell patch-clamping, with a difference of nearly ten fold (Feuerbach *et al.*, 2005). This may be due to different concentrations of agonist required to give the maximal calcium response compared to the whole cell reponse. Alternatively, as the EC_{50} for the calcium assay is lower, it may be that this method is more sensitive thus will register responses as low concentrations that elicit no visible response in whole cell recording.

By using whole-cell patch-clamp recording, it was possible to examine various functional properties of the functional chimeras and compare them, directly to the homomeric 5-HT_{3A} subunit, and indirectly to values reported previously for the homomeric α7 subunit. The rectification values of the chimeras were not significantly different to that with the 5-HT_{3A} subunit. This is as may be expected as the rectification has been attributed to the M2 channel domain of these receptors (Forster and Bertrand, 1995), and this is the region that the three chimeras have in common with the 5-HT_{3A} subunit.

The results of desensitization characteristics were less clear cut. Chimeras that contained the N-terminal of the α7 subunit desensitise faster than expected for the homomeric 5-HT_{3A} subunit thus the N-terminal domain may be important determinant of the rate of desensitization. The N-terminal domain has been reported to be important for desensitization of the β2 and β4 subunit nAChRs (Bohler *et al.*, 2001; Francis *et al.*, 2000). There were also significant differences in the rate of desensitization for the two chimeras that had the same α7 N-terminal domain. The $\alpha7^{V201\text{-}5\text{-}HT3A}$ and $\alpha7^{4TM\text{-}5\text{-}HT3A}$ chimeras had different large cytoplasmic M3-M4 domains, thus this domain may also determine the speed of desensitization. The rat α7 subunit and the mouse 5-HT_{3A} have different potential phosphorylation sites in the M3-M4 domain (Séguéla *et al.*, 1993; Maricq *et al.*, 1993), which may contribute to differing properties of desensitization as phosphorylation has been proposed to be a mechanism of regulation of desensitization (Quick and Lester, 2002). It should also be mentioned that these two chimeras had desensitization characteristics that

were different to the homomeric α7 receptor. This implies that the channel domain is also important in determining the rate of desensitization.

The steady state percentage desensitization was estimated from the exponential fitting of responses to a 20 second agonist application. The $\alpha7^{V201\text{-}5\text{-}HT3A}$ and $\alpha7^{4TM\text{-}5\text{-}HT3A}$ chimeras showed a steady state level of activation of approximately 30%. The homomeric 5-HT_{3A} receptor showed significantly less activation (only 9.3±0.9%), and the homomeric rat α7 receptor is know to fully desensitize within a few seconds (see Chapter 4, Section 4.). Thus it seems that the equilibrium between the open and desensitized states of these two chimeras is different from both the 5-HT_{3A} and homomeric α7 subunit receptors.

An unexpected finding to emerge from this study was evidence that subunit domains other than the putative transmembrane regions have a significant influence upon single-channel conductance. Extensive experimental evidence exists to suggest that the M2 domain of ligand-gated ion channels lines the channel pore and exerts a direct influences upon ion channel properties. Residues within the M2 region of the *Torpedo* nAChR can be photo affinity labelled by channel blockers (Giraudat *et al.*, 1986; Hucho *et al.*, 1986). The influence of residues within the M2 domain upon ion channel properties has been demonstrated by construction of subunit chimeras (Imoto *et al.*, 1986) and by site-directed mutagenesis (Imoto *et al.*, 1988; Leonard *et al.*, 1988; Charnet *et al.*, 1990; Villarroel *et al.*, 1991).

This study provides evidence obtained from the series of subunit chimeras to demonstrate that single-channel conductance is influenced by regions other than the predicted transmembrane regions. The result that the cytoplasmic M3-M4 loop domain of the nAChR α7 subunit can influence channel conductance agrees with a recent investigation of the human 5-HT_3 receptor channel conductance which examined chimeras constructed between the 5-HT_{3A} and 5-HT_{3B} subunits (Kelley *et al.*, 2003). This study identified three arginine residues within the amphipathic helix in the large M3-M4 cytoplasmic loop as being critical in influencing 5-HT_3 receptor single-channel conductance. These arginine residues are present in the 5-HT_{3A} but not the 5-HT_{3B}. A mutated 5-HT_{3A} subunit without these arginine residues has a

greater single-channel conductance (25.1±0.8 pS) than the wild type homomeric receptor (0.76±0.22 pS). The murine 5-HT_{3A} subunit also has these arginine residues, which the rat α7 subunit lacks. The results in this study confirm that constructs that contain a M3-M4 cytoplasmic loop without these arginine residues have a greater signal channel conductance. In terms of the 3-dimensional receptor struture the large intracellular loop may form part of a cage-like structure beneath the inner mouth of the ion channel that is seen by electron microscopy (Figure 1.5). Residues in the structure may act to control the flow of ions into the channel. In this case the positively charged arginines may form an electrostatic barrier making it harder for cations to enter the channel, resulting in a smaller conductance compared to cation channels without these positive residues.

In addition, evidence has been obtained that conductance can be influenced by the extracellular N-terminal domain of ligand-gated ion channels. When the 5-HT_{3A} N-terminal domain is replaced by that of α7, the single-channel conductance estimate increases about two fold. This could be an intrinsic characteristic of the protein, or dependent on the interaction of a specific type of ligand with the protein. It would be difficult to determine more precisely which region of the N-terminal is responsible as changes in the ligand-binding domain could easily effect agonist binding and result in a chimera that was not functional. Recently a compound (PSAB-OFP) has been described which is an agonist of both the α7 and the 5-HT_{3A} subunits (Broad *et al.*, 2002). It would be interesting to use this to examine the conductance in the functional chimeras from this study.

CHAPTER 4

RIC3 affects functional expression of multiple nAChR subtypes and the 5-HT_{3A} receptor.

4.1 Introduction

The α7 nAChR subunit has been shown to form functional receptors in *Xenopus* oocytes (Couturier *et al.*, 1990a) and some mammalian cell lines (Puchacz *et al.*, 1994; Gopalakrishnan *et al.*, 1995). However, no evidence of functional expression of α7 nAChRs can be detected when the α7 subunit is expressed in a number of other mammalian cell lines, for example HEK cells (Cooper and Millar, 1997; Sweileh *et al.*, 2000). There has also been difficulty expressing functional chick α8 receptors in this cell line (Cooper and Millar, 1998) despite the ability of α8 to form functional nAChRs in *Xenopus* oocytes (Gerzanich *et al.*, 1994; Gotti *et al.*, 1994). This implies that the host cell environment may be important for the correct subunit folding, assembly and cell surface expression of these ligand-gated ion channels. A number of nAChR-interacting proteins have been identified and have been shown to enhance the expression of nAChRs. Calnexin and BiP are involved in the assembly of muscle nAChRs (Gelman *et al.*, 1995; Blout and Merlie, 1991), and chaperone protein 14-3-3η has been shown to increase the levels of α4β2 receptors (Jeanclos *et al.*, 2001). Until recently, no factors have been identified which facilitate the functional expression of α7 or α8 subunits in HEK cells.

A recent study with *Caenorhabditis elegans* has identified a protein encoded by the gene *ric-3* (Halevi *et al.*, 2002). Mutations of this protein cause the intracellular accumulation of nicotinic receptors, suggesting that this protein has a role in the maturation of nAChRs (Halevi *et al.*, 2002). Co-expression of *C. elegans* RIC3 with the *C. elegans* nAChR DEG-3/DES-2 in *Xenopus* oocytes revealed an enhancement of the nAChR function (Halevi *et al.*, 2002). This enhancement was not restricted to *C. elegans* nAChRs, and has also been observed with homomeric rat α7 receptors expressed in *Xenopus* oocytes (Halevi *et al.*, 2002). The RIC3 protein has been shown to have no effect on functional expression of some other ligand-gated ion channels, for example the GABA, glutamate and glycine receptors (Halevi *et al.*, 2002; Halevi *et al.*, 2003). However RIC3 has been reported to reduce functional expression of the murine 5-HT_{3A} receptor expressed in *Xenopus* oocytes (Halevi *et al.*, 2003).

Vertebrate and invertebrate homologues of the *C.elegans* RIC3 protein have been cloned and this family of proteins are predicted to have two transmembrane domains separated by a proline-rich spacer region (Halevi *et al.*, 2003). The *C.elegans* RIC3 is predicted to have two coiled-coil domains after the second transmembrane domain, whereas all the other RIC3 genes examined (*Ostertagia ostertagi, Drosophila melanogaster, Danio rerio, Xenopus leavis,* murine and human; Figure 4.1B) have one predicted coiled coil domain (Halevi *et al.*, 2003). The proposed topology of this protein places the N-terminal and C-terminal on the cytoplasmic side of the membrane (Figure 4.1A; Halevi, *et al.*, 2003).

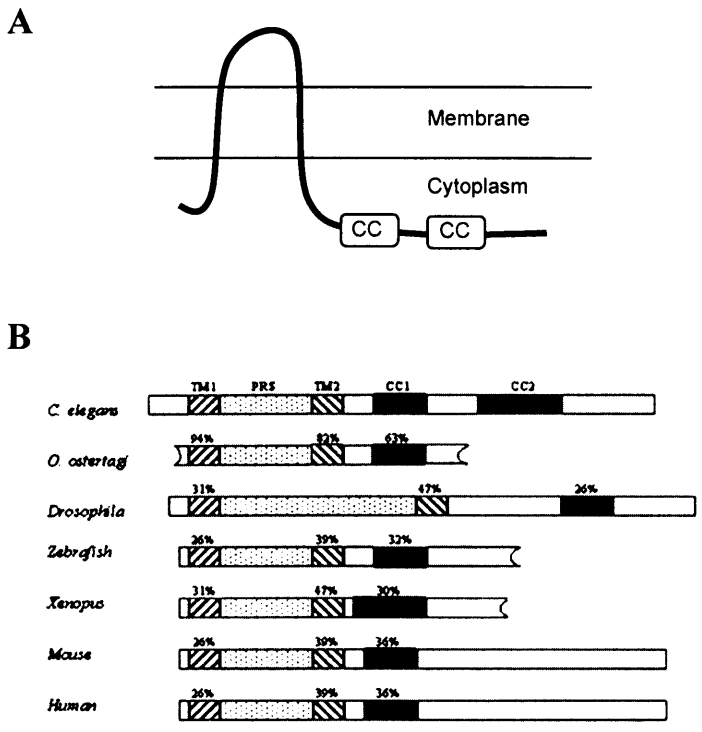

Figure 4.1 *Structure and topology of the RIC3 proteins*

The *C. elegans* RIC3 protein is predicted to have two transmembrane domains separated by a proline rich domain, followed by two coiled coil domains (predicted by Halevi *et al.*, 2002; Halevi *et al.*, 2003). (A) shows the predicted topology of the *C.elegans* RIC3 protein. (B) is adapted from Halevi *et al.*, 2003 and shows the structure and conservation within the RIC3 gene family.

The human RIC3 homologue has been reported to enhance the function of the α7 nAChR (both the human and rat), but reduce the function of the heteromeric α4β2

and α3β4 nAChRs and the murine 5-HT_{3A} receptor when expressed in *Xenopus* oocytes (Halevi *et al.*, 2003). Human and *C. elegans* RIC3 have also been co-expressed with the α7 subunit in HEK cells, to investigate whether this would result in correctly folded α7 receptors in this cell line. A significant level of [^{125}I]α-BTX binding (Lansdell *et al.*, 2005) and fluorescent labelled α-BTX (human RIC3 only Williams *et al.*, 2005) has been reported on the surface of these cells that is not detected when the α7 subunit is expressed alone. The human RIC3 protein has been demonstrated to associate with the human α7 subunit (Williams *et al.*, 2005, human RIC3 only; Lansdell *et al.*, 2005). There is also a significant increase in cell surface radioligand binding when RIC3 was co-expressed with either the chick α8 subunit or one of a number of heteromeric nAChR subunit combinations (α3β2, α3β4, α4β2 and α4β4; Lansdell *et al.*, 2005). It is not clear what effect RIC3 has upon 5-HT_{3A}, as there are differences depending on the assay used and the species of the 5-HT_{3A} subunit and the RIC3 protein expressed (Doward, 2005).

This chapter examines whether nAChR subunits can form functional receptors when co-expressed with RIC3 in a HEK cell line (tsA201). Although not known at the time this part of the current project was performed, data published subsequently (Williams *et al.*, 2005), has reported that the human α7 forms functional receptors in HEK cells when co-expressed with human RIC3. For this chapter whole-cell patch-clamping has been used to examine the effect of RIC3 when co-expressed in HEK cells with the following nAChRs: human and rat α7, chick α8 and rat α3β2 subunits, thus results with all but one of these combinations are novel. In addition the effect of RIC3 upon the functional expression of the 5-HT_{3A} subunit was also examined.

RESULTS

4.2 Functional α7 receptors formed when co-expressed with RIC3

As has been discussed previously (Cooper and Millar, 1997) difficulties have been reported in attempts to detect functional homomeric α7 nAChRs in transfected HEK cells. In the present study, HEK tsA201 cells were transfected with the α7 subunit alone and examined by whole-cell patch-clamping. None of the cells examined showed a response to ACh (n=17, Figure 4.2). These results are consistent with

A

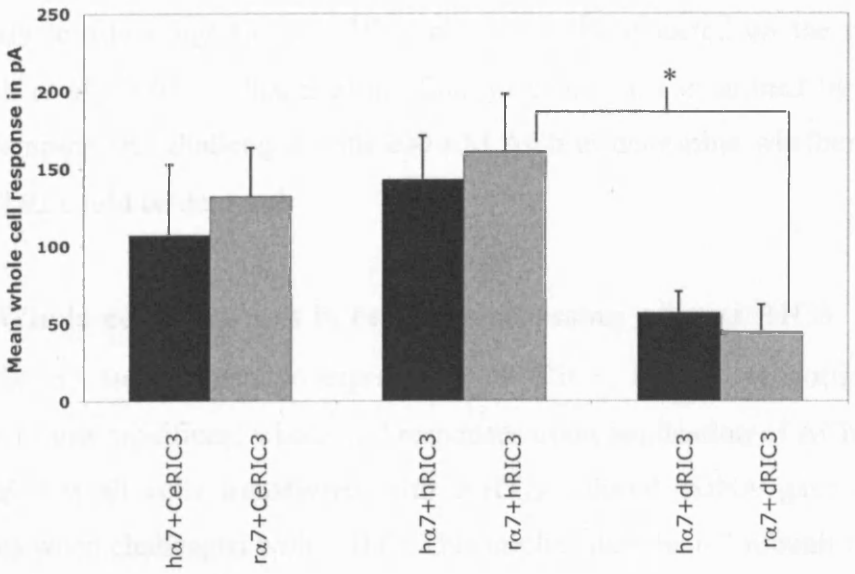

B

	α7 alone	+ Ce RIC3	+ hRIC3	+dRIC3
Human α7	0/9	9/11	13/17	5/5
Rat α7	0/8	6/7	8/8	4/6

Number of cells that responded / total number of cells challenged with 200 μM ACh

Figure 4.2 *Mean size of whole-cell responses of α7 co-expressed with RIC3 in tsA201 cells..*

(A) Mean size of responses in cells transfected with either the human or rat α7 subunit, and either *C.elegans* RIC3, human RIC3 or *Drosophila* RIC3. (B) The table indicates the fraction of cells that responded to 200 μM ACh. The *n* number for the calculated mean is in larger type. The differences between groups were tested for significance with using either a student's t-test or a modified Z test. * indicates $p<0.05$

previous studies that show that no significant α-BTX binding can be detected on the surface of transfected HEK cells when the α7 subunit is expressed alone (Cooper and Millar, 1997). HEK tsA201 cells were transfected with the α7 subunit (human or rat) and RIC3 (*C. elegans*, human or *Drosophila*), which has been shown previously to allow significant α-BTX binding to be detected on the cell surface (Lansdell *et al.*, 2005; Williams *et al.*, 2005). Cells were examined by whole-cell patch-clamping and challenged with 200 μM ACh to determine whether functional α7 nAChRs could be detected.

4.2.1 Whole-cell responses in cells co-expressing α7 and RIC3

When the α7 subunit was co-expressed with RIC3, a large proportion of cells examined show significant whole-cell responses upon application of ACh. It should be noted that all cells transfected with 5-HT_{3A} subunit cDNA gave whole cell responses when challenged with 5-HT. This implies that the α7 subunit is still no as efficient as the 5-HT_{3A} subunit at forming functional receptors even when expressed with RIC3. All combinations of the α7 nAChR subunit (human or rat) and the RIC3 protein (*C. elegans*, human or *Drosophila*) tested showed function in most cells examined (examples of whole-cell responses in Figures 4.3 and 4.4). Of the cells transfected with human α7 subunit and a RIC3 protein, 27/33 gave whole-cell responses when challenged with ACh. Similarly, most cells transfected with rat α7 subunit and a RIC3 protein gave whole-cell responses (18/21). The whole-cell responses ranged from 20 to 300 pA. There was no significant difference in the size of the responses between the human and rat α7 subunit transfections (Figure 4.2). There was also no significant difference in the size of the responses of cells transfected with the human α7 subunit, although it did appear that cells co-expressing the human α7 subunit with the *Drosophila* RIC3 had smaller responses (Figure 4.2). There was no significant difference between the size of the responses in cells with the rat α7 subunit co-expressed with either *C.elegans* or human RIC3, but the responses were significantly smaller in cells co-expressing the rat α7 subunit and *Drosophila* RIC3 (Figure 4.2, $p<0.05$). These data show that the RIC3 protein enables the α7 subunit to fold correctly and form functional receptors. This occurs with mammalian α7 subunits and human, *C. elegans* or *Drosophila* RIC3 proteins, although this appears less efficient with the *Drosophila* RIC3.

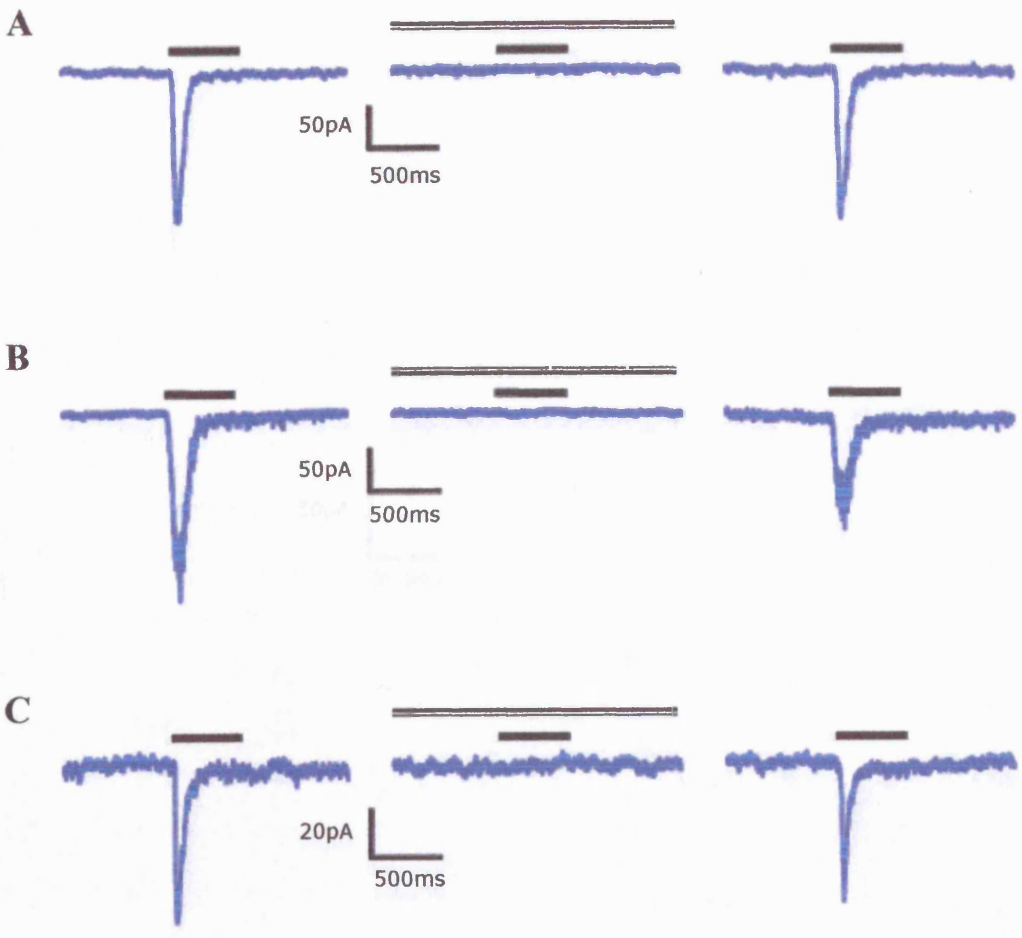

Figure 4.3 *Whole-cell responses of human α7 co-expressed with RIC3 in tsA201 cells.*

Examples of whole-cell responses in cells transfected with the human α7 subunit either with (A) *C.elegans* RIC3, (B) human RIC3 or (C) *Drosophila* RIC3. The lower black bar indicates the application of 200 μM ACh, the upper line indicates the bath application of 100 nM MLA. The right hand column shows responses after the antagonist was washed off.

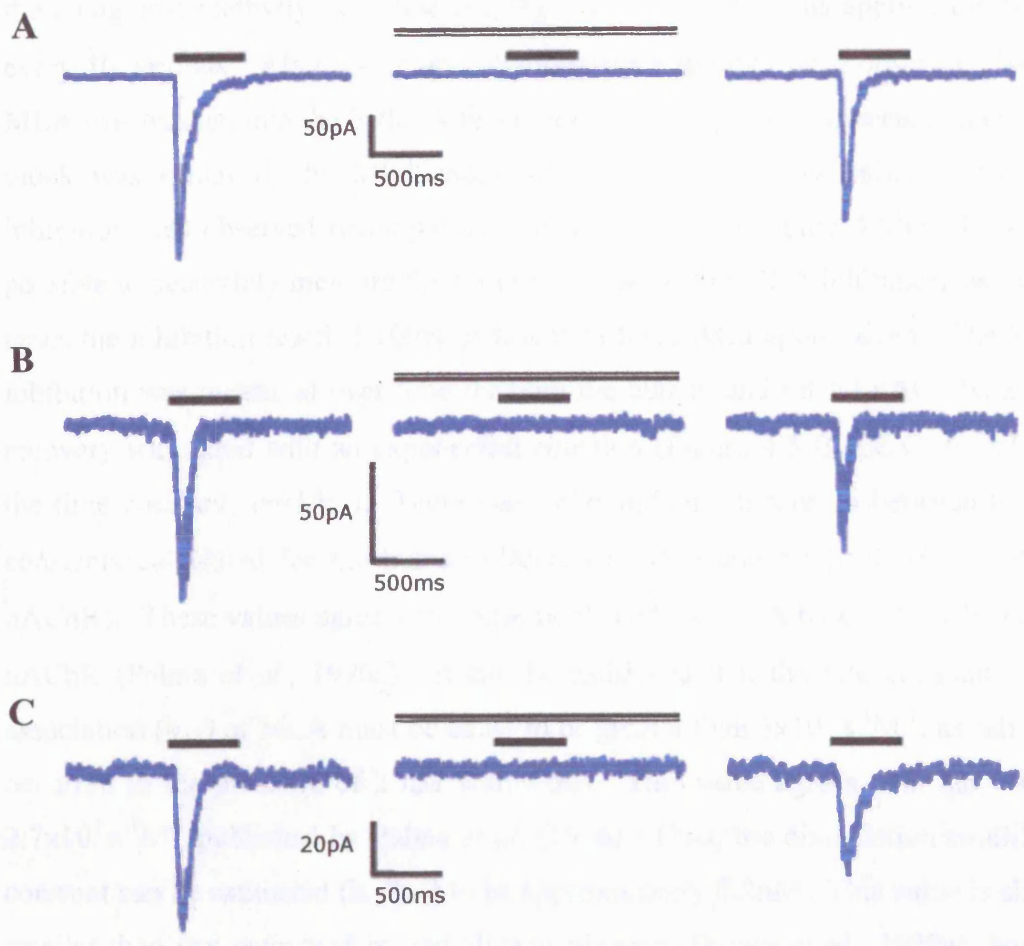

Figure 4.4 *Whole-cell responses of rat α7 co-expressed with RIC3 in tsA201 cells.*

Examples of whole-cell responses in cells transfected with the rat α7 subunit either with (A) *C.elegans* RIC3, (B) human RIC3 or (C) *Drosophila* RIC3. The lower black bar indicates the application of 200 μM ACh, the upper line indicates the bath application of 100 nM MLA. The right hand column shows responses after the antagonist was washed off.

4.2.2 Inhibition of whole-cell responses with an α7 nAChR antagonist

A reversible block of whole-cell responses to ACh was observed on application of the antagonist methyllycaconitine (MLA). ACh (200 μM) was applied for 500 ms every 10 seconds. After stable and reproducible responses were observed, 100 nM MLA was washed into the bath. A fast block of the response was seen, and once full block was achieved, the MLA was washed off and a slow recovery from the inhibition was observed (example of one cell shown in Figure 4.5A). It was not possible to accurately measure the on-time course of the MLA inhibition, as in most cases the inhibition reached 100% in less than three ACh applications. The loss of inhibition was measured over time for both the human and rat α7 nAChRs, and the recovery was fitted with an exponential equation (Figure 4.5 B and C) to calculate the time constant ($\tau=1/k_{-1}$). There was no significant difference between the time constants calculated for the human (189±26 s, n=6) and rat (204±16 s, n=6) α7 nAChRs. These values agree with those published for MLA block of the human α7 nAChR (Palma *et al.*, 1996a). It can be estimated that the rate constant for the association (k_{+1}) of MLA must be equal to or greater than $3x10^7$ $s^{-1}M^{-1}$, as full block occurred in the presence of 2 nM within 30s. This value agrees with the value of $2.7x10^7$ $s^{-1}M^{-1}$ published by Palma *et al.* (1996). Thus, the dissociation equilibrium constant can be estimated (k_{-1}/k_{+1}) to be approximately 0.2nM. This value is slightly smaller than that estimated by radioligand binding (Davies *et al.*, 1999a), however this was done on homogenised rat brain membranes which may not have contained only homomeric α7 nAChRs.

4.3 Functional α8 receptors formed when co-expressed with RIC3

The chick α8 subunit shows close sequence similarity to the α7 subunit (Schoepfer *et al.*, 1990). This subunit can form functional homomeric nAChRs when expressed in *Xenopus* oocytes (Gerzanich *et al.*, 1994, Gotti *et al.*, 1994), and is blocked by the antagonists α-BTX and MLA. Just as with the α7 subunit, there have been problems expressing functional α8 receptors in cell lines such as tsA201 (Cooper and Millar, 1998). It has been shown that when the α8 subunit is co-expressed with RIC3, significant [^{125}I]α-BTX binding can be detected on the cell surface (Lansdell *et al.*, 2005). Surprisingly, when the α8 subunit was expressed alone in tsA201 cells

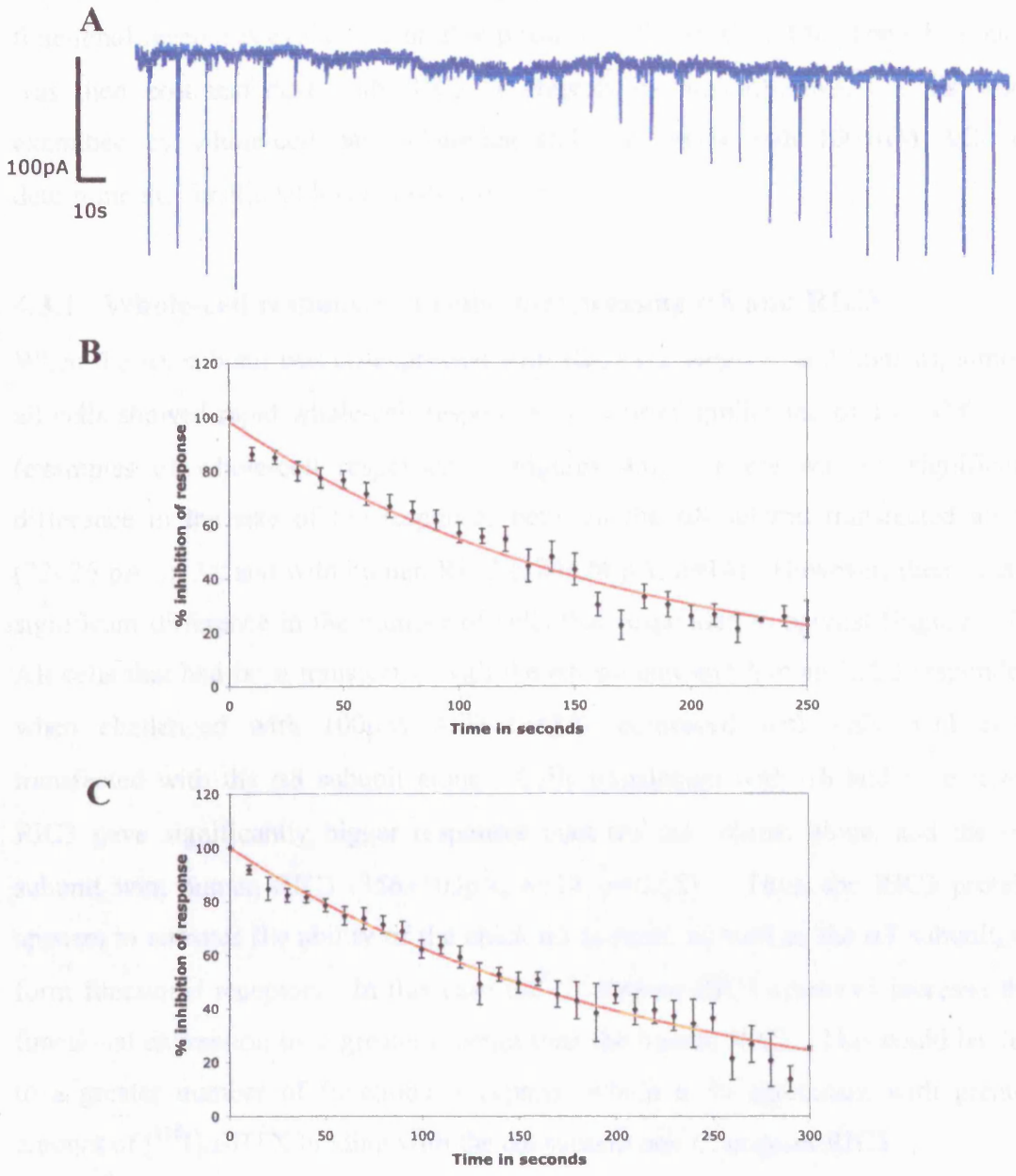

Figure 4.5 *MLA inhibition of response to ACh in tSA201 cells transfected with α7 andRIC3.*

(A) An example of responses to brief (500 ms) agonist applications (200 μM ACh) every 10 seconds, from a cell transfected with the the human α7 subunit and *C.elegans* RIC3. (B) and (C) plot of % of inhibition with time during wash off of MLA for (B) the human α7 subunit co-expressed with RIC3 (n=6) and (C) the rat α7subunit co-expressed with RIC3 (n=5). % of inhibition was calculated by comparing the reponses on recovery to the average of 3 responses before antagonist application.

and examined by whole-cell patch-clamping, a small number of cells (3/11) showed functional responses evoked by brief applications of 100 μM ACh. The α8 subunit was then co-transfected with RIC3 (*C.elegans* or human) DNA. Cells were examined by whole-cell patch-clamping and challenged with 100 μM ACh to determine the functional level of α8 nAChRs.

4.3.1 Whole-cell responses in cells co-expressing α8 and RIC3

When the α8 subunit was co-expressed with RIC3 (*C. elegans* and human), almost all cells showed rapid whole-cell responses upon brief application of 100 μM ACh (examples of whole-cell responses in Figures 4.6). There was no significant difference in the size of the responses between the α8 subunit transfected alone (72±26 pA, n=3), and with human RIC3 (124±24 pA, n=14). However, there was a significant difference in the number of cells that responded to agonist (Figure 4.7). All cells that had been transfected with the α8 subunit and human RIC3 responded when challenged with 100μM ACh (n=14), compared with only 3/11 cells transfected with the α8 subunit alone. Cells transfected with α8 and *C. elegans* RIC3 gave significantly bigger responses than the α8 subunit alone, and the α8 subunit with human RIC3 (356±103pA, n=14, p<0.05). Thus, the RIC3 protein appears to enhance the ability of the chick α8 subunit, as well as the α7 subunit, to form functional receptors. In this case the *C. elegans* RIC3 seems to increase the functional expression by a greater amount than the human RIC3. This could be due to a greater number of functional receptors, which is in agreement with greater amount of [^{125}I]α-BTX binding with the α8 subunit and *C. elegans* RIC3.

4.3.2 Inhibition of whole-cell responses with nicotinic antagonists

MLA was used to block whole-cell responses in cells transfected with α8 and RIC3, but in most cases there was no recovery from this inhibition during the length of the recording. Concentrations as low as 2 nM blocked the response and no recovery was seen with 11/12 cells, even after 25 minutes in one case. The nicotinic antagonist, d-tubocurarine was used as an alternative antagonist that is known to be reversible. Four cells showed reversible block with this antagonist (10 μM, examples of this can be seen in Figure 4.6). The nicotinic antagonist α-BTX (10 nM) was also applied to

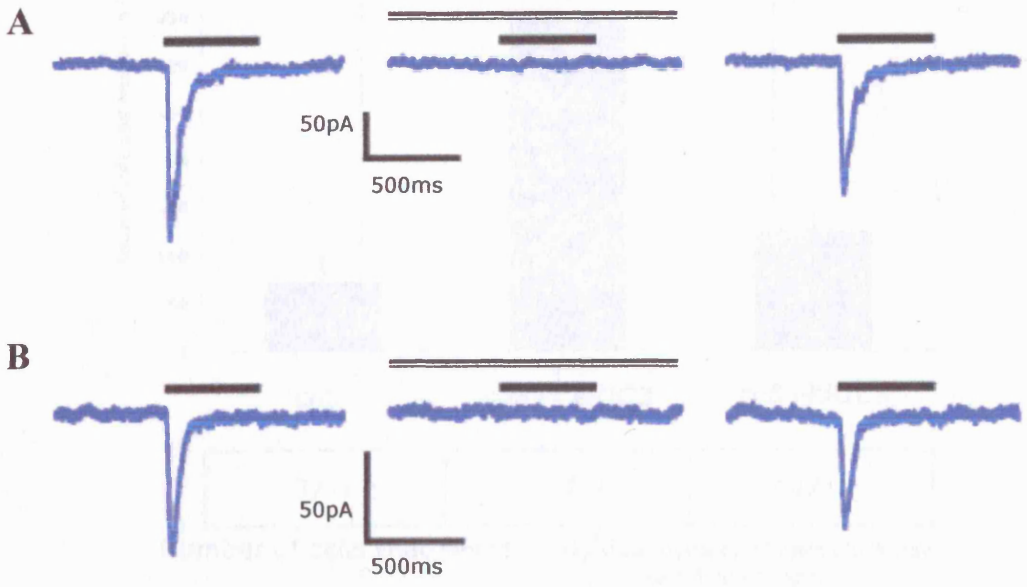

Figure 4.6 *Whole-cell responses of chick α8 co-expressed with RIC3 in tsA201 cells.*

Examples of whole-cell responses in cells transfected with the chick α8 subunit either with (A) *C.elegans* RIC3 or (B) human RIC3. The lower black bar indicates the application of 100 μM ACh, the upper line indicates the bath application of 10 μM d-TC. The right hand column shows responses after the antagonist was washed off.

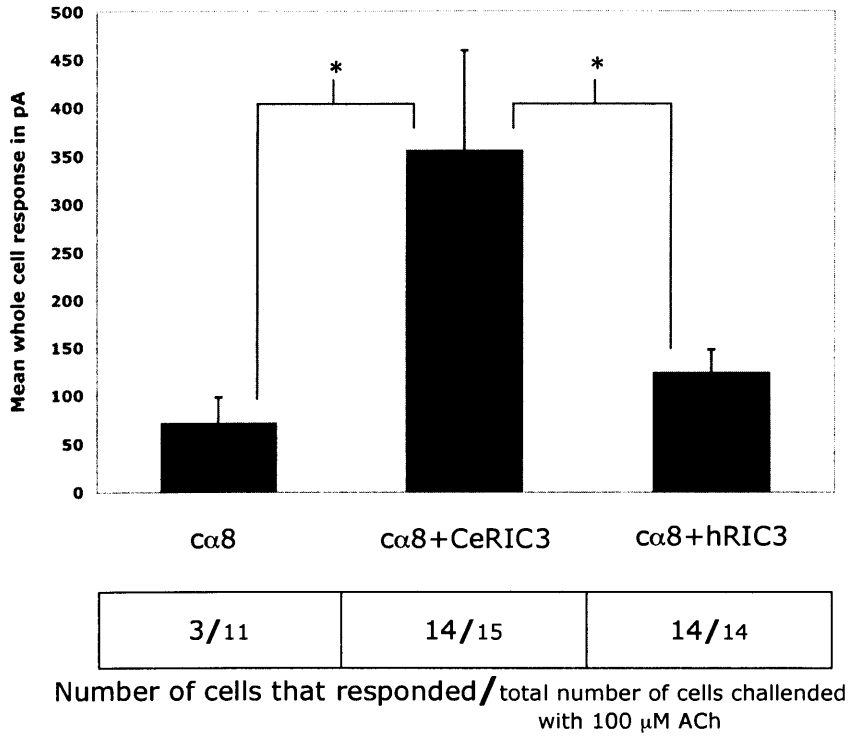

Figure 4.7 *Mean size of whole-cell responses of chick α8 co-expressed with RIC3 in tsA201 cells.*

Mean size of responses in cells transfected with the chick α8 subunit either alone or with *C.elegans* RIC3 or human RIC3. The table below indicates the fraction of cells that responded to 100 μM ACh. The *n* number for the calculated mean is in larger type. The differences between groups were tested for significance with using either a student's t-test or a modified Z test.. * indicates $p<0.05$

two cells that showed some recovery in only a few minutes after washing, implying that this antagonist may be quickly reversible at the chick α8 receptor, unlike the α7 receptor. This rapidly reversible block of α8 with α-BTX has not previously reported. Because the α8 receptor was slower to recover from desensitization than the α7 receptors, it was more difficult to obtain the data required to examine the time course of recovery with this concentration of agonist. The recovery from desensitization was almost as slow as the recovery from block. For this reason there is no analysis on the time course of recovery of antagonist on cells expressing the α8 receptor.

4.4 Functional α3β2 receptors formed when co-expressed with RIC3

Functional expression of rat α3β2 has been reported in *Xenopus* oocytes (Boulter *et al.*, 1987; Luetje and Patrick, 1991; Fenster *et al.*, 1997; Covernton and Connolly, 2000), however there are no reports in mammalian cells. Specific radioligand binding of [^{3}H]epibatidine has been reported to cells transfected with the rat α3 and β2 subunits, but this level of binding is low compared to other nAChR subunit combinations. Co-expression of the rat α3 and β2 subunits with human RIC3 significantly increases the level of binding over four fold (Lansdell *et al.*, 2005). When the rat α3 and β2 subunits were transfected into tsA201 cells and examined by whole-cell patch-clamping, only a few cells showed functional responses (2/10) to 400 μM ACh. The α3 and β2 subunits were also transfected with RIC3 (*C.elegans* or human) and again cells were examined by whole-cell patch-clamping and challenged with 400 μM ACh to determine the functional level of α3β2 nAChRs.

4.4.1 Whole-cell responses in cells co-expressing α3β2 and RIC3

When the α3 and β2 subunits, and RIC3 were transfected together, all the cells patched showed whole-cell responses upon application of ACh (n=18, example traces of responses from cells expressing the α3 and β2 subunits and RIC3 are shown in Figure 4.8). Cells transfected with the α3 and β2 subunits and RIC3 showed significantly larger responses than cells expressing the receptor subunits

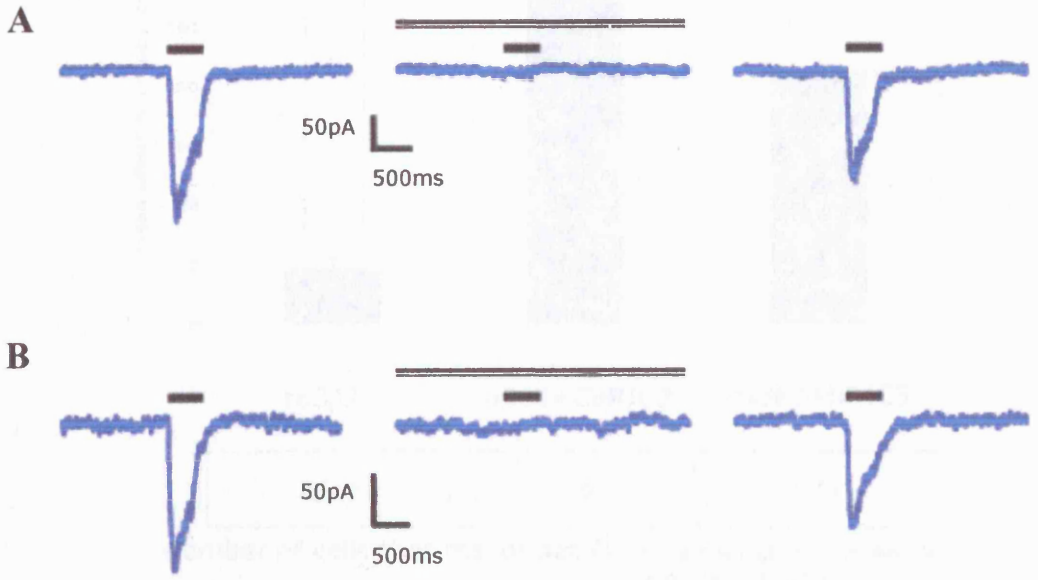

Figure 4.8 *Whole-cell responses of rat α3β2 co-expressed with RIC3 in tsA201 cells.*

Examples of whole-cell responses in cells transfected with rat α3 and β2 subunit either with (A) *C.elegans* RIC3 or (B) human RIC3. The lower black bar indicates the application of 100 μM ACh, the upper line indicates the bath application of 10 μM dTC. The right hand column shows responses after the antagonist was washed off.

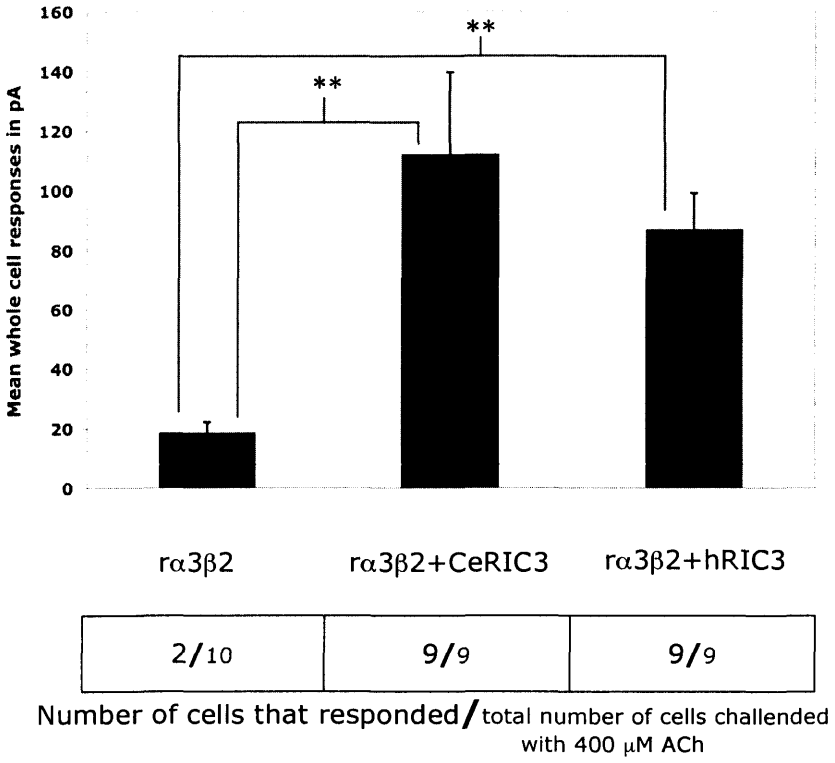

Figure 4.9 *Mean size of whole-cell responses of rat α3β2 co-expressed with RIC3 in tsA201 cells.*

Mean size of responses in cells transfected with the rat α3 and β2 subunits either alone or with *C.elegans* RIC3 or human RIC3. The table below indicates the fraction of cells that responded to 400 μM ACh. The *n* number for the calculated mean is in larger type. The differences between groups were tested for significance with using either a student's t-test or a modified Z test.. ** indicates $p<0.01$

alone (19±3pA, n=2, p<0.01). The mean response with *C. elegans* RIC3 was 112±27pA (n=9), and with human RIC3 was 86±12pA (n=9). There was no significant difference in the size of the responses in cells transfected with the α3 and β2 subunits with *C. elegans* RIC3 compared to human RIC3. Thus co-expression of RIC3 increases the number of cells expressing functional rat α3β2 receptors and also increases the size of the response (Figure 4.9).

4.4.2 Inhibition of whole-cell responses with a nicotinic antagonist

Whole-cell responses were reversibly blocked by the nicotinic antagonist d-tubocurarine (examples shown in Figure 4.8). A complete block of responses to ACh was obtained with 10 μM d-tubocurarine. As with the chick α8 receptor, the rat α3β2 receptor did not recover from desensitization as quickly as the α7 receptor. For this reason, only two responses were made every minute, which made it more difficult to examine the time course of the recovery from block.

4.5 Functional level of 5-HT_{3A} receptors co-expressed with RIC3

The 5-HT_{3A} subunit belongs to the same ligand-gated ion channel family as α7, however it is able to form functional receptors in the cell lines in which no functional α7 receptors can be detected (Cooper and Millar, 1997; Gunthorpe *et al.*, 2000). The murine 5-HT_{3A} subunit has been co-expressed with human RIC3 in *Xenopus* oocytes, and this resulted in the loss of 5-HT-induced currents (Halevi *et al.*, 2003). Human or murine 5-HT_{3A} subunits were expressed alone in tsA201 cells, and examined by whole-cell patch-clamping. Large whole-cell responses were obtained upon application of 2μM 5-HT (see figure 4.10), a value close to the EC_{50} for both the human and murine subunits (Brown *et al.*, 1998; Hubbard *et al.*, 2000). There was no significant difference in the size of the currents obtained with the murine and human 5-HT_{3A} receptors (Figure 4.11). HEK tsA201 cells were transfected with the 5-HT_{3A} subunits (human or murine) and RIC3 (*C. elegans* or human). Cells were examined by whole-cell patch-clamping and challenged with 2 μM 5-HT to determine the functional level of 5-HT_3 receptors.

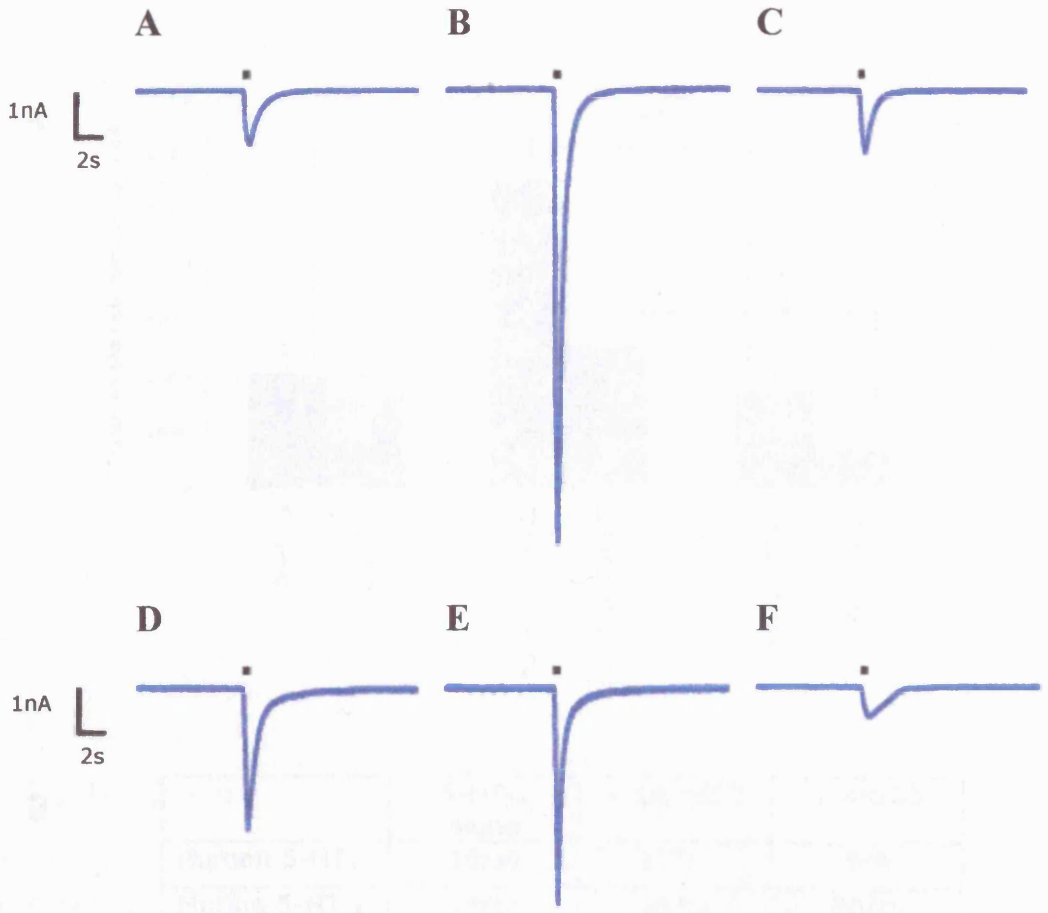

Figure 4.10 *Whole-cell responses of 5-HT_{3A} receptors co-expressed with RIC3 in tsA201 cells.*

Examples of whole-cell responses in cells transfected with the human (A,B and C) or murine (D,E and F) $5HT_{3A}$ subunit either alone (A and D) or with *C.elegans* RIC3 (B and E) or human RIC3 (C and F). The black bars indicate the 500 ms application of 2 μM 5HT.

A

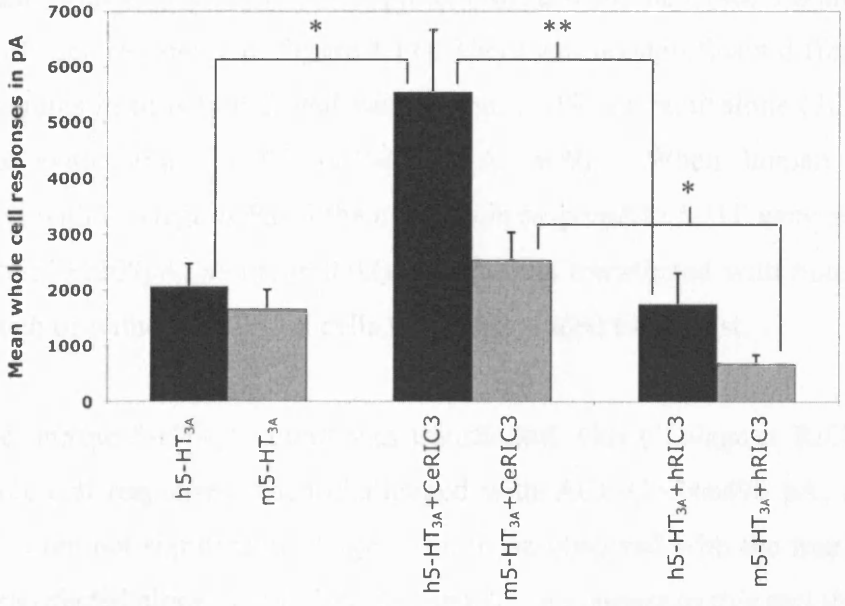

B

	5-HT_{3A} alone	+ Ce RIC3	+ hRIC3
Human 5-HT_{3A}	10/10	11/11	9/9
Murine 5-HT_{3A}	14/14	16/16	20/25

Number of cells that responded/total number of cells challenged with 2 μM 5-HT

Figure 4.11 *Mean size of whole-cell responses of 5-HT_{3A} receptors co-expressed with RIC3 in tsA201 cells..*

(A) Mean size of responses in cells transfected with either human or murine 5-HT_{3A}, and either *C.elegans* RIC3 or human RIC3. (B) The table indicates the fraction of cells that responded to 2 μM 5-HT. The *n* number for the calculated mean is in larger type. Note that all cells tested responded except in the case of murine 5-HT_{3A} co-expressed with hRIC3, where 5/25 cells did not respond. The differences between groups were tested for significance with using either a student's t-test or a modified Z test.. * indicates $p<0.05$, ** indicates $p<0.01$.

4.5.1 Whole-cell responses in cells co-expressing 5-HT_{3A} and RIC3

When 5-HT_{3A} is transfected with RIC3 there are different effects upon the level of function (enhancement versus reduction) depending on which species of 5-HT_{3A} subunit and which species of RIC3 protein were examined (see Figure 4.10 and mean whole-cell responses in Figure 4.11). There was no significant difference in the size of currents in cells transfected with human 5-HT_{3A} subunit alone (2069±397pA, n=10), or with human RIC3 (1750±558pA, n=9). When human 5-HT_{3A} is transfected with *C. elegans* RIC3 the currents in response to 5-HT were significantly greater (5551±1109pA, n=11, p<0.02). With cells transfected with human 5-HT_{3A} subunit with or without RIC3, all cells tested responded to agonist.

When the murine 5-HT_{3A} subunit was transfected with *C. elegans* RIC3, all cells gave whole-cell responses when challenged with ACh (2534±496 pA, n=16), and responses were not significantly larger than those observed with the murine 5-HT_{3A} subunit transfected alone (1651±359 pA, n=14). In contrast to this and the result for the human 5-HT_{3A} subunit, when the murine 5-HT_{3A} subunit was transfected with human RIC3, the whole-cell responses obtained were significantly smaller (669±172 pA, n=20, p<0.05). Also, five of the twenty-five cells tested showed no response to agonist. These results agree with those obtained by using a calcium-influx assay (Doward, 2005). Thus, it seems that the RIC3 protein has differential effects that depend on the which species of the 5-HT_{3A} subunit and the RIC3 protein are co-expressed.

4.6 Functional characteristics of α7 and 5-HT_{3A} expressed with RIC3

The effect on functional characteristics upon co-expression of RIC3 with the α7 and 5-HT_{3A} subunits was examined. It has been reported that interacting proteins can affect the functional characteristics of receptors, for example VILIP-1 and the α4β2 nAChR (Lin *et al.*, 2002) and calmodulin and NMDARs (Ehlers *et al.*, 1996; Rycroft and Gibb, 2002). The rat α7 subunit or murine 5-HT_{3A} subunit was transfected with human RIC3 into HEK tsA201 cells. Rat α7 and murine 5-HT_{3A} were chosen to be investigated as chimeras have been constructed from these two subunits (Chapter 3).

Human RIC3 protein was chosen as it caused an increase in functional expression of the rat α7 receptor and a reduction in functional expression of the murine 5-HT_{3A} receptor (Section 4.2 and 4.5). Rectification, desensitization and single-channel conductance were investigated as described in the Chapter 2, Section 2.7.

4.6.1 Rectification of α7 and 5-HT_{3A} expressed with human RIC3

Previous studies have demonstrated that there is no significant difference between the reversal potentials of the homomeric α7 and 5-HT_{3A} receptors (Puchacz *et al.*, 1994; Hubbard *et al.*, 2000). In contrast, the α7 receptor has been shown to exhibit much greater rectification compared with the 5-HT_{3A} receptor (Puchacz *et al.*, 1994; Hubbard *et al.*, 2000). The current-voltage relationship of the α7 or 5-HT_{3A} subunits co-expressed with RIC3 was investigated by obtaining triplicate responses at holding potentials from -60 to +40 mV (see, for example, Figure 4.12A). The reversal potential and rectification were determined from the current-voltage relations (Figure 4.12B and C). There was no significant difference in the reversal potential between the rat α7 subunit (8.1±2.4 mV, n=6) and the murine 5-HT_{3A} subunit (9.0±3.0 mV, n=5). Co-expression of RIC3 with murine 5-HT_{3A} subunit caused no significant difference in the reversal potential compared to murine 5-HT_{3A} subunit alone (1.2±1.3 mV, n=5). There was also no significant difference between the rat α7 subunit and three α7/5-HT_{3A} chimeras ($\alpha7^{V2015\text{-}HT_{3A}}$, 4.8±2.6 mV; $\alpha7^{4TM\text{-}5\text{-}HT_{3A}}$, 6.6±2.4 mV; $5\text{-}HT_{3A}^{3\text{-}4Loop\text{-}\alpha7}$, 5.8±2.6 mV; n=5, Chapter 3). Thus it appears that the RIC3 protein does not alter the reversal potential when expressed with the murine 5-HT_{3A} receptor subunit.

The rectification characteristics of the murine 5-HT_{3A} receptor were not affected by co-expression of RIC3. There was little or no rectification seen in the current-voltage relation for the 5-HT_{3A} subunit expressed alone (Figure 3.10B) or with human RIC3 (Figure 4.12B). There was no significant difference in the coefficient of rectification (method of calculation in Chapter 2, Section 2.7.3) between the murine 5-HT_{3A} subunit expressed alone (0.93±0.08, n=5), or with human RIC3 (0.95±0.20, n=5). As has been shown previously for the α7 receptor, the rat α7 receptor showed much greater rectification, that can be seen in the current-voltage relationship (Figure 3.10A and C). The coefficient of rectification was significantly lower with

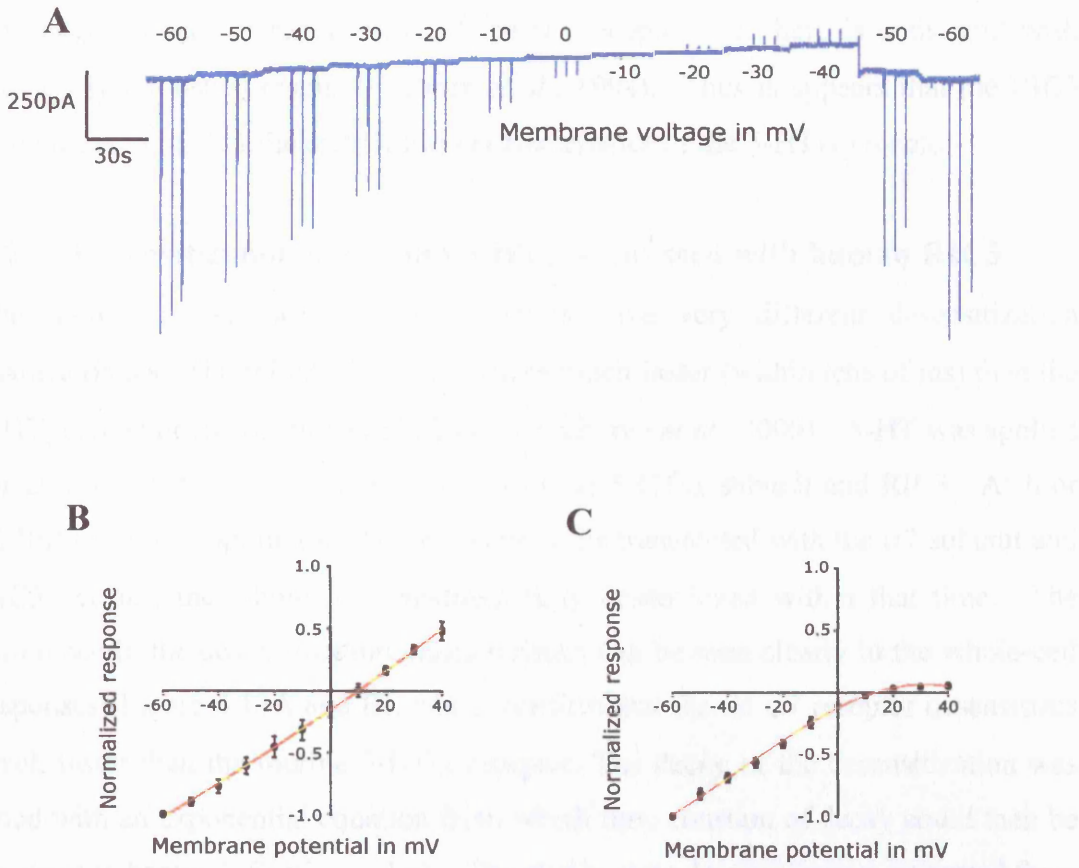

Figure 4.12 *Current voltage relations of whole-cell responses from tsA201 cells transiently transfected with 5-HT_{3A} or α7 and RIC3.*

(A), an example of brief (500 ms) agonist applications (200 μM ACh) done in triplicate to obtain current-voltage relation, with a cell transfected with the rat α7 subunit and human RIC3. (B) and (C) current-voltage plot for murine $5HT_{3A}$ co-expressed with human RIC3 (B) and rat α7 co-expressed with human RIC3 (C), The responses were normalised to the response obtained at -60 mV. *n*=5-6.

the α7 subunit (0.18±0.04, n=6, p<0.005), than observed with the 5-HT_{3A} subunit (transfected with or without human RIC3), or any of the three α7/5-HT_{3A} chimeras ($\alpha7^{V2015\text{-}HT_{3A}}$, 0.94±0.08; $\alpha7^{4TM\text{-}5\text{-}HT_{3A}}$, 1.01±0.15; 5-$HT_{3A}^{3\text{-}4Loop\text{-}\alpha7}$, 1.08±0.04; n=5). The large amount of rectification of the α7 receptor seen here is consistent with previously published results (Puchacz *et al.*, 1994). Thus is appears that the RIC3 protein does not alter the rectification characteristics of the 5-HT_{3A} receptor.

4.6.2 Desensitization of α7 and 5-HT_{3A} expressed with human RIC3

The homomeric α7 and 5-HT_{3A} receptors have very different desensitization characteristics. The α7 nAChR desensitizes much faster (within tens of ms) than the 5-HT_{3A} receptor (Ragozzino *et al.*, 1997; Gunthorpe *et al.*, 2000). 5-HT was applied for 20 seconds to the cells transfected with the 5-HT_{3A} subunit and RIC3. ACh or DMPP were only applied for 500 ms to the cells transfected with the α7 subunit and RIC3 because the whole-cell responses fully desensitized within that time. The difference in the desensitization characteristics can be seen clearly in the whole-cell responses (Figure 4.13A and B), which confirm that the rat α7 receptor desensitizes much faster than the murine 5-HT_{3A} receptor. The decay of the desensitization was fitted with an exponential equation from which time constant of decay could then be obtained (Chapter 2, Section 2.7.4). The steady state desensitization estimated from the single exponential fitting of a response from a 20 second agonist application for 5-HT_{3A} and 500 ms agonist application for α7 was also compared.

There was no significant difference in either the time constant of decay or the percentage of desensitization of whole-cell responses between cells transfected with the murine 5-HT_{3A} subunit alone, or with human RIC3. The time constant for decay for the murine 5-HT_{3A} subunit with human RIC3 (6895±1682 ms, n=6, Figure 4.13C) was not significantly smaller than the 5-HT_{3A} subunit alone (9201±1345 ms, n=6). The steady state desensitization was approximately the same with murine 5-HT_{3A} with RIC3 (91.7±3.2%) as with murine 5-HT_{3A} alone (89.9±2.5%). It appears that the co-expression of the murine 5-HT_{3A} subunit with human RIC3 does not affect the characteristics of desensitization of this receptor.

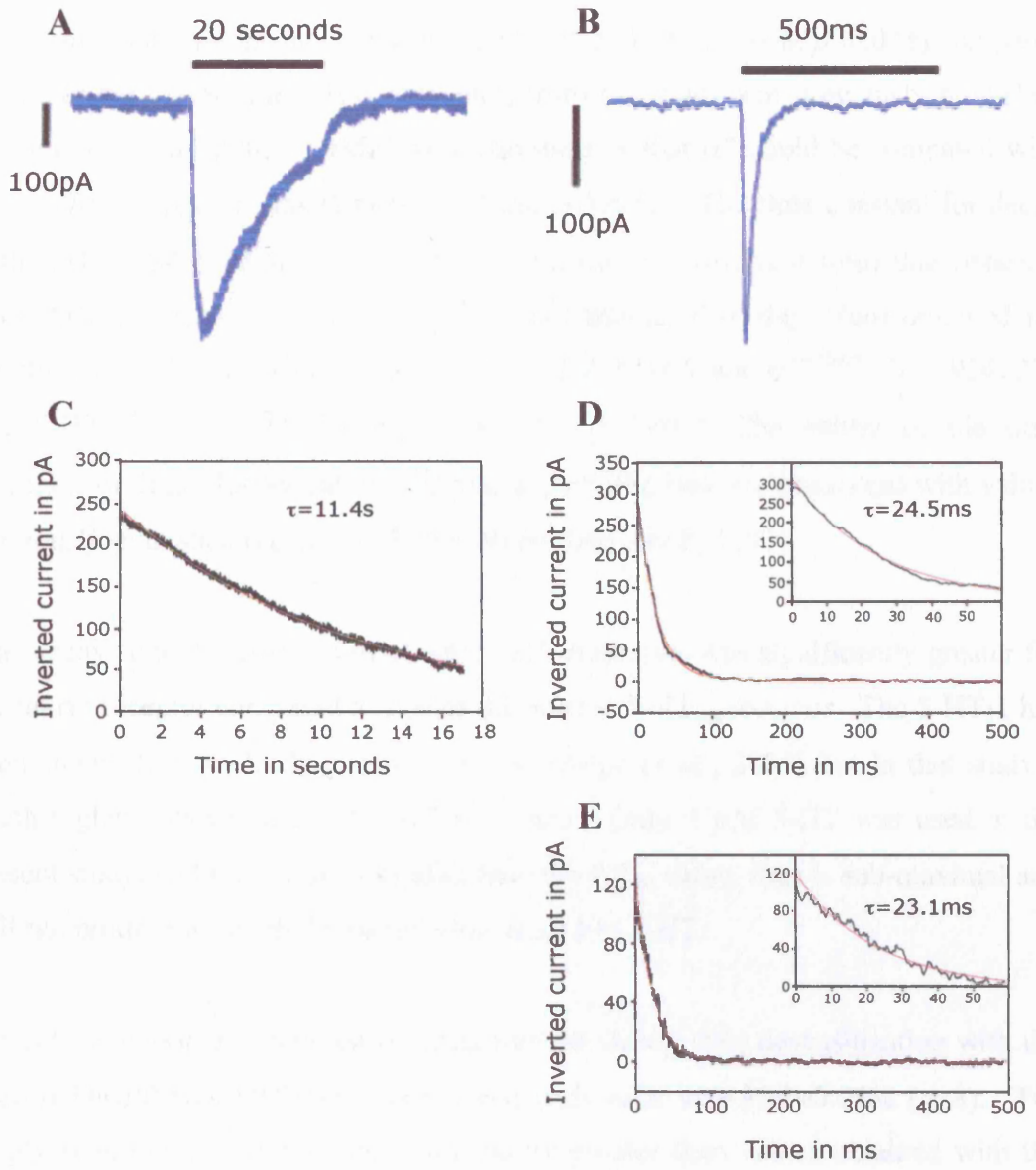

Figure 4.13 *Desensitization analysis of whole-cell responses from tsA201 cells transiently transfected with 5-HT$_{3A}$ or α7, and RIC3.*

Whole cell responses were analysed to obtain the time constant of decay and the percentage of desensitization. (A) and (C): the murine 5-HT$_{3A}$ subunit co-expressed with human RIC3, with a 20 second application of 1 μM 5-HT. (B), (D) and (E): the rat α7 subunit co-expressed with human RIC3, with 500 ms application of (D) 200 μM ACh and (E) 200 μM DMPP. (A) and (B) show examples of the redordings used for analysis. (C), (D) and (E) show examples of average of the responses from one cell (n=3-5), inverted and fitted with an exponential equation to estimate the time constant of decay and the percentage of desensitization.

Cells expressing the rat α7 subunit and human RIC3 gave whole-cell responses that had significantly faster time constants (ACh, 66.5±12.8 ms, n=8, p<0.001) compared to values for the murine 5-HT_{3A} receptor, from this study and previously published (Gunthorpe *et al.*, 2000). DMPP was also used so that α7 could be compared with three α7/5-HT_{3A} chimeras (Chapter 3, Section 3.6.1). The time constant for decay with DMPP (54.7±16.5ms, n=7) was not significantly different from that obtained from ACh applications, and was significantly smaller than the values obtained for the three α7/5-HT_{3A} chimeras ($\alpha7^{V2015\text{-}HT_{3A}}$, 223.2±31.5 ms; $\alpha7^{4TM\text{-}5\text{-}HT_{3A}}$, 924±220 ms; 5-$HT_{3A}^{3\text{-}4Loop\text{-}\alpha7}$, 7067±878 ms; n=6-8) (p<0.001). The values of the time constants of decay for the rat α7 receptor determined here are consistent with values previously published (chick α7, 75 ms; Ragozzino *et al.*, 1997).

The steady state desensitization of whole-cell responses was significantly greater for the rat α7 receptor compared to that of the murine 5-HT_{3A} receptor. The 5-HT_{3A} has been shown to completely desensitize (Gunthorpe *et al.*, 2000) but in that study a much higher concentration of 5-HT was used. Only 1 μM 5-HT was used in the present study, and this value is smaller than the EC_{50} value, thus is sub-maximal and will not produce as much desensitization as 30 μM 5-HT.

For cells expressing functional α7 receptors the steady state desensitization with the agonist DMPP was 99.9±0.6% (n=7) and with ACh was 99.5±0.03% (n=8). The steady state desensitization was significantly greater than values obtained with the same concentration of DMPP, from cell transfected with one of two α7/5-HT_{3A} chimeras ($\alpha7^{V2015\text{-}HT_{3A}}$, 70.8±3.2%; $\alpha7^{4TM\text{-}5\text{-}HT_{3A}}$, 64.6±2.9%; p<0.001). There was no difference in the steady state desensitization after 500 ms with ACh compared to DMPP. This complete desensitization seen for the rat α7 receptor is consistent with responses reported previously (Gopalakrishnan *et al.*, 1995).

4.6.3 Single-channel conductance of 5-HT_{3A} expressed with human RIC3

Single-channel conductance was estimated for the murine 5-HT_{3A} receptor using noise analysis. Due to the rapid desensitization of the rat α7 receptor it was not possible to obtain a reliable estimate. A very large number of responses (>100) would be needed per cell to perform the analysis as the responses are so short. The

murine 5-HT_{3A} receptor has been shown to have a small single-channel conductance of about 0.7±0.1 pS (Chapter 3, Section 3.6.3, Hussy *et al.*, 1994; Kelley *et al.*, 2003).

As with murine 5-HT_{3A} subunit transfected alone, there was little detectable noise during agonist application in cells where the murine 5-HT_{3A} subunit was co-expressed with human RIC3 (Figure 3.14A). Noise analysis was performed on long responses (as described in Chapter 2, Section 2.7.5). There was no significant difference in the estimate of the single-channel conductance by the variance method for the murine 5-HT_{3A} subunit alone (0.50±0.06 pS, n=8) compared with the 5-HT_{3A} subunit expressed with human RIC3 (0.62±0.15pS, n=6). Noise power spectral density analysis also showed no significant effect of RIC3 on single-channel conductance. The single-channel conductance of the 5-HT_{3A} subunit expressed alone was 0.67±0.10pS (n=8), and the 5-HT_{3A} subunit expressed with RIC3 was 0.81±0.13pS (n=6). Using the noise power spectral density method of analysis the kinetics of channel gating were characterized (see Chapter 2 Section 2.7.5.2). There was no significant difference between the mean single-channel open time of the murine 5-HT_{3A} alone (τ=24.2±4.3 ms, n=8) and with human RIC3 (τ=36.9±11.4 ms, n=6). Thus, co-expression of human RIC3 does not appear to change the single-channel conductance or the channel kinetics of the murine 5-HT_{3A} receptor.

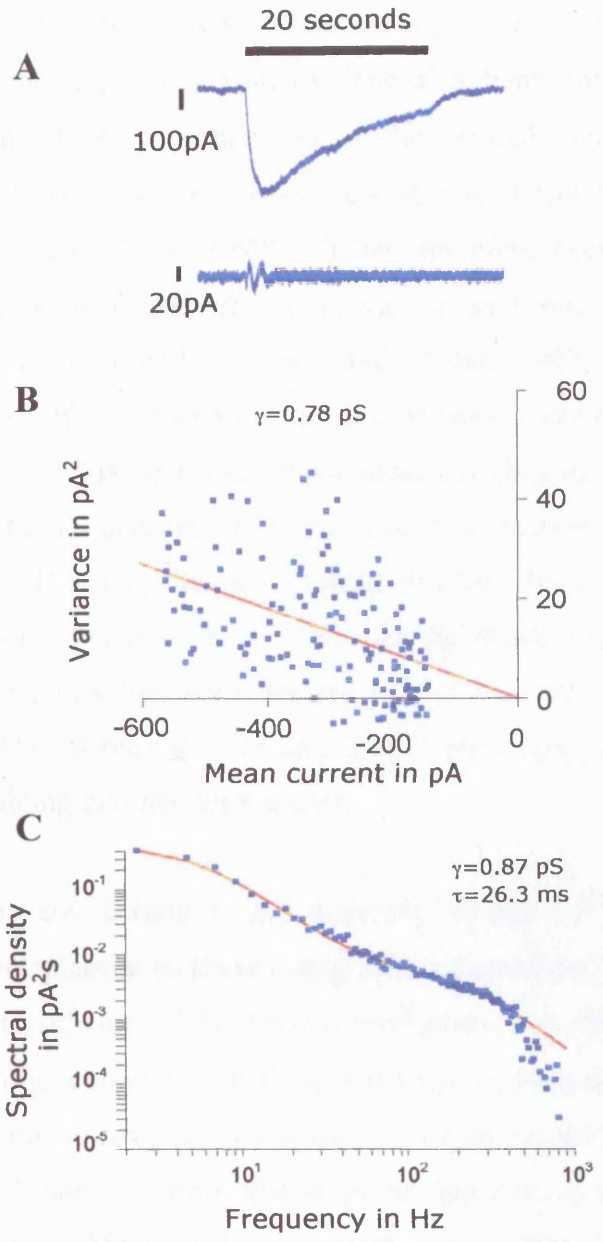

Figure 4.14 *Noise analysis of whole-cell responses from tsA201 cells transiently transfected with 5-HT$_{3A}$ and RIC3.*

20 second agonist applications were analysed to obtain the single channel conductance of the 5-HT$_{3A}$ subunit. Results for one cell are shown. (A), An example of a response, the black above the trace indicates the agonist application. (B), Estimation of single channel conductance by the variance method. (C), Estimation of single channel conductance by the noise power spectral density.

4.7 Discussion

There have been difficulties reported for the expression of functional α7 nAChRs in many heterologous expression systems. The α7 subunit protein can be detected, for example by immunoprecipitation, but neither specific binding with α-BTX nor conformationally sensitive antibodies were able to detect the appropriately folded protein (Cooper and Millar, 1997). It has, therefore been proposed that the α7 subunit is incorrectly folded when expressed in such host cell types as HEK and chinese hamster ovary cells (Cooper and Millar, 1997; Sweileh *et al.*, 2000). Although the α7 subunit forms functional homomeric receptors in *Xenopus* oocytes (Couturier *et al.*, 1990a) and some mammalian cell lines such as GH_4C_1 (Virginio *et al.*, 2002), little is understood about how this protein folds into the correct conformation. The *Torpedo* and muscle nAChRs have been more extensively studied (Chapter 1, Section 1.3.1). Although the muscle nAChR forms receptors in many cell lines, this has been shown to be slow and inefficient (Merlie and Lindstrom, 1983, Wanamaker *et al.*, 2003), with only 20-30% of synthesized subunits assembling into mature receptors.

Various factors are thought to aid assembly of non-α7 nAChR subunits. For example the endoplasmic reticulum chaperone calnexin has been shown to associate with nascent α1 subunits. This interaction decreases shortly before assembly with other subunits (Gelman *et al.*, 1995) and calnexin has been shown to enhance surface expression of muscle nAChRs when they are co-expressed in HEK cells (Chang *et al.*, 1997). BiP has also been shown to be involved in the assembly of muscle nAChR (Blount and Merlie, 1991; Forsayeth *et al.*, 1992). The neuronal subunit α4 interacts with the chaperone protein 14-3-3η, and this interaction significantly increases the steady state levels of α4β2 receptors (Jeanclos *et al.*, 2001). Thus it was not unexpected to find a protein that, when co-expressed with the α7 subunit, increased cell surface expression and function of this nAChR.

The RIC3 protein has been shown to have an effect on nicotinic receptors of *C. elegans* (Halevi *et al.*, 2002). RIC3 has also been shown to cause a functional upregulation of rat and human α7 receptors when expressed in *Xenopus* oocytes, indicating that it may interact with these receptors (Halevi *et al.*, 2002; Halevi *et al.*,

2003). These results suggest that the RIC3 protein may enable the α7 subunit to fold correctly in cells that are not normally permissive, allowing the formation of functional receptors. Radioligand binding and immunoblotting studies in HEK cells have shown that both human and rat α7 subunits, when co-expressed with human or *C. elegans* RIC3, form α-BTX binding sites on the cell surface (Lansdell *et al.*, 2005; Williams *et al.*, 2005). The human α7 subunit has been shown to co-assemble with the human RIC3 protein, as demonstrated by co-immunoprecipitation (Lansdell *et al.*, 2005, Williams *et al.*, 2005). These results support the idea that RIC3 associates with α7 and helps the protein fold correctly. This chapter has investigated the effect of RIC3 upon the level of functional α7 receptors and some of the functional characteristics of the receptor.

4.7.1 RIC3 co-expressed with the α7 nAChR subunit

In the present study, no functional human or rat α7 receptors could be detected in tsA201 cells transfected with only the α7 cDNA. When any of the three RIC3 constructs (*C. elegans*, human or *Drosophila*) were co-expressed with the α7 receptors, whole-cell responses were seen in response to ACh in a large proportion of the cells. Thus, in the presence of RIC3, not only is the α7 protein now folded in such a way that it allows α-BTX to bind, but the subunits assemble into functional receptors. The whole-cell responses that were obtained with ACh could be blocked with the α7/α8 selective antagonist MLA. The recovery from block by MLA displayed a time course that was consistent with data previously reported for α7 (Palma *et al.*, 1996a). The rat α7 receptors expressed with human RIC3 have functional characteristics that are typical for the α7 receptor. They show strong inward rectification, which has been reported repeatedly for α7 receptors (Puchacz *et al.*, 1994; Forster and Bertrand, 1995). The α7 receptors are known to desensitize rapidly (Virginio *et al.*, 2002; Ragozzino *et al.*, 1997). The results from this thesis show clearly that, when expressed with human RIC3, the rat α7 also desensitizes rapidly, with a time constant of only tens of ms with both the natural agonist ACh and also in response to DMPP.

Thus it seems that the RIC3 protein associates with the α7 subunits, and allows the subunits to fold correctly or associate with each other correctly to form both the α-BTX binding site and a functional receptor. This agrees with the results of Castillo *et al.* (2005), who suggest that the RIC3 protein acts to both increase the number of mature or correctly folded receptors and also facilitate the transport of the receptor to the cell surface. As functional characteristics of the rat α7 receptor with RIC3 are in agreement with data already published in the literature (Puchacz *et al.*, 1994; Gopalakrishnan *et al.*, 1997; Ragozzino *et al.*, 1997), it is possible that in all the expression systems where the α7 subunit is able to form functional receptors an endogenous RIC3 protein may be expressed. A *Xenopus* RIC3 homologue has been cloned (Halevi *et al.*, 2003), and endogenous RIC3 transcripts have been identified in SH-SY5Y cells, a human neuroblastoma cell line (Lansdell *et al.*, 2005), which expresses functional endogenous α7 receptors (Puchacz *et al.*, 1994).

4.7.2 RIC3 co-expressed with other nAChR subunits

RIC3 has been reported to increase the levels of other nicotinic receptors. The α8 subunit gives no specific binding when expressed alone (Cooper and Millar, 1998), and the rat α3 and β2 subunits give low levels (Xiao and Kellar, 2004; Lansdell *et al.*, 2005). Radioligand binding studies with the chick α8 and rat α3β2 nicotinic receptors (with [^{125}I]α-BTX and [^{3}H]epibatidine respectively) showed increased number of radioligand binding sites when co-expressed with RIC3 (Lansdell *et al.*, 2005). The effect of RIC3 upon the level of functional expression of these nicotinic receptors was investigated to determine if, as with the α7 receptor, co-expression of RIC3 increases the expression of functional receptors.

When the α8 subunit was expressed alone, most cells examined by whole-cell patch-clamping gave no response to agonist, although 3/11 gave small whole-cell responses. Response in cells expressing only the α8 subunit was unexpected because no specific binding has been detected with [^{125}I]α-BTX when the α8 subunit was expressed alone (Cooper and Millar, 1998). The absence of specific [^{125}I]α-BTX binding could be due to only a very small number of cells expressing correctly folded and thus functional receptors, so small that it cannot be detected by radioligand binding. This conclusion is supported by the results that when cells are

transfected with both the α8 subunit and the RIC3 protein (*C.elegans* or human), there was a significant level of binding (Lansdell *et al.*, 2005) and 28 out of 29 cell examined gave whole-cell responses when challenged with an agonist. The whole-cell responses were blocked by the α7/α8 selective antagonist MLA and recovery did not occur within the time of the whole-cell recording. There is no data published on the reversibility of the block by MLA on recombinant α8 receptors. The nicotinic antagonist d-tubocurarine reversibly blocked the whole-cell responses. The antagonist α-BTX was also used to block the responses, but it was ambiguous whether this block was reversible. Thus it seems that the RIC3 protein allows more α8 subunits to fold correctly or associate with each other correctly to form both the α-BTX binding site and a functional receptor.

When the rat α3 and β2 subunits were expressed together most cells patched gave no response to agonist, although 2/9 cells gave measurable whole-cell responses. This is in agreement with the low level of radioligand binding observed compared to other subunit combinations such as α3β4, which has a B_{max} 150 times greater than α3β2 (Xiao and Kellar, 2004). No data has been published on the function of rat α3β2 receptors in mammalian cells. This is not surprising as the 2 out of 9 cells that did respond to agonist had very small responses to 400μM ACh, a concentration more than 2 fold greater than the EC_{50} obtained in *Xenopus* oocytes (two components: 6.9±2.0μM and 170±120μM; Covernton and Connolly, 2000). Such a small number of cells producing functional receptors would make it difficult to examine function by whole-cell patch-clamping. When the rat α3 and β2 subunits were co-expressed with RIC3 (*C. elegans* or human) all cells that were challenged with agonist gave whole-cell responses, and the mean size of the responses was significantly greater than that of responses obtained in cells without RIC3. These responses were reversibly blocked with d-tubocurarine, a nicotinic antagonist.

The action of RIC3 is not restricted to the α7 nAChR. RIC3 causes the functional upregulation of both chick α8 and rat α3β2 receptors. In addition it has been shown that human RIC3 also increases the number of epibatidine binding sites and the calcium influx upon agonist application in cells expressing rat α3β4, α4β2 and α4β4, (Lansdell *et al.*, 2005). Human RIC3 assembles with rat α4β2, shown by

immunoprecipitation (Lansdell *et al.*, 2005). It has also been demonstrated that co-expression of RIC3 has no effect on α9α10 receptor expression in tsA201 cells (Lansdell *et al.*, 2005). Thus, RIC3 is a general nicotinic receptor-associated protein that can up regulate the functional expression of many but not all nicotinic subtypes.

4.7.3 RIC3 co-expressed with 5-HT_{3A} receptors

The nicotinic receptors are not the only ligand-gated ion channels that are affected by RIC3. Human RIC3 has been shown to almost completely abolish function of the murine 5-HT_{3A} receptor expressed in *Xenopus* oocytes (Halevi *et al.*, 2003). Human 5-HT_{3A} has also been shown to transiently interact with human RIC3 (Cheng *et al.*, 2005). Radioligand binding studies conducted in a mammalian cell line have shown that the total number of 5-HT_3 receptor binding sites is greater with co-expression of either *C.elegans* or human RIC3 (Doward, 2005). However use of an enzyme-linked antibody assay has revealed differences between the murine and human forms of 5-HT_{3A} (Doward, 2005). There is no difference in the amount of murine 5-HT_{3A} receptor detected on the cell surface with or without RIC3 (*C.elegans* or human), but a greater amount of human 5-HT_{3A} receptor has been detected on the cell surface when co-expressed with RIC3 (Doward, 2005). In the present study the effect of RIC3 upon the level of functional expression of human and rat 5-HT_{3A} receptors in tsA201 cells was investigated to determine if, as with the α7 receptor, co-expression of RIC3 increases the level of functional expression. Radioligand binding assays show more 5-HT_{3A} receptor on the cell surface with co-expression of RIC3, suggesting that the level of function expression should also be greater. However, the enzyme-linked antibody assay show no difference in the level of murine 5-HT_{3A} subunit on the cell surface when it is co-expressed with RIC3, which suggests that level of functional expression of this receptor will be no different.

The 5-HT_{3A} receptor (human or rat) gave whole-cell responses from all cells challenged with 5-HT. When *C. elegans* RIC3 was co-expressed with the murine 5-HT_{3A} subunit no difference was detected in the size of the responses. In contrast there was an increase the mean size of the responses to 5-HT in cells expressing the human 5-HT_{3A} subunit and *C. elegans* RIC3 compared to human 5-HT_{3A} alone. When human RIC3 was co-expressed with the human 5-HT_{3A} subunit it had no

effect on the level of receptor function. This agrees with the results of Cheng *et al.*, 2005, who also showed that increasing the amount of RIC3 DNA used for transfection of cells caused an increase in the number of surface receptors and in receptor function in a concentration-dependent manner. Co-expression of human RIC3 with murine 5-HT_{3A} caused a reduction in the magnitude of responses (mean response was decreased to 40% of the size of the response with murine 5-HT_{3A} alone), and some cells showed no response at all. This reduction is not as great a decrease as seen in *Xenopus* oocytes (Halevi *et al.*, 2003), which highlights again the differences that the expression system appears to exert. The functional characteristics of the murine 5-HT_{3A} subunit when expressed with RIC3 are not significantly different from the murine 5-HT_{3A} subunit expressed alone (Chapter 3, Section 3.6). The desensitization, reversal potential and rectification, and single-channel conductance are all the same with and without the RIC3 protein.

The presence of an extracellular isoleucine (I^{218}) just before the first putative transmembrane domain has been reported as responsible for the loss of functional murine 5-HT_{3A} receptors in *Xenopus* oocytes, by hindering the transport of mature receptors to the cell surface (Castillo *et al.*, 2005). However, in mammalian cells the human RIC3 protein causes a decrease in function (assayed by recordings of agonist-induced changed in levels of intracellular calcium and by whole-cell electrophysiological recording), but no change in the surface levels of the murine 5-HT_{3A} receptor (Doward, 2005). These results seem contradictory, however these differences could be explained by a decrease in the agonist sensitivity of the 5-HT_{3A} receptor. The alteration of agonist sensitivity of a nAChR has been shown previously with VILIP-1 and the $\alpha4\beta2$ receptors (Lin *et al.*, 2002). However the human RIC3 and the 5-HT_{3A} subunit have been shown to interact only transiently (Cheng *et al.*, 2005), so if RIC3 does affect the agonist sensitivity, this might require a long-lasting modification of the receptor that was retained after the two proteins separated. Alternatively, the human RIC3 protein might decrease the proportion of functional murine 5-HT_{3A} receptors expressed on the cell surface, without affecting the total amount of subunit protein. This does not agree with the radioligand binding data, which suggests that there are more correctly folded 5-HT_{3A} receptors on the cell surface when the subunit is co-expressed with RIC3.

Further experiments with RIC3 need to be performed to investigate the discrepancies between the radioligand binding, enzyme-linked assays and functional assays and also to confirm the mechanism of action of RIC3 upon the subcellular trafficking and the resulting functional expression of the 5-HT_{3A} subunit. Future studies can do be done to examine which regions of the subunits that have been shown to interact with RIC3 are needed for this interaction.

CHAPTER 5
CONCLUSION

5.1 Inefficient folding of the α7 nAChR subunit

The folding and assembly of the muscle nAChR has been demonstrated to be inefficient, with only 30% of synthesized α subunits assembling into receptors (Merlie and Lindstrom, 1993). The α7 subunit has been reported to form no functional recombinant receptors in some cell lines (for example HEK and COS) in which functional recombinant muscle nAChR, other neuronal nAChRs and 5-HT_3Rs are detected (Cooper and Millar, 1997; Sweileh *et al.*, 1998; Gunthorpe *et al.*, 2000). The α7 subunit is able to form functional receptors in *Xenopus* oocytes (Couturier *et al.*, 1990a) and some neuronal cell lines (Puchaz *et al.*, 1994; Cooper and Millar, 1997; Virginio *et al.*, 2002) and the protein is detected in HEK cells by antibodies to a linear epitope, but not by conformationally sensitive antibodies (Cooper and Millar, 1997). Thus, it has been suggested that some cell lines lack factors such as chaperones that are needed for the α7 subunit to fold correctly. Both the α7 subunit and the 5-HT_{3A} subunit are able to form functional homomeric receptors in *Xenopus* oocytes, but despite forming similarly complex structures to make functional receptors, the 5-HT_{3A} has been demonstrated to do this efficiently in all cell lines tested.

5.1.1 α7/5-HT_{3A} chimeras

A chimera with the N-terminal extracellular domain of α7 and the transmembrane and intracellular domains of the 5-HT_{3A} subunit has been demonstrated to form functional receptors gated by ACh in HEK cells, where no α7 function is detected (Eiselé *et al.*, 1993; Cooper and Millar, 1997). The present study has extended the research previously published by narrowing down which regions within the transmembrane and C-terminal domains of the 5-HT_{3A} subunit confer the ability to fold and assemble efficiently into functional receptors in HEK tsA201 cells.

A series of α7/5-HT_{3A} chimeras was constructed replacing various domains of α7 for the equivalent 5-HT_{3A} sequence (Chapter 3, Figure 3.1) and the cell surface expression of correctly folded receptors was established by radioligand binding and enzyme-linked assays. Chimeras showing cell surface expression were then tested for function using a calcium-sensitive dye in a FLIPR based assay and by whole-cell patch-clamp recording. In each case where surface expression was found, the

receptors were functional suggesting only correctly folded (and hence functional) receptors are transported to the cell surface. All chimeras that contained the four transmembrane domains of 5-HT_{3A} showed significant radioligand binding and were found to be functional. These results suggest that all four transmembrane domains of the 5-HT_{3A} subunit are necessary for efficient expression of correctly folded functional receptors. The large cytoplasmic M3-M4 domain has been proposed to influence folding and assembly of neurotransmitter receptors as this region has been shown to interact with a range of intracellular proteins (Maimone and Enigk, 1999; Jeanclos *et al.*, 2001; Lin *et al.*, 2002). However, there was no detrimental effect on serotonergic radioligand binding when the 5-HT_{3A} large cytoplasmic loop was replaced with the equivalent α7 sequence. Additionally, when the α7 intracellular loop was replaced with the 5-HT_{3A} intracellular loop the receptor still formed no α-BTX binding sites. Thus, from the results obtained in this study, it was concluded that only the regions from just before M1 to the end of M3, and just before M4 to the end of the protein determine the efficiency of folding and assembly of these receptors.

5.1.2 The α7 subunit co-expressed with RIC3

The wild-type α7 subunit is able to form functional receptors in some mammalian cell lines, for example in SH-SY5Y cells which contain endogenous α7 receptors and can express heterologous α7 receptors efficiently (Puchacz *et al.*, 1994). Also GH_4C_1 cells which do not express endogenous α7 receptors, can express heterologous α7 receptors and (Virginio *et al.*, 2002). This has been attributed to host-cell specific factors that aid the correct folding and assembly of α7 subunits in a small number of expression systems that include *Xenopus* oocytes. Recently the RIC3 family of proteins has been identified and implicated in the maturation of several nAChR subtypes, including the α7 nAChRs, when expressed in *Xenopus* oocytes (Halevi *et al.*, 2002; Halevi *et al.*, 2003). A correlation between the expression of RIC3 and the ability to express functional α7 receptors has been shown: the presence of RIC3 transcripts was demonstrated in SH-SY5Y cells that endogenously express α7 receptors, but no RIC3 transcript could be detected in HEK tsA201 cells, which are unable to express functional heterologous α7 receptors (Lansdell *et al.*, 2005). Co-expression of α7 and RIC3 in HEK cells has been

demonstrated to result in cell surface expression of an α7 nAChR capable of binding α-BTX (Williams *et al.*, 2005; Lansdell *et al.*, 2005). The aim of this study was to examine how co-expression of RIC3 affected the level of functional expression of α7 nAChRs expressed in HEK tsA201 cells. This was investigated by whole-cell patch-clamp recording of cells transfected with cDNAs of different species of α7 and of RIC3.

It has been demonstrated in this thesis that functional α7 nAChRs can be detected only when the subunit is co-expressed with RIC3 (Chapter 4, Section 4.2). Co-expression of the human α7 subunit and human RIC3 resulted in functional nAChRs, as has also been demonstrated by Williams *et al.* (2005). The combinations of human or rat α7 subunit and human or *C.elegans* RIC3 all gave mean whole-cell responses of approximately the same size (Chapter 4, Section 4.2.1). Co-expressing the α7 subunit with *Drosophila* RIC3 also resulted in functional α7 nAChRs, but gave smaller whole-cell responses with human or *C.elegans* RIC3.

The functional characteristics of the rat α7 nAChR when co-expressed with human RIC3 were investigated by examining whole-cell responses. The reversal potential, rectification characteristics and desensitization (Chapter 4, Section 4.6) were all very similar to those reported previously for α7 receptors expressed in *Xenopus* oocytes or studied in native cells such as cultured hippocampal neurones (Mike *et al.*, 2000). When expressed with human RIC3, both the human and rat α7 subunit formed receptors which were blocked by the antagonist MLA (Chapter 4, Section 4.2.2). The recovery from block had characteristics similar to those previously published for the α7 receptor (Palma *et al.*, 1996a). These results indicate that the functional characteristics of the channel have either not been altered by co-expression with RIC3, or, that all other cells expressing functional α7 receptors also co-express RIC3. It is possible that the RIC3 protein may act by enhancing the efficiency of subunit folding, assembly. It has been proposed that RIC3 does not affect receptor trafficking as it has been reported that there was no difference in the amount of cell surface α7 subunit detected in the presence or absence of RIC3 (Williams *et al.*, 2005). However, it has also been suggested that the effect of RIC3 upon the α7 subunit in *Xenopus* oocytes is mediated at two levels; an increase in the number of

mature receptors and facilitation of transport to the plasma membrane (Castillo *et al.*, 2005).

The RIC3 protein co-assembles with the α7 subunit, as demonstrated by immunoprecipitation (Doward, 2005; Williams *et al.*, 2005); thus the action of RIC3 upon the α7 subunit may be mediated directly through the association of these proteins. This may be a transient association as it has been demonstrated in *Xenopus* oocytes that labelling of the α7 subunit only coincides in some places with RIC3 labelling (Castillo *et al.*, 2005).

5.1.3 RIC3 co-expressed with other neurotransmitter receptor subunits

In this thesis it has been demonstrated that the RIC3 protein can affect the expression of nicotinic neurotransmitter receptor subunits other than α7 (Chapter 4, Section 4.3-4.4; Lansdell *et al.*, 2005). When the α8 nicotinic subunit was expressed alone in fibroblast cells, no α8 receptor can be detected with radioligand binding (Cooper and Millar, 1998). However, when RIC3 is co-expressed in HEK with the α8 subunit specific radioligand binding is detected (Lansdell *et al.*, 2005). In this thesis, it was investigated whether the level of functional expression assayed by whole-cell patch-clamp recording, would increase with co-expression of RIC3. In cells expressing the α8 subunit alone three out of 11 cells responded to ACh (Chapter 4, Section 4.3). This was unexpected as no specific radioligand binding with this subunit has been demonstrated previously (Cooper and Millar, 1997; Lansdell *et al.*, 2005). A much greater proportion of the cells tested showed functional expression when the α8 subunit was co-expressed with RIC3 and the responses were of greater magnitude (Chapter 4, Section 4.3.1).

Radioligand binding assays demonstrate that cell expressing the α3 and β2 subunits show low levels of specific binding in comparison to other subunit combinations such as α4β2 (Xiao and Kellar, 2004; Lansdell *et al.*, 2005). When α3 and β2 subunits were co-expressed, only two out of ten cells showed small whole-cell responses (Chapter 4, Section 4.4). When RIC3 was co-expressed with the α3 and β2 subunits an increase in radioligand binding and an increase in calcium influx upon application of nicotinic agonist has been demonstrated (Lansdell *et al.*, 2005).

When tested with whole-cell patch-clamp recording, the whole-cell responses were larger and a higher proportion of cells responded to agonist in the presence of RIC3 (Chapter 4, Section 4.4.1).

Additionally, when co-expressed with RIC3, an increase has been reported in the number of radioligand binding sites, and in agonist-induced intracellular calcium influx in cells expressing α4β2, α4β4 or α3β4 nAChRs (Lansdell *et al.*, 2005). These results and the results in this thesis indicate that RIC3 is a general nAChR associated protein that acts to increase the number of functional receptors. Previously reported nAChR-accessory proteins (Calnexin, BiP and 14-3-3η) have been demonstrated to up-regulate only muscle nAChR (Chang *et al.*, 1997; Forsayeth *et al.*, 1992) and α4β2 receptors (Jeanclos *et al.*, 2001).

The RIC3 protein also affects the functional expression of 5-HT_{3A} receptors (Chapter 4, Section 4.5). Co-expression of human RIC3 with murine 5-HT_{3A} has been shown to result in the loss of functional expression of this receptor when expressed in *Xenopus* oocytes (Halevi *et al.*, 2002). In contrast, when this receptor is expressed in a mammalian cell line (HEK), there is an increase in radioligand binding (Doward 2005) and cell surface receptors (Cheng *et al.*, 2005) when the 5-HT_{3A} subunit is co-expressed with RIC3. There are differences in the effect of RIC3 upon the expression of 5-HT_{3A}, depending on the species of RIC3, the species of 5-HT_{3A} and the technique used to examine the levels of expression. For example, compared to expressing the subunit alone, co-expression of human 5-HT_{3A} with human RIC3 gave a greater number of surface receptors, but the same level of functional expression as assayed by agonist-induced calcium influx (Doward, 2005). There is no difference in cell surface receptor expression with murine 5-HT_{3A} alone and with human RIC3 (Doward, 2005); however agonist-induced calcium influx is lower when human RIC3 is co-expressed with the murine 5-HT_{3A} subunit (Doward, 2005; Chapter 4, Section 4.5.1). This thesis examines the functional expression of the 5-HT_{3A} receptor by whole-cell patch-clamp recording as an alternative method to the calcium-influx assay.

All cells expressing one of the 5-HT_{3A} subunits (human or murine) responded to 5-HT (Chapter 4, Section 4.5). Upon co-expression of *C. elegans* RIC3, there was an increase in the size of whole-cell responses from cells expressing the human 5-HT_{3A} subunit, but no difference in cells expressing the murine 5-HT_{3A} subunit. In contrast, when human RIC3 was co-expressed with the human or murine 5-HT_{3A} subunit there was no difference in the size of the whole-cell response from human 5-HT_{3A} receptors, but a decrease in response from the murine 5-HT_{3A} receptor (Chapter 4, Section 4.5.1). Thus this thesis shows that no generalization can be made about the action of RIC3 upon the 5-HT_{3A} receptor. In the future it would be interesting to clone the murine RIC3 protein and see what effect it would have upon the murine 5-HT_{3A} subunit. Also, since the cell line used in these experiments was of human origin, it would be interesting to investigate if there were any difference if a murine cell line was used.

It has been demonstrated that if the ratio of human RIC3 to the human 5-HT_{3A} subunit is increased, the level of functional expression also increases (Cheng *et al.*, 2005). The RIC3 protein (when in sufficient quantities) may increase the level of functional expression of the human 5-HT_{3A} subunit, but may act differently at the murine 5-HT_{3A} subunit. When expressed in *Xenopus* oocytes the lack of detectable functional murine 5-HT_{3A} receptors when co-expressed with human RIC3 has been attributed to inhibition of export of the receptor to the plasma membrane. This requires an extracellular isoleucine close to the first transmembrane receptor domain (Castillo *et al.*, 2005). It would be interesting to see if loss of this isoleucine also abolished the effect of co-expression of human RIC3 in HEK tsA201 cells. As yet there is no hypothesis as to how RIC3 enhances the functional expression of human 5-HT_{3A}. By using the chimeric subunits described in Chapter 3, studies can be performed in the future to examine which part of the subunits are necessary for both the interaction with RIC3 and the resultant effect on function.

Human RIC3 has been shown to co-assemble with the α3, α4, β2 and β4 nAChR subunits and the 5-HT_{3A} subunit (Lansdell *et al.*, 2005; Williams *et al.*, 2005; Cheng *et al.*, 2005). This suggests that, as for the α7 subunit, the action of RIC3 upon these subunits may involve direct interaction with the RIC3 protein. The co-assembly of

human RIC3 and human 5-HT_{3A} has been proposed to be transient as RIC3 and 5-HT_{3A} co-immunoprecipitate only a few hours after metabolic labelling (Cheng *et al.*, 2005). In this case RIC3 may promote some posttranslational modifications, for example palmitoylation (Drisdel *et al.*, 2004) that is required for forming the correct receptor structure or transport to the cell surface (Cheng *et al.*, 2005).

The RIC3 protein has been demonstrated to have multiple actions. It increases the number of nAChRs and their transport to the membrane, but also acts on the 5-HT_{3A} subunit, and affects the level of functional expression. In the future, the chimeras constructed between the rat α7 and murine 5-HT_{3A} subunits can be co-expressed with RIC3 to identify which regions of the subunits are important for the association with RIC3 and the effect that RIC3 has upon the receptor subunit. It has been reported that amino acids in the putative amphipathic helix in the large cytoplasmic loop of the human α7 subunit are necessary for the positive effect of RIC3 upon the number of surface α-BTX binding sites (Castillo *et al.*, 2005). This intracellular loop region does not affect the efficiency of protein folding of the α7 subunit as demonstrated in Chapter 3 (Section 3.3.2), where exchange of the 5-HT_{3A} and α7 M3-M4 sequences did not effect the number of radioligand binding sites. However, this region may important for the mechanism by which RIC3 enables α7 to fold to form α-BTX binding sites.

5.2 Functional characteristics of the homomeric α7 and 5-HT_{3A} receptors

The α7 nAChR subunit and 5-HT_{3A} subunit have approximately 33% sequence similarity, but they have very different functional properties, thus it was of interest to examine which of the sequence differences were important for function. Out of the thirteen chimeras constructed from the α7 and 5-HT_{3A} subunits in this study, three were functional (5-$HT_{3A}^{3\text{-}4Loop\text{-}\alpha7}$, $\alpha7^{V201\text{-}5\text{-}HT3A}$ and $\alpha7^{4TM\text{-}5\text{-}HT3A}$). The functional characteristics of these three chimeras were compared with the 5-HT_{3A} receptor (Chapter 3, Section 3.6) and the α7 receptor (co-expressed with RIC3; Chapter 4, Section 4.6).

5.2.1 Reversal potential and rectification

There was no significant difference in the reversal potential of the homomeric α7 and 5-HT_{3A} receptors, and the three chimeras also had similar reversal potentials. The α7 receptor shows much greater rectification then the 5-HT_{3A} receptor, and the chimeras all resembled the 5-HT_{3A} receptor. The 5-HT_{3A} subunit and the three chimeras share only the four transmembrane domains. Thus the results in this thesis suggest that this is the region that determines the rectification characteristics of these receptors. Surprisingly, rectification is not affected by the large cytoplasmic loop, even though this region contains amino acids that affect the single-channel conductance (see below).

5.2.2 Desensitization characteristics

The α7 receptor desensitizes approximately 40 times faster than the 5-HT_{3A} receptor. The 5-$HT_{3A}^{3\text{-}4Loop\text{-}\alpha7}$ chimera had desensitization characteristics similar to the 5-HT_{3A} receptor, but the $\alpha7^{V201\text{-}5\text{-}HT3A}$ and $\alpha7^{4TM\text{-}5\text{-}HT3A}$ chimeras had rates of desensitization that were in between the α7 and 5-HT_{3A} receptors. Also the rate of desensitization was significantly faster for the $\alpha7^{V201\text{-}5\text{-}HT3A}$ chimera, compared to the $\alpha7^{4TM\text{-}5\text{-}HT3A}$ chimera. These results demonstrate that multiple regions may determine the rate of desensitization. Both the α7 and 5-HT_{3A} subunits and the 5-$HT_{3A}^{3\text{-}4Loop\text{-}\alpha7}$ chimera desensitize to a greater degree than the $\alpha7^{V201\text{-}5\text{-}HT3A}$ and $\alpha7^{4TM\text{-}5\text{-}HT3A}$ chimeras, which had a high level of residual activation after desensitization (~30%). Having the N-terminal extracellular region of α7 but the transmembrane domains of 5-HT_{3A} results in a receptor that does not fully desensitize even upon long agonist applications.

5.2.3 Single-channel conductance

The single-channel conductance of the α7 receptor is approximately 50 times greater than that of the receptor formed form 5-HT_{3A} subunits. Previously the transmembrane domains, and particularly M2, have been postulated to determine the single-channel conductance of nicotinic receptors (Imoto *et al.*, 1986). However the results of this thesis and also work published by Kelley *et al.* (2003) suggest otherwise. Using noise analysis to determine the single-channel conductance, the three chimeras were shown to have significantly greater single-channel conductance

than the 5-HT_{3A} receptor, despite all four constructs containing the same transmembrane domains. Inclusion of the large cytoplasmic loop of the α7 receptor (comparing 5-HT_{3A} to 5-$HT_{3A}^{3\text{-}4Loop\text{-}\alpha7}$, and $\alpha7^{V201\text{-}5\text{-}HT3A}$ to $\alpha7^{4TM\text{-}5\text{-}HT3A}$) increased the conductance ten fold, and inclusion of the N-terminal domain of α7 (comparing 5-HT_{3A} to $\alpha7^{V201\text{-}5\text{-}HT3A}$, 5-$HT_{3A}^{3\text{-}4Loop\text{-}\alpha7}$ to $\alpha7^{4TM\text{-}5\text{-}HT3A}$) increased the conductance two fold. Thus, both the large cytoplasmic loop and the N-terminal domain are involved in determining the single-channel conductance of the α7 and 5-HT_{3A} receptors. It has been demonstrated that the low conductance of the 5-HT_{3A} receptor can be attributed to three arginine residues in the large cytoplasmic loop (Kelley *et al.*, 2003), and the α7 sequence contains none of these arginine residues.

5.3 Summary

The aim of this thesis was to further investigate structural domains responsible for the inefficient folding, assembly and functional expression of the α7 subunit. The exchange of a minimum of two domains of the α7 subunit cDNA sequence (including M1 to M3 and M4 to the end of the subunit) for that of the 5-HT_{3A} subunit, created chimeras that were able to form functional receptors. Thus the domains that dictate the correct folding and assembly of these receptors have been narrowed down. It was also demonstrated that the transmembrane domains determine the rectification of the receptors and that the large cytoplasmic loop and the N-terminal domain determine the single-channel conductance.

The α7 subunit forms functional receptor in some mammalian cell lines, and this has recently been suggested to be due to the presence of the RIC3 protein. This thesis demonstrates that the α7 subunit forms functional receptors only when co-expressed with RIC3 in HEK cells. It has also been demonstrated that RIC3 increases the functional expression of other nicotinic receptors (α8 and α3β2), and influences the functional expression of the 5-HT_{3A} receptor.

REFERENCES

Alkondon, M., Braga, M. F., Pereira, E. F., Maelicke, A., Albuquerque, E. X. (2000). α7 nicotinic acetylcholine receptors and modulation of GABAergic synaptic transmission in the hippocampus. *Eur. J. Pharm.*, **393**, 59-67.

Alkondon, M., Pereira, E. F., Cortes, W. S., Maelicke, A., Albuquerque, E. X. (1997) Choline is a selective agonist of α7 nicotinic acetylcholine receptors in the rat brain neurons. *Eur. J. Neurosci.*, **9**, 2734-42.

Anand. R., Conroy. W. G., Schoepfer. R., Whiting. P., Lindstrom. J. (1991). Neuronal nicotinic acetylcholine receptors expressed in *Xenopus* oocytes have a pentameric quaternary structure. *J. Biol. Chem.*, **266**, 11192-8.

Anand, R., Peng, X., Lindstrom, J. (1993). Homomeric and native α7 acetylcholine receptors exhibit remarkably similar but non-identical pharmacological properties, suggesting that the native receptor is a heteromeric protein complex. *FEBS Letts*, **327,** 241-6.

Art, J. J., Fettiplace, R., Fuchs, P. A. (1984) Synaptic hyperpolarization and inhibition of turtle cochlear hair cells *J. Physiol.*, **356**, 25-50.

Auerbach. A. (2003) Life at the top: the transition state of AChR gating *Sci. STKE.*, **188,** 11-23.

Baker, R. B. (2003). Molecular and cell biological charaterisation of neuronal nicotinic acetylcholine receptors. PhD thesis at University College London.

Barnard, E. A., Miledi, R., Sumikawa, K. (1982). Translation of exogenous messenger RNA coding for nicotinic acetylcholine receptors produces functional receptors in *Xenopus* oocytes. *Proc. R. Soc. Lond. B.*, **215,** 241-6.

Barnes, N. M. and Sharp, T. (1999). A review of central 5-HT receptors and function. *Neuropharm.*, **38,** 1083-152.

Belelli, D., Balcarek, J. M., Hope, A. G., Peters, J. A., Lambert, J. J., Blackburn, T. P. (1995). Cloning and functional expression of a human 5-hydroxytryptamine type 3AS receptor subunit. *Molec. Pharm.*, **48,** 1054-62.

Benwell, M. E. M., Balfour, D. J. K., Anderson, J. M. (1988). Evidence that tobacco smoking increases the density of (-)-[^{3}H]nicotine binding sites in human brain. *J. Neurochem.*, **50,** 1243-7.

Bertrand, D., Devillers-Thiery, A., Revah, F., Galzi, J. L., Hussy, N., Mulle, C., Bertrand, S., Ballivet, M., Changeux, J. P. (1992). Unconventional pharmacology of a neuronal nicotinic receptor mutated in the channel domain *Proc. Natl. Acad. Sci. U. S. A.*, **89,** 1261-5.

Bertrand, D., Galzi, J. L., Devillers-Thiery, A., Bertrand, S., Changeux, J. P. (1993). Mutations at two distinct sites within the channel domain M2 alter calcium permeability of neuronal α 7 nicotinic receptor. *Proc. Natl. Acad. Sci. U. S. A.*, **90,** 6971-5.

Bhatnagar, S., Nowak, N., Babich, L., Bok, L. (2004a). Deletion of the 5-HT3 receptor differentially affects behavior of males and females in the Porsolt forced swim and defensive withdrawal tests. *Behav. Brain. Res.*, **153**, 527-35.

Bhatnagar, S., Sun, L. M., Raber, J., Maren, S., Julius, D., Dallman, M. F. (2004b). Changes in anxiety-related behaviors and hypothalamic-pituitary-adrenal activity in mice lacking the 5-HT_{3A} receptor. *Physiol. Behav.*, **81**, 545-55.

Blount, P. and Merlie, J. P. (1991). BIP associates with newly synthesized subunits of the mouse muscle nicotinic receptor. *J. Cell Biol.*, **113,** 1125-32.

Blount, P., Smith, M. M., Merlie, J. P. (1990). Assembly intermediates of the mouse muscle nicotinic acetylcholine receptor in stably transfected fibroblasts. *J. Cell Biol.*, **111,** 2601-11.

Blumenthal, E. M., Conroy, W. G., Romano, S. J., Kassner, P. D., Berg, D. K. (1997). Detection of functional nicotinic receptors blocked by α-bungarotoxin on PC12 cells and dependence of their expression on post-translational events. *J. Neurosci.*, **17**, 6094-104.

Boess, F. G., Beroukhim, R., Martin, I. L. (1995). Ultrastructure of the 5-HT_3 receptor. *J. Neurochem.*, **64,** 1401-5.

Boess, F. G., Steward, L. J., Steele, J. A., Liu, D., Reid, J., Glencorse, T. A. and Martin, I. L. (1997). Analysis of the ligand binding site of the 5-HT_3 receptor using site directed mutagenesis: importance of glutamate 106. *Neuropharm.*, **36,** 637-47.

Bohler, S., Gay, S., Bertrand, S., Corringer, P. J., Edelstein, S. J., Changeux, J. P., Bertrand, D. (2001). Desensitization of neuronal nicotinic acetylcholine receptors conferred by N-terminal segments of the β2 subunit. *Biochem.*, **40**, 2066-74.

Boorman, J. P., Groot-Kormelink, P. J., Sivilotti, L. G. (2000). Stoichiometry of human recombinant neuronal nicotinic receptors containing the b3 subunit expressed in *Xenopus* oocytes. *J. Physiol.*, **529,** 565-77.

Boulter, J., Connolly, J., Deneris, E., Goldman, D., Heinemann, S., Patrick, J. (1987). Functional expression of two neuronal nicotinic acetylcholine receptors from cDNA clones identifies a gene family. *Proc. Natl. Acad. Sci. U. S. A.*, **84,** 7763-7767.

Boulter, J., Luyten, W., Evans, K., Mason, P., Ballivet, M., Goldman, D., Stengelin, S., Martin, G., Heinemann, S., Patrick, J. (1985). Isolation of a clone coding for the α-subunit of a mouse acetylcholine receptor. *J. Neurosci.*, **5,** 2545-52.

Boulter, J., O'Shea-Greenfield, A., Duvoisin, R. M., Connolly, J. G., Wada, E., Jensen, A., Gardner, P. D., Ballivet, M., Deneris, E. S., McKinnon, D., Heinemann, S., Patrick, J. (1990). α3, α5, and β4: three members of the rat neuronal nicotinic acetylcholine receptor-related gene family form a gene cluster. *J. Biol. Chem.*, **265,** 4472-82.

Boyd, G. W., Doward, A. I., Kirness, E. F., Millar, N. S., Connolly, C. N. (2003). Cell surface expression of 5-hydroxytryptamine type 3 receptors is controlled by an endoplasmic reticulum retention signal. *J. Biol. Chem.*, **278,** 27681-7.

Boyd, G. W., Low, P., Dunlop, J. I., Robertson, L. A., Vardy, A., Lambert, J. J., Peters, J. A., Connolly, C. N. (2002). Assembly and cell surface expression of homomeric and heteromeric 5-HT_3 receptors: the role of oligomerization and chaperone proteins. *Mol. Cell. Neurosci.*, **21,** 38-50.

Brejc, K., van Dijk, W. J., Klaassen, R. V., Schuurmans, M., van der Oost, J., Smit, A. B., Sixma, T. K. (2001). Crystal structure of an ACh-binding protein reveals the ligand-binding domain of nicotinic receptors. *Nature*, **411,** 269-76.

Brisson, A. and Unwin, P. N. (1985) Quarternary structure of the acetylcholine receptor *Nature,* **315,** 474-7.

Britto, L. R., Hamassaki-Britto, D. E., Ferro, E. S., Keyser, K. T., Karten, H. J., Lindstrom, J. M. (1992) Neurons of the chick brain and retina expressing both α-bungarotoxin-sensitive and α-bungarotoxin-insensitive nicotinic acetylcholine receptors: an immunohistochemical analysis *Brain Res.*, **590,** 193-200.

Broad, L. M., Felthouse, C., Zwart, R., McPhie, G., Pearson, K. H., Craig, P. J., Wallace, L., Broadmore, R. J., Boot, J. R., Keenan, M., Baker, S. R. and Sher, E. (2002). PSAB-OFP, a selective α7 nicotinic receptor agonist, is also a potent agonist of the 5-HT_3 receptor. *Eur. J. Pharm.*, **452,** 137-144.

Brown, A. M., Hope, A. G., Lambert, J. J., Peters, J. A. (1998). Ion permeation and conduction in a human recombinant 5-HT_3 receptor subunit (h5-HT_{3A}). *J. Physiol.*, **507,** 653-65.

Brüss, M., Barann, M., Hayer-Zillgen, M., Eucker, T., Gothert, M., Bonisch, H. (2000). Modified 5-HT_{3A} receptor function by co-expression of alternatively spliced human 5-HT_{3A} receptor isoforms. *Naunyn Schmiedebergs Arch. Pharm.*, **362,** 392-401.

Brüss, M., Molderings, G.J., Bonisch, H., Gothert, M. (1999). Pharmacological differences and similarities between the native mouse 5-HT_3 receptor in N1E-115 cells and a cloned short splice variant of the mouse 5-HT_3 receptor expressed in HEK 293 cells. *Naunyn Schmiedebergs Arch. Pharm.,* **360**, 225-33.

Buisson, B., Gopalakrishnan, M., Arneric, S. P., Sullivan, J. P., Bertrand, D. (1996) Human α4β2 neuronal nicotinic acetylcholine receptor in HEK 293 cells: A patch-clamp study *J. Neurosci.,* **16,** 7880-91.

Buisson. B, and Bertrand, D. (2001) Chronic exposure to nicotine upregulates the human α4β2 nicotinic acetylcholine receptor function *J. Neurosci.*, **21,** 1819-29.

Campos-Caro, A., Rovira, J. C., Vicente-Agullo, F., Ballesta, J. J., Sala, S., Criado, M., Sala, F. (1997). Role of the putative transmembrane segment M3 in gating of neuronal nicotinic receptors. *Biochem.*, **36**, 2709-15.

Carbonetto, S.T., Fambrough, D.M., Muller, K.J. (1978). Nonequivalence of α-bungarotoxin receptors and acetylcholine receptors in chick sympathetic neurons. *Proc. Natl. Acad. Sci. U. S. A.,* 75, 1016-20.

Cartier, G. E., Yoshikami, D., Gray, W. R., Luo, S., Olivera, B. M., McIntosh, J. M. (1996) A new α-conotoxin which targets α3β2 nicotinic acetylcholine receptors *J. Biol. Chem.,* **271,** 7522-8.

Castillo, M., Mulet, J., Gutierrez, L. M., Ortiz, J.A., Castelan, F., Gerber, S., Sala, S., Sala, F., Criado, M. (2005). Dual role of the RIC-3 protein in trafficking of serotonin and nicotinic acetylcholine receptors. *J. Biol Chem.,* **280**, 27062-8.

Chang, W., Gelman, M. S., Prives, J. M. (1997). Calnexin-dependent enhancement of nicotinic acetylcholine receptor assembly and surface expression. *J. Biol. Chem.*, **272,** 28925-32.

Changeux, J.-P., Kasai, M., Lee, C. Y. (1970). Use of a snake venom toxin to characterise the cholinergic receptor protein. *Proc. Natl. Acad. Sci. U. S. A.*, **67,** 1241-7.

Charnet, P., Labarca, C., Leonard, R. J., Vogelaar, N. J., Czyzyk, L., Gouin, A., Davidson, N., Lester, H. A. (1990). An open-channel blocker interacts with adjacent turns of α-helices in the nicotinic acetylcholine receptor. *Neuron,* **4**, 87-95.

Chen, D. and Patrick, J. W. (1997). The a-bungarotoxin-binding nicotinic acetylcholine receptor from rat brain contains only the α7 subunit. *J. Biol. Chem.*, **272,** 24024-9.

Cheng, A., McDonald, N. A., Connolly, C. N. (2005) Cell surface expression of 5-hydroxytryptamine type 3 receptors is promoted by RIC-3 *J. Biol. Chem.*, **280,** 22502-7.

Chiara, D. C., Middleton, R. E., Cohen, J. B. (1998). Identification of tryptophan 55 as the primary site of [^{3}H]nicotine photoincorporation in the γ subunit of the *Torpedo* nicotinic acetylcholine receptor. *FEBS Lett.*, **423,** 223-6.

Chiara, D. C., Xie, Y., Cohen, J. B. (1999). Structure of the agonist-binding sites of the *Torpedo* nicotinic acetylcholine receptor: affinity-labeling and mutational analyses identify γTyr-111/δArg-113 as antagonist affinity determinants. *Biochem.*, **38,** 6689-98.

Clarke, P. B., Schwartz, R. D., Paul, S. M., Pert, C. B., Pert A. (1985) Nicotinic binding in rat brain: autoradiographic comparison of [^{3}H]acetylcholine, [^{3}H]nicotine, and [^{125}I]α-bungarotoxin. *J. Neurosci.*, **5**, 1307-15.

Claudio, T., Ballivet, M., Patrick, J., Heinemann, S. (1983) Nucleotide and deduced amino acid sequences of *Torpedo californica* acetylcholine receptor γ subunit. *Proc. Natl. Acad. Sci. U. S. A.*, **80**, 1111-5.

Connolly, J., Boulter, J., Heinemann, S. F. (1992). α4β2 and other nicotinic acetylcholine receptor subtypes as targets of psychoactive and addictive drugs. *Br. J. Pharm.*, **105**, 657-66.

Conroy, W. G. and Berg, D. K. (1995). Neurons can maintain multiple classes of nicotinic acetylcholine receptors distinguished by different subunit compositions. *J. Biol. Chem.*, **270,** 4424-31.

Conroy, W. G. and Berg, D. K. (1998) Nicotinic receptor subtypes in the developing chick brain: appearance of a species containing the α4, β2, and α5 gene products *Mol. Pharm.*, **53,** 392-401.

Conroy, W. G., Vernallis, A. B., Berg, D. K. (1992). The α5 gene product assembles with multiple acetylcholine receptor subunits to form distinctive receptor subtypes in brain. *Neuron*, **9,** 679-91.

Cooper, E., Couturier, S., Ballivet, M. (1991). Pentameric structure and subunit stoichiometry of a neuronal nicotinic acetylcholine receptor. *Nature*, **350,** 235-8.

Cooper, S. T. and Millar, N. S. (1997). Host cell-specific folding and assembly of the neuronal nicotinic acetylcholine receptor α7 subunit. *J. Neurochem.*, **68,** 2140-51.

Cooper, S. T. and Millar, N. S. (1998). Host cell-specific folding of the neuronal nicotinic receptor α8 subunit. *J. Neurochem.*, **70,** 2585-93.

Cooper, S. T., Harkness, P. C., Baker, E. R., Millar, N. S. (1999). Upregulation of cell-surface α4β2 neuronal nicotinic receptors by lower temperature and expression of chimeric subunits. *J. Biol. Chem.*, **274,** 27145-52.

Cooper, S.T. (1998). Host cell-specific folding of the neuronal nicotinic acetylcholine receptor α7 and α8 subunits. PhD thesis at University College London.

Corcia, G., Blasetti, A., De Simone, M., Verrotti, A., Chiarelli, F. (2005). Recent advances on autosomal dominant nocturnal frontal lobe epilepsy: "understanding the nicotinic acetylcholine receptor (nAChR)". *Eur. J. Paediatr. Neurol.*, **9**, 59-66.

Cordero-Erausquin, M., Marubio, L. M., Klink, R., Changeux, J.-P. (2000). Nicotinic receptor function: new perspectives from knockout mice. *Trends Pharm. Sci.*, **21,** 211-7.

Corringer, P. J., Bertrand, S., Bohler, S., Edelstein, S. J., Changeux, J. P., Bertrand, D. (1998) Critical elements determining diversity in agonist binding and desensitization of neuronal nicotinic acetylcholine receptors *J. Neurosci.*, **18**, 648-57.

Corringer, P.-J., Bertrand, S., Galzi, J.-L., Devillers-Thiéry, A., Changeux, J.-P., Bertrand, D. (1999). Mutational analysis of the charge selectivity filter of the $\alpha 7$ nicotinic acetylcholine receptor. *Neuron*, **22,** 831-43.

Corringer, P.-J., Galzi, J.-L., Eiselé, J.-L., Bertrand, S., Changeux, J.-P., Bertrand, D. (1995). Identification of a new component of the agonist binding site of the nicotinic $\alpha 7$ homooligomeric receptor. *J. Biol. Chem.*, **270**, 11749-52.

Corringer, P.-J., Le Novére, N., Changeux, J.-P. (2000). Nicotinic receptors at the amino acid level. *Ann. Rev. Pharm. Toxicol.*, **40,** 431-8.

Corriveau, R. A. and Berg, D. K. (1993). Coexpression of multiple acetylcholine receptor genes in neurons: quantification of transcripts during development. *J. Neurosci.*, **13,** 2662-71.

Couturier, S., Bertrand, D., Matter, J. M., Hernandez, M. C., Bertrand, S., Millar, N., Valera, S., Barkas, T., Ballivet, M. (1990a). A neuronal nicotinic acetylcholine receptor subunit ($\alpha 7$) is developmentally regulated and forms a homo-oligomeric channel blocked by α-BTX. *Neuron*, **5,** 847-56.

Couturier, S., Erkman, L., Valera, S., Rungger, D., Bertrand, S., Boulter, J., Ballivet, M., Bertrand, D. (1990b). $\alpha 5$, $\alpha 3$, and non-$\alpha 3$. Three clustered avian genes encoding neuronal nicotinic acetylcholine receptor-related subunits. *J. Biol. Chem.*, **265,** 17560-7.

Covernton, P.J. and Connolly J.G. (2000). Multiple components in the agonist concentration-response relationships of neuronal nicotinic acetylcholine receptors. *J. Neurosci. Methods*, **96**, 63-70.

Cuevas, J., Roth, A. L., Berg, D. K. (2000) Two distinct classes of functional 7-containing nicotinic receptor on rat superior cervical ganglion neurons *J. Physiol.*, **525**, 735-46.

Czajkowski, C., Kaufmann, C., Karlin, A. (1993) Negatively charged amino acid residues in the nicotinic receptor δ subunit that contribute to the binding of acetylcholine *Proc. Natl. Acad. Sci. U. S. A.*, **90,** 6285-9.

Dale, H. H. (1914). *J. Pharm.* **6**, 147. Discussed in the Nobel Lecture 1936 given by Sir Henry Dale, "Some recent extentions of the chemical transmission of the effects of nerve impulses", www.nobelprize.org/medicine/laureates/1936/dale-lecture.html

Davies, A. R., Hardick, D. J., Blagbrough, I. S., Potter, B. V., Wolstenholme, A. J., Wonnacott, S. (1999a). Characterisation of the binding of [^{3}H]methyllycaconitine: a new radioligand for labelling α 7-type neuronal nicotinic acetylcholine receptors. *Neuropharm.*, **38**, 679-90.

Davies, P. A., Pistis, M., Hanna, M. C., Peters, J. A., Lambert, J. J., Hales, T. G., Kirkness, E. F. (1999b). The 5-HT$_{3B}$ subunit is a major determinant of serotonin-receptor function. *Nature*, **397,** 359-63.

Deane, C. M. and Lummis, S. C. (2001) The role and predicted propensity of conserved proline residues in the 5-HT3 receptor *J. Biol. Chem.*, **276,** 37962-6.

Deneris, E. S., Boulter, J., Swanson, L. W., Patrick, J., Heinemann, S. (1989). β3: a new member of nicotinic acetylcholine receptor gene family is expressed in brain. *J. Biol. Chem.*, **264**, 6268-72.

Deneris, E. S., Connolly, J., Boulter, J., Wada, E., Wada, K., Swanson, L. W., Patrick, J., Heinemann, S. (1988). Primary structure and expression of β2: a novel subunit of neuronal nicotinic acetylcholine receptors. *Neuron*, **1,** 45-54.

Derkach, V., Surprenant, A., North, R. A. (1989). 5-HT$_3$ receptors are membrane ion channels. *Nature*, **339,** 706-9.

Dineley, K. T. and Patrick, J. W. (2000). Amino acid determinants of α7 nicotinic acetylcholine receptor surface expression. *J. Biol. Chem.*, **275,** 13974-85.

DiPaola, M., Czajkowski, C., Karlin, A. (1989). The sidedness of the COOH terminus of the acetylcholine receptor δ subunit. *J Biol Chem*, **264,** 15457-63.

Dourado, M., Sargent, P. B. (2002). Properties of nicotinic receptors underlying Renshaw cell excitation by α-motor neurons in neonatal rat spinal cord. *J. Neurophysiol.*, **87**, 3117-25.

Doward, A. I. (2005). Assembly and trafficking of nicotinic and 5HT$_3$ receptors. PhD thesis at University College London.

Drisdel, R. C. and Green, W. N. (2000). Neuronal α-bungarotoxin receptors are α7 subunit homomers. *J. Neurosci.*, **20**, 133-9.

Drisdel, R. C., Manzana, E., Green, W. N. (2004). The role of palmitoylation in functional expression of nicotinic $\alpha 7$ receptors. *J. Neurosci.*, **24,** 10502-10.

Dubin, A. E. (2002). DNA encoding a human subunit 5-HT_{3C} serotonin receptor. *http://v3.espacenet.com; patent no. WO 01/16297.*

Dubin, A. E., Huvar, R., Dandrea, M. R., Pyati, J., Zhu, J. Y., Joy, K. C., Wilson, S. J., Galindo, J. E., Glass, C. A., Luo, L., Jackson, M. R., Lovenberg, T. W., Erlander, M. G. (1999). The pharmacological and functional characteristics of the serotonin 5-HT_{3A} receptor are specifically modified by a 5-HT_{3B} receptor subunit. *J. Biol. Chem.*, **274,** 30799-810.

Duvoisin, R. M., Deneris, E. S., Patrick, J., Heinemann, S. (1989). The functional diversity of the neuronal nicotinic acetylcholine receptors is increased by a novel subunit: β 4. *Neuron,* **3**, 487-96.

Ehlers, M. D., Zhang, S., Bernhadt, J. P., Huganir, R. L. (1996). Inactivation of NMDA receptors by direct interaction of calmodulin with the NR1 subunit. *Cell*, **84,** 745-55.

Eiselé, J.-L., Bertrand, S., Galzi, J.-L., Devillers-Thiéry, A., Changeux, J.-P., Bertrand, D. (1993). Chimaeric nicotinic-serotonergic receptor combines distinct ligand binding and channel specificities. *Nature*, **366,** 479-83.

Elgoyhen, A. B., Johnson, D. S., Boulter, J., Vetter, D. E., Heinemann, S. (1994). α9: an acetylcholine receptor with novel pharmacological properties expressed in rat cochlear hair cells. *Cell*, **18,** 705-15.

Elgoyhen, A. B., Vetter, D. E., Katz, E., Rothlin, C. V., Heineman, S. F., Boulter, J. (2001). α10: a determinant of nicotinic cholinergic receptor function in mammakian vestibular and cochlear mechanosensory hair cells. *Proc. Natl. Acad. Sci. U. S. A*, **98,** 3501-6.

Fatt, P. (1949). The depolarizing action of acetylcholine on muscle. *J. Physiol.*, **109**, 10.

Fenster, C. P., Rains, M. F., Noerager, B., Quick, M. W., Lester, R. A. (1997) Influence of subunit composition on desensitization of neuronal acetylcholine receptors at low concentrations of nicotine *J. Neurosci.*, **17,** 5747-59.

Feuerbach, D., Lingenhohl, K., Dobbins, P., Mosbacher, J., Corbett, N., Nozulak, J., Hoyer, D. (2005). Coupling of human nicotinic acetylcholine receptors $\alpha 7$ to calcium channels in GH3 cells. *Neuropharm.*, **48**, 215-27.

Fletcher, S., Lindstrom, J. M., McKernan, R. M., Barnes, N. M. (1998). Evidence that porcine native 5-HT_3 receptors do not contain nicotinic acetylcholine receptor subunits. *Neuropharm.*, **37,** 397-9.

Flores, C. M., DeCamp, R. M., Kilo, S., Rogers, S. W., Hargreaves, K. M. (1996). Neuronal nicotinic receptor expression in sensory neurons of the rat trigeminal ganglion: Demonstration of $\alpha 3\beta 4$, a novel subtype in the mammalian nervous system. *J. Neurosci.*, **16,** 7892-901.

Forsayeth, J. R. and Kobrin, E. (1997). Formation of oligomers containing the $\beta 3$ and $\beta 4$ subunits of the rat nicotinic receptor. *J. Neurosci.*, **17,** 1531-8.

Forsayeth, J. R., Gu, Y., Hall, Z. W. (1992). BiP forms stable complexes with unassembled subunits of the acetylcholine receptor in transfected COS cells and in C2 muscle cells. *J. Cell Biol.*, **117,** 841-7.

Forster, I. and Bertrand, D. (1995). Inward rectification of neuronal nicotinic acetylcholine receptors investigated by using the homomeric $\alpha 7$ receptor *Proc. Biol. Sci.*, **260,** 139-48.

Francis, M. M., Vazquez, R. W., Papke, R. L., Oswald, R. E. (2000). Subtype-selective inhibition of neuronal nicotinic acetylcholine receptors by cocaine is determined by the $\alpha 4$ and $\beta 4$ subunits. *Mol. Pharm.*, **58**, 109-19.

Freedman, R., Adams, C. E., Leonard, S. (2000). The $\alpha 7$-nicotinic acetylcholine receptor and the pathology of hippocampal interneurons in schizophrenia. *J. Chem. Neuroanat.*, **20**, 299-306.

Froehner, S.C. (1991). The submembrane machinery for nicotinic acetylcholine receptor clustering. *J. Cell. Biol.*, **114**, 1-7.

Fucile, S. (2004) Ca2+ permeability of nicotinic acetylcholine receptors. *Cell Calcium*, **35,** 1-8.

Fucile, S., Palma, E., Martinez-Torres, A., Miledi, R., Eusebi, F. (2002). The single-channel properties of human acetylcholine α 7 receptors are altered by fusing $\alpha 7$ to the green fluorescent protein. *Proc. Natl. Acad. Sci. U. S. A.*, **99**, 3956-61

Galzi, J. L., Devillers-Thiery, A., Hussy, N., Bertrand, S., Changeux, J. P., Bertrand, D. (1992). Mutations in the channel domain of a neuronal nicotinic receptor convert ion selectivity from cationic to anionic. *Nature*, **359,** 500-5.

Galzi, J. L., Revah, F., Black, D., Goeldner, M., Hirth, C., Changeux, J. P. (1990). Identification of a novel amino acid α-tyrosine 93 within the cholinergic ligands-binding sites of the acetylcholine receptor by photoaffinity labeling. Additional evidence for a three-loop model of the cholinergic ligands-binding sites. *J. Biol. Chem.*, **265,** 10430-7.

Galzi, J. L., Revah, F., Bouet, F., Menez, A., Goeldner, M., Hirth, C., Changeux, J. P. (1991). Allosteric transitions of the acetylcholine receptor probed at the amino acid level with a photolabile cholinergic ligand. *Proc. Natl. Acad. Sci. U. S. A.*, **88,** 5051-5.

Galzi, J.-L. and Changeux, J.-P. (1995). Neuronal nicotinic receptors: Molecular organization and regulations. *Neuropharm.*, **34,** 563-582.

Geerts, H. (2005). Indicators of neuroprotection with galantamine. *Brain res. Bull.*, **64**, 519-24.

Gehle, V. M., Walcott, E. C., Nishizaki, T., Sumikawa, K. (1997). *N*-glycosylation at the conserved sites ensures the expression of properly folded functional ACh receptors. *Mol. Brain Res.*, **45,** 219-29.

Gelman, M. S., Chang, W., Thomas, D. Y., Bergeron, J. J. M., Prives, J. M. (1995). Role of the endoplasmic reticulum chaperone calnexin in subunit folding and assembly of nicotinic acetylcholine receptors. *J. Biol. Chem.*, **270,** 15085-15092.

Gentry, C. L., Wilkins, L. H. Jr., Lukas, R. J. (2003) Effects of prolonged nicotinic ligand exposure on function of heterologously expressed, human α4β2- and α4β4-nicotinic acetylcholine receptors *J. Pharm. Exp. Ther.*, **304**, 206-16.

Gerzanich, V., Anand, R., Lindstrom, J. (1994). Homomers of α8 and α7 subunits of nicotinic receptors exhibit similar channels but contrasting binding site properties. *Mol. Pharm.*, **45,** 212-20.

Gerzanich, V., Wang, F., Kuryatov, A., Lindstrom, J. (1998) α5 subunit alters desensitization, pharmacology, Ca^{2+} permeability and Ca^{2+} modulation of human neuronal α3 nicotinic receptors *J. Pharm. Exp. Ther.*, **286,** 311-20.

Gething, M. J. and Sambrook, J. (1992) Protein folding in the cell *Nature*, **355,** 33-45.

Giraudat, J., Dennis, M., Heidmann, T., Chang, J.-Y., Changeux, J.-P. (1986). Structure of the high-affinity binding site for non-competitive blockers of the acetylcholine receptor: serine-262 of the δ subunit us labelled by [^{3}H]chlorpromazine. *Proc. Natl. Acad. Sci. U. S. A.*, **83,** 2719-723.

Glitsch, M., Wischmeyer, E., Karschin, A. (1996). Functional characterisation of two 5-HT_3 receptor splice variants isolated from a mouse hippocampal cell line. *Pflugers Arch. - Eur. J. Physiol.*, **432,** 134-43.

Goldman, D., Deneris, E., Luyten, W., Kochhar, A., Patrick, J., Heinemann, S. (1987). Members of a nicotinic acetylcholine receptor gene family are expressed in different regions of the mammalian central nervous system. *Cell*, **48,** 965-73.

Gopalakrishnan, M., Buisson, B., Touma, E., Giordano, T., Campbell, J. E., Hu, I. C., Donnelly-Roberts, D., Arneric, S. P., Bertrand, D., Sullivan, J. P. (1995). Stable expression and pharmacological properties of the human $\alpha 7$ nicotinic acetylcholine receptor. *Eur. J. Pharm.*, **290,** 237-46.

Gopalakrishnan, M., Molinari, E. J., Sullivan, J.P. (1997) Regulation of human $\alpha 4\beta 2$ neuronal nicotinic acetylcholine receptors by cholinergic channel ligands and second messenger pathways *Mol. Pharm.*, **52,** 524-34.

Gotti, C., Hanke, W., Maury, K., Moretti, M., Ballivet, M., Clementi, F., Bertrand, D. (1994). Pharmacology and biophysical properties of $\alpha 7$ and $\alpha 7$-$\alpha 8$ α-bungarotoxin receptor subtypes immunopurified from the chick optic lobe. *Eur. J. Neurosci.*, **6,** 1281-1291.

Green, W. N. and Claudio, T. (1993). Acetylcholine receptor assembly: subunit folding and oligomerization occur sequentially. *Cell*, **74,** 57-69.

Green, W. N. and Millar, N. S. (1995). Ion-channel assembly. *Trends Neurosci.*, **18,** 280-7.

Green, W. N. and Wanamaker, C. P. (1997). The role of the cystine loop in acetylcholine receptor assembly. *J. Biol. Chem.*, **272,** 20945-53.

Gu, Y., Forsayeth, J. R., Verral, S., Yu, X. M., Hall, Z. W. (1991) Assembly of the mammalian muscle acetylcholine receptor in transfected COS cells. *J. Cell. Biol.*, **114**, 799-807.

Gunthorpe, M. J. and Lummis, S. C. R. (2001). Conversion of the ion selectivity of the 5-HT_{3A} receptor from cationic to anionic reveals a conserved feature of the ligand-gated ion channel superfamily. *J. Biol. Chem.*, **276,** 10977-83.

Gunthorpe, M. J., Peters, J. A., Gill, C. H., Lambert, J. J., Lummis, S. C. (2000). The 4'lysine in the putative channel lining domain affects desensitization but not the single-channel conductance of recombinant homomeric 5-HT_{3A} receptors. *J. Physiol.*, **522**, 187-98.

Gurley, D. A. and Lanthorn, T. H. (1998). Nicotinic agonists competitively antagonize serotonin at 5-HT_3 receptors expressed in *Xenopus* oocytes. *Neurosci. Letters*, **247,** 107-10.

Halevi, S., McKay, J., Palfreyman, M., Yassin, L., Eshel, M., Jorgensen, E. M., Treinin, M. (2002). The *C.elegans ric-3* gene is required for maturation of nicotinic acertylcholine receptors. *EMBO Journal*, **21,** 1012-20.

Halevi, S., Yassin, L., Eshel, M., Sala, F., Sala, S., Criado, M., Treinin, M. (2003). Conservation within the RIC-3 gene family: effectors of mammalian nicotinic acetylcholine receptor expression. *J. Biol. Chem.*, **278,** 34411-7.

Hamilton, S. L., McLaughlin, M., Karlin, A. (1979). Formation of disulphide linked oligomers of acetylcholine receptor in membrane from *Torpedo* electric tissue. *Biochem.*, **18,** 155-63.

Hanna, M. C., Davies, P. A., Hales, T. G., Kirkness, E. F. (2000). Evidence for expression of heteromeric serotonin 5-HT_3 receptors in rodents. *J. Neurochem.*, **75,** 240-7.

Hargreaves, A. C., Lummis, S. C., Taylor, C. W. (1994). Ca^{2+} permeability of cloned and native 5-hydroxytryptamine type 3 receptors. *Mol. Pharm.*, **46,** 1120-8.

Harkness, P. C. and Millar, N. S. (2001). Inefficient cell-surface expression of hybrid complexes formed by the co-assembly of neuronal nicotinic acetylcholine receptor and serotonin receptor subunits. *Neuropharm.*, **41,** 79-87.

Hiel, H., Elgoyhen, A. B., Drescher, D. G., Morley, B. J. (1996) Expression of nicotinic acetylcholine receptor mRNA in the adult rat peripheral vestibular system *Brain Res.*, **738,** 347-52.

Hope, A. G., Downie, D. L., Sutherland, L., Lambert, J. J., Peters, J. A., Burchell, B. (1993). Cloning and functional expression of an apparent splice variant of the murine 5-HT_3 receptor A subunit. *Eur. J. Pharm.*, **245,** 187-192.

Hope, A. G., Peters, J. A., Brown, A. M., Lambert, J. J., Blackburn, T. P. (1996). Characterization of a human 5-hydroxytryptamine$_3$ receptor type A (h5-HT$_{3AS}$ R) subunit stably expressed in HEK 293 cells. *Br. J. Pharm.*, **118,** 1237-45.

Hsu, Y. N., Amin, J., Weiss, D. S., Wecker, L. (1996) Sustained nicotine exposure differentially affects α3 β2 and α4 β2 neuronal nicotinic receptors expressed in *Xenopus* oocytes *J. Neurochem.*, **66,** 667-75.

Hubbard, P. C., Thompson, A. J., Lummis, S. C. R. (2000). Functional differences between splice variants of the murine 5-HT$_{3A}$ receptor: possible role for phosphorylation. *Mol. Brain Res.*, **81,** 101-8.

Hucho, F., Layer, P., Kiefer, H.R., Bandini, G. (1976). Photoaffinity labeling and quaternary structure of the acetylcholine receptor from *Torpedo californica. Proc. Natl. Acad. Sci. U. S. A.*, **73**, 2624-8.

Hucho, F., Oberthür, W., Lottspeich, F. (1986). The ion channel of the nicotinic acetylcholine receptor is formed by the homologous helices M2 of the receptor subunits. *FEBS Lett.*, **205,** 137-42.

Huganir, R. L. and Greengard, P. (1990). Regulation of neurotransmitter receptor desensitization by protein phosphorylation. *Neuron*, **5,** 555-67.

Hussy, N., Lukas, W., Jones, K. A. (1994). Functional properties of a cloned 5-hydroxytryptamine ionotropic receptor subunit: comparison with native mouse receptors. *J. Physiol.*, **481,** 311-23.

Imoto, K., Busch, C., Sakmann, B., Mishina, M., Konno, T., Nakai, J., Bujo, H., Mori, Y., Fukuda, K., Numa, S. (1988). Rings of negatively charged amino acids determine the acetylcholine receptor channel conductance. *Nature*, **335,** 645-8.

Imoto, K., Methfessel, C., Sakmann, B., Mishina, M., Mori, Y., Konno, T., Fukuda, K., Kurasaki, M., Bujo, H., Fujita, Y., *et al.* (1986) Location of a δ-subunit region determining ion transport through the acetylcholine receptor channel *Nature*, **324,** 670-4.

Isenberg, K. E., Ukhun, I. A., Holstad, S. G., Jafri, S., Uchida, U., Zorumski, C. F., Yang, J. (1993). Partial cDNA cloning and NGF regulation of a rat 5-HT$_3$ receptor subunit. *Neuroreport*, **5,** 121-4.

Jackson, M. B. and Yakel, J. L. (1995). The 5-HT$_3$ receptor channel. *Ann. Rev. Physiol.*, **57,** 447-68.

Jagger, D. J., Griesinger, C. B., Rivolta, M. N., Holley, M. C., Ashmore, J. F. (2000) Calcium signalling mediated by the α9 acetylcholine receptor in a cochlear cell line from the immortomouse *J. Physiol.*, **527,** 49-54.

Jeanclos, E. M., Lin, L., Treuil, M. W., Rao, J., DeCoster, M. A., Anand, R. (2001). The chaperone protein 14-3-3h interacts with the nicotinic acetylcholine receptor α4 subunit. *J. Biol. Chem.*, **276,** 28281-90.

Johnson, D. S. and Heinemann, S. F. (1992). Cloning and expression of the rat 5-HT_3 receptor reveals species-specific sensitivity to curare antagonism. *Soc. Neurosci. Abstracts*, **18,** 249.

Jones, B. J. and Blackburn, T. P. (2002). The medical benefit of 5-HT research. *Pharm., Biochem. Behav.*, **71,** 555-68.

Jones, S., Sudweeks, S., Yakel, J. L. (1999). Nicotinic receptors in the brain: correlating physiology with function. *Trends Neurosci.*, **22,** 555-61.

Kao, P. N. and Karlin, A. (1986). Acetylcholine receptor binding site contains a disulfide cross-link between adjacent half-cystinyl residues. *J. Biol. Chem.*, **261,** 8085-8.

Kao, P. N., Dwork, A. J., Kaldany, R. R. J., Silver, M., Wideman, J., Stein, J., Karlin, A. (1984). Identification of the α-subunit half cysteine specifically labeled by an affinity reagent for acetylcholine receptor binding site. *J. Biol. Chem.*, **259,** 11662-5.

Karlin, A., Holtzman, E., Yodh, N., Lobel, P., Wall, J., Hainfeld, J. (1983). The arrangement of the subunits of the acetylcholine receptor of *Torpedo californica*. *J. Biol. Chem.*, **258**, 6678-81

Kassner, P. D. and Berg, D. K. (1997). Differences in the fate of neuronal acetylcholine receptor protein expressed in neurons and stably transfected cells. *J. Neurobiol.*, **33,** 968-82.

Kawai, H. and Berg, D. K. (2001). Nicotinic acetylcholine receptors containing α7 subunits on rat cortical neurons do not undergo long-lasting inactivation even when up-regulated by chronic nicotine exposure *J. Neurochem.*, **78,** 1367-78.

Keller, S. H., Lindstrom, J., Taylor, P. (1996). Involvement of the chaperone protein calnexin and the acetylcholine receptor β subunit in the assembly and cell surface expression of the receptor. *J. Biol. Chem.*, **271,** 22871-7.

Kelley, S. P., Dunlop, J. I., Kirkness, E. F., Lambert, J. J., Peters, J. A. (2003). A cytoplasmic region determines single-channel conductance in 5-HT_3 receptors. *Nature*, **424,** 321-4.

Keyser, K. T., Britto, L. R., Schoepfer, R., Whiting, P., Cooper, J., Conroy, W., Brozozowska-Prechtl, A., Karten, H. J., Lindstrom, J. (1993). Three subtypes of a-bungarotoxin-sensitive nicotinic acetylcholine receptors are expressed in chick retina. *J. Neurosci.*, **13,** 442-54.

Khiroug, S. S., Harkness, P. C., Lamb, P. W., Sudweeks, S. N., Khiroug, L., Millar, N. S., Yakel, J. L. (2002). Rat nicotinic receptor α7 and β2 subunits co-assemble to form functional heteromeric nicotinic receptor channels. *J. Physiol.*, **540,** 425-34.

Kihara, T., Shimohama, S., Sawada, H., Honda, K., Nakamizo, T., Shibasaki, H., Kume, T., Akaike, A. (2001). α7 nicotinic receptor transduces signals to phosphatidylinositol 3-kinase to block β-amyloid-induced neurotoxicity. *J. Biol. Chem.*, **276**, 13541-6.

Kilpatrick, G. J., Jones, B. J., Tyers, M. B. (1987) Identification and distribution of 5-HT_3 receptors in rat brain using radioligand binding. *Nature,* **330**, 746-8.

Kriegler, S., Sudweeks, S., Yakel, J. L. (1999). The nicotinic α4 receptor subunit contributes to the lining of the ion channel pore when expressed with the 5-HT_3 receptor subunit. *J. Biol. Chem.*, **274,** 3934-6.

Kurosaki, T., Fukuda, K., Konno, T., Mori, Y., Tanaka, K., Mishina, M., Numa, S. (1987). Functional properties of nicotinic acetylcholine receptor subunits expressed in various combinations. *FEBS Lett.*, **214**, 253-8.

Kuryatov, A., Gerzanich, V., Nelson, M., Olale, F., Lindstrom, J. (1997). Mutation causing autosomal dominant nocturnal frontal lobe epilepsy alters Ca^{2+} permeability, conductance, and gating of human α4β2 nicotinic acetylcholine receptors. *J. Neurosci.*, **17**, 9035-47.

Kuryatov, A., Olale, F., Cooper, J., Choi, C. Lindstrom, J. (2000). Human α6 AChR subtypes: subunit composition, assembly, and pharmacological responses. *Neuropharm.*, **39,** 2570-90.

Kusano, K., Miledi, R., Stinnakre, J. (1977). Acetylcholine receptors in the oocyte membrane. *Nature,* **270**, 739-41.

La Torre, J. L., Lunt, G. S., De Robertis, E. (1970). Isolation of a cholinergic proteolipid receptor from electric tissue. *Proc. Natl. Acad. Sci. U. S. A.*, **65**, 716-20.

Labarca, P., Lindstrom, J., Montal, M. (1984). Acetylcholine receptor in planar lipid bilayers. Characterization of the channel properties of the purified nicotinic acetylcholine receptor from *Torpedo californica* reconstituted in planar lipid bilayers. *J. Gen. Physiol.*, **83**, 473-96.

Lambert, J. J., Belelli, D., Hill-Venning, C. Peters, J. A. (1995). Neurosteroids and $GABA_A$ receptor function. *Trends Pharm. Sci.*, **16,** 295-303.

Lankiewicz, S., Huser, M. B., Heumann, R., Hatt, H. Gisselmann, G. (2000). Phosphorylation of the 5-hydrotryptamine$_3$ (5-HT_3) receptor expressed in HEK293 cells. *Receptors and Channels*, **7,** 9-15.

Lankiewicz, S., Lobitz, N., Wetzel, C. H. R., Rupprecht, R., Gisselmann, G. Hatt, H. (1998). Molecular cloning, functional expression, and pharmacological characterization of 5-hydroxytryptamine$_3$ receptor cDNA and its splice variants from guinea pig. *Mol. Pharm.*, **53,** 202-12.

Lansdell, S. J., Gee, V. J., Harkness, P. C., Doward, A. I., Baker, E. R., Gibb, A. J., Millar, N. S. (2005). RIC3 enhances functional expression of multiple nicotinic acetylcholine receptor subtypes in mammalian cells. *Mol. Pharm. [Epub ahead of print]*

LaPolla, R. J., Mayne, K. M., Davidson, N. (1984). Isolation and characterisation of a cDNA clone for the complete coding region of the δ subunit of the mouse acetylcholine receptor. *Proc. Natl. Acad. Sci. U. S. A.*, **81,** 7970-4.

Lax, P., Fucile, S., Eusebi, F. (2002). Ca^{2+} permeability of human heteromeric nAChRs expressed by transfection in human cells. *Cell Calcium,* **32**, 53-8.

Lee, C. Y. and Chang, C. C. (1966). Modes of action of purified toxins from elapid venoms on neuromuscular transmission. *Mem. Inst. Butantan. Sao Paulo*, **33,** 555-72.

Lena, C. and Changeux, J.-P. (1998). Allosteric nicotinic receptors, human pathologies. *J. Physiol.*, **92,** 63-74.

Leonard, R. J., Labarca, C. G., Charnet, P., Davidson, N., Lester, H. A. (1988) Evidence that the M2 membrane-spanning region lines the ion channel pore of the nicotinic receptor *Science*, **242,** 1578-81.

Levin, E. D. and Simon, B. B. (1998). Nicotinic acetylcholine involvement in cognitive function in animals. *Psychopharm.*, **138,** 217-30.

Lewis, T. M., Harkness, P. C., Sivilotti, L. G., Colquhoun, D., Millar, N. S. (1997) The ion channel properties of a rat recombinant neuronal nicotinic receptor are dependent on the host cell type *J. Physiol.*, **505,** 299-306.

Lin, L., Jeanclos, E. M., Treuil, M. W., Braunewell, K.-H., Gundelfinger, E. D., Anand, R. (2002). The calcium sensor protein visinin-like protein-1 modulates the surface expression and agonist-sensitivity of the α4β2 nicotinic acetylcholine receptor. *J. Biol. Chem.*, **277,** 41872-8.

Lips, K. S., Pfeil, U., Kummer, W. (2002) Coexpression of α9 and α10 nicotinic acetylcholine receptors in rat dorsal root ganglion neurons *Neurosci.*, **115**, 1-5

Lobitz, N., Gisselmann, G., Hatt, H., Wetzel, C. H. (2001). A single amino-acid in the TM1 domain is an important determinant of the desensitization kinetics of recombinant human and guinea pig α-homomeric 5-hydroxytryptamine type 3 receptors. *Mol. Pharm.*, **59**, 844-51.

Luetje, C. W., Patrick, J. (1991). Both α- and β-subunits contribute to the agonist sensitivity of neuronal nicotinic acetylcholine receptors. *J. Neurosci.*, **11**, 837-45.

Ma, D. and Jan, L. Y. (2003). ER transport signals and trafficking of potassium channels and receptors. *Curr. op. pharm.*, **12**, 287.

Macor, J. E., Gurley, D., Lanthorn, T., Loch, J., Mack, R. A., Mullen, G., Tran, O., Wright, N., Gordon, J. C. (2001). The 5-HT_3 antagonist tropisetron (ICS 205-930) is a potent and selective α7 nicotinic receptor partial agonist. *Bioorganic and Medicinal Chemistry Letters*, **11,** 319-21.

Maimone, M. M. and Enigk, R. E. (1999). The intracellular domain of the nicotinic acetylcholine receptor α subunit mediates its coclustering with rapsyn. *Mol Cell Neurosci.* **14**, 340-54.

Mair, I. D., Lambert, J. J., Yang, J., Dempster, J., Peters, J. A. (1998) Pharmacological characterization of a rat 5-hydroxytryptamine type 3 receptor subunit (r5-$HT_{3A(b)}$) expressed in *Xenopus* laevis oocytes *Br. J. Pharm.*, **124**, 1667-74.

Mandelzys, A., Pié, B., Deneris, E. S., Cooper, E. (1994). The developmental increase in ACh current densities on rat sympathetic neurons correlates with changes in nicotinic ACh receptor a-subunit gene expression and occurs independent of innervation. *J. Neurosci.*, **14,** 2357-64.

Mansvelder, H. D. and McGehee, D. S. (2000). Long-term potentiation of excitatory inputs to brain reward areas by nicotine. *Neuron*, **27,** 349-57.

Mansvelder, H. D. and McGehee, D. S. (2002). Cellular and synaptic mechanisms of nicotine addiction. *J. Neurobiol.*, **53,** 606-17.

Mansvelder, H. D., Keath, J. R., McGehee, D. S. (2002). Synaptic mechanisms underlie nicotine-induced excitability of brain reward areas. *Neuron*, **33**, 905-19.

Marazziti, D., Betti, L., Giannaccini, G., Rossi, A., Masala, I., Baroni, S., Cassano, G. B., Lucacchini, A. (2001). Distribution of [^{3}H]GR65630 binding in human brain postmortem. *Neurochem. Res.*, **26,** 187-90.

Maricq, A. V., Peterson, A. S., Brake, A. J., Myers, R. M., Julius, D. (1991). Primary structure and functional expression of the $5HT_3$ receptor, a serotonin-gated ion channel. *Science*, **254,** 432-7.

Marks, M. J., Pauly, J. R., Gross, S. D., Deneris, E. S., Hermans-Borgmeyer, I., Heinemann, S. F., Collins, A. C. (1992). Nicotine binding and nicotinic receptor subunit RNA after chronic nicotine treatment. *J. Neurosci.* **12**, 2765-84.

Martin, M., Czajkowski, C., Karlin, A. (1996). The contribution of aspartyl residues in the acetylcholine receptor γ and δ subunits to the binding of agonists and competitive antagonists. *J. Biol. Chem.*, **271,** 13497-503.

Martin-Ruiz, C. M., Court, J. A., Molnar, E., Lee, M., Gotti, C., Mamalaki, A., Tsouloufis, T., Tzartos, S., Ballard, C., Perry, R. H., Perry, E. K. (1999). α4 but not α3 and α7 nicotinic acetylcholine receptor subunits are lost from the temporal cortex in Alzheimer's disease. *J. Neurochem.*, **73**, 1635-40.

Marubio, L. M., del Mar Arroyo-Jimenez, M., Lena, C., Le Novére, N., Kerchove d'Exaerde, A., Huchet, M., Damaj, M. I., Changeux, J.-P. (1999). Reduced antinociception in mice lacking neuronal nicotinic receptor subunits. *Nature*, **398,** 805-10.

McGehee, D. S. and Role, L. W. (1995). Physiological diversity of nicotinic acetylcholine receptors expressed by vertebrate neurons. *Annu. Rev. Physiol.*, **57,** 521-46.

McMahon, L. L. and Kauer, J. A. (1997). Hippocampal interneurons are excited via serotonin-gated ion channels. *J. Neurophysiol.*, **78**, 2493-502

Merlie, J. P. and Lindstrom, J. (1983). Assembly in vivo of mouse muscle acetylcholine receptor: identification of an α subunit species that may be an assembly intermediate. *Cell*, **34,** 747-57.

Miledi, R., Molinoff, P., Potter, L. T. (1971). Isolation of the cholinergic receptor protein of *Torpedo* electric tissue. *Nature*, **229**, 554-7.

Millar, N. S. (2003). Assembly and subunit diversity of nicotinic acetylcholine receptors. *Biochem. Soc. Trans.*, **31,** 869-74.

Mike, A., Castro, N. G., Albuquerque, E. X. (2000). Choline and acetylcholine have similar kinetic properties of activation and desensitization on the α7 nicotinic receptors in rat hippocampal neurons. *Brain Res.*, **882**, 155-68.

Miquel, M. C., Emerit, M. B., Gingrich, J. A., Nosjean, A., Hamon, M., El Mestikawy, S. (1995). Developmental changes in the differential expression of two serotonin 5-HT_3 receptor splice variants in the rat. *J. Neurochem.,* **65,** 475-83.

Mishina, M., Takai, T., Imoto, K., Noda, M., Takahashi, T., Numa, S., Methfessel, C., Sakman, B. (1986). Molecular distinction between fetal and adult forms of muscle acetylcholine receptor. *Nature*, **313,** 364-9.

Miyake, A., Mochizuki, S., Takemoto, Y., Akuzawa, S. (1995). Molecular cloning of human 5-hydroxytryptamine$_3$ receptor: heterogeneity in distribution and function among species. *Mol. Pharm.*, **48,** 407-16.

Miyazawa, A., Fujiyoshi, Y., Unwin, N. (2003). Structure and gating mechanism of the acetylcholine receptor pore. *Nature*, **423,** 949-55.

Miyazawa, A., Fujiyoshi, Y., Stowell, M., Unwin, N. (1999). Nicotinic acetylcholine receptor at 4.6Å resolution: transverse tunnels in the channel wall. *J. Mol. Biol.*, **288,** 765-86.

Mochizuki, S., Miyake, A., Furuichi, K. (1999). Identification of a domain affecting agonist potency of meta-chlorophenylbiguanide in 5-HT_3 receptors. *Eur. J. Pharm.*, **369,** 125-32.

Molinari, E. J., Delbono, O., Messi, M. L., Renganathan, M., Arneric, S. P., Sullivan, J. P., Gopalakrishnan, M. (1998). Up-regulation of human $\alpha 7$ nicotinic receptors by chronic treatment with activator and antagonist ligands. *Eur. J. Pharm.*, **347**, 131-9.

Monk, S. A., Desai, K., Brady, C. A., Williams, J. M., Lin, L., Princivalle, A., Hope, A. G., Barnes, N. M. (2001) Generation of a selective 5-HT_{3B} subunit-recognising polyclonal antibody; identification of immunoreactive cells in rat hippocampus *Neuropharm.*, **41,** 1013-6.

Morales, M. and Wang, S.-D. (2002). Differential composition of 5-HT_3 receptors synthesized in the rat CNS and peripheral nervous system. *J. Neurosci.*, **22,** 6732-41.

Morens, D. M., Grandinetti, A., Reed, D., White, L. R., Ross, G. W. (1995). Cigarette smoking and protection from Parkinson's disease: false association or etiologic clue? *Neurology*, **45**, 1041-51.

Nayak, S. V., Rondé, P., Spier, A. D., Lummis, S. C. R., Nichols, R. A. (2000). Nicotinic receptors co-localize with 5-HT_3 serotonin receptors on striatal nerve terminals. *Neuropharm.*, **39,** 2681-90.

Nef, P., Mauron, A., Stalder, R., Alliod, C., Ballivet, M. (1984). Structure, linkage and sequence of the two genes encoding the δ and γ subunits of the nicotinic acetylcholine receptor. *Proc. Natl. Acad. Sci. U. S. A.*, **81,** 7975-9.

Nelson, M. E., Kuryatov, A., Choi, C. H., Zhou, Y., Lindstrom, J. (2003). Alternate stoichiometries of α4β2 nicotinic acetylcholine receptors. *Mol. Pharm.*, **63,** 332-41.

Neubig, R. R., Krodel, E.K., Boyd, N. D., Cohen, J. B. (1979). Equilibrium binding of [^{3}H]tubocurarine and [^{3}H]acetylcholine by *Torpedo* postsynaptic membranes: stoichiometry and ligand interactions. *Biochem.*, **18**, 5464-75.

Niemeyer, M.-I. and Lummis, S. C. R. (1998). Different efficacy of specific agonists at 5-HT_3 receptor splice variants: the role of the extra six amino acid segment. *Br. J. Pharm.*, **123,** 661-6.

Niesler, B., Frank, B., Kapeller, J., Rappold, G. A. (2003). Cloning, physical mapping and expression analysis of the human 5-HT_3 serotonin receptor-like genes *HTR3C*, *HTR3D* and *HTR3E*. *Gene*, **310,** 101-11.

Nisell, M., Nomikos, G. G., Svensson, T. H. (1994). Systemic nicotine-induced dopamine release in the rat nucleus accumbens is regulated by nicotinic receptors in the ventral tegmental area. *Synapse*, **16,** 36-44.

Noda, M., Furutani, Y., Takahashi, H., Toyosato, M., Tanabe, T., Shimizu, S., Kikyotani, S., Kayano, T., Hirose, T., Inayama, S., *et al.* (1983a). Cloning and sequence analysis of calf cDNA and human genomic DNA encoding α-subunit precursor of muscle acetylcholine receptor. *Nature*, **305**, 818-23.

Noda, M., Takahashi, H., Tanabe, T., Toyosato, M., Kikyotani, S., Furutana, Y., Hirose, T., Takashima, H., Inayama, S., Miyata, T., Numa, S. (1983b). Stuctural homology of *Torpedo californica* acetylcholine receptor subunits. *Nature*, **302,** 528-32.

Noda, M., Takahashi, H., Tanabe, T., Toyosato, M., Furutani, Y., Hirose, T., Asai, M., Inayama, S., Miyata, T., Numa, S. (1982). Primary structure of α-subunit precursor of *Torpedo californica* acetylcholine receptor deduced from cDNA sequence. *Nature*, **299**, 793-7.

Nomoto, H., Takahashi, N., Nagaki, Y., Endo, S., Arata, Y., Hayashi, K. (1986). Carbohydrate structures of acetylcholine receptor from *Torpedo californica* and distribution of oligosaccharides among the subunits. *Eur. J. Biochem.*, **157,** 133-42.

Olale, F., Gerzanich, V., Kuryatov, A., Wang, F., Lindstrom, J. (1997). Chronic nicotine exposure differentially affects the function of human α3, α4, and α7 neuronal nicotinic receptor subtypes. *J. Pharm. Exp. Ther.*, **283,** 675-83.

Orr-Urtreger, A., Goldner, F. M., Saeki, M., Lorenzo, I., Goldberg, L., De Biasi, M., Dani, J. A., Patrick, J. W., Beaudet, A. L. (1997). Mice deficient in the α7 neuronal nicotinic acetylcholine receptor lack a-bungarotoxin binding sites and hippocampal fast nicotinic currents. *J. Neurosci.*, **17,** 9165-71.

Ortells, M. O., Lunt, G. G. (1995). Evolutionary history of the ligand-gated ion-channel superfamily of receptors. *Trends Neurosci.*, **18**, 121-7.

Palma, E., Bertrand, S., Binzoni, T., Bertrand, D. (1996). Neuronal nicotinic α7 receptor expressed in *Xenopus* oocytes presents five putative binding sites for methyllycaconitine. *J. Physiol.*, **491,** 151-61.

Palma, E., Maggi, L., Barabino, B., Eusebi, F., Ballivet, M. (1999). Nicotinic acetylcholine receptors assembled from the α7 and β3 subunits. *J. Biol. Chem.*, **274,** 18335-40.

Palma, E., Mileo, A. M., Eusebi, F., Miledi, R. (1996b). Threonine-for-leucine mutation within domain M2 of the neuronal α7 nicotinic receptor converts 5-hydroxytryptamine from antagonist to agonist. *Proc. Natl. Acad. Sci. U. S. A.*, **93**, 11231-5.

Panicker, S., Cruz, H., Arrabit, C., Slesinger, P. A. (2002) Evidence for a centrally located gate in the pore of a serotonin-gated ion channel *J. Neurosci.*, **22**, 1629-39.

Papke, R. L., Boulter, J., Patrick, J., Heinemann, S. (1989). Single-channel currents of rat neuronal nicotinic acetylcholine receptors expressed in *Xenopus* oocytes. *Neuron.*, **3**, 589-96.

Parker, M. J., Beck, A., Luetje, C. W. (1998). Neuronal nicotinic receptor β2 and β4 subunits confer large differences in agonist binding affinity. *Mol. Pharm.*, **54**, 1132-9.

Paterson, D. and Nordberg, A. (2000). Neuronal nicotinic receptors in the human brain. *Prog. Neurobiol.*, **61,** 75-111.

Patrick. J. and Stallcup. W.B. (1977). Immunological distinction between acetylcholine receptor and the α-bungarotoxin-binding component on sympathetic neurons. *Proc. Natl. Acad. Sci. U. S. A.*, **74**, 4689-92.

Paulson, H. L., Ross, A. F., Green, W. N., Claudio, T. (1991). Analysis of early events in acetylcholine receptor assembly. *J. Cell Biol.*, **113,** 1371-84.

Pedersen, S. E. and Cohen, J. B. (1990). *d*-Tubocurarine binding sites are located at α–γ and α–δ subunit interfaces of the nicotinic acetylcholine receptor. *Proc. Natl. Acad. Sci. U. S. A.*, **87,** 2785-9.

Peng, X., Gerzanich, V., Anand, R., Wang, F., Lindstrom, J. (1997). Chronic nicotine treatment up-regulates α3 and α7 acetylcholine receptor subtypes expressed by the human neuroblastoma cell line SH-SY5Y. *Mol. Pharm.*, **51,** 776-84.

Peng, X., Katz, M., Gerzanich, V., Anand, R., Lindstrom, J. (1994). Human α7 acetylcholine receptor: cloning of the α7 subunit from the SH-SY5Y cell line and determination of pharmacological properties of native receptors and functional α7 homomers in *Xenopus* oocytes. *Mol. Pharm.*, **45,** 546-54.

Picciotto, M. R. and Zoli, M. (2002). Nicotinic receptors in aging and dementia. *J. Neurobiol.*, **53,** 641-55.

Picciotto, M. R., Brunzell, D. H., Caldarone, B. J. (2002). Effect of nicotine and nicotinic receptors on anxiety and depression. *Neuroreport*, **13**, 1097-106.

Picciotto, M. R., Zoli, M., Lena, C., Bessis, A., Lallemand, Y., Le Novére, N., Vincent, P., Merlo Pich, E., Brulet, P., Changeux, J.-P. (1995). Abnormal avoidance learning in mice lacking functional high-affinity nicotine receptor in the brain. *Nature*, **374,** 65-7.

Picciotto, M. R., Zoli, M., Rimondini, R., Lena, C., Marubio, L. M., Merlo Pich, E., Fuxe, K., Changeux, J.-P. (1998). Acetylcholine receptors containing the β2 subunit are involved in the reinforcing properties of nicotine. *Nature*, **391,** 173-7.

Prince, R. J. and Sine, S. M. (1996). Molecular dissection of subunit interfaces in the acetylcholine receptor. *J. Biol. Chem.*, **271,** 25770-7.

Puchacz, E., Buisson, B., Bertrand, D., Lukas, R. L. (1994). Functional expression of nicotinic acetylcholine receptors containing rat α7 subunits in human SH-SY5Y neuroblastoma cells. *FEBS Letters*, **354,** 155-9.

Pugh, P. C., Corriveay, R. A., Conroy, W. G., Berg, D. K. (1995). Novel subpopulation of neuronal acetylcholine receptors among those binding a-bungarotoxin. *Mol. Pharm.*, **47,** 717-25.

Pym, L., Kemp, M., Raymond-Delpech, V., Buckingham, S., Boyd, C. A., Sattelle, D. (2005). Subtype-specific actions of β-amyloid peptides on recombinant human neuronal nicotinic acetylcholine receptors (α7, α4β2, α3β4) expressed in *Xenopus laevis* oocytes. *Br. J. Pharm., [Epub ahead of print]*

Quick, M. W. and Lester, R. A. (2002) Desensitization of neuronal nicotinic receptors *J. Neurobiol.,* **53,** 457-78.

Quik, M. and Kulak, J. M. (2002). Nicotine and nicotinic receptors; relevance to Parkinson's disease. *Neurotox.*, **23**, 581-94.

Quirk, P. L., Rao, S., Roth, B. L., Siegel, R. E. (2004). Three putative N-glycosylation sites within the murine 5-HT_{3A} receptor sequence affect plasma membrane targeting, ligand binding, and calcium influx in heterologous mammalian cells. *J. Neurosci. Res.*, **77,** 498-506.

Racchi, M., Mazzucchelli, M., Porrello, E., Lanni, C., Govoni, S. (2004). Acetylocholine inhibitors: novel activities of old molecules. *Pharmacological Res.*, **50**, 441-51.

Ragozzino, D., Barabino, B., Fucile, S., Eusebi, F. (1998). Ca^{2+} permeability of mouse and chick nicotinic acetylcholine receptors expressed in transiently transfected human cells. *J. Physiol.*, **507**, 749-57.

Ragozzino, D., Fucile, S., Giovannelli, A., Grassi, F., Mileo, A. M., Ballivet, M., Alema, S. and Eusebi, F. (1997). Functional properties of neuronal nicotinic acetylcholine receptor channels expressed in transfected human cells. *Eur. J. Neurosci.*, **9,** 480-8.

Rakhilin, S., Drisdel, R. C., Sagher, D., McGehee, D. S., Vallejo, Y., Green, W., N. (1999). α-bungarotoxin receptors contain $\alpha 7$ subunits in two different disulfide-bonded conformations. *J. Cell Biol.*, **146,** 203-17.

Ramirez-Latorre, J., Yu, C. R., Qu, X., Perin, F., Karlin, A., Role, L. (1996) Functional contributions of $\alpha 5$ subunit to neuronal acetylcholine receptor channels *Nature*, **380,** 347-51.

Rangwala, F., Drisdel, R. C., Rakhilin, S., Ko, E., Atluri, P., Harkins, A. B., Fox, A. P., Salman, S. B., Green, W. N. (1997). Neuronal a-bungarotoxin receptors differ structurally from other nicotinic acetylcholine receptors. *J. Neurosci.*, **17,** 8201-12.

Reeves, D. C. and Lummis, S. C. R. (2000). Mutation of an isoleucine residue M2 alters the Ca^{2+} permeability of 5-HT_{3A} receptors. *Br. J. Pharm.*, **129,** 39P.

Reeves, D. C., Goren, E. N., Akabas, M. H., Lummis, S. C. R. (2001). Structural and electrostatic properties of the 5-HT_3 receptor pore revealed by substituted cysteine accessibility mutagenesis. *J. Biol. Chem.*, **276,** 42035-42.

Reeves, D. C., Sayed, M. F. R., Chau, P.-L., Price, K. L., Lummis, S. C. R. (2003). Prediction of 5-HT_3 receptor agonist-binding residues using homology modeling. *Biophys. J.*, **84,** 2238-344.

Reeves, D.C. and Lummis, S. C. (2002) The molecular basis of the structure and function of the 5-HT3 receptor: a model ligand-gated ion channel. *Mol. Membr. Biol.*, **19,** 11-26.

Revah, F., Bertrand, D., Galzi, J. L., Devillers-Thiery, A., Mulle, C., Hussy, N., Bertrand, S., Ballivet, M., Changeux, J. P. (1991). Mutations in the channel domain alter desensitization of a neuronal nicotinic receptor. *Nature*, **353,** 846-9.

Revah, F., Galzi, J. L., Giraudat, J., Haumont, P. Y., Lederer, F., Changeux, J. P. (1990). The noncompetitive blocker [^{3}H]chlorpromazine labels three amino acids of the acetylcholine receptor γ subunit: implications for the α-helical organization of regions MII and for the structure of the ion channel. *Proc. Natl. Acad. Sci. U. S. A.*, **87,** 4675-9.

Reynolds, J. A. and Karlin, A. (1978). Molecular weight in detergent solution of acetylcholine receptor from *Torpedo californica. Biochem.*, **17,** 2035-8.

Roerig, B., Nelson, D. A., Katz, L. C. (1997). Fast synaptic signaling by nicotinic acetylcholine and serotonin 5-HT_3 receptors in developing visual cortex. *J. Neurosci.*, **17,** 8353-62.

Role, L. W. and Berg, D. K. (1996). Nicotinic receptors in the development and modulation of CNS synapses. *Neuron*, **16,** 1077-85.

Role, L.W. (1992). Diversity in primary structure and function of neuronal nicotinic acetylcholine receptor channels. *Curr. Opin. Neurobiol.*, **2,** 254-62.

Roth, A. L., Shoop, R. D., Berg, D. K. (2000) Targeting α7-containing nicotinic receptors on neurons to distal locations *Eur. J. Pharm.*, **393,** 105-12.

Rust, G., Burgunder, J.-M., Lauterburg, T. E., Cachelin, A. B. (1994). Expression of neuronal nicotinic acetylcholine receptor subunit genes in the rat autonomic nervous system. *Eur. J. Neurosci.*, **6,** 478-85.

Rycroft, B. K. and Gibb, A.J. (2002). Direct effects of calmodulin on NMDA receptor single-channel gating in rat hippocampal granule cells. *J. Neurosci.*, **22,** 8860-8.

Salpeter, M. M. and Harris, R. (1983) Distribution and turnover rate of acetylcholine receptors throughout the junction folds at a vertebrate neuromuscular junction *J. Cell Biol.*, **96,** 1781-5.

Sargent, P. B. (1993). The diversity of neuronal nicotinic acetylcholine receptors. *Annu. Rev. Neurosci.*, **16,** 403-43.

Schoepfer, R., Conroy, W. G., Whiting, P., Gore, M., Lindstrom, J. (1990). Brain α-bungarotoxin binding protein cDNAs and mAbs reveal subtypes of this branch of the ligand-gated ion channel gene superfamily. *Neuron*, **5,** 35-48.

Schoepfer, R., Whiting, P., Esch, F., Blacher, R., Shimasaki, S., Lindstrom, J. (1988). cDNA clones coding for the structural subunit of a chicken brain nicotinic acetylcholine receptor. *Neuron*, **1,** 241-8.

Sealock, R. (1982). Visualization at the mouse neuromuscular junction of a submembrane structure in common with *Torpedo* postsynaptic membranes. *J. Neurosci.*, **2,** 918-23.

Séguéla, P., Wadiche, J., Dineley-Miller, K., Dani, J. A., Patrick, J. W. (1993). Molecular cloning, functional properties, and distribution of rat brain α7: a nicotinic cation channel highly permeable to calcium. *J. Neurosci.*, **13,** 596-604.

Servent, D. Winckler-Dietrich, V., Hu, H.-Y., Kessler, P., Drevet, P., Betrand, D., Ménez, A. (1997). Only snake curaremimetic toxins with a fifth disulfide bond have high affinity for the neuronal α7 nicotinic receptor. *J. Biol. Chem.*, **272,** 24279-86.

Severance, E. G., Zhang, H., Cruz, Y., Pakhlevaniants, S., Hadley, S. H., Amin, J., Wecker, L., Reed , C., Cuevas, J. (2004). The α7 nicotinic acetylcholine receptor subunit exists in two isoforms that contribute to functional ligand-gated ion channels. *Mol. Pharm.*, **66**, 420-9.

Severance, E. G. and Cuevas, J. (2004) Distribution and synaptic localization of nicotinic acetylcholine receptors containing a novel α7 subunit isoform in embryonic rat cortical neurons *Neurosci. Lett.*, **372**, 104-9.

Sine, S. M. (1993) Molecular dissection of subunit interfaces in the acetylcholine receptor: identification of residues that determine curare selectivity *Proc. Natl. Acad. Sci. U. S. A.*, **90,** 9436-40.

Smit, A. B., Syed, N. I., Schaap, D., van Minnen, J., J., K., Kits, K. S., Lodder, H., van der Schors, R. C., van Elk, R., Sorgedrager, B., Brejc, K., Sixma, T., Geraerts, W. P. M. (2001). A glial-derived acetylcholine-binding protein that modulates synaptic transmission. *Nature*, **411,** 261-8.

Sorenson, E. M., El-Bogdadi, D. G., Nong, Y., Chiappinelli, V. A. (2001) α7-Containing nicotinic receptors are segregated to the somatodendritic membrane of the cholinergic neurons in the avian nucleus semilunaris *Neurosci.*, **103**, 541-50.

Spier, A. D. and Lummis, S. C. R. (2000). The role of tryptophan residues in 5-hydroxytryptamine(3) receptor ligand binding domain. *J. Biol. Chem.*, **275,** 5620-5.

Spier, A. D., Wotherspoon, G., Nayak, S. V., Nichols, R. A., Priestly, J. V., Lummis, S. C. R. (1999). Antibodies against the extracellular domain of the 5-HT_3 receptor label both native and recombinant receptors. *Mol. Brain Res.*, **67,** 221-30.

Steinlein, O. K., Mulley, J. C., Propping, P., Wallace, R. H., Phillips, H. A., Sutherland, G. R., Scheffer, I. E., Berkovic, S. F. (1995). A missense mutation in the neuronal nicotinic acetylcholine receptor α4 subunit is associated with autosomal dominant nocturnal frontal lobe epilepsy. *Nat. Genet.*, **11**, 201-3.

Steward, L. J., Boess, F. G., Steele, J. A., Liu, D., Wong, N., Martin, I. L. (2000). Importance of phenylalanine 107 in agonist recognition by the 5-hydroxytryptamine (3A) receptor. *Mol. Pharm.*, **57,** 1249-55.

Stewart, A., Davies, P. A., Kirkness, E. F., Safa, P., Hales, T. G. (2003). Introduction of the 5-HT_{3B} subunit alters the functional properties of 5-HT_3 receptors native to neuroblastoma cells. *Neuropharm.*, **44,** 214-23.

Stroud, R. M., McCarthy, M. P., Shuster, M. (1990). Nicotinic acetylcholine receptor superfamily of ligand-gated ion channels. *Biochem.*, **29,** 11009-23.

Sugita, S., Shen, K. Z., North, R. A. (1992). 5-hydroxytryptamine is a fast excitatory transmitter at 5-HT_3 receptors in rat amygdala. *Neuron*, **8,** 199-203.

Sumikawa, K., Houghton, M., Emtage, J. S., Richards, B. M., Barnard, E. A. (1981). Active multi-subunit ACh receptor assembly by translation of heterologous mRNA in *Xenopus* oocytes. *Nature*, **292,** 862-4.

Swanson, L. W., Simmons, D. M., Whiting, P. J., Lindstrom, J. (1987) Immunohistochemical localization of neuronal nicotinic receptors in the rodent central nervous system *J. Neurosci.*, **7,** 3334-42.

Sweileh, W., Wenberg, K., Xu, J., Forsayeth, J., Hardy, S., Loring, R. H. (2000). Multistep expression and assembly of neuronal nicotinic receptors is both host-cell- and receptor-subtype-dependent. *Mol. Brain Res.*, **75,** 293-302.

Takai, T., Noda, M., Mishina, M., Shimizu, S., Furutani, Y., Kayano, T., Ikeda, T., Kubo, T., Takahashi, H., Takahashi, T., Kuno, M., Numa, S. (1985). Cloning, sequencing and expression of cDNA for a novel subunit of acetylcholine receptor from calf muscle. *Nature*, **315,** 761-764.

Tanabe, T., Noda, M., Furutani, Y., Takai, T., Takahashi, H., Tanaka, K., Hirose, T., Inayama, S., Numa, S. (1984). Primary structure of β subunit precursor of calf muscle acetylcholine receptor deduced from cDNA sequence. *Eur. J. Biochem.*, **144**, 11-7.

Taylor, P., Malany, S., Molles, B. E., Osaka, H., Tsigelny, I. (2000). Subunit interface selective toxins as probes of nicotinic acetylcholine receptor struture. *Eur. J. Physiol.*, **440,** R115-117.

Thompson, A. J. and Lummis. S. C. (2003) A single ring of charged amino acids at one end of the pore can control ion selectivity in the 5-HT_3 receptor *Br. J. Pharm.*, **140,** 359-65.

Traynelis, S. F. and Jaramillo, F. (1998). Getting the most out of noise in the central nervous system. *Trends Neurosci.*, **21**, 137-45.

Trautmann, A. (1982). Curare can open and block ionic channels associated with cholinergic receptors. *Nature*, **298**, 272-5.

Unwin, N. (1993). Nicotinic acetylcholine receptor at 9 Å resolution. *J. Mol. Biol.*, **229,** 1101-1124.

Unwin, N. (2003). Structure and action of the nicotinic acetylcholine receptor explored by electron microscopy. *Febs Lett*, **555,** 91-95.

Unwin, N. (2005). Refined structure of the nicotinic acetylcholine receptor at 4 Å resolution. *J. Mol. Biol.*, **346,** 967-989.

Vailati, S., Moretti, M., Balestra, B., McIntosh, M., Clementi, F., Gotti, C. (2000) β3 subunit is present in different nicotinic receptor subtypes in chick retina *Eur. J. Pharm.*, **393,** 23-30.

Valor, L. M., Mulet, J., Sala, F., Sala, S., Ballesta, J. J., Criado, M. (2002). Role of the large cytoplasmic loop of the $\alpha 7$ neuronal nicotinic acetylcholine receptor subunit in receptor expression and function. *Biochem.*, **41**, 7931-8.

van Hooft, J. A. and Vijverberg, H. P. M. (2000). 5-HT_3 receptors and neurotransmitter release in the CNS: a nerve ending story? *Trends Neurosci.*, **23,** 605-610.

van Hooft, J. A., Kreikamp, A. P., Vijverberg, H. P. (1997). Native serotonin 5-HT_3 receptors expressed in *Xenopus* oocytes differ from homopentameric 5-HT_3 receptors. *J. Neurochem.*, **69**, 1318-21.

van Hooft, J. A., Spier, A. D., Yakel, J. L., Lummis, S. C. R., Vijverberg, H. P. M. (1998). Promiscuous coassembly of serotonin 5-HT_3 and nicotinic α4 receptor subunits into Ca^{2+}-permeable ion channels. *Proc. Natl. Acad. Sci. U. S. A.*, **95,** 11456-11461.

van Hooft, J. A., van der Haar, E., Vijverberg, H. P. M. (1997). Allosteric potentiation of the 5-HT_3 receptor-mediated ion current in N1E-115 neuroblastoma cells by 5-hydroxyindole and analogues. *Neuropharm.*, **36,** 649-653.

Vazquez, R. W. and Oswald, R. E. (1999) Identification of a new amino acid residue capable of modulating agonist efficacy at the homomeric nicotinic acetylcholine receptor, α7 *Mol. Pharm.*, **55**, 1-7.

Vernallis, A. B., Conroy, W. G., Berg, D. K. (1993). Neurons assemble acetylcholine receptors with as many as three kinds of subunits while maintaining subunit segregation among receptor subtypes. *Neuron*, **10,** 451-64.

Villarroel, A. and Sakmann, B. (1996). Calcium permeability increase of endplate channels in rat muscle during postnatal development. *J. Physiol.*, **496** , 331-8.

Villarroel, A., Herlitze, S., Koenen, M., Sakmann, B. (1991). Location of a threonine residue in the α-subunit M2 transmembrane segment that determines the ion flow through the acetylcholine receptor channel. *Proc. Biol Sci.*, **243**, 69-74.

Virginio, C., Giacometti, A., Aldegheri, L., Rimland, J. M., Terstappen, G. C. (2002). Pharmacological properties of rat α7 nicotinic receptors expressed in native and recombinant cell systems. *Eur. J. Pharm.*, **445,** 153-61.

Wada, K., Ballivet, M., Boulter, J., Connolly, J., Wada, E., Deneris, E. S., Swanson, L. W., Heinemann, S., Patrick, J. (1988). Functional expression of a new pharmacological subtype of brain nicotinic acetylcholine receptor. *Science*, **240**, 330-4.

Wanamaker, C. P., Christianson, J. C., Green, W. N. (2003) Regulation of nicotinic acetylcholine receptor assembly *Ann. N. Y. Acad. Sci.*, **998,** 66-80.

Wang, F., Gerzanich, V., Wells, G. B., Anand, R., Peng, X., Keyser, K., Lindstrom, J. (1996) Assembly of human neuronal nicotinic receptor $\alpha 5$ subunits with $\alpha 3$, $\beta 2$, and $\beta 4$ subunits *J. Biol. Chem.*, **271,** 17656-65.

Wang, F., Nelson, M. E., Kuryatov, A., Olale, F., Cooper, J., Keyser, K., Lindstrom, J. (1988). Chronic nicotine treatment up-regulates human $\alpha 3\beta 2$ but not $\alpha 3\beta 4$ acetylcholine receptors stably transfected in human embryonic kidney cells. *J. Biol. Chem.*, **273**, 28721-32.

Wang, J.-M., Zhang, L., Yao, Y., Viroonchatapan, N., Rothe, E., Wang, Z.-Z. (2002). A transmembrane motif governs the surface trafficking of nicotinic acetylcholine receptors. *Nature Neurosci.*, **5,** 963-70.

Weiland, S., Witzemann, V., Villarroel, A., Propping, P., Steinlein, O. K. (1996). An amino acid exchange in the second transmembrane segment of a neuronal nicotinic receptor causes partial epilepsy by altering its desensitization kinetics. *FEBS Lett.*, **398,** 91-6.

Whitehouse, P. J., Hedreen, J. C., White, C. L. 3rd, Price, D. L. (1983). Basal forebrain neurons in the dementia of Parkinson disease. *Ann. Neurol.*, **13**, 243-8.

Whitehouse, P. J., Martino, A. M., Wagster, M. V., Price, D. L., Mayeux, R., Atack, J. R., Kellar, K. J. (1988). Reductions in [^{3}H]nicotinic acetylcholine binding in Alzheimer's disease and Parkinson's disease: an autoradiographic study. *Neurology*, **38**, 720-3.

Williams, B. M., Temburni, M. K., Levey, M. S., Bertrand, S., Bertrand, D., Jacob, M. H. (1998). The long internal loop of the $\alpha 3$ subunit targets nAChRs to subdomains within individual synapses on neurons in vivo. *Nature Neurosci.*, **1**, 557-62.

Williams, M. E., Burton, B., Urrutia, A., Shcherbatko, A., Chavez-Noriega, L. E., Cohen, C. J., Aiyar, J. (2005). RIC-3 promotes functional expression of the nicotinic acetylcholine receptor $\alpha 7$ subunit in mammalian cells. *J. Biol. Chem.*, **280,** 1257-63.

Wonnacott, S. (1997). Presynaptic nicotinic ACh receptors. *Trends Neurosci.*, **20,** 92-8.

Wonnacott, S., Kaiser, S., Mogg, A., Soliakov, L., Jones, A. W. (2000). Presynaptic nicotinic receptors modulating dopamine release in the rat striatum. *Eur. J. Pharm.*, **393,** 51-8.

Xiao, Y. and Kellar, K. J. (2004). The comparative pharmacology and up-regulation of rat neuronal nicotinic receptor subtype binding sites stably expressed in transfected mammalian cells. *J. Pharm. Exp. Ther.*, **310**, 98-107.

Yakel, J. L., Lagrutta, A., Adelman, J. P., North, R. A. (1993). Single amino acid substitution affects desensitization of the 5-hydroxytryptamine type 3 receptor expressed in *Xenopus* oocytes. *Proc. Natl. Acad. Sci. U. S. A.*, **90,** 5030-3.

Yan, D., Schulte, M. K., Bloom, K. E., White, M. M. (1999). Structural features of the ligand-binding domain of the serotonin $5HT_3$ receptor. *J. Biol. Chem.*, **274,** 5537-41.

Yu, C. R. and Role, L. W. (1998a). Functional contribution of the α5 subunit to neuronal nicotinic channels expressed by chick sympathetic ganglion neurones. *J. Physiol.*, **509,** 667-81.

Yu, C. R. and Role, L. W. (1998b). Functional contribution of the $\alpha 7$ subunit to multiple subtypes of nicotinic receptors in embryonic chick sympathetic neurones. *J. Physiol.*, **509,** 651-65.

Zhao, L., Kuo, Y. P., George, A. A., Peng, J. H., Purandare, M. S., Schroeder, K. M., Lukas, R. J., Wu, J. (2003). Functional properties of homomeric, human $\alpha 7$-nicotinic acetylcholine receptors heterologously expressed in the SH-EP1 human epithelial cell line. *J. Pharm. Exp. Ther.*, **305**, 1132-41.

Zoli, M., Lena, C., Picciotto, M. R., Changeux, J.-P. (1998). Identification of four classes of brain nicotinic receptors using β2 mutant mice. *J. Neurosci.*, **18,** 4461-72.

Zwart, R., De Filippi, G., Broad, L. M., McPhie, G. I., Pearson, K. H., Baldwinson, T., Sher, E. (2002). 5-Hydroxyindole potentiates human $\alpha 7$ nicotinic receptor-mediated responses and enhances acetylcholine-induced glutamate release in cerebellar slices. *Neuropharm.*, **43,** 374-84.

Zwart, R. and Vijverberg, H. P. M. (1998). Four pharmacologically distinct subtypes of α4β2 nicotinic acetylcholine receptor expressed in *Xenopus laevis* oocytes. *Mol. Pharm.*, **54,** 1124-31.